REFERENCE ONLY

UNIVERSITY OF LONDON THESIS

Degree PhD Year 2006 Name of Author PURI, T. S.

Characterisation of the human TIP48 and TIP49 AAA^+ proteins and their complex

By

TEENA PURI

Thesis admitted to the University of London for the degree of doctor of philosophy 2005

ProQuest LLC
789 East Eisenhower Parkway
P.O. Box 1346
Ann Arbor, MI 48106-1346

ABSTRACT

TIP48 and TIP49 are two closely related proteins, which are highly conserved in all eukaryotes. They are crucial components of various nuclear complexes involved in transcription activation, DNA repair, and snoRNP accumulation and trafficking, but the function of TIP48 and TIP49 within these complexes is not understood. They are part of the AAA^+ family of ATPases and show homology to the bacterial branch migration motor RuvB. However, reports about their enzymatic activities, such as DNA helicase activities, are contradictory and subject to speculations.

In this study the enzymatic activities of recombinant TIP48, TIP49 and catalytically inactive mutants were examined. The proteins displayed very low ATPase activities, which were not stimulated in the presence of DNA, and no DNA helicase activities. Both TIP48 and TIP49 bound adenine nucleotides. However, whilst TIP48 formed oligomers, upon incubation with adenine nucleotides, TIP49 did not.

An equimolar TIP48/TIP49 complex was assembled in solution and purified. The ATPase activity of the complex was significantly higher than the activities of the constituent proteins. Within this complex, both proteins bound and hydrolyzed ATP, as shown by using catalytically inactive mutant. The ATPase activity of the complex was not stimulated in the presence of DNA and no DNA helicase or branch migration activities were detected. The TIP48/TIP49 complex consists of two stacked hexameric rings with C6 symmetry as shown by electron microscopy. Structural differences between the top and bottom rings indicate that the complex may consist of two homohexamers.

The localizations of TIP48 and TIP49 in cells were examined by immunofluoresence microscopy. Both proteins showed specific localisation to the mitotic spindle, which strongly suggests a novel role in mitosis. Surprisingly, a dramatic accumulation of TIP48 at the midbody was observed in the late stages of mitosis, which differed from that of TIP49. The observations suggest that TIP48 may have a separate function at this stage of the cell cycle.

Acknowledgements

I would like to thank my supervisor Dr. Irina Tsaneva for allowing me to work on the project and for all the help she has given me over the last few years to complete this work. I would also like to thank people in the lab, past and present, for their help and advice with all the little and big things that I needed. I would like to especially thank Barbara Sigala who has helped me throughout the entire period with many things and also contributed to some aspects of the project, including some of the cloning and obtaining the antibodies used in this work. I would also especially like to thank Petra Wendler from the Birkbeck School of crystallography, who collaborated with us on the electron microscopy work and provided the images for this thesis. I would also like to thank her for helping me write that particular section in Chapter 5. Thank you also to Mina Edwards and Jodie Gwalter who grew and provided us with HeLa and Fibroblast cells for the immunofluorescence work. Lastly, I would like to thank my parents and my brother and sister who have put up with me for the last few years, while I tried to finish this work. I would also like thank everyone else; family and friends for all the support they have given me.

CONTENTS

Figures and Tables

ABBREVIATIONS

AAA^+	ATPases with different Associated Activities +
aa	Amino acid
ADP	Adenosine 5'-diphosphate
AMP	Ampicillin
AMPNP	5'-Adenylylimido diphosphate
APO128	Polyoxethelene (8) dodecyl ether
APS	Ammonium persulphate
ATP	Adenosine 5'-triphosphate
ATPγS	Adenosine 5'O-(3-thiotriphosphate)
bp	Base pair
BCIP/NBT	5-Bromo-4-chloro-3-indoyl phosphate/ nitro blue tetrazolium
βME	2-β mercaptoethanol
BSA	Bovine serum albumin
$CaCl_2$	Calcium Chloride
CB	Carbenicillin
Ci	Curie
CM	Chloroamphenicol
CIP	Calf intestinal (alkaline) phosphatase
ChIP	Chromatin immunoprecipitation
Coomassie BB	Coomassie brilliant blue
CPT	Camptothecin
Da	Dalton
DEAE	Diethylaminoethyl
DNA	Deoxyribonucleic acid
ssDNA	Single-stranded DNA
dsDNA	Double-stranded DNA
dNTP	Deoxyribonucleotide triphosphate
DSB	Double-strand breaks

DTT	Dithiothreitol
EDTA	Ethylenediaminetetraacetic acid
EM	Electron microscopy
FPLC	Fast protein liquid chromatography
g	Gram
g	g-force/relative centrifugal force (RCF)
HCl	Hydrochloric acid
HRP	Horse radish peroxidase
IPTG	Isopropyl-1-thio-β-D-galactopyranoside
IR	Ionizing Radiation
k	Kilo
KCl	Potassium chloride
K_2HPO_4	Dipotassium hydrogen phosphate
KH_2PO_4	Potassium dihydrogen phosphate
KOH	Potassium hydroxide
l	Litre
LB	Luria Broth
M	Molar
m	Milli
m	Metre
MCM	Mini chromosome maintenance
$MgSO_4$	Magnesium sulphate
MMS	Methylmethane sulphonate
Mol	Mole
MOPS	(3-[N-Morpholino] propane sulphonoic acid
n	Nano
NaI	Sodium iodide
NaCl	Sodium Chloride
Na_2HPO_4	Disodium hydrogen phosphate
NaH_2PO_4	Sodium dihydrogen phosphate
NaOH	Sodium hydroxide

NHEJ	Non-homologous end joining
NP40	Nonidet P40
nt	Nucleotide
p	Pico
PCR	Polymerase chain reaction
PBS	Phosphate buffered saline
PEI	Poly(ethyenimine)
OD	Optical density
ORF	Open reading frame
PAGE	Polyacrylamide gel electrophoresis
PBS	Phosphate buffered saline
PCNA	proliferating cell nuclear antigen
PMSF	Phenyl methyl sulphonyl fluoride
PNK	Polynucleotide kinase
PVDF	Polyvinylidene fluoride
$RbCl_2$	Rubidium chloride
RFC	Replication protein C
RNA	Ribonucleic acid
rRNA	Ribosomal RNA
RNP	Ribonucleoprotein
RPM	Revolutions per minute
SDM	Site directed mutagenesis
SDS	Sodium dodecyl sulphate
SSC	Sodium chloride-Sodium Citrate
TAE	Tris, Acetic acid and EDTA (buffer)
TB	Tris borate
TBP	Tata binding protein
TBS	Tris buffered saline
TCA	Trichloric acid
TE	Tris EDTA (buffer)
TEMED	N,N,N',N'-Tetra-methyl-ethylenediamine

TLC	Thin layer chromatography
T_m	Melting temperature
TRIS	Tris (hydroxymethyl) aminoethane
Triton X-100	Octyl phenol ethoxylate
Tween 20	Poloxyethylene Sorbitan Monolaurate
U	Unit
UV	Ultra violet
v/v	Volume to volume
X-gal	5-brom-4-chloro-3-indolyl-beta-D-galactopyranoside
Å	Angstrom
µ	Micro
[α-^{32}P]-ATP	Adenosine 5'-[α^{32}P] diphosphate
[γ-^{32}P]-ATP	Adenosine 5'-[γ^{32}P] triphosphate
[γ^{32}P] 2-azido ATP	2-azidoadenosine 5'-[γ^{32}P] triphosphate

CHAPTER 1

INTRODUCTION

1.1 Homologous recombination

Homologous recombination is a process that occurs in both prokaryotes and eukaryotes and is required for the generation of genetic diversity between organisms as well as for the repair of DNA double-strand breaks (DSBs) (Helleday, 2003; Johnson and Jasin, 2001). DSBs occur through the action of external factors, such as ionizing radiation and DNA damaging chemicals, and internal factors, such as oxidizing agents and DNA endonucleases. It is therefore important that these damaged regions are repaired by pathways, employed by the cell, to prevent chromosomal aberrations that lead to the onset of cancer and cell death (Elliott and Jasin, 2002; Pfeiffer et al., 2000). The mechanism of homologous recombination has a very important role in prokaryotes for the repair of DSBs and, as shown in the last few years, in eukaryotes as well (Dudas and Chovanec, 2004; Johnson and Jasin, 2001; Osman and Subramani, 1998).

Homologous recombination involves the interaction of the broken ends of one DNA molecule with homologous segments of another DNA molecule. This is followed by a strand exchange event and the formation of a heteroduplex crossover intermediate (Figure 1.1). Homologous pairing and strand exchange is catalyzed in bacteria by the RecA protein (West, 1994b) and in eukaryotes, by its functional homologue Rad51 (Baumann and West, 1998). The heteroduplex intermediated formed, is known as the Holliday junction, named after Robin Holliday (Holliday, 1964). To complete the recombination reaction the Holliday junction needs to be processed by specialised enzymes that promote branch migration and endonucleolytic resolution of the crossover. A specialised enzymatic system for processing Holliday junctions exists in prokaryotes and involves the RuvABC proteins, which have been extensively characterised (Reviewed in (West, 1994b; West, 1996)).

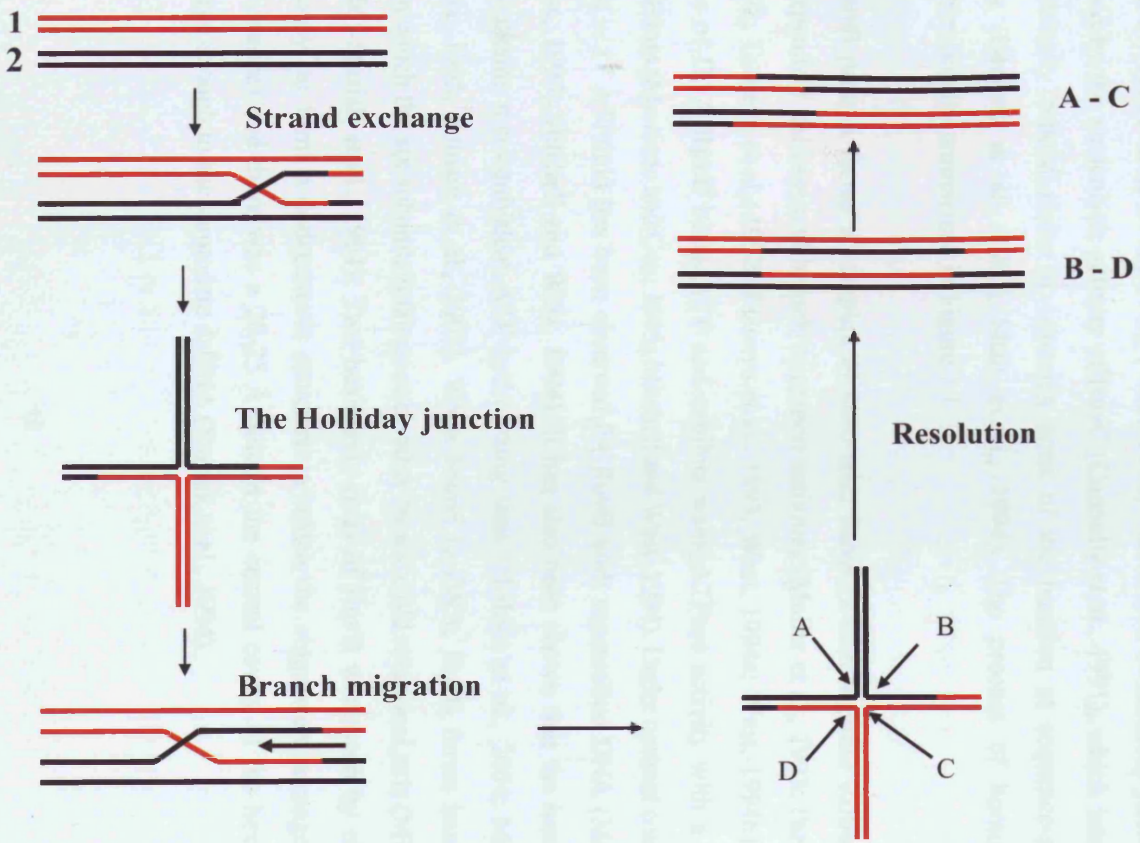

FIGURE 1.1 : The process of Homologous recombination

Two homologous segments of DNA undergo a strand exchange event, forming a heteroduplex intermediate known as the Holliday junction (Holliday.R. 1964). In prokaryotes RuvAB binds at the junction and translocates along the DNA to extend the region of heteroduplex DNA in a process known as branch migration. RuvC then loads onto the junction and cleaves it at specfic sequences to produce the 'splice' (A-C) or 'patch' recombination products (B-D) (reviewed in West.S.C 1997).

In prokaryotes, RuvA binds the Holliday junction with a high affinity (Iwasaki et al., 1992; Parsons et al., 1992) and opens it up into a square planar structure in which DNA is thought to be sandwiched between two RuvA tetramers (Parsons et al., 1995b; Rafferty et al., 1996; Yu et al., 1997). Two RuvB hexamers, which are orientated in opposite directions, encompass the DNA duplex on two arms of the junction, sandwiching the RuvA tetramers (Parsons et al., 1995a; Parsons et al., 1992; Stasiak et al., 1994). The RuvAB complex then drives branch migration of the junction (Iwasaki et al., 1992; Muller et al., 1993; Parsons et al., 1992; Parsons and West, 1993; Tsaneva et al., 1992) This process extends the region of heteroduplex DNA by the action of the RuvB hexameric rings, which act as molecular pumps rotating DNA and passing it through the central hole of each ring (West, 1996). Resolution of Holliday junctions is catalysed by the nucleolytic activity of RuvC (Connolly et al., 1991), which introduces symmetrically related nicks in opposing arms of the junction at sequence-specific regions (Bennett et al., 1993; Shah et al., 1994). The process of homologous recombination is summarized in Figure 1.1

The RuvB protein forms a complex *in vitro* with RuvA, which together exhibit both ATP dependent helicase and branch migration activities (Muller et al., 1993; Parsons et al., 1992; Tsaneva et al., 1992; Tsaneva et al., 1993; West, 1994a; West, 1994b). In the absence of DNA RuvB binds ATP and exhibits weak ATPase activity with a k_{cat} of ~ 5 ATP/min (Marrione and Cox, 1995; Mitchell and West, 1994). Under optimal conditions a k_{cat} of ~ 17 ATP/min has been observed for RuvB with supercoiled DNA (Marrione and Cox, 1995; Mitchell and West, 1994). It has also been shown that the hexameric RuvB contains non-equivalent ATP hydrolyzing sites (Hishida et al., 2004; Marrione and Cox, 1995; Putnam et al., 2001). When bound to DNA, RuvB forms hexameric rings, in which the six subunits relate to each other by a sixfold rotational axis (Miyata et al., 2000; Stasiak et al., 1994). Two hexameric rings of RuvB were seen by electron microscopy, to form a dodecameric structure in which the rings were arranged in a bipolar manner and there was a 20-25 Å hole in the central cavity of the hexameric ring, large enough to accommodate dsDNA (Stasiak et al., 1994).

Functional homologues of RuvA and RuvB are yet to be discovered in eukaryotes. However, two eukaryotic proteins, TIP48 and TIP49, share sequence homology with RuvB from different eubacteria species (Kanemaki et al., 1999; Kanemaki et al., 1997; Qin et al., 1994). On the basis of these sequence similarities and published data reporting DNA helicase activities of the two proteins (Kanemaki et al., 1999; Makino et al., 1999), we speculated at the beginning of the project that TIP48 and TIP49 may be potential DNA translocation or branch migration motors in eukaryotes, similar to RuvB.

1.2 The TIP48 and TIP49 proteins

Two highly conserved eukaryotic proteins, TIP48 and TIP49, with sequence homology to each other were discovered in different eukaryotic species by several groups (Bauer et al., 1998; Ikura et al., 2000; Kanemaki et al., 1999; Kanemaki et al., 1997; Kikuchi et al., 1999; Qiu et al., 1998; Shen et al., 2000; Wood et al., 2000). They are part of the super-family of proteins known as "**A**TPases **A**ssociated with different cellular **A**ctivities +" or AAA^+ proteins (Neuwald et al., 1999) and are believed to be most closely related to the bacterial RuvB protein (Kanemaki et al., 1999; Kanemaki et al., 1997; Putnam et al., 2001; Qiu et al., 1998), which is also part of the AAA^+ superfamily (Neuwald et al., 1999). The acronym TIP stands for both **T**BP **I**nteracting **P**rotein and **T**ransactivation domain **I**nteraction **P**rotein (Kanemaki et al., 1997; Wood et al., 2000) (see below).

Both proteins have acquired a plethora of names in the literature, some of which refer the proteins to be "RuvB-like" proteins. TIP49 is also known as Rvb1p or Tih1p in yeast (Jonsson et al., 2001; Lim et al., 2000; Shen et al., 2000) and in mammals as RUVBL1, TIP49a, NMP238, p50, Pontin52, ECP-54 and TAP54α (Bauer et al., 1998; Holzmann et al., 1998; Ikura et al., 2000; Kikuchi et al., 1999; Makino et al., 1999; Qiu et al., 1998; Salzer et al., 1999). TIP48 is also known as Rvb2p or Tih2p in yeast (Jonsson et al., 2001; Lim et al., 2000; Shen et al., 2000) and in mammals as RUVBL2, TIP49b, p47, Reptin52, ECP-51 TAP54β (Bauer et al., 2000; Gohshi et al., 1999; Ikura et al., 2000;

Kanemaki et al., 1999; Salzer et al., 1999). From here on, the human homologues will be referred to as TIP48 and TIP49. The homologues from different eukaryotic species will be indicated with abbreviations, as and when mentioned; yeast homologues from *Saccharomyces cerevisiae* (*sc*), *Schizosacchromyces pombe* (*sp*); or higher eukaryotes *Drosophila melanogaster* (d), *Caenorhabditis elegans* (*ce*), *Xenopus laevis* (x), Zebrafish (z), Mouse (m) or Rat (r); and an archaea species *Archaeoglobus fulgidus* (*Af*).

TIP49 was first discovered through interactions with the TATA-binding protein (TBP) (Kanemaki et al., 1997). It was then isolated by a yeast 2-hybrid system using the 14 kDa sub-unit of replication protein A (hsRPA3) as bait (Qiu et al., 1998). In addition, database searches revealed the presence of a TIP49 related protein in yeast and humans (Kanemaki et al., 1999; Qiu et al., 1998), namely TIP48. Since then a number of groups have found both TIP48 and TIP49 in various complexes from yeast to humans, such as; chromatin modifying complexes, transcription-activating complexes and small nucleolar ribonucleoprotein complexes (snoRNPs). Some of the transcription-activating proteins that TIP48 and TIP49 interact with have the potential to initiate cancer, and TIP49 has been shown directly to be an important cofactor for their activity (Dugan et al., 2002; Feng et al., 2003; Wood et al., 2000). The strong links to chromatin modifying complexes, their interaction with hsRPA, which is involved in DNA transactions during replication, repair and recombination (Baumann and West, 1998; Stillman, 1992), and a wider role in transcription and oncogenesis, all make TIP48 and TIP49 very important proteins to study. In the following sections a more detailed account of the relationship of TIP48 and TIP49 with other AAA^+ proteins, localization of the proteins in cells, interactions with other proteins and their participation in large complexes will be discussed.

1.3 Sequence homology of TIP48 and TIP49 to AAA$^+$ proteins

1.3.1 Conservation of TIP48 and TIP49 in different species

The cDNA of TIP49 encodes an open reading frame of 456 amino acids with a calculated molecular mass of approximately 50 kDa (Qiu et al., 1998). Database searches revealed the presence of TIP49 homologues in various eukaryotic organisms. The amino acid sequences of the rat and human TIP49 are almost identical, apart from Ile291 in the human TIP49 being replaced by a valine residue in rTIP49a (Kanemaki et al., 1997; Qiu et al., 1998). The mouse homologue is over 99 % identical to the human protein (Lim et al., 2000; Newman et al., 2000), while chicken and *S. cerevisiae* TIP49 proteins are 95 % and 70 % identical, respectively (Lim et al., 2000; Makino et al., 1999). These findings show that TIP49 proteins are highly conserved between distantly related eukaryotic species, suggesting an important biological role.

Examination of the amino acid sequence of TIP49 revealed that the protein contains Walker A and Walker B motifs. The Walker A (G4xGKT) and Walker B (4 hydrophobic-DExH) motifs are characteristic of proteins that bind and hydrolyze ATP (also known as P-loop ATPases/NTPases) and are present in a vast number of ATPase proteins (Koonin, 1993a; Koonin, 1993b; Patel and Latterich, 1998).

The cDNA of human TIP48 encodes an open reading frame of 463 amino acids and has a calculated molecular mass of 51 kDa (Kanemaki et al., 1999). It was shown to be highly conserved in other eukaryotes with over 99 % amino acid sequence identity to mouse and rat homologues (Lim et al., 2000; Newman et al., 2000) and 65 % identity to the *sc*TIP48 (Kanemaki et al., 1999; Lim et al., 2000). Like TIP49, TIP48 contains the Walker A and Walker B motifs. Both proteins are also found in the plant species *Arabidopsis thaliana* (Fritsch et al., 2004) and, as described in more detail below, one of the homologues is present in archaea (Makino et al., 1999; Newman et al., 2000). This suggests that both TIP48 and TIP49 have very important roles in the cell, as they are conserved across the three kingdoms of living organisms.

Although TIP48 and TIP49 form two distinct families of proteins, which show high conservation between family members, there is significant sequence similarity between the two proteins. The amino acid sequences of the two human proteins are 42 % identical and 68 % similar (Kanemaki et al., 1999). More detailed comparison showed that the homology was particularly high in the regions containing the Walker A and Walker B motifs, and a region between these two motifs (residues 179-195 of TIP48 and residues 177-197 of TIP49), which showed 69 % identity (Putnam et al., 2001),(Figure 1.2b). The significance of this highly homologous region is unknown, as it does not correspond to any regions found in other known AAA^+ proteins, including the bacterial RuvB protein. These findings demonstrate that although they form their own family of proteins, TIP48 and TIP49 are closely related, and probably diverged from a common ancestor early on in evolution; most likely at the time eukaryotes appeared.

In support of this idea, there is a single homologue of TIP48 and TIP49 in the archaea species *Archaeoglobus fulgidus*. This homologue first came up in database searches with TIP49 (Makino et al., 1999), but later on, when TIP48 was identified, it was shown that this archaeal homologue showed much more homology to TIP48 (Kanemaki et al., 1999). Comparisons of the regions containing the Walker A and Walker B motifs showed that the archaeal homologue was 51 % and 66 % identical with human TIP48, respectively. These identities were much higher than those shown with the human TIP49 protein (Kanemaki et al., 1999). As there is only one homologue of TIP48 and TIP49 in this ancient species, it is likely that it is the ancestor of TIP48, based on these sequence comparisons. Therefore, TIP49 probably arose later on during evolution, after duplication of the TIP48 gene.

FIGURE 1.2: RuvB crystal structure and sequence alignment with TIP48 and TIP49

(A) *T. maritima* RuvB crystal structure determined by (Putnam et al., 2001). The three RuvB structural domains are shown with an ADP molecule bound at the interface between the AAA^+ class ATPase domains I (blue) and II (gold). The winged-helix domain III (green) is also shown.

(B) Sequence alignment of *T. maritima* (TMA) RuvB, *E. coli* (ECO) RuvB, *H. sapiens* TIP49 (TIP49A), and *H. sapiens* TIP48 (TIP49B) proteins displayed with the *T. maritima* secondary structure assignment. Gaps in the sequence are displayed as dashes. Red residues are those conserved not only in the presented sequences, but also across an additional 15 different bacterial RuvB sequences. Red dots above the sequence represent strong and/or moderate dominant negative mutations isolated in the *E. coli* RuvB protein (Iwasaki et al., 2000). (This figure was taken from (Putnam et al., 2001)).

A

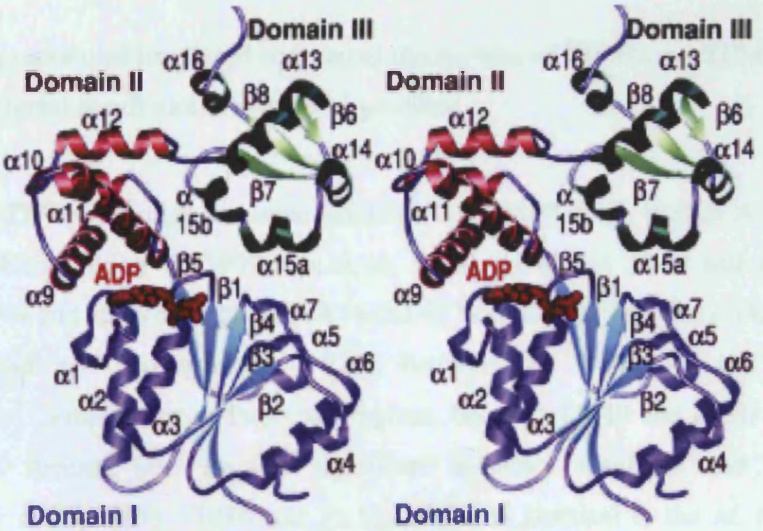
Domain III
Domain II
α16
α13
β8
β6
α12
α14
α10
α15b
β7
α11
ADP
β5
α15a
α9
β1
α7
β4
α5
β3
α6
α1
α2
β2
α3
α4
Domain I

B

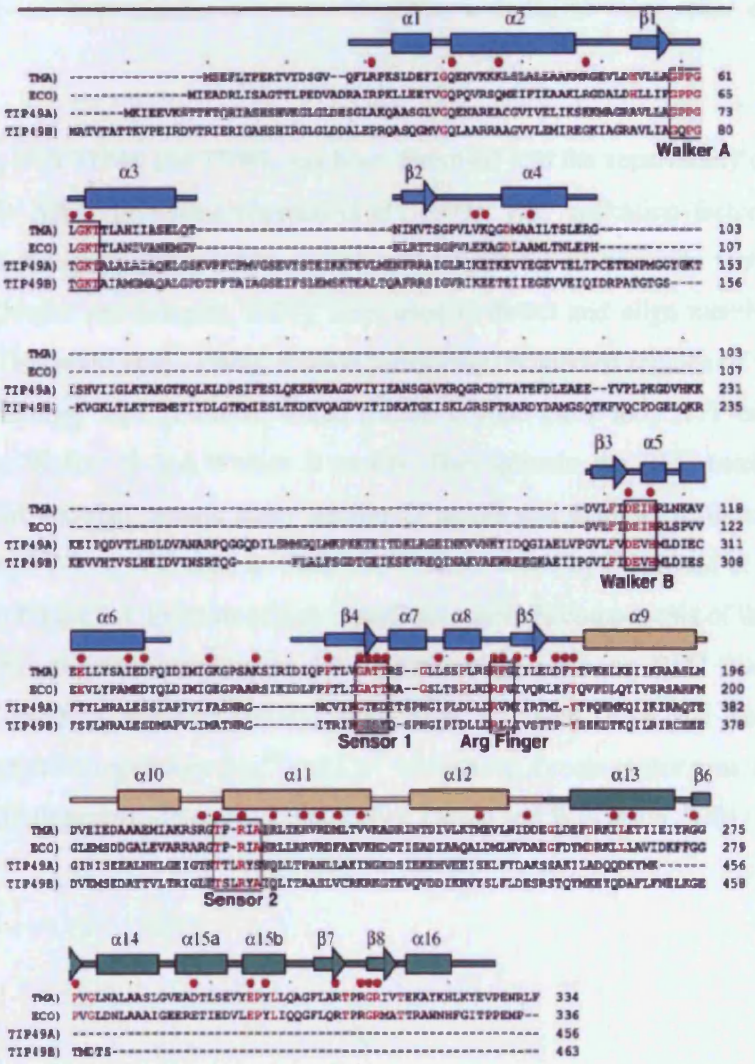
α1
α2
β1
Walker A
α3
β2
α4
β3
α5
Walker B
α6
β4
α7
α8
β5
α9
Sensor 1
Arg Finger
α10
α11
α12
α13
β6
Sensor 2
α14
α15a
α15b
β7
β8
α16

1.3.2 Sequence and predicted structural similarities of TIP48 and TIP49 to bacterial RuvB and other AAA^+ proteins

TIP48 and TIP49 have high sequence similarity with RuvB in the Walker A and Walker B motifs (Kanemaki et al., 1999; Qiu et al., 1998). TIP49 (aa 26-88 and aa 277-425) showed 38 % and 25 % identity, and 54 % and 46 % similarity with the *T. thermophilius* RuvB amino acid sequence (aa 1-226), between the Walker A and B motifs, respectively. Comparisons of these two regions, between TIP49 and RuvB from other eubacterial species, also showed significant sequence identities and similarities (Kanemaki et al., 1997). TIP48 was 31 % and 34 % identical to the *M. tuberculosis* RuvB amino acid sequence in the Walker A and Walker B motifs, respectively (Kanemaki et al., 1999), although the size of the regions compared was not stated. TIP48 is also likely to have similar sequence identities with RuvB from other eubacterial species.

RuvB, along with TIP48 and TIP49, has been classified into the superfamily of proteins known as the AAA^+ proteins (Neuwald et al., 1999). The replication factor C (RFC) proteins, which form a clamp-loader complex that loads the processivity factor PCNA, onto DNA (Majka and Burgers, 2004), were used to detect and align members of the AAA^+ class (Neuwald et al., 1999). Several previously undetected regions of significant sequence homology were revealed, which feature beyond the P-loop NTP-binding site including the Walker A and Walker B motifs. They contain the RFC boxes and the sensor 1 motif but also contain many additional motifs that distinguish them from the other classes of P-loop ATPases, as described in more detail by (Neuwald et al., 1999), and shown in Figure 7.1. Proteins in this superfamily include components of the Lon and Clp proteases; proteins involved in DNA replication, such as RFC clamp-loader proteins, MCM DNA licensing factors, SV40 large T antigen DnaA and RuvB; NtrC-related transcription regulators; Mg^{2+} and Co^{2+} chelatases; dynein motor proteins and the TIP48 and TIP49 proteins (Neuwald et al., 1999; Ogura and Wilkinson, 2001).

A subfamily within the AAA^+ superfamily is the AAA family of proteins (ATPases Associated with different cellular Activities), defined a few years earlier (Beyer, 1997). They share a common sequence feature, the AAA motif that contains the Walker A and Walker B motifs (Confalonieri and Duguet, 1995; Patel and Latterich, 1998), but are characterized by possessing a second region of homology (SRH) (Lupas and Martin, 2002; Neuwald et al., 1999; Ogura and Wilkinson, 2001; Patel and Latterich, 1998) (Figure 1.3). Members of this family include proteins involved in organelle biogenesis, such as N-ethylmaleimide-sensitive factor (NSF) and p97; some are metalloproteases, such as the FtsH protein; and others are part of the proteosome complex.

The crystal structure for some AAA^+ and AAA proteins have been solved (reviewed in (Lupas and Martin, 2002; Neuwald et al., 1999; Ogura and Wilkinson, 2001)) and have given an insight into their mechanism of action. Although the functions of AAA^+ proteins are diverse, many of these structures have common features. Therefore, the mechanisms of action employed by AAA^+ proteins are likely to be similar, as discussed by (Ogura and Wilkinson, 2001). Two atomic structures for RuvB have been solved, one from *Thermotoga martima* and the other from *Thermus thermophilus* (Putnam et al., 2001; Yamada et al., 2001). The crystal structure of *Thermotoga martima* RuvB, solved to 1.6 Å will be described below (Putnam et al., 2001) along with a predicted structural alignment of the TIP48 and TIP49 amino acid sequences that was also carried out by this group.

The RuvB monomer contains 3 domains forming a triangular shaped molecule (Figure 1.2a). The N-terminal domain 1 is an ATPase domain and makes up around half of the protein. It contains five β-strands, which form a parallel β-sheet, which is then surrounded by eight α-helices. Domain 2 is much smaller and is mainly α-helical, while the C terminal domain 3 is a mixture of α-helices and β-strands. Both domains 2 and 3 are packed against the C-terminal edges of the β-sheet of domain 1. All three domains are linked by extended loops, which were thought to allow movement between the domains (Putnam et al., 2001).

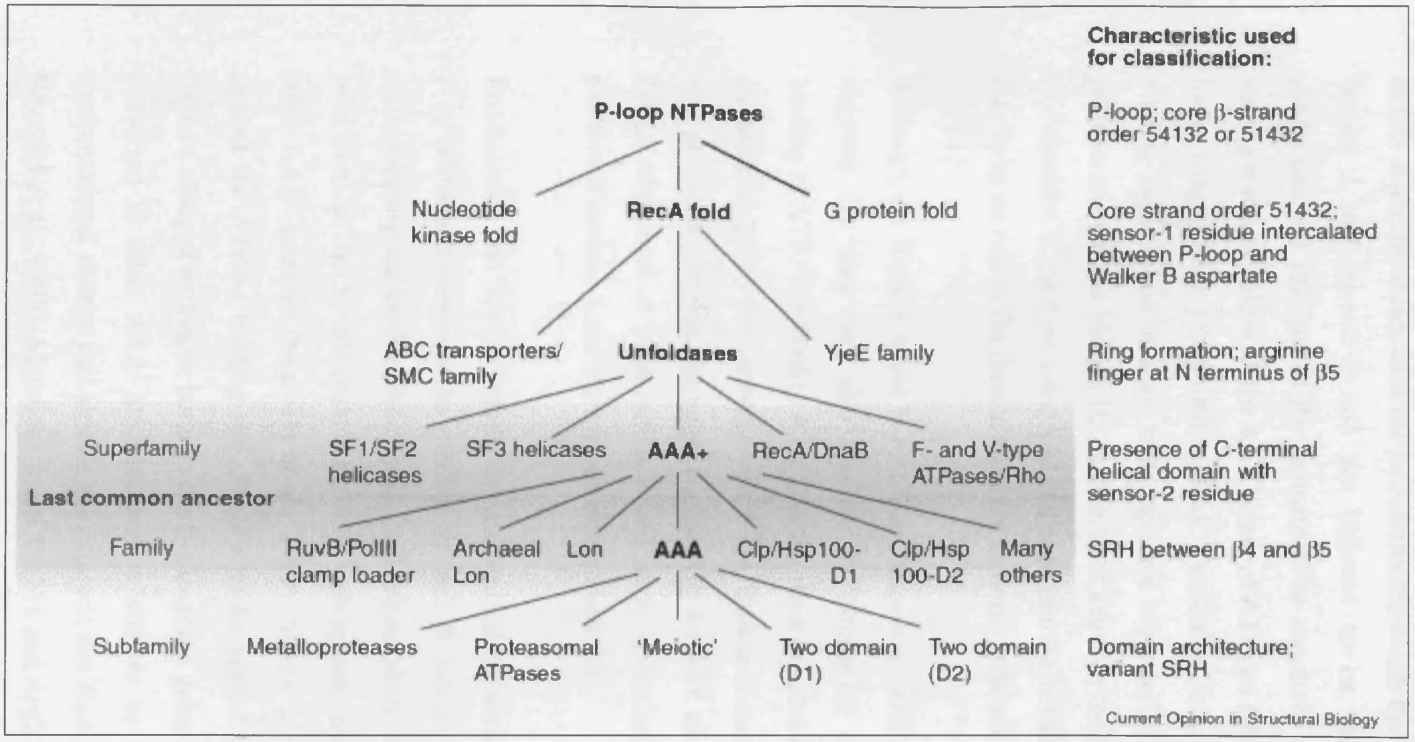

FIGURE 1.3: Phylogenetic classification of AAA domains within the P-loop NTPases
The criteria used for classification at each node are listed on the right. (This figure is taken from Lupas and Martin 2002)

An ADP molecule was shown to bind at the interface of domains 1 and 2. There are four motifs at the boundary of these two domains, which include the Walker A, Walker B, Sensor 1 and Sensor 2 and are believed to be important in nucleotide–driven conformational changes of the domains. The structures of domains 1 and 2 of RuvB share a common fold with the AAA^+ class of ATPases (Neuwald et al., 1999). Domain 3 has a winged-helix DNA-binding fold, a modified form of the helix-turn-helix DNA-binding motif found in many transcriptional regulators and non-specific DNA-binding proteins such as the histone H5. A dominant negative mutation in *E. coli* RuvB suggests that domains 1 and 2 are preserved and pack into the hexamer, while domain 3 is not and may have no role in the formation of the hexamer structure (Iwasaki et al., 2000).

Although the Walker A and B motifs are known to drive ATP hydrolysis, the structure suggests that they may also function in introducing conformational changes upon binding of ATP. The Walker A motif is involved in coordinating ATP and presenting the γ-phosphate group for cleavage, while the Walker B motif coordinates divalent metal ions and could activate the water nucleophile for ATP cleavage (Ogura and Wilkinson, 2001). Alignment of these motifs would result in conformational changes, altering the position of domain 3 and the subunit-subunit interface.

The Sensor 1 and Sensor 2 motifs are also critical for sensing nucleotide binding. Sensor 1 is positioned between the Walker A and B motifs and is likely to function in distinguishing nucleotide diphosphate and triphosphate states, by forming a hydrogen bond from its Thr158 side chain to the ATP γ-phosphate group. This residue is conserved in other AAA^+ proteins (Neuwald et al., 1999). Sensor 2, in domain 2 is found packed against the ATPase binding site. Pro216 packs against the adenine face and Arg217 forms a charged hydrogen bond to the β-phosphate group. This arginine residue is also conserved in other AAA^+ proteins and is seen to be important, as it may induce conformational change that shields the catalytic site from water (Guenther et al., 1997; Neuwald et al., 1999). Mutations in the Pro216 and Arg217 residues affect the ATPase activity of the protein (Putnam et al., 2001). Both residues interact with components that

are present in ADP and ATP. Therefore, the role of this motif is probably to distinguish between nucleotide-bound and unbound states, as well as constraining the ATP-bound conformational state, so that non-productive binding is prevented.

The RuvB monomer can exist in three states: ATP-bound, ADP-bound and empty (Putnam et al., 2001). The Walker A and B motifs, along with Sensor 1, respond to the ATP bound, with the interaction of the γ-phosphate group and divalent cation. This ATP-bound state most likely exists in a strained conformation (Putnam et al., 2001). Sensor 2 recognizes ADP by interaction with the sugar and diphosphate as well as hydrophobic collapse around the adenine ring. The different conformational states of the domains provide the chemomechanical force that drives branch migration. The molecular interfaces of the RuvB dimers in the crystal structure, show that the hexameric structure formed could be similar to those observed in the Hs1U and NSF-D2 hexameric AAA $^{+}$ class ATPases (Bochtler et al., 2000; Lenzen et al., 1998; Yu et al., 1998). The RuvB domain I was superimposed onto the HsIU conserved domain. This superimposition resulted in a polar RuvB hexamer that satisfies known constraints and dimensions observed by electron microscopy (Stasiak et al., 1994).

The subunit interface made up of domains 1 and 2 is hydrophilic and complementary in shape, which most likely allows domain 1 to bind within the cleft formed by domains 1 and 2 of the adjacent subunit. This could affect subunit-subunit interactions by shifting the positions of the subunit during the reaction cycle. Although it is known that RuvB is functional as a hexamer (Marrione and Cox, 1995; Mitchell and West, 1994), the ADP-bound RuvB in the crystal structure assembles into a helix with six subunits per turn, rather than a ring. This indicated that the asymmetry, which occurs in the RuvB, arises due to assembly, and not all the subunits can exist in an ADP form. This type of asymmetry has been seen in other hexameric helicases such as the T7gp4 protein (Singleton et al., 2000).

There is a strictly conserved arginine that follows the Walker A and B motifs in AAA^{+} class ATPases (Ogura and Wilkinson, 2001). Mutation of the Arg170 residue in *T. martima* RuvB caused deficiency in the ATPase activity of the protein, even when

bound to DNA (Putnam et al., 2001). Similar results were shown with mutants of the *E. coli* FtSH ATPase-dependent protease and *E. coli* RuvB (Iwasaki et al., 2000). The hexameric assembly of RuvB suggests that the arginine residue approaches the phosphate group and functions to regulate hydrolysis of ATP. The ATP binding in one subunit may drive ATP hydrolysis in the adjacent molecule, providing the mechanism by which ATP is both substrate and allosteric effector (Marrione and Cox, 1995; Marrione and Cox, 1996).

Figure 1.2b shows a sequence alignment of the *T. martima* RuvB amino acid sequence with the human TIP48, TIP49 and *E. coli* RuvB sequences. The secondary structure assignment of the *T. maritima* RuvB amino acid sequence is also shown above the alignment (Putnam et al., 2001). It can be seen that the TIP48 and TIP49 proteins share significant predicted structural homology with domains 1 and 2 from the *T. martima* RuvB structure. However, TIP48 and TIP49 contain insertions of approximately 190 amino acids between the two homologous regions of RuvB; the first containing the Walker A motif; and the second, the Walker B motif, Sensor 1, Sensor 2 and the arginine finger (Figure 1.2b).

It has been suggested that RuvB is structurally similar to the subunits of clamp-loader complexes (Guenther et al., 1997), which also contain insertions of different sizes between the regions containing the Walker A and B motifs. The crystal structure of *T. martima* RuvB rationalizes these insertions and deletions found in the eukaryotic and archaeal TIP48/TIP49 proteins. TIP48 and TIP49 lack domain 3 of RuvB (Figure 1.2a and 1.2b). However, the insert between α3 and β3 of the RuvB structure, which is unique to the TIP48/49 proteins, could be positioned where domain 3 sits in RuvB, at the C-terminal face of the domain 1 β-sheet. Therefore, it is speculated that this insertion could function similarly to the RuvB domain 3 for DNA binding activities, or interactions with other proteins.

1.4 Cell and tissue distribution of TIP48 and TIP49

Deletion of either *TIP48* or *TIP49* genes in *S. cerevisiae* showed that both proteins are essential in yeast and encode non-redundant functions (Kanemaki et al., 1999; Lim et al., 2000; Qiu et al., 1998). Similarly, deletion of either *dTIP48* or *dTIP49* in *Drosophila* was lethal (Bauer et al., 2000). Further experiments by the same group showed that both genes encode proteins with non-redundant functions during early development of *Drosophila*. Due to these findings, similar important functions are likely to exist in humans.

The tissue distribution of both proteins demonstrated that they are ubiquitously expressed (Kanemaki et al., 1999; Makino et al., 1999). Western blot analysis revealed that TIP49 is moderately expressed in the spleen, thymus and the lungs, and abundantly in the testes (Makino et al., 1999). The protein was expressed mainly in the germ line cells from late pachytene spermatocytes to round spermatides, indicating that this protein could be involved in recombination. The distribution of TIP48 in rat tissues was found to be similar, with high expression in the testes and thymus (Kanemaki et al., 1999). The distribution pattern of these two proteins was compared, and stated to be similar to that of the recombination protein RAD51 (Kanemaki et al., 1999; Makino et al., 1998). Other studies have shown by both RT-PCR and northern blot analysis that TIP48 and TIP49 mRNA is expressed in a large array of tissues (Parfait et al., 2000; Salzer et al., 1999). Several *in situ* hybridizations of *Drosophila* and *Xenopus* embryos showed that *TIP48* and *TIP49* have similar embryonic transcription patterns (Bauer et al., 2000; Etard et al., 2000).

Fluorescence *in situ* hybridization analysis demonstrated that *TIP49* is located on chromosome 3 in band q21 (3q21) (Qiu et al., 1998). This is a region, which has frequent rearrangements in different types of leukemia and solid tumors (Rynditch et al., 1997), but it is unknown whether *TIP49* is close to rearrangement breakpoints. The *TIP48* gene was identified at the 19q13.3 chromosomal region (Parfait et al., 2000), which is frequently amplified in breast cancer (Parfait et al., 2000). *TIP48* gene

expression was quantified by measuring mRNA in a series of breast tumors and compared to the endogenous levels in six normal human breast tissues (Parfait et al., 2000). None of the tumor samples showed increase in *TIP48* expression at the transcription level, therefore not demonstrating any type of contribution in cancerous cells.

Immunofluoresence microscopy using anti-TIP49 antibodies showed a dot-shaped nuclear staining pattern, which suggested that TIP49 was included in a macromolecular structure in the nucleus (Bauer et al., 1998; Makino et al., 1998). Two-dimensional SDS gel electrophoresis of nuclear matrix proteins revealed that TIP49 was a ubiquitously occurring nuclear matrix protein found in both normal and cancer tissues and cells (Holzmann et al., 1998). In addition, TIP49 also contains nuclear localization signals (Holzmann et al., 1998). Both mTIP48 and mTIP49 were found predominantly in the nucleoplasm, with little indication that either was present in the nucleolus (King et al., 2001; Newman et al., 2000). *sc*TIP48 was primarily localized in the nucleus and specifically in the nucleoplasm (King et al., 2001; Lim et al., 2000).

TIP48 and TIP49 have been found in large nuclear complexes *in vivo* (Kanemaki et al., 1999). Immunoprecipitation experiments were carried out using mouse polyclonal anti-TIP49 antibody and TIP48 in the immunoprecipitates was detected using anti-TIP48 antibody. TIP49 was detected using anti-TIP49 antibody from immunoprecipitates prepared with anti-TIP48 antibody. These experiments showed that both proteins were included in the same complex. HeLa cell nuclear extracts were also fractionated by size exclusion chromatography, and the presence of TIP48 and TIP49 was analyzed (Kanemaki et al., 1999). TIP48 and TIP49 co-eluted in fractions with molecular masses between 2000-500 kDa and also co-eluted in fractions with molecular masses between 800-600 kDa fractions. These results indicated that both proteins exist together in large nuclear complexes.

Although both proteins seem to be predominantly nuclear, cytoplasmic localization of TIP49 was observed by immunoblotting cytosol preparations (Holzmann et al., 1998). It

was also shown by confocal microscopy that TIP49 was present both within the nucleus and cytoplasm of U937 cells (Gartner et al., 2003). Both TIP48 and TIP49 were isolated from human erythrocyte cytosol by affinity chromatography, using a peptide of an integral membrane protein, stomatin (Salzer et al., 1999). TIP49 was shown to interact with profibrinolytic plasminogen on the cell surface of U937 cells (Hawley et al., 2001). TIP49 was also shown to act as an auto-antigen in the sera of some patients with autoimmune diseases such as polymyositis/dermatisis and hepatitis (Makino et al., 1998). These results indicate there may be mechanisms for the localization of TIP48 and TIP49 to the cytoplasm and TIP49 to the cell surface.

TIP49 was recently shown to interact with tubulin, both *in vitro* and *in vivo,* and to co-localize with tubulin during mitosis (Gartner et al., 2003). Confocal immunofluoresence microscopy revealed that during prophase and prometaphase, TIP49 localized at the centrosome and branching microtubule spindles. At metaphase TIP49 accumulated at the centrosome and sites of tubulin polymerization. The topology of the protein at the nuclear spindle changed as cells passed from metaphase to anaphase and subsequently to telophase. At anaphase it was concentrated at the zone of tubule interdigitation and when the cells progressed to telophase, TIP49 was found at the polar tubule overlap. At cytokinesis, however, it reappeared at the site of chromosome decondensation within the daughter cells. Therefore the association of TIP49 with tubulin was dependent on progression through cell division.

Although TIP48 and TIP49 can be detected in the cytoplasm, which indicates that they may have functions there, TIP48 and TIP49 localize mainly in the nucleus. Therefore, the majority of their activities are likely to be in the nucleus. Hence, participation of TIP48 and TIP49 in large nuclear complexes and interactions with specific nuclear factors will be described in the next three sections, to gain a better understanding of their functions *in vivo*.

1.5 Association of TIP48 and TIP49 with chromatin modifying complexes from yeast and mammals

Very little is understood about the function of the TIP48 and TIP49 proteins individually, however, it is hypothesized that together these two proteins play an active role in chromatin modifying complexes in both yeast and mammals (Jonsson et al., 2004). By examining the function and roles of these complexes we may begin to understand the functions of TIP48 and TIP49. Previous studies have elucidated that TIP48 and TIP49 are part of complexes, which display chromatin remodeling, histone exchange or histone acetylase activities (Fuchs et al., 2001; Ikura et al., 2000; Kobor et al., 2004; Krogan et al., 2003; Kusch et al., 2004; Shen et al., 2000) (Figure 1.4). Recent studies have shown that, as well as being required for the transcription of a certain number of genes (Ebbert et al., 1999; Galarneau et al., 2000; Kobor et al., 2004; Krogan et al., 2003), these chromatin modifying complexes are also involved in DNA damage repair (Downs et al., 2004; Kusch et al., 2004; Morrison et al., 2004; van Attikum et al., 2004). In the absence of TIP48 and TIP49 some of these complexes are inactive, indicating an important role for the two proteins in chromatin modification (Jonsson et al., 2004).

Although TIP48 and TIP49 are essential in *S. cerevisiae,* the catalytic subunits of some of these complexes are not (Krogan et al., 2003; Shen et al., 2000). Therefore, the activities of TIP48 and TIP49 that make them essential are not likely to be associated with one single complex. They obviously play an important role as part of several complexes, which affect many other pathways in the cell, such as transcription and DNA damage repair. Below is an account of three complexes (*sc*INO80, TIP60 and P400/scSWR1) that TIP48 and TIP49, or their homologues in other species, are part of. Although we are interested in the function of the human proteins, studies on the yeast complexes will be discussed, as more information on the function of these complexes has been obtained and can be used as a model for the function of the human chromatin modifying complexes.

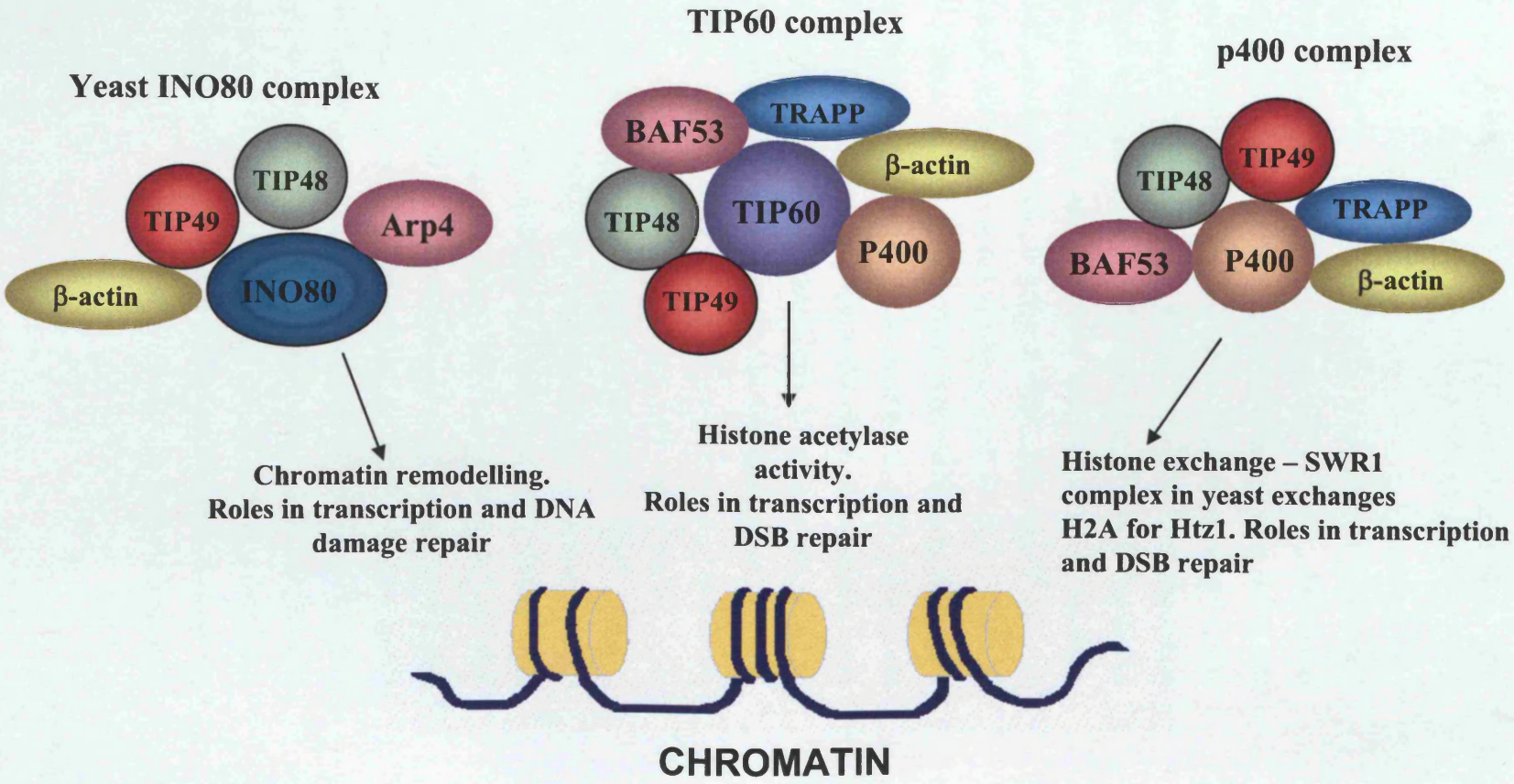
Yeast INO80 complex
TIP48
TIP49
Arp4
β-actin
INO80
Chromatin remodelling.
Roles in transcription and DNA
damage repair
TIP60 complex
BAF53
TRAPP
β-actin
TIP48
TIP60
P400
TIP49
Histone acetylase
activity.
Roles in transcription and
DSB repair
p400 complex
TIP48
TIP49
TRAPP
BAF53
P400
β-actin
Histone exchange – SWR1
complex in yeast exchanges
H2A for Htz1. Roles in transcription
and DSB repair
CHROMATIN

FIGURE 1.4: Chromatin modifying complexes that contain TIP48 and TIP49

The three main chromatin modifying complexes, which contain TIP48 and TIP49 or their homologues in *S.cerevisiae,* are illustrated (Ikura et al., 2000; Kobor et al., 2004; Krogan et al., 2003; Shen et al., 2000). The catalytic subunits of these complexes, namely Ino80p, TIP60 and p400 are shown in the centre of each complex. Other subunits that are common to these complexes are also shown.

1.5.1 Yeast INO80 complex

a) Chromatin remodeling activities

The primary unit of chromatin is the nucleosome, which has ~146 bp of DNA wrapped around the histone protein core; an octamer, comprised of a pair of each of the core histone proteins H2A, H2B, H3 and H4. Arrays of nucleosomes form a further higher-order of chromatin structure. Chromatin allows compact storage of DNA in the nucleus and additionally restricts access of nuclear proteins to DNA. There are mechanisms that regulate chromatin structure, which allow subsequent processes that require protein-DNA interactions. Chromatin remodeling is one of these mechanisms that regulate some of these processes, such as transcription (Peterson, 1996). One complex from yeast that has been studied extensively is the SWI/SNF ATP-dependent chromatin-remodeling complex (Tsukiyama et al., 1999). Several other complexes have also been identified, which all contain a putative ATPase subunit that belongs to the SWI2/SNF2 superfamily of proteins. Among these is the Ino80 protein (Ino80p) which derived its name from its activity in inositol biosynthesis (Ebbert et al., 1999; Shen et al., 2000). The Ino80p is part of a larger chromatin remodeling complex, the INO80 complex, which includes both *sc*TIP48 and *sc*TIP49, as described below. A similar complex has not been isolated from mammals, however the data presented below will give an idea of the role of TIP48 and TIP49 in a large chromatin remodeling complex.

To study Ino80p biochemically, a double-FLAG tag was inserted at the C-terminus of the *INO80* chromosomal gene by homologous recombination (Shen et al., 2000). A complex of proteins associated with Ino80p, termed the INO80 complex, was immunoprecipitated with anti-FLAG agarose. The complex was shown to contain 12 polypeptides, most of which were present in equal amounts. A number of these proteins were identified by mass spectrometry. The proteins β-actin and three actin-related proteins Arp4, Arp5 and Arp8 (Poch and Winsor, 1997) were associated with the complex along with Ino80p. *sc*TIP48 and *sc*TIP49 were also identified as part of the INO80 chromatin-remodeling complex.

A specific interaction was seen between Ino80p and *sc*TIP48, after immunoprecipitating *sc*TIP48, which suggested that *sc*TIP48 was a true component of the complex, most likely along with *sc*TIP49. Immunoprecipitation of *sc*TIP48 showed that 11 out of the 12 proteins of the complex co-purified with *sc*TIP48, and the twelfth polypeptide, Arp4, may have been obscured by the TIP48-Flag protein band (Shen et al., 2000). Glycerol gradient centrifugation also showed that the 12 proteins sediment together. Interestingly, a number of other polypeptides co-purified with the *sc*TIP48 protein that are not part of the INO80 complex, which widens the roles of *sc*TIP48, and may explain why *scTIP48* mutants are lethal and *ino80* mutants are not (Ebbert et al., 1999; Kanemaki et al., 1999).

Analysis of the protein bands of *sc*TIP48, *sc*TIP49 and actin in the INO80 complex, using densitometry, showed that the molar ratios of *sc*TIP49 to sc*TIP48 to actin were: 6.5 and 5.6 to 1, respectively (silver stain) and 6.3 and 6.7 to 1, respectively (Coomassie stain). This shows an approximate 6:1 stoichiometry of *sc*TIP48 and *sc*TIP49 compared to the other proteins in the complex, which corresponds well to the hexameric structure observed with other AAA^+ proteins (Ogura and Wilkinson, 2001).

The INO80 complex showed high intrinsic ATPase activity, which was mainly ascribed to Ino80p, as a yeast strain carrying a mutation in the ATP-binding site (K737A) showed significantly reduced activity (Shen et al., 2000). It is thought that the rest of the ATPase activity (~ 5 %) was contributed to by the other subunits. The ATPase activity was stimulated in the presence of DNA or nucleosomes. This showed that, like SWI/SNF and the RSC chromatin remodeling complexes, the INO80 complex displays DNA-dependent ATPase activity. The complex also displayed helicase activity as it was able to displace a primer annealed to single-stranded ϕX174 DNA (Shen et al., 2000). The polarity of the helicase activity was found to be 3' to 5'. The Ino80p K737A mutant did not show DNA helicase activity, demonstrating that the Ino80p is the catalytic subunit of the complex. The complex was also shown to directly bind free DNA, in an ATP independent manner (Shen et al., 2003) and mobilize nucleosomes in an ATP-dependent manner (Jonsson et al., 2001; Jonsson et al., 2004; Shen et al., 2003). Catalytically active Ino80p was required for these activities (Jonsson et al., 2001; Jonsson et al., 2004; Shen

et al., 2003). As well as requiring Ino80p, the complex also depended on the presence of the actin-related proteins Arp5 and Arp8 for its ATPase, DNA binding and nucleosome mobilization activities (Shen et al., 2003).

Although the INO80 complex was characterized *in vitro*, as described above, it was not shown until only recently, that *sc*TIP48 and *sc*TIP49 are both required for the chromatin remodeling activity of the INO80 complex (Jonsson et al., 2004). Strains were obtained, which expressed a FLAG-tagged Ino80p; with or without *sc*TIP48 that was fused to a temperature-degradable fusion tag (*sc*TIP48-td); and a heat-inducible Myc-UBR1 tag, to aid degradation when the temperature was shifted to 38 °C. Complexes obtained from wild-type cells showed robust ATP-dependent chromatin remodeling activity, while complexes, obtained from the degron strain, which had been depleted of *sc*TIP48-td, were completely inactive. The complex obtained from the degron strain lacked *sc*TIP49, although it was abundant in the cell, which suggests that both *sc*TIP48 and *sc*TIP49 are needed for the chromatin remodeling activity of the INO80 complex and have to come together before incorporating into the INO80 complex. In addition, the Ino80p was shown to be essential for the chromatin remodeling activity of the complex and therefore likely to be the catalytic subunit (Jonsson et al., 2004).

Further experiments in the same study showed that *sc*TIP48 and *sc*TIP49 were required for the correct assembly of the INO80 complex, as the Arp5 subunit was absent in the complex obtained from the *sc*TIP48-td strain (Jonsson et al., 2004). A recombinant *sc*TIP48/TIP49 binary complex, purified from insect cells, exhibited no chromatin remodeling activity. When this complex was added to the INO80 mutant complex, it failed to restore chromatin remodeling activity, indicating that Arp5 was required for the activity of the complex, as shown previously (Shen et al., 2003). A functional complex was, however, reconstituted *in vivo*, using wild-type and an ATP hydrolysis-defective mutant of *sc*TIP48 (E297G). The INO80 complex also displayed chromatin remodeling activity in the presence of *sc*TIP48E297G, indicating ATP hydrolysis by *sc*TIP48 was not required for chromatin remodeling by the INO80 complex. This study showed that

rather than having activities on DNA, *sc*TIP48 and *sc*TIP49 were actually required for the assembly of the INO80 complex, so that it could function correctly.

b) Links to transcription

It has been shown that the INO80 complex is required for the transcription of a number of genes (Ebbert et al., 1999; Shen et al., 2000; Steger et al., 2003). *sc*TIP48 and *sc*TIP49 are also required for the transcription of a number of genes (Jonsson et al., 2001; Ohdate et al., 2003), as will be described in section 1.6. Therefore, it is likely that the effect of *sc*TIP48 and *sc*TIP49 on promoters is directly through the INO80 complex.

Cells lacking *ino80* showed a reduced transcription in a number of reporter constructs (Ebbert et al., 1999). RNA levels for endogenous *INO1*, *PHO5* and *Ty1* genes decreased in the absence of Ino80p, while the RNA levels of other genes such as *INO2*, *PHO8* and *ACT1* were unaffected (Shen et al., 2000; Steger et al., 2003). It was also shown that when the Arp5 and Arp8 components of the INO80 complex were not present, there was a reduced transcription of the *INO1* gene, which demonstrated that the whole complex is required for the regulation of certain genes (Shen et al., 2003).

The effect of the INO80 complex on promoters was studied after depleting Ino80p and *sc*TIP48 from cells (Jonsson et al., 2004). It was first shown that the removal of either slowed down the growth of yeast. Then pairwise comparisons of the mRNA levels were carried out between the Ino80p-td, *sc*TIP48-td and wild-type cells. Out of 5602 genes examined, 150 showed a 2-fold change in mRNA level when Ino80 was removed, and 503 genes showed a 2-fold change when *sc*TIP48 was removed. In both cases, almost an equal number of genes were up-regulated verses down-regulated. There was also a significant overlap of genes regulated by *sc*TIP48 and Ino80p and a strong positive correlation in the direction and magnitude of change in gene expression.

A separate study compared the changes in transcription of a small number of genes in a temperature sensitive *sc*TIP48 mutant strain (*tih2-ts160*) and *ino80* null cells (Ohdate et

al., 2003). It was observed that all the genes, which decreased in expression in the *tih2-ts160* mutant, also decreased in the *ino80* null cells. However, some of the genes that showed increased expression in the *tih2-ts160* mutant did not increase in the *ino80* null cell, confirming that *sc*TIP48 and Ino80 target genes overlap, but are not identical. Hence, *sc*TIP48 (and *sc*TIP49) are likely to regulate promoters via other chromatin modifying complexes too, as discussed later.

Ino80p and *sc*TIP48 are required for the regulation of two phosphate-regulated genes *PHO5* and *PHO84* (Jonsson et al., 2004). It was shown that the induction of *PHO5* and *PHO84* was impaired in a phosphate-depleted medium, when Ino80p was deleted. A similar effect was seen when *sc*TIP48 was depleted from the cell, showing that both Ino80p and *sc*TIP48 are required for the regulation of *PHO5* and *PHO84* promoters. *sc*TIP48 and *sc*TIP49 could not be detected on these promoters, whereas Ino80p and TBP clearly associated with the promoters. It was also shown that the association of Ino80p on *PHO84* was not affected in the absence of *sc*TIP48, whereas there was a decrease of Ino80p on the *PHO5* promoter in the absence of *sc*TIP48, indicating differing functions of *sc*TIP48 for different promoters.

c) Links to DNA repair

As well as being involved in transcription regulation, the INO80 complex has been implicated in DNA damage repair (Shen et al., 2000; Shen et al., 2003; van Attikum et al., 2004). This finding is quite important as it has been speculated that *sc*TIP48 and *sc*TIP49 may be functioning as 'RuvB-like' helicases and branch migration motors to repair DSBs *in vivo* (Cairns, 2004). However, the exact role of *sc*TIP48 and *sc*TIP49 in this pathway has not yet been determined, so it is unknown whether they are involved directly in repairing DSBs. Nevertheless, as both *sc*TIP48 and *sc*TIP49 are important for the function of the INO80 complex, the role of the complex in this process will be described below.

The *ino80* null mutant was shown to be sensitive to hydroxyurea (HU) and the alkylating agent MMS, (Shen et al., 2000), both of which affect DNA metabolism, and MMS is known to cause single- and DSBs. The mutant was also sensitive to UV light and ionizing radiation, the latter introducing DSBs directly. The *arp5Δ* and *arp8Δ* mutants were shown to mimic the *ino80Δ* phenotype as they were hypersensitive to growth in the presence of hydroxyurea and MMS (Shen et al., 2003; van Attikum et al., 2004). It was also shown that in the plant species *Arabidopsis thaliana*, the Ino80p homologue controls homologous recombination (Fritsch et al., 2004). These experiments showed the involvement of the INO80 complex in the repair of DSBs.

The sensitivity, of the *arp5Δ* and *arp8Δ* to DNA-damaging agents was not caused by checkpoint inactivation (Morrison et al., 2004; van Attikum et al., 2004), as the phosphorylation of a central checkpoint kinase, Rad53, which depends on the activity of the ATR-like kinase Mec1, still occurred (van Attikum et al., 2004). It was also shown that other downstream targets of Mec1, the ribonucleotide reductase genes *RNR1* and *RNR2* were induced in *ino80* null cells after treatment with HU, and the cells showed normal cell cycle arrest in presence of HU (Morrison et al., 2004).

INO80 did not appear to affect repair indirectly by regulating gene expression (Morrison et al., 2004; van Attikum et al., 2004). No genes that are implicated in DNA repair or checkpoint response were repressed in *ino80* or *arp8* mutants (van Attikum et al., 2004). To be sure that the effects of INO80 on DNA repair were not due to indirect effects through the transcription of genes, 702 genes were focused on, which are relevant for repair, DNA processing or cell cycle regulation (van Attikum et al., 2004). Fifteen of these genes were shown to be mis-regulated in the *ino80* strain. Out of these, three were also mis-regulated in *arp8* cells. One of these genes was DNA ligase 4, which is involved specifically in another DSB repair pathway, known as non-homologous end joining (NHEJ), which is distinct from homologous recombination. Both *arp5* and *arp8* strains were also shown to be compromised for NHEJ. This showed that out of all the genes studied that are involved in DNA repair or damage response, this was the only one

that was potentially affected by the INO80 complex, at the transcription level. It was therefore concluded that INO80 was involved in DNA repair directly.

Ino80p, Arp5 and Arp8 were shown to bind near sites of DNA damage, which provides evidence that the IN080 complex has a more direct role in DNA repair (Morrison et al., 2004; van Attikum et al., 2004). The presence of the INO80 complex was assessed at HO endonuclease induced DSBs and all three proteins were shown to be recruited near the HO-induced DSBs. The recruitment was similar to that of many proteins involved in DSB repair, by both homologous recombination and NHEJ, such as Rad51, Rad52, Rad54, Rad55 and Yku80 (Morrison et al., 2004).

In higher eukaryotes an early event in response to DNA damage is the phosphorylation of the histone variant of H2A, H2AX, at sites close to DSBs (Redon et al., 2002). The phosphorylated H2AX, known as γ-H2AX, forms foci that are required for the onset of DNA repair. In yeast there is no H2A variant, but H2A is transcribed from two genes *HTA1* and *HTA2*, which both carry the target serine 129, found four residues away from the carboxyl terminus, similar to the mammalian H2AX. In response to DNA damage this residue also becomes phosphorylated by ATM- and ATR- related kinases (Downs et al., 2000). The INO80 complex was shown to directly interact with γ-H2AX. There was no recruitment of the complex to damaged DNA in strains that had both HTA loci mutated at the serine 129 (van Attikum et al., 2004). Moreover, it was shown that when the Mec1 and Tel1 kinases, which induce the formation of γ-H2AX were deleted from cells, INO80 recruitment was significantly reduced (Morrison et al., 2004). The SWI/SNF chromatin remodelling complex failed to interact with γ-H2AX but the SWR1 complex, which contains the Swr1 ATPase and is related to Ino80, also interacted with γ-H2AX, but much more weakly (Morrison et al., 2004).

By creating a series of strains, mutated for particular subunits of the INO80 complex, it was shown that Arp4 and Arp8 were not required for the interaction of INO80 with γ-H2AX (Morrison et al., 2004), even though both subunits have been shown to interact with histones (Harata et al., 1999; Shen et al., 2003). However, the association of the

INO80 complex with γ-H2AX was significantly reduced in the absence of Nhp10 (Morrison et al., 2004). Nhp10 is a HMG-like protein which can potentially bind DNA with particular structures (i.e. Holliday junctions) and is not present in the Swr1 complex or any other known chromatin remodelling complexes. Therefore, this signifies a unique role for Nhp10 in specifying the interaction between γ-H2AX and the INO80 complex.

1.5.2 The TIP60 and p400 complexes

a) Composition of TIP60 and p400 complexes

The human Tip60 protein (Tip60p) was first isolated as an HIV-1-Tat-interacting protein (Kamine et al., 1996) and was shown to be a histone acetyltransferase (Yamamoto and Horikoshi, 1997) The *S. cerevisiae* homologue, known as Esa1, is an essential histone acetyltransferase (Clarke et al., 1999; Smith et al., 1998) and is part of the NuA4 histone acetyltransferase complex (Allard et al., 1999). A similar complex was isolated from human cells and was termed the TIP60 complex (Ikura et al., 2000) or the human NuA4 complex (Doyon et al., 2004).

S. cerevisiae NuA4 contains 12 subunits, most of which have been identified, and 10 out of 12 have clear homologues in higher eukaryotes. Included among the subunits are Esa1p; Tra1p, an essential ATM related protein; Epl1, the homologue of Drosophila E(P)c (*enhancer of polycomb*) protein, which is a suppressor of position effect variegation; actin; and the actin-related protein Arp4, which is also part of the INO80 complex (see above). The purified human TIP60 complex (Doyon et al., 2004; Ikura et al., 2000) has 11 subunits that have homologues in the yeast NuA4 complex. Some of these include; the TRRAP protein, the homologue of Tra1; the E(P)c homologue; β-actin; and the actin-related protein BAF53, which is the homologue of Arp4. The TIP60 complex contains additional subunits, which are not found in the yeast NuA4 complex, which include TIP48; TIP49; the SWI/SNF2-like protein p400; and a bromodomain-containing protein Brd8, which has a homologue in yeast, Bdf1, but is not part of the

NuA4 complex. A similar TIP60 complex was purified from *Drosophila* and contained the dTIP48, dTIP49, dp400/domino and E(P)c proteins (Kusch et al., 2004).

The p400 protein was found associated with the E1A oncoprotein, along with the TRRAP protein (Fuchs et al., 2001). In this report the recombinant FLAG-tagged p400 and its associated proteins were purified from nuclear extracts by immunoaffinity chromatography. TIP48 and TIP49 co-purified with p400, as did BAF53, β-actin and the enhancer of polycomb homologue, which are all part of the TIP60 complex. Interestingly, Tip60p was not present in this complex, suggesting that the p400 and TIP60 complexes are distinct. This will be discussed in more detail below. TIP48 and TIP49 were shown to interact with p400 in the SWI2/SNF2 like N-terminal domain. This region also binds the adenovirus E1A oncoprotein (Fuchs et al., 2001).

The Swr1 protein in *S. cerevisiae* is related to p400, as it contains the SWI2-like ATPase domain, homologous to the one in p400. The SWR1 complex in *S. cerevisiae* has also been purified by a number of groups (Kobor et al., 2004; Krogan et al., 2003; Mizuguchi et al., 2004) and has been shown to be distinct from the NuA4 complex, although like the human TIP60 and p400 complexes, they share specific subunits such as Arp4 and actin. The complex includes *sc*TIP48, *sc*TIP49, similar to the human TIP60 and p400 complexes.

The fact that the homologues of p400, TIP48 and TIP49 are not present in the yeast NuA4 complex, led one group to believe that the TIP60 complex was not the functional equivalent to the yeast NuA4 complex (Doyon et al., 2004). However, closer examination of the p400 protein reveals that apart from the SWI2 related domain, three additional domains are present in p400, which are also found in the yeast NuA4 subunit Eaf1 (Doyon et al., 2004). Therefore p400 is likely to be the functional homologue of Eaf1 in humans. Interestingly, the SWI2-related domain in p400 recruits TIP48 and TIP49 to the p400 complex (Fuchs et al., 2001). This explains why *sc*TIP48 and *sc*TIP49 are not part of the yeast NuA4 complex, as NuA4 does not contain a protein with this SWI2-related domain, to recruit *sc*TIP48 and *sc*TIP49.

It is striking that the homology of subunits shared by the TIP60 and p400 complexes from yeast to humans is so close (Doyon et al., 2004; Fuchs et al., 2001; Ikura et al., 2000; Kusch et al., 2004). In yeast there are clearly two complexes, NuA4 and SWR1, but they share many common subunits, so it is quite feasible from this information alone that there is a common link between these two (Kobor et al., 2004). In humans and *Drosophila* this is even more obvious as evolution seems to have brought the two complexes together through the p400 subunit, which has homology to two separate proteins in yeast; one of which is present in the NuA4 complex and the other found in the Swr1 complex (Doyon et al., 2004). However, it is quite clear that the p400 complex can be isolated on its own. Therefore, it is likely that TIP48 and TIP49 are initially members of the p400 complex, before they form a complex with TIP60, going by the compositions of the yeast NuA4 and SWR1 complexes. The functional significance of these complexes will be described below.

b) Function of the TIP60 complex

Recombinant Tip60p is able to acetylate free histones H2A, H3 and H4 (Ikura et al., 2000; Yamamoto and Horikoshi, 1997), but was unable to acetylate histones within nucleosomes. However, the purified TIP60 complex was able to efficiently acetylate histones within nucleosomes (Ikura et al., 2000), which indicates that components of the TIP60 complex allow the catalytic subunit, Tip60p, to acetylate histones within nucleosomes. Similar observations were made with the yeast NuA4 complex and its catalytic subunit Esa1p (Allard et al., 1999; Clarke et al., 1999).

The purified TIP60 complex exhibited robust ATPase activity (Ikura et al., 2000). It was assumed that this activity was derived from the TIP48 and TIP49 proteins, since both β-actin and BAF53 have already been shown to exhibit weak ATPase activities (Zhao et al., 1998). The ATPase activity of the TIP60 complex was compared to the activities of purified recombinant TIP48, TIP49 and the equimolar TIP48/TIP49 complex formed *in vitro* (Ikura et al., 2000). The activities of the recombinant proteins, individually and as a complex, were significantly weaker than the activity of the purified TIP60 complex. It

was also shown in this study that the recombinant TIP48, TIP49 and the TIP49/TIP48 complex did not bind to dsDNA or any DNAs with particular structures, such as replication fork-like three-way junctions and Holliday junctions. However, the TIP60 complex had high affinity for three-way and Holliday junctions, but did not bind to duplex DNA. The TIP60 complex also showed ATP dependent DNA helicase activity with a 3' to 5'polarity of unwinding. However, the recombinant TIP48, TIP49 and TIP49/TIP48 complex did not display detectable helicase activity (Ikura et al., 2000).

c) Function of p400/*sc*SWR1 complexes

Recombinant human p400 protein was purified from Sf9 insect cells and both insect homologues of TIP48 and TIP49 were shown to co-purify with p400 (Fuchs et al., 2001). A p400 deletion/ point mutant (Δ1-1044/m), which contains a large N-terminal deletion and a point mutation (K to A) in the putative ATP binding site (residue 1086), failed to bind insect TIP48 and TIP49, underlying the conserved nature of all these proteins, as well as the strong interactions between the TIP48 and TIP49 proteins with the p400 protein. The p400 complex demonstrated concentration-dependent ATPase activity (Fuchs et al., 2001). Addition of DNA to the complex only stimulated the ATPase activity slightly. When the complex was treated with DNaseI a reduced ATPase activity was observed, indicating endogenous DNA within the complex that stimulated the ATPase activity. Although the p400 protein displayed helicase activity, the p400 mutant (Δ1-1044/m) did not. This implied that TIP48 and TIP49 may be required for the helicase activity of the p400 protein (Fuchs et al., 2001). In addition, the p400 complexes purified in the same study, did not display chromatin remodeling activities on either mononucleosomal or polynucleosomal templates.

As the SWR1 complex from *S. cerevisiae* contains similar subunits to the p400 complex in humans, it is thought that they function in a similar way and some evidence for this is presented in section 1.5.2e. The SWR1 complex has been characterized slightly more than the p400 complex. It was shown to co-purify with the histone variant of histone H2A; histone Htz1 (Mizuguchi et al., 2004). Other groups also showed the association of the SWR1 complex with histone Htz1 (Kobor et al., 2004; Krogan et al., 2004;

Krogan et al., 2003). Furthermore, Htz1 was shown to require the Swr1 complex for its recruitment into chromatin *in vivo* (Krogan et al., 2003). Experiments carried out *in vitro* demonstrated that the SWR1 complex catalyzed the exchange of H2A-H2B dimers for Htz1-H2B dimers into nucleosomes (Mizuguchi et al., 2004). This catalytic exchange of nucleosomal H2A for Htz1 variant suggests a previously unknown mechanism of chromatin remodeling that would require the disruption of histone-histone as well as histone-DNA contacts. A similar mechanism may be employed by the p400 complex, as suggested in (Kusch et al., 2004) that will be described later.

d) Links to transcription

Both TIP60 (NuA4) and p400 (SWR1) complexes have been shown to be involved in the transcription of a certain number of genes (Galarneau et al., 2000; Kobor et al., 2004; Krogan et al., 2003; Mizuguchi et al., 2004). TIP48 and TIP49 regulate a number of promoters and interact with some transcription-activating proteins (see section 1.6). As TIP48 and TIP49 are also part of the TIP60 and p400 complexes it is likely that their effects on promoters are directly through these complexes, similar to the yeast INO80 complex (section 1.5.1b). Therefore the function of the TIP60 and p400 complexes in transcription will be described briefly below.

The NuA4 complex affects the transcription of some genes. Arp4, a subunit of the NuA4 complex, was shown to bind H3, H4 and H2A N-termini and mutations in lysines of the H4 tail eliminated this binding (Galarneau et al., 2000). Cells with mutant Arp4 were also shown to be deficient in acetylation of histone H4 (Galarneau et al., 2000). In addition, both Arp4 and Esa1 mutant cells showed decreased mRNA levels of specific genes such as *HIS4*, *LYS2* and *PHO5*. In fact, it was reported later that the NuA4 complex is critical for chromatin remodeling over the *PHO5* promoter, prior to activation (Nourani et al., 2004). Esa1 was also shown to localize precisely throughout the nucleus but did not overlap with silent chromatin marker Sir3, which implicates a role for NuA4 in transcribed regions of the genome (Krogan et al., 2003).

There is also evidenced that the TIP60 complex is required for gene expression. It contains TRRAP, which is an essential cofactor for both E2F and c-Myc, and is necessary for the transformation activity of both proteins. It was also shown that c-Myc, E2F and β-catenin all recruit the TIP60 complex to chromatin (Feng et al., 2003; Frank et al., 2003; Taubert et al., 2004). It is interesting that all these transcription factors also directly interact with TIP48 and TIP49, which will be presented in more detail in section 1.6.

The Swr1 complex plays an important role in the transcription of genes. Microarray analysis revealed that Htz1-activated genes cluster near telomeres and near the silent HMR mating-type locus (Meneghini et al., 2003). Htz1 is enriched in euchromatin regions and acts synergistically with boundary elements, to prevent the spread of heterochromatin. The Swr1 complex functions to recruit Htz1 in certain chromatin regions (Kobor et al., 2004; Krogan et al., 2003; Mizuguchi et al., 2004). Cells lacking Swr1, revealed a profound defect in the deposition of Htz1 at euchromatin sites that flank the HMR silent mating type cassette, as well as other chromosomal sites (Kobor et al., 2004). Htz1 also binds near the telomere where Sir2 and Sir3 proteins bind, indicating that the protein is recruited to both non-transcribed and transcribed regions (Krogan et al., 2003). As p400 is homologous to the Swr1 enzyme and the p400 complex contains subunits that are homologous to the Swr1 complex, including TIP48 and TIP49, it may have similar functions and links to transcription like the Swr1 complex.

e) Links to DNA repair

The TIP60 and NuA4 complexes have been implicated in DSB repair (Bird et al., 2002; Downs et al., 2004; Ikura et al., 2000). A more recent report revealed the mechanism by which the TIP60/p400 complex functions to repair DSBs (Kusch et al., 2004). It is not known how the TIP48 and TIP49 proteins are involved in this process but, as mentioned in section 1.5.1c, they may act as 'RuvB-like' branch migration motors to repair DSBs

in vivo. The involvement of the TIP60 (NuA4) and p400 (SWR1) complexes in DNA damage repair will be presented below.

It was shown that cells expressing a histone acetylase-defective Tip60 mutant were unable to repair DSBs (Ikura et al., 2000). The kinetics of DNA DSB repair in mutant Tip60-expressing cells was compared to those of wtTip60-expressing cells and non-transfected cells. The cells expressing mutated Tip60 were unable to repair DSBs efficiently, especially during the first 30 min, when only 5 % of the repair had occurred. In the non-transfected cells, 40 % of the breaks had been repaired and cells expressing wild-type Tip60p had more efficient DSB repair (Ikura et al., 2000). These results showed that histone acetylation by the TIP60 complex, is likely to play a role in DSB repair.

Cells that are DNA repair-efficient can signal the presence of DNA lesions to the apoptotic machinery, so that cells that fail to repair DNA lesions, undergo apotosis (D'Atri et al., 1998). After γ-irradiation, control and wild-type TIP60-expressing cells were able to induce apoptosis (Ikura et al., 2000). However, mutant TIP60-expressing cells were resistant to apoptosis. This showed that the TIP60-dependent DSB repair pathway is likely to be involved in signaling to the apoptotic machinery. As the mutated TIP60 protein is unable to acetylate histones, the DNA repair machinery is probably unable to access the DNA and hence, the whole process of DNA repair and signaling to the apoptotic machinery is inhibited (Ikura et al., 2000). The Holliday junction intermediates have been seen to be the preferred DNA binding substrates of the TIP60 complex *in vitro* (Ikura et al., 2000). If it is the same case *in vivo,* then the TIP60 complex may monitor not only DNA lesions, such as DSBs, but also the later intermediates, such as Holliday junctions, and hence, recruit factors that can process these intermediates (Ikura et al., 2000). Whether TIP48 and TIP49 are involved in processing these Holliday junctions, is unknown.

In *S. cerevisiae* acetylation of histone H4 by Esa1p is essential in two separate pathways of DSB repair: NHEJ and replication-coupled repair (Bird et al., 2002). When all four

tail lysines in histone H4 were replaced by glutamines, in this study, cells containing this mutant showed sensitivity to camptothecin (CPT) and MMS, both of which induce DNA DSBs. By addition of a single lysine on the H4 tail, hypersensitivity to DSB-inducing reagents was rescued and this lysine was shown to be acetylated. Some temperature-sensitive mutants of Esa1, which prefers H4 as a substrate *in vitro*, showed hypersensitivity to CPT and MMS (Bird et al., 2002). Within these mutants, the level of H4 acetylation was diminished showing that Esa1 is required for acetylation of H4 for DSB repair. No genes involved in DSB repair showed a substantial decrease in expression with these mutants (Bird et al., 2002). These results therefore indicated a direct involvement of Esa1 in DSB repair, similar to TIP60. The DSB repair pathway affected in these mutants was NHEJ. However, there was evidence that another main pathway was important in restoring CPT-induced damage, which causes DSBs at the replication fork. This pathway, referred to as replication coupled pathway (Bird et al., 2002), could involve homologous recombination.

Arp4, which has been shown to bind the wild-type histone H4 tail sequence *in vitro* (Harata et al., 1999), was unable to bind to histone H4, when the tail lysines had been mutated (Bird et al., 2002). It was shown to be recruited to DSBs *in vivo*, suggesting that both Esa1 and Arp4, within the NuA4 complex, have a direct role in the repair process. Purified NuA4 complex also showed striking preference for nucleosomal histones in a linear array template over a circular array template, indicating the complex has the ability to recognize DSBs within chromatin (Bird et al., 2002).

(Downs et al., 2004) confirmed the interaction of the NuA4 complex with DSBs through the Arp4 subunit. γ-H2AX, as mentioned in section 1.5.1c, is found at DSBs. Components of the NuA4 complex were pulled down from whole cell extracts with a γ-H2AX peptide but not a H2A peptide (Downs et al., 2004). Purified recombinant Arp4 protein bound specifically to the γ-H2AX peptide, but in *arp4* mutant cells the NuA4 complex failed to interact with the peptide, demonstrating that Arp4 is required for the interaction to γ-H2AX. NuA4 acetylates the N-teriminal tails of histone H2A and H4. Strains lacking histone H2A N-terminal tails were shown to be hypersensitive to MMS,

which indicated that the substrate of NuA4 is important for DNA damage response (Downs et al., 2004). Mutants of Arp4 that affect NuA4 function also showed hypersensitivity to MMS. *In vivo*, γ-H2AX was found close to regions of induced DNA DSBs, as expected, along with components of the NuA4 complex; Esa1, Epl1, Eaf1 and Arp4. This recruitment of the NuA4 complex did not occur in mutant *arp4* cells.

The chromatin remodeling complexes INO80 and SWR1 were also shown, by pull down assays to interact with γ-H2AX peptide but not the H2A peptide (Downs et al., 2004). An enrichment of the INO80 complex, and specifically *sc*TIP49, was seen around induced DSB sites *in vivo* (Downs et al., 2004). However, no such binding was seen in *arp4* mutant cells. This confirmed to an extent that *sc*TIP49-containing complexes were recruited to these DSBs via Arp4 (Downs et al., 2004). There was also an order of recruitment of the complexes to the DSBs. Phosphorylation of H2A at Ser129 and recruitment of Eaf1 was observed in the first 60 min, whereas *sc*TIP49 accumulates between 2-4 hours. This suggests that INO80/SWR1 complexes arrive at a later stage than NuA4 complexes. Accumulation of *sc*TIP49 was greatly diminished in *esa1* mutant cells implicating that acetylation by NuA4 is required for binding of SWR1 and INO80 complexes (Downs et al., 2004).

In *Drosophila* the histone variant equivalent to the mammalian H2AX, known as H2Av, becomes phosphorylated at sites of DNA damage and was shown to be acetylated by the dTIP60 complex (Kusch et al., 2004). The dTIP60 complex was shown, in this study, to acetylate and exchange the phosphorylated histone variant with unmodified H2Av *in vitro*. Upon induction of DSBs, phosphor-H2Av rapidly accumulates on chromatin but phosphorylation becomes undetectable within 180 min (Madigan et al., 2002). dTIP60 and another subunit of the complex dMrg15 were depleted from cells by RNAi (Kusch et al., 2004). When cells were exposed to γ irradiation to induce DSBs, phospho-H2Av levels remained high in cells after 180 min. This showed that the dTIP60 complex was needed *in vivo* to acetylate and remove phospho-H2Av from nucleosomes. The exchange of phospho-H2Av for H2Av occurs in an ATP-dependent manner, most probably by the activity of the p400/domino protein, due to its similarity to Swr1 (Kusch

et al., 2004). In fact *swr1* and *htz1* null mutants are sensitive to caffeine and MMS, and weakly sensitive to UV irradiation, implicating a role for both proteins in DNA damage repair (Mizuguchi et al., 2004). This study (Kusch et al., 2004) is the first evidence of the dTIP60 and p400 complexes working together in a higher eukaryote in the process of DNA damage repair.

1.6 The interaction of TIP48 and TIP49 with transcription activation factors

The *S. cerevisiae* homologues of TIP48 and TIP49 regulate a number of genes (Jonsson et al., 2001; Lim et al., 2000). Genome-wide microarray analysis confirmed that they regulate over 5 % of genes in *S. cerevisiae*, and as described in section 1.5.1, many of these overlap with the genes regulated by the Ino80 protein (Jonsson et al., 2001; Jonsson et al., 2004). This indicates that while a number of genes are regulated by the INO80 complex, others may also be regulated by other *sc*TIP48- and *sc*TIP49-containing complexes. Some genes that were affected after the inactivation of *sc*TIP48 were also affected by the inactivation of *sc*TIP49 (Jonsson et al., 2001). Yet, it was shown that overall, the removal of *sc*TIP48 had a stronger negative effect on transcription than the removal of *sc*TIP49, indicating that the two proteins may have functions independent of each other. There was also an indication that *sc*TIP48 and *sc*TIP49 may act in opposite directions on some promoters, although the effects of the experimental conditions, in this respect, was not ruled out (Jonsson et al., 2001).

In human cells TIP48 and TIP49 interact with a number transcription-activating proteins, such as c-Myc, β-catenin and E2F1, that all seem to also recruit TIP60/p400 complexes to promoter sites (Figure 1.5). It has been shown, in some recent reports, that the TIP60/p400 complex is recruited for the acetylation histones at promoter sites to initiate transcription (Feng et al., 2003; Frank et al., 2003; Taubert et al., 2004). Intriguingly, these factors are also implicated in oncogenic transformation and TIP49 in particular, has been shown to be an essential cofactor for oncogenic transformation and

apoptosis, induced by these proteins (Dugan et al., 2002; Feng et al., 2003; Wood et al., 2000). TIP48 and TIP49 have been shown to interact with TATA binding protein (TBP) (Bauer et al., 2000; Bauer et al., 1998; Ohdate et al., 2003), which confirms that these proteins do have a role in the transcription of some genes. Below, the details of the interactions and functions with some transcription activators will be described.

1.6.1 TATA binding protein and RNA polymerase II holoenzyme

TBP is thought to initiate the assembly of the pre-initiation complex, for the onset of transcription by RNA polymerase II (Zawel and Reinberg, 1993). A histidine-tagged TBP was used to affinity purify interacting proteins from rat liver nuclear extracts (Kanemaki et al., 1997). rTIP49 protein was pulled out from these extracts. Immunprecipitation analysis, however failed to confirm that the two proteins interact *in vivo* and further experiments were unable to show that the proteins interact *in vitro*. Nevertheless, the interaction has been shown *in vitro* by (Bauer et al., 1998), who also showed that TIP48 interacts with TBP (Bauer et al., 2000). Although, these experiments were carried out using the human proteins as opposed to the rat proteins, similar interactions with TBP were seen using the *S. cerevisiae* TIP48 and TIP49 homologues (Ohdate et al., 2003). The fact that TBP interacts with the two proteins in yeast and humans, signifies that they must also interact in rats, and it may be due to experimental conditions that direct interactions were not seen by (Kanemaki et al., 1997).

*sc*TIP48 and TBP interact genetically (Ohdate et al., 2003). Mutants of TBP, which were unable to bind the TATA element displayed severe synthetic growth defects in the presence of a *sc*TIP48 mutant (scTIP48-160). Transcription of *SPL2* and *PHO84* genes that are targets of *sc*TIP48 were also investigated in TBP mutants (Ohdate et al., 2003). Transcription was severely reduced in both the *tih2-ts160 sc*TIP48 mutant and a certain TBP mutant (Ohdate et al., 2003). Other genes affected in *tih2-ts160* were also investigated and were affected in some TBP mutant strains (Ohdate et al., 2003). These results showed that the transcription of some genes depends on the functions of both *sc*TIP48 and TBP.

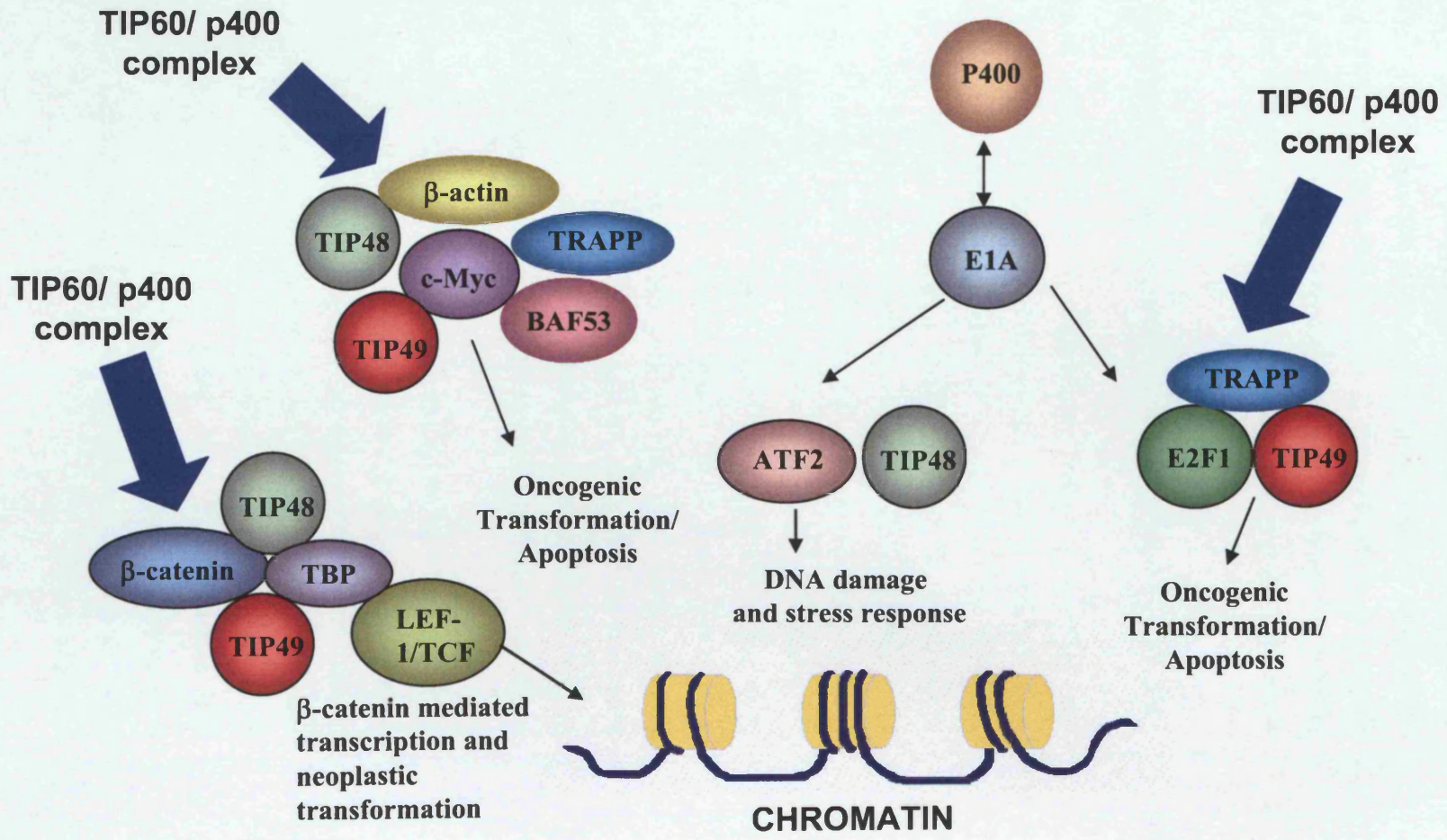
TIP60/ p400 complex
β-actin
TIP48
TRAPP
c-Myc
BAF53
TIP49
TIP60/ p400 complex
TIP48
β-catenin
TBP
TIP49
LEF-1/TCF
β-catenin mediated transcription and neoplastic transformation
Oncogenic Transformation/ Apoptosis
P400
E1A
ATF2
TIP48
DNA damage and stress response
TIP60/ p400 complex
TRAPP
E2F1
TIP49
Oncogenic Transformation/ Apoptosis
CHROMATIN

FIGURE 1.5: Interactions of TIP48 and TIP49 with transcription activating proteins

Interactions of TIP48 and TIP49 with the transcription-activating proteins, c-Myc, β-catenin, E2F1 and ATF2 are illustrated (Bauer et al., 2000; Cho et al., 2001; Dugan et al., 2002; Wood et al., 2000). Other proteins that also interact with these transcription activators are shown and their roles or interactions are described in the text. The recruitment of the TIP60/p400 chromatin modifying complex, by some of these transcription activators is also shown (Frank et al., 2003; Fuchs et al., 2001; Taubert et al., 2004).

TIP49 was shown to co-purify with RNA polymerase II after fractionation of HeLa cells (Qiu et al., 1998). This implies that TIP49 has a role in transcription. TIP49 was first identified in a yeast two-hybrid screen using hRPA3 (Qiu et al., 1998). hRPA3 is a subunit of hRPA, which plays a role in DNA replication (Stillman, 1992) and is an important accessory factor in pairing and strand exchange by hRad51 (Baumann and West, 1998). Both hRPA and Rad51 have been shown to be present in RNA polymerase II, under certain conditions (Maldonado et al., 1996). Therefore, as well as having links to transcription, TIP49 may also be involved in DNA replication or recombination repair, due to its interaction with hRPA3. However, as TIP49 did not immunoprecipitate hRPA3, this interaction is likely to be transient and does not show conclusively that TIP49 is involved in recombination repair.

1.6.2 c-Myc and E2F1

TIP48 and TIP49 have been found in a complex with the transcription factor oncoprotein, c-Myc (Wood et al., 2000). c-Myc is one of the most frequent sites of mutation in human cancer (Cole, 1986; Henriksson and Luscher, 1996) and mutations in the DNA binding domain abolishes the oncogenic activity, which shows that this ability is dependent on the regulation of gene expression (Amati et al., 1993; Stone et al., 1987). Its activity involves the activation of target genes. The N-terminus of the protein contains two regions called the Myc homology box I (MbI) and Myc homology box II (MbII) and the latter is needed for nearly all c-Myc biological activities, including oncogenic transformation, apoptosis, the ability to block differentiation and auto-suppression of the *c-myc* promoter (Stone et al., 1987; Wood et al., 2000). The N-terminus has been seen to have a function that is distinct from the recruitment of basal transcription factors. It is believed that the N-terminus interacts with cofactors needed for c-Myc function (Wood et al., 2000).

The TRRAP protein was identified as a c-Myc N-terminus interacting protein (McMahon et al., 1998). Its ortholog in *S. cerevisiae*, Tra1 is essential for viability, and both the yeast and mammalian proteins are part of the SAGA/PCAF chromatin-remodeling complex, which contain the histone acetyltransferase GCN5p or

hGCN5/PCAF in mammals (Grant et al., 1998; McMahon et al., 1998; Ogryzko, 2000). TRRAP is also part of the TIP60 histone acetylase complex (section 1.5.2).

TIP48 and TIP49 were pulled out of HeLa cells by affinity purification, using the c-Myc N-terminus (amino acids 1-262) (Wood et al., 2000). The association of TIP48 and TIP49 with c-Myc was confirmed *in vivo*, as both TIP48 and TIP49 co-immunoprecipitated with c-Myc. Deletion mutants of c-Myc were used to map the regions of the N-terminus needed for interaction with TIP48 and TIP49. Both bound to a transformation-defective mutant of c-Myc, deleted in the N-terminus (Δ20-48), which has been shown to bind poorly to TRRAP (McMahon et al., 1998). The MbII region of c-Myc (Δ118-152 and Δ129-145) was shown to be necessary to bind to both TIP48 and TIP49. Binding was reduced by a single missense mutation W136E in MbII, which has also been shown to impair the oncogenic activity of c-Myc (Brough et al., 1995). As TIP48 and TIP49 bound the MbII domain, both proteins were thought to be critical cofactors for c-Myc (Wood et al., 2000).

Endogenous TRRAP did not co-precipitate with Flag-TIP48 or Flag-TIP49 (Wood et al., 2000). TIP48 and TIP49 are therefore unlikely to exist in a complex with TRRAP and therefore probably bind c-Myc independently of TRRAP. Deletion mutants of TIP49 were made and it was shown the interaction with c-Myc required the region between residues 136-187 of TIP49 (Wood et al., 2000). This deletion did not completely eliminate binding; therefore the region of interaction could be much larger. Deletion of the Walker A and B motifs, in the same study, had no effect on the binding to c-Myc.

A point mutation was introduced into the Walker B box of TIP49 (D302N) (Wood et al., 2000), equivalent to a mutation that has been shown to create a dominant negative allele of RuvB, which cannot hydrolyze ATP efficiently *in vitro* (Mezard et al., 1997). The mutated protein was able to interact efficiently with c-Myc and endogenous TIP49 and TIP48. The ability of this protein to interfere with c-Myc function was then tested in a transformation assay. It was shown that the TIP49D302N mutant was able to completely inhibit c-Myc-mediated transformation. Both the wild-type TIP49 and the mutant

proteins were assayed for toxicity or non-specific growth inhibition; neither of which had arisen (Wood et al., 2000). Therefore, this mutation caused a dominant negative effect on c-Myc mediated transformation (Wood et al., 2000). It was also demonstrated that this mutation introduced into the yeast homologue *sc*TIP49, failed to rescue *sc*TIP49 deficiency strains, which shows that this mutation resulted in a non-functional protein (Wood et al., 2000).

The E1A protein from adenovirus has similarities to the Myc family of proteins as it can transform and immortalize cells, induce cell proliferation and apoptosis and block differentiation (Nevins, 1995). However, unlike c-Myc, it is unable to bind DNA but instead modulates the activity of E2F transcription factors, so they act as direct mediators of E1A function. One of the ways E1A does this is by sequestering the Rb tumor suppressor, which normally masks the transactivation domain of E2F and prevents it from activating gene expression (Dyson, 1998). It was shown that, like c-Myc, the E2F1 transactivation domain binds to the TRRAP protein (McMahon et al., 1998). Immunoprecipitation experiments also showed that TIP49 binds to the transactivation domain of E2F1 (Dugan et al., 2002). Co-transfection with TIP49 had a modest inhibitory effect on oncogenic focus formation, whereas TIP49D302N completely abolished focus formation (Dugan et al., 2002). The inhibitory effect of TIP49 was, however, lost when lower concentrations of expression vector were transfected, indicating that over-expression of the protein in the first instance caused an imbalance in cellular complexes containing TIP49. This experiment showed that TIP49 is essential for E1A mediated oncogenesis.

Both c-Myc and E2F1 can induce apoptosis that may oppose the proliferation of cancer cells. The mechanism by which these proteins can switch from promoting cell growth to promoting cell death is unknown but is quite an important area that needs to be researched. Interestingly, E2F1 has the ability to induce apoptosis independently of E1A function (Hsieh et al., 1997), indicating, that there are multiple apoptotic pathways.

When cells were starved in 0.1 % serum, c-Myc induced apoptosis (Dugan et al., 2002). A similar observation was made in the same study when cells were starved in the presence of E2F1. Apoptosis in both cases was modestly enhanced by the presence of TIP49 and significantly in the presence of TIP49D302N. These results indicate that disrupting the ATPase domain of TIP49 enhanced the ability of c-Myc and E2F1 to induce apoptosis. In similar experiments TRRAP had no effect on apoptosis induced by the two proteins. These experiments showed that TIP49 and TRRAP have different roles in oncogenesis and apoptosis.

c-Myc complexes have been shown to have histone acetylase activity. The TRRAP protein mediates the recruitment of histone acetylase hGCN5 by c-Myc (McMahon et al., 2000) providing a mechanism for c-Myc to mediate gene regulation. hGCN5 was, however, only able to restore a limited amount of oncogenic activity to transformation-defective c-Myc mutants (McMahon et al., 2000). Therefore other nuclear factors could be essential for oncogenic transformation by c-Myc. TIP48 and TIP49 as described above are essential cofactor for c-Myc. Interestingly, c-Myc co-immunoprecipitates with the TIP60 complex *in vivo* (Frank et al., 2003). c-Myc was also shown in the same study, to bind to specific sites in genomic DNA and induce histone acetylationat these sites. Tip60p was recruited to the nucleolin (NUC) intron 1 by c-Myc, together with TRRAP, TIP48, TIP49, p400, and was accompanied by H4 and H3 acetylation and the induction of NUC mRNA expression. In c-Myc$^{-/-}$ rat cells the induction of H4 acetylation at the NUC site was defective, but could be restored by infection of the cells with a c-Myc expressing adenovirus (AdMYC) , which also restored the recruitment of Tip60p and TRRAP to the NUC site (Frank et al., 2003).

c-Myc interacts specifically with the p400 protein (Fuchs et al., 2001) and as TIP48, TIP49 and TRRAP are part of both the p400 and TIP60 complexes (Fuchs et al., 2001; Ikura et al., 2000), these data confirmed that both p400/TIP60 complexes are recruited by c-Myc to target loci. It was also demonstrated that TIP60 has a role in c-Myc-induced acetylation (Frank et al., 2003). Wild-type Tip60p and an inactive Tip60p mutant were expressed in c-Myc$^{-/-}$ cells infected with AdMYC (Frank et al., 2003). The TIP60 mutant

caused a delay of approximately 1 hour in H4 acetylation at target loci, indicating that it is required for acetylation at these loci via c-Myc recruitment. The mutant also reduced the level of c-Myc binding to some of these sites demonstrating that the TIP60 acetylation also has a role in stabilizing c-Myc binding to chromatin (Frank et al., 2003).

Members of the E2F family, including E2F1, are required for hyperacetylation at target chromatin sites (Taubert et al., 2004). E2F species associate with target promoters in late G1 and this association was concurrent with H3 and H4 acetylation. The acetylation was shown to be directly promoted by E2F *in vivo* and affected expression of E2F target genes (Taubert et al., 2004). The TRRAP protein was recruited to the same promoter sites where E2F1 was found; with similar kinetics as E2F1 binding. Recruitment of the hGCN5 HAT complex was however, not observed, whereas the TIP60 complex was found at these sites. Three subunits of the TIP60 complex also found at these sites were, TIP48, TIP49 and p400. Co-immunoprecipitation confirmed E2F1 and Tip60p can interact physically in cells, however, it is unknown whether the interaction is direct or through other E2F1 interacting proteins such as TRRAP or TIP49 (Taubert et al., 2004). Expression of a dominant negative E2F1 mutant blocked recruitment of Tip60, TIP48, TIP49, TRRAP and p400 to target sites, confirming that E2F recruits this complex to promoter sites (Taubert et al., 2004). It was also shown that TIP48 and TIP49 are found on target promoters, independent of E2F (and c-Myc) stimulation (Taubert et al., 2004). This suggests that TIP48 and TIP49 are part of other transcriptional regulatory complexes apart from the TIP60/p400 complexes.

1.6.3 BAF53

A 45 kDa protein BAF53 and the 41 kDa protein β-actin, were pulled out by affinity purification with the N-terminus of c-Myc along with TIP48 and TIP49 (Park et al., 2002; Wood et al., 2000). BAF53 and β-actin have been found in the SWI/SNF-related chromatin remodeling complex BAF (Zhao et al., 1998). BAF is formed by proteins, known as BRM/BRG associated proteins, encoded by a family of related genes. These form a complex that associates with SWI2 related mammalian proteins BRG or hBRM to give rise to different chromatin remodeling complexes, both of which exhibit

nucleosome remodeling activity (Zhao et al., 1998). BAF53 shows extensive homology to β-actin and the essential actin-related protein in yeast, Arp4 (Poch and Winsor, 1997; Zhao et al., 1998), which is part of the NuA4, SWR1 and INO80 complexes. Arp4 interacts with histones and may have a role in maintenance or reconfiguration of chromatin structure (Harata et al., 1999). BAF53, as mentioned in section 1.5.2, is also part of the TIP60 and p400 complexes.

It was shown that BAF53 interacts with c-Myc *in vivo* when expressed at normal physiological levels (Park et al., 2002). However, the Brg1 and Brm proteins from the BAF complex did not co-precipitate with c-Myc showing that the interaction of BAF53 and β-actin is independent of the BAF complex. Deletion mutants of the N-terminus of c-Myc were used to map the domain that interacts with BAF53 (Park et al., 2002). A deletion mutant of the MBII domain in c-Myc (Δ118-152) was unable to bind to BAF53. This binding was similar but distinguishable from the binding of TRRAP. It was also shown that, similar to TIP49, deletion mutants of BAF53 resulted in the inhibition of c-Myc-mediated transformation.

Immunoprecipitation experiments showed that a complex consisting of TIP48, TIP49 and BAF53 was present in cells. This indicated that these cofactors come together for the function of c-Myc (Park et al., 2002). To rule out the possibility that the interactions were bridged by c-Myc, FLAG-TIP49 was expressed in *c-myc* null cells. Immunoprecipitation with anti-FLAG antibody showed again co-precipitation of TIP49 with endogenous BAF53, which confirmed that the interactions were not mediated by c-Myc (Park et al., 2002). The TRRAP protein was not co-immunoprecipitated with TIP49 indicating that there was no interaction of TRRAP with the BAF53-TIP49 complex. It is unknown, however, if other components of TIP49 containing complexes (such as TIP60 or p400), were present in these immunoprecipitates.

It was also shown that the TIP49-TIP48-BAF53 complex did not display any histone acetylase activity (Park et al., 2002), unlike TRAPP containing complexes (Grant et al., 1998; McMahon et al., 2000; Ogryzko, 2000). Immunoprecipitation of Flag-TRRAP did not precipitate TIP48 and TIP49, and co-transfection of Flag-TIP49 with wild type c-

Myc did not stimulate the binding of TIP49 or BAF53 to endogenous TRRAP. This shows that the c-Myc transactivation domain does not bridge the TIP49-TIP48-BAF53 complex to TRRAP, and c-Myc binds these co-factors independently. Nevertheless, they could be recruited sequentially to similar chromosomal sites. Furthermore, BAF53 co-immunoprecipitated a complex that contained TRAPP and this complex also displayed a unique histone acetylase activity, different to the one seen with TIP60 (Ikura et al., 2000). This suggested that BAF53 forms separate complexes with TIP48/TIP49 (and TIP60), and TRRAP.

1.6.4 β-catenin

The TIP49 protein was found to be associated with β-catenin, which was initially identified as a central component of E-cadherin-cantenin cell to cell adhesion complex (Aberle et al., 1996). β-catenin plays an important role in the Wnt signaling pathway (Willert and Nusse, 1998). This signaling pathway increases and stabilizes the cytoplasmic pool of β-catenin, which then becomes available to interact with transcription factors of the lymphocyte enhancer factor-1/T-cell factor (LEF-1/TCF) family. These factors then cause the accumulation of β-catenin in the nucleus. LEF-1/TCF transcription factors are able to bind DNA target sequences but have little or no transcription activation potential, while β-catenin has no DNA binding capacity but contains a transactivation domain in its C-terminus. Both are needed to activate target genes of the Wnt signaling pathway.

Binding partners of β-catenin were screened for in colon carcinoma cells using a β-catenin-GST fusion protein (Bauer et al., 1998). A 52 kDa protein was identified, namely TIP49. Immunoprecipitation experiments showed that TIP49 interacted with β-catenin *in vivo* (Bauer et al., 1998). A direct interaction between the two proteins was also observed *in vitro*, using tagged recombinant TIP49 and β-catenin proteins. It was shown that the β-catenin region containing the Armadillo-repeat motif (aa 187-284) was needed for binding of TIP49 (Bauer et al., 1998). A direct interaction between TIP49 and TBP was also observed *in vitro*, within this study. The same experiment using

recombinant LEF-1 did not however show interactions with TIP49. Nevertheless, a complex consisting of LEF-1, β-catenin, and TIP49 was co-immunoprecipitated from cell lysates using anti-TIP49 antibodies. The experiments suggested that TIP49 most likely acts as a bridge between the LEF-1-β-catenin complex to TBP, and the transcriptional machinery and hence was named Pontin52 from the latin *pons*, which means bridge (Bauer et al., 1998). It was also shown that TIP48 (named Reptin52) interacted directly with β-catenin and TBP (Bauer et al., 2000). The binding of TIP48 was mapped to β-catenin and found to lie between residues 1-284. This shows that both TIP49 and TIP48 interact with the same domain of β-catenin *in vitro*, in the amino acid region of 183/187-210.

Reporter gene assays were used to test if TIP48 and TIP49 influenced the β-catenin-TCF transactivation potential (Bauer et al., 2000). When hTCF4 and β-catenin proteins were expressed in cells ectopically, the reporter expression was stimulated by a factor of eight. Co-expression with TIP49 did not significantly modify the reporter. However, co-expression with TIP48 caused a strong repressive effect, reducing the activity to 50 % compared to that obtained with hTCF4 and β-catenin alone. Co-expression with both TIP49 and TIP48 resulted in an identical inhibitory effect. A titration analysis with increasing amounts of TIP49 or TIP48 showed clearly that TIP49 was able to activate the promoter, while TIP48 repressed it (Bauer et al., 2000). This showed that these two proteins have opposing effects on the transcriptional activity of the β-catenin/hTCF4 complex and the abundance of TIP48 and TIP49 may regulate this activity. The inhibitory effect of TIP48 was dependent on the presence of β-catenin in the transactivation complex (Bauer et al., 2000). TIP48 and TIP49 have also been shown to be antagonistic regulators of wing development in *Drosophila* (Bauer et al., 2000) and heart growth in zebrafish embryos (Rottbauer et al., 2002).

(Feng et al., 2003) investigated how TIP49 regulates TCF-dependent gene expression and β-catenin-mediated neoplastic transformation. The same TIP49 mutant (TIP49D302N) that interfered with c-Myc mediated transformation (Wood et al., 2000) was made to see if it could affect activation of the a model TCF reporter construct. Ectopic expression of an oncogenic form of β-catenin (β-catenin S33Y) strongly

activated TCF-dependent transcription, but expression of wtTIP49 did not enhance this transcription. However, expression of TIP49D302N mutant had a modest ability to inhibit the effect of β-catenin on TCF-dependent reporter activity.

The β-catenin S33Y mutant induced the formation of foci in an E1A-immortalized rat epithelial cell line (RK3E) (Feng et al., 2003). In the presence of wtTIP49 the number of foci was similar, whereas in cells expressing TIP49302N mutant, 70-80 % less foci were generated. A similar effect was observed in a human cancer cell line with defective β-catenin regulation. A substantial reduction in colony formation was seen in cells expressing TIP49D302N compared to the control and cells expressing wtTIP49. This indicates that TIP49 plays a role in β-catenin-mediated neoplastic transformation and its ATPase activity is important for this function (Feng et al., 2003).

The inhibitory effect of TIP49D302N in the reporter gene assay was quite modest, compared to the strong inhibition of β-catenin mediated neoplastic transformation by TIP49D302N. The oncogenic activity of β-catenin has been shown to be related to its transcriptional activity (Kolligs et al., 1999), therefore, it was predicted that the effect of TIP49 on β-catenin/TCF transcription may be more apparent if the DNA templates were part of higher order chromatin structure, rather than introduced as a reporter construct (Feng et al., 2003). Two genes *ITF-2* and *Axil* were highly expressed in a β-catenin-transformed cell lines compared to the parental cells. Expression of TIP49D302N protein in the β-catenin transformed cells or depletion of TIP49 by RNAi, reduced the expression of *ITF-2* and *Axil* compared to cells expressing wtTIP49 (Feng et al., 2003). This showed that TIP49 is required for transcription of endogenous genes that are regulated by β-catenin and the Wnt signaling pathway.

Experiments were then carried out, which showed that TIP49 was recruited by β-catenin to the promoters of TCF-target genes (Feng et al., 2003). This affected histone acetylation of nearby nucleosomes by the TIP60 complex, to increase transcriptional activity of these genes. Both BAF53 and β-catenin were shown to co-immunoprecipitate with FLAG-tagged TIP49. ChIP studies then showed that TIP49, TRRAP, TCF-4 and

TIP60 co-immunoprecipitated with sequences containing a TCF site in the human *ITF-2* promoter region. As TRRAP and TIP60 are present at the promoter site and both TRRAP and TIP49 are part of the TIP60 complex (Ikura et al., 2000), it was thought that the whole TIP60 complex, affects chromatin structure to allow β-catenin/TCF mediated transcription (Feng et al., 2003). ChIPs using antibodies against acetylated histone H4, showed that histone acetylation of the *ITF-2* promoter region covering the TCF binding site was greatly reduced in cells expressing TIP49D302N compared to control cells and cells expressing TIP49 (Feng et al., 2003). This suggests that TIP49 mediates histone H4 acetylation through the TIP60 complex to facilitate β-catenin/TCF mediated transcription (Figure 1.5).

1.6.5 ATF2 interaction with TIP48

Activating transcription factor 2 (ATF2) is a member of the ATF-CREB family of transcription factors that have been implicated in growth control, cell cycle progression, differentiation, transformation, stress and DNA damage response (Bhoumik et al., 2001; Cho et al., 2001). A yeast 2 hybrid screen showed that TIP48 associates with ATF2 and immunoprecipitation experiments confirmed the interaction (Cho et al., 2001). The TIP48D299N mutant was able to interact with ATF2 to the same extent as the wild-type protein. However, TIP49 and its mutant (TIP49D302N) did not form a complex with ATF2, indicating a selective association of TIP48 over TIP49, by the ATF2 protein. Furthermore it was revealed that ATF2 associates with the C-terminal region of TIP48 (Cho et al., 2001), which contains neither Walker A nor B motifs (Figure 1.2).

The association between endogenous TIP48 and ATF2 increased after the UV irradiation of the cells (Cho et al., 2001). This increase coincided with the phosphorylation of ATF2, suggesting that the interaction between the two is dependent on this phosphorylation. Ionizing radiation (IR) also increased the interaction between TIP48 and ATF2. ATF2 mutated on the specific phosphoacceptor sites allowed only a weak association between TIP48 and ATF2, providing direct evidence that the association between the two proteins is phosphorylation-dependent (Cho et al., 2001).

Further experiments showed that the ectopic expression of TIP48 attenuated the increase in ATF2-transcriptional activities after UV irradiation or IR (Cho et al., 2001). The same experiments were carried out with TIP49 but no change in transcriptional activities, mediated by ATF2, was observed. Moreover, expression of the TIP48D299N mutant showed the same results as the wild-type protein, indicating that the ATPase activity of TIP48 was not responsible for attenuating the transcriptional activities of ATF2. It was shown that the effect of TIP48 to attenuate ATF2 did not require the activities of other TIP48-interacting transcription activation factors, such as c-Myc or β-catenin. The expression of the $ATF^{150-248}$ domain also did not have an effect on either c-Myc or β-catenin activities confirming that the activity of TIP48 on ATF2 is specific (Cho et al., 2001).

1.7 The association of TIP48 and TIP49 with snoRNPs

The synthesis and processing of eukaryotic ribosomal RNAs (rRNAs) takes place in the nucleolus (Lafontaine and Tollervey, 2001). Within the nucleolus there are a number of small nucleolar RNAs (snoRNAs), which are involved in processing pre-rRNA. They function as sequence-specific guides in the modification of rRNA but some are also required for RNA folding and cleavage events (Filipowicz et al., 1999; Lafontaine and Tollervey, 2001; Terns and Terns, 2002; Weinstein and Steitz, 1999). There are two major families of snoRNAs known as the H/ACA and box C/D snoRNAs, which are classified on the basis of conserved sequence motifs. H/ACA snoRNAs function in the site-specific isomerization of uridine to pseudouridine, whereas C/D snoRNAs direct the 2'O methylation or ribose moieties within rRNA (Filipowicz et al., 1999; Lafontaine and Tollervey, 2001; Terns and Terns, 2002; Weinstein and Steitz, 1999). The C and D nucleotide boxes are also required for snoRNA processing and transport into the nucleolus. Most of the snoRNAs are derived from introns of protein genes, which are assembled into ribonucleoprotein complexes (RNP) in the nucleoplasm and then transported into the nucleolus (Newman et al., 2000).

It was shown by one group that specific nuclear proteins associate with the box C/D core motif *in vitro* (Watkins et al., 1998). Using a box C/D motif derived from the mouse U14 snoRNA, four mouse proteins were affinity purified and identified, which included mTIP48 and mTIP49 (Newman et al., 2000). They were shown to localize predominantly in the nucleoplasm, which suggested a possible role in snoRNA production and maybe also transport of snoRNAs into the nucleoli (Newman et al., 2000). In fact, it was shown in yeast that repressing the synthesis of *sc*TIP48 mRNA resulted in a reduced accumulation of C/D and H/ACA snoRNAs (King et al., 2001). This was a direct effect due to the loss of *sc*TIP48, because the expression of certain genes, that encode elements for snoRNA production, were not affected by the loss of *sc*TIP48 (King et al., 2001). Moreover, mutations in the Walker A domain of *sc*TIP48 caused a severe defect in the accumulation of snoRNAs (King et al., 2001). Depletion of *sc*TIP48 also caused a delocalization of both C/D and H/ACA small nucleolar RNPs (snoRNPs) (King et al., 2001), as observed by immunofluorescence microscopy.

The accumulation and nucleolar localization of snoRNAs require the function of a number of other box C/D snoRNA-associated proteins (Watkins et al., 2002). The association of TIP48 and TIP49 to the snoRNP complex was shown to be dependent on the presence of the Nop58 protein (Watkins et al., 2002). A more recent study examined the association of TIP48 and TIP49 with snoRNAs (Watkins et al., 2004). Both TIP48 and TIP49 associated with the precursor forms of U3 snoRNA but TIP49 also associated with the mature form (Watkins et al., 2004). Depletion of TIP49 by siRNA resulted in a reduction of box C/D snoRNA levels. However, the effect on the box C/D snoRNA levels after depleting TIP48 was much weaker. It was also observed that after RNA processing, the nucleoplasmic U3 snoRNP was still associated with many proteins that are not present in the mature nucleolar snoRNPs (Watkins et al., 2004), suggesting that a further maturation step was necessary to generate a mature snoRNP complex. Examination of the salt-sensitivity of the association of some snoRNP proteins with the U3 snoRNP complex, demonstrated that there was a major difference in the stability of the core snoRNP complex found in the nucleoplasm and that in the nucleolus (Watkins et al., 2004). These data suggest that one or more of the snoRNP associated proteins

cause a restructuring event, which leads to the stabilization of the core box C/D complex before it enters the nucleous. The authors suggested that TIP48 and TIP49 would be likely candidates in this process as they are AAA^+ proteins and could function as molecular motors within the complex.

In conclusion, complexes containing TIP48 and TIP49 are diverse. Both proteins tend to associate with chromatin modifying complexes that exhibit different activities such as histone acetylase, nucleosomal sliding and histone exchange. There is also a common theme for the two proteins to interact with a number of transcription activating proteins, which require TIP48 and TIP49 for their function. However, there is evidence that this transcription activation is directly linked to chromatin modification by the complexes that TIP48 and TIP49 are part of. Both proteins have links to DNA repair, but again this is in the context of chromatin-modifying complexes. There is also evidence that TIP48 and TIP49 exert opposite effects on β-catenin-mediated transcription. This observation is difficult to explain in terms of chromatin remodelling, as all chromatin-modifying complexes identified so far, contained both proteins. In addition, both proteins are involved in snoRNP function. While this study was in progress, it was shown that TIP49 interacts with tubulin during mitosis. All this, implies a more general activity for the two proteins as molecular motors or a chaperone-like function. Hence, they may be involved in remodelling protein/protein interactions. Below the published biochemical properties of the individual proteins and their complex will be described.

1.8 Biochemical properties of the TIP48 and TIP49 proteins

1.8.1 Characterization of TIP48 and TIP49 *in vitro*

Several groups have purified recombinant TIP48 and TIP49 proteins and have tried to characterize their activities *in vitro* (Ikura et al., 2000; Kanemaki et al., 1999; Makino et al., 1999; Qiu et al., 1998). However, the results that have been published are contradictory and therefore it is still unknown what the functions of these two proteins are. Below, the experiments carried with the individual proteins will be described.

Recombinant rat TIP49 was cloned with two affinity tags and purified from *E. coli* by nickel affinity chromatography, followed by FLAG affinity chromatography and MonoQ anion-exchange (Makino et al., 1999). The final fractions of the purification were found to contain no contaminating protein, by SDS-PAGE, and were used for biochemical assays. The results showed that TIP49 had weak ATPase activity in the absence of DNA, which correlated well with the amount of TIP49 in each MonoQ fraction. The ATPase activity of TIP49 was strongly stimulated by the presence of single stranded DNA (~10-fold). Closed circular double stranded plasmid DNA only weakly stimulated the ATPase activity and RNA homopolymers and cellular RNAs had no effect. These results demonstrated that TIP49 was a ssDNA-stimulated ATPase. The purified TIP49 showed DNA helicase activity, as it displaced a radiolabeled 30-mer oligonucleotide that was annealed to M13 ssDNA, with 3' to 5' polarity. Helicase activity was dependent on the presence of Mg^{2+} and ATP hydrolysis, as ATPγs, ADP or AMP did not display cofactor abilities.

A UV cross-linking assay confirmed that TIP49 bound radiolabelled ATP specifically (Makino et al., 1999). The labelling was inhibited strongly by the presence of unlabelled ATP. The addition of unlabelled UTP had little effect on the labelling, while unlabelled GTP and CTP moderately reduced the labelling of TIP49. This showed that the labelling of TIP49 is due to a specific interaction with ATP. The nucleotide specificity for hydrolysis by TIP49 was also investigated by using unlabelled nucleoside triphosphates as competitors. The addition of UTP had little effect on the ATPase activity, in the presence of M13 ssDNA, whereas GTP and CTP moderately reduced it. These results are consistent with the cross-linking results, and show that TIP49 interacts specifically with ATP and is unable to efficiently interact with other nucleotides and hydrolyse them (Makino et al., 1999).

The results described above contradicted data published previously. Human TIP49 was overexpressed in insect cells, using a baculovirus expression system (Qiu et al., 1998). The TIP49 protein purified from these cells did not hydrolyse ATP, when tested under a

range of conditions. The reactions were carried out in the absence and presence of various DNAs including linear ssDNA and dsDNA, circular plasmid or phage DNAs and synthetic Holliday junction DNA but ATP hydrolysis was not observed under any conditions tested. The protein also did not exhibit branch migration or helicase activities, although it was unlikely to carry out these activities due to the absence of ATPase activity.

The reported biochemical properties of TIP48 are also contradictory. Human TIP48 was overexpressed in *E. coli* cells (Kanemaki et al., 1999). The protein was purified on a nickel agarose column followed by hydroxyapatite and MonoQ columns. It was found, that only a faint ATPase activity was detected in the peak fractions from the MonoQ column. However, the ATPase activity was stimulated considerably by ssDNA (~ 40-fold). This indicated that TIP48 was a ssDNA-dependent ATPase, similar to TIP49 (Makino et al., 1999). dsDNA only slightly stimulated the ATPase activity. The purified TIP48 also had DNA helicase activity, and the reaction absolutely required ATP and Mg^{2+}. ADP and ATPγS could not substitute ATP. The polarity of unwinding was shown to be in the 5' to 3' direction, opposite to that of TIP49. A UV cross-linking experiment also showed that TIP48 specifically bound ATP.

Recombinant human TIP48 and TIP49 proteins were expressed in *E. coli* and were purified by another group under slightly different purification schemes, which included a Superdex 200 size exclusion chromatography (Ikura et al., 2000). It was shown that very little ATPase activity was seen with TIP49, which eluted at the position of a monomer. TIP48 however showed weak ATPase activity, which eluted at the position of a dimer/trimer. Helicase and DNA binding activities were not observed with these proteins (Ikura et al., 2000).

These studies reported by three different groups (Ikura et al., 2000; Kanemaki et al., 1999; Makino et al., 1999; Qiu et al., 1998) were carried out in slightly different ways, due to the purification schemes employed to purify TIP48 and TIP49. The first group (Kanemaki et al., 1999; Makino et al., 1999) cloned TIP48 and TIP49 with N-terminal

His_6 and FLAG tags and used two affinity purification steps. The second group (Ikura et al., 2000) cloned TIP48 and TIP49 with just a His_6-tag but it did not specify whether the tag was N- or C- terminal. They employed size exclusion chromatography in the purification; a step that was not used by first group. The third group (Qiu et al., 1998) purified non-tagged TIP49 from insect cells using conventional chromatography but the system of expression is completely different from *E. coli*. Therefore, it is unknown why so much contradiction in the activity of the two proteins was reported by the three groups. Either the proteins purified by (Ikura et al., 2000; Qiu et al., 1998) were inactive and therefore exhibited no helicase activity; or the proteins purified by (Kanemaki et al., 1999; Makino et al., 1999) carried contaminating bacterial helicases.

1.8.2 The TIP48/TIP49 complex

It was discovered by several groups that TIP48 and TIP49 interact *in vivo* (Bauer et al., 2000; Gohshi et al., 1999; Kanemaki et al., 1999; Wood et al., 2000) and later on it was also shown that the two proteins form a large complex *in vitro* (Ikura et al., 2000; Jonsson et al., 2004). TIP48 was identified as an interacting partner of TIP49 by a yeast two-hybrid screen, using the full-length cDNA of TIP49 as bait to screen a human fetal cDNA library (Bauer et al., 2000). *In vivo* interactions of the two proteins were also observed when TIP49 immunoprecipitated TIP48 and *vice versa* and self-interaction of the two proteins was also seen (Bauer et al., 2000; Wood et al., 2000). These experiments confirmed that both proteins form heterotypic and homotypic interactions *in vivo*. It was also shown that the two *S. cerevisiae* homologues interact *in vivo*. Fusion constructs of the two proteins were created and expressed in yeast strains and interactions were then shown by immunoprecipitation experiments (Lim et al., 2000). Deletion of the Walker A (Δ63-135) or Walker B (Δ290-366) motifs in a transiently expressed TIP49 protein eliminated the binding of TIP49 to the endogenous TIP48 and TIP49 proteins (Wood et al., 2000). However, mutants with deletions between the two motifs had no effect on binding of either endogenous TIP48 or TIP49. These results therefore showed that the ATPase motifs of TIP49 are critical for complex formation between TIP48 and TIP49, but subtle mutations in the ATPase motif showed no inhibition of interaction between the proteins (Wood et al., 2000).

As described in section 1.4, TIP48 and TIP49 are found in large complexes *in vivo* (Kanemaki et al., 1999). It was also shown by another group that rTIP48 eluted in large protein complexes in the presence of $MgCl_2$. Glycerol gradient centrifugation and size exclusion chromatography analysis demonstrated that in the rat liver nuclear matrix, TIP48 existed in complexes of 697 kDa (Gohshi et al., 1999). The sedimentation coefficient and Stokes' radius of the rTIP48 complex were similar compared to those of rTIP49 (Kikuchi et al., 1999). The complexes that contained rTIP49 and rTIP48, sedimented in glycerol gradients and eluted from the size exclusion chromatography column at the same position (Gohshi et al., 1999). No other protein was seen with the same sedimentation profile as rTIP49 and rTIP48. This therefore suggested that in the nuclear matrix, the major components of the rTIP49 and rTIP48 complexes were these proteins themselves. The molecular mass also suggested that the complex consisted of six rTIP49 and six rTIP48 proteins, and there may also be some other minor components. However the authors speculated that the two proteins could also be contained in distinct complexes (Gohshi et al., 1999).

Other groups have used pull-down assays to show that TIP48 and TIP49 form a complex *in vitro*. Fusion TIP48 and TIP49 proteins carrying different tags were used to demonstrate heterotypic and homotypic interactions for both TIP48 and TIP49 (Bauer et al., 2000; Kanemaki et al., 1999). Purified recombinant TIP48 and TIP49 were used to reconstitute a complex *in vitro* (Ikura et al., 2000). Both proteins were incubated in equimolar amounts and the formation of a complex containing equimolar ratios of the two proteins was demonstrated by size exclusion chromatography on Superdex 200 column. The peak fractions eluted around 500 kDa and the ATPase activity of this complex was significantly stronger than that of the individual subunits. These results showed that the formation of the multimeric complex involving the two proteins is important for efficient ATP hydrolysis. Significantly, this complex, like the individual proteins, exhibited no helicase activity (Ikura et al., 2000). More recently, an *S. cerevisiae* TIP48/TIP49 complex was purified by co-expressing His_6-*sc*TIP49 and *sc*TIP48-$FLAG_2$ in insect cells (Jonsson et al., 2004). The binary complex was purified on a nickel metal affinity column followed by MonoQ anion exchange. Dynamic light

scattering revealed a monodispersed species with virtually all the protein in a complex of 615 kDa. This suggested that the *sc*TIP48/*sc*TIP49 complex forms a structure consistent with a double hexamer.

1.8.3 Effects of mutations in TIP48 and TIP49

Mutations have been made in both human and yeast proteins and their effects assessed. As mentioned in section 1.6, a mutation in the Walker B motif of TIP49, where the conserved aspartate (aa 302) was changed to an asparagine, showed a dominant negative effect on the activity of some transcription activation factors (Dugan et al., 2002; Feng et al., 2003; Wood et al., 2000). This mutation is similar to one that was made in bacterial RuvB protein, which also showed a dominant negative effect *in vivo* and had an inhibitory affect on the ATP hydrolysis activity, *in vitro* (Mezard et al., 1997). The same mutation made in *sc*TIP49 and *sc*TIP48 was lethal in yeast cells (King et al., 2001; Wood et al., 2000). Another mutation at the conserved glutamate of the *sc*TIP48 and *sc*TIP49 Walker B motifs also proved to be lethal (Jonsson et al., 2001), whereas another group showed that it only caused a conditional temperature sensitivity phenotype in *sc*TIP48 (King et al., 2001). The difference seen in the two studies may have been due to yeast strain background. These mutations show, however, that the Walker B motif, which is required for ATP hydrolysis, is essential for the function of both proteins *in vivo*.

It was shown by two groups that the mutation of the conserved lysine in the Walker A motif of *sc*TIP48 (aa 81) and *sc*TIP49 (aa 85) was lethal (Jonsson et al., 2001; Lim et al., 2000). However, the same mutation made in *sc*TIP48 by another group only caused a conditional temperature sensitivity phenotype, which again may be due to yeast strain background (King et al., 2001). A mutation at the conserved glycine in the Walker A motif in *sc*TIP48 (aa 80) also caused a conditional temperature sensitivity phenotype while mutation of the other conserved glycine (aa 75) proved to be lethal (King et al., 2001). A mutation at the conserved threonine (aa 82) also caused a conditional temperature sensitivity phenotype (King et al., 2001).

A mutant allele of TIP48, which was embryonic lethal, was identified in Zebrafish (Rottbauer et al., 2002). The recessive Zebrafish mutation *liebeskummer* causes cardiac hyperplasia in developing embryos. The *lik* mutant carries an in-frame insertion of three amino acids in zTIP48 caused by abnormal splicing at the exon7-exon8 boundary. The mutation is within the conserved 200 amino acid stretch between the Walker A and Walker B motifs (Figure 1.2). It was shown that *sc*TIP48-*lik* expressed in *scTIP48* mutant yeast cells, did not support viability.

Recombinant wild-type zTIP48, which was expressed and purified from insect cells, eluted as a homotypic hexamer (~310 kDa) and dimer (~110 kDa) (Rottbauer et al., 2002). The mutant protein, however, did not peak as a hexamer or dimer but instead, formed larger aggregates (more than 670 kDa) that had high ATPase activity. However, both proteins clearly co-purified with other insect proteins and the results are difficult to interpret. The *lik* mutant was shown to enhance the transcriptional repressor activity of zTIP48 in the β-catenin/TCF pathway. As shown in other systems (Bauer et al., 2000), zTIP49 had an effect, opposite to that of zTIP48. Depletion of zTIP49 caused cardiac hyperplasia in embryos, which indicated that zTIP49 acts as a negative regulator upon heart cell growth.

TIP48 and TIP49 are required for the activity of various complexes and obviously their ATPase activity is required for some, if not all, their functions *in vivo*. However, it is unknown how ATP hydrolysis by the two proteins is coupled to their function. One possibility suggested by reports of their DNA helicase activity, is that they have DNA translocation and unwinding activities (Kanemaki et al., 1999; Makino et al., 1999). This is supported by the fact that they show homology to the RuvB translocation motor (Putnam et al., 2001). There are also numerous speculations in the literature about branch migration of Holliday junctions by TIP48 and TIP49, particularly as the TIP60 complex binds Holliday junctions (Ikura et al., 2000) and both the TIP60/p400 and yeast INO80 complexes are involved in DSB repair (Downs et al., 2004; Ikura et al., 2000; Morrison et al., 2004; van Attikum et al., 2004). However, reports about their DNA

helicase activities are controversial (Ikura et al., 2000; Kanemaki et al., 1999; Makino et al., 1999; Qiu et al., 1998) and need to be clarified, so that the function of TIP48 and TIP49 can be elucidated. Moreover, the two proteins clearly interact to form a complex (Bauer et al., 2000; Ikura et al., 2000), which seems to be central to their activity (Jonsson et al., 2004). The molecular architecture and contribution of the individual proteins, to the activity of the complex has not been investigated. Therefore these questions need to be addressed, which leads to the aims of the project.

1.9 Aims and experimental design

The main aims of this project were to characterize the biochemical activities of purified recombinant TIP48 and TIP49 proteins and the TIP48/TIP49 complex. In particular, we were interested in their ATPase and ATP-binding activities and, possibly, DNA unwinding and branch migration activities. As little characterization has been carried out on the TIP48/TIP49 complex we were particularly interested in the contribution of the individual subunits to the ATPase activity of the complex. As well as this, we wanted to determine the subunit structure of the TIP48 and TIP49 proteins individually and as a complex, and in particular whether they formed hexamers *in vitro*. Lastly, we wanted to carry out further investigations into the roles of TIP48 and TIP49 *in vivo*, to gain a better idea of their functions in the cell. Below specific aims are presented and the experiments that were used to address these aims are outlined, which will lead us to the following chapters.

- **Purification of the recombinant TIP48 and TIP49 proteins.**

This was done by making bacterial expression constructs and expressing the 6x histidine (His_6) tagged proteins in *E. coli*. Both proteins were purified by metal affinity chromatography and subsequent chromatography steps. Catalytically inactive proteins containing a point mutation in the conserved aspartate residue of the Walker B motif of both proteins (TIP48D299N or TIP49D302N) were also expressed and purified under similar conditions.

- **Purification of the TIP48/TIP49 complex.**

Co-expression of TIP48 and TIP49-His_6 from a dual expression cassette in *E. coli* did not yield soluble proteins. However, upon refolding from urea, the two proteins assembled into a defined stable soluble complex. A TIP48/TIP49 complex was obtained under native conditions by mixing purified recombinant TIP48-His_6 and partially purified TIP49 in solution. The complex was captured on a metal affinity column and fractionated further by size exclusion chromatography. Mutant complexes were also made that comprised of either TIP48-His_6/TIP49D302N or TIP49/TIP48D299N-His_6.

- **ATPase and ATP binding activities of TIP48, TIP49 and their complex *in vitro*.**

ATPase activities of the proteins were measured. As both TIP48 and TIP49 seemed to carry ATPase contaminants that were stimulated in the presence of ssDNA, an additional purification step by ssDNA cellulose chromatography was employed to remove the contaminants. ATPase activity was then again measured as was ATP binding using a radio-labelled ATP analogue ([γ^{32}P] 2 azido-ATP). The ATPase activities of the refolded and native complex were determined. ATP binding to the TIP48/TIP49 complex was examined as it was it was important to determine if both TIP48 and TIP49 bind ATP within the complex. The ATPase activities of the mutant complexes (TIP48-His_6/TIP49D302N or TIP49/TIP48D299N-His_6) were determined to see if both proteins are required for the ATPase activity of the complex. ATPase activities of the individual proteins or the TIP48/TIP49 complex were tested in the presence of different DNA forms and an interacting partner β-catenin.

- **DNA helicase and branch migration activities of TIP48, TIP49 and the TIP48/TIP49 complex?**

DNA helicase and branch migration substrates were made and assays with the individual proteins and the TIP48/TIP49 complex were carried out using RuvAB as controls.

- **The subunit structure of TIP48 and TIP49 individually and as a complex.**

These studies were carried out by size exclusion chromatography and electron microscopy by negative staining. The subunit organizations of TIP48 and TIP49 were

determined by size exclusion chromatography, both in the absence and presence of adenine nucleotides. Binding experiments using these adenine nucleotides as competitors to [γ^{32}P] 2 azido-ATP were also carried out to confirm that TIP48 and TIP49 could bind them. The TIP48/TIP49 complex eluted as a large oligomer from size exclusion chromatography in the absence of adenine nucleotide cofactors. A sample of this was studied by electron microscopy to determine whether the TIP48/TIP49 complex formed a double hexameric structure typical of other AAA^+ proteins (Ogura and Wilkinson, 2001). Electron microscopy was also employed because it may indicate whether the complex comprises of two homo-hexamers or two hetero-hexamers of TIP48 and TIP49

- **Localizations of TIP48 and TIP49 *in vivo*.**

Antibodies were raised against the recombinant TIP48 and TIP49 proteins. Localization studies were carried out in HeLa and mouse fibroblast cells using immunofluorescence microscopy. As TIP48 and TIP49 showed different patterns of localization during mitosis the localizations of other proteins that interact with TIP48 and TIP49, namely BAF53 and β-catenin, were also examined and compared to TIP48 and TIP49.

CHAPTER 2

Materials and Methods

2.1 Materials

2.1.1. Reagents

Affinity Labelling Technologies: [γ^{32}P] 2 azido-ATP (10-15 Ci/mmol)

Amersham Pharmacia: ECL plus reagents

Anatrace: APO128 detergent

BD Biosciences: Agar, Tryptone, Yeast extract

BDH: Acetone, Boric acid, $CaCl_2$, EDTA, Ethanol, Formic acid, Glacial acetic acid, Glycerol, HCl, Isopropanol, KCl, K_2HPO, KH_2PO, KOH, LiCl, Methanol, NaCl, Na_2HPO, NaH_2PO, NaOH, Sodium acetate, Urea, TCA.

Bio-Rad: (30 %, 29:1) acrylamide bis-acrylamide, (30 %, 19:1) acrylamide bis-acrylamide, Agarose (0.5 % or 0.8 % made in 1x TAE), Ammonium persulphate, Bradford reagent, Bromophenol blue, Coomassie Brilliant blue (R250), Ethidium Bromide (added to agarose to a final concentration of 0.5 μg/ml), Glycine (electrophoresis grade), SDS (electrophoresis grade), TEMED, Tris (electrophoresis grade), Xylene cyanol FF.

Fisher Scientific: DTT

Gibco: Dulbecco's modified Eagle Medium (DMEM), Donor calf serum, Fetal bovine serum, penicillin/streptomycin.

Perkin and Elmer: [α-^{32}P]-ATP (800 Ci/mmol), [γ-^{32}P]-ATP (3000 Ci/mmol).

Roche: EDTA free cocktail protease inhibitor tablets for 50 ml samples, containing pancreas-extract, Chymotrypsin, Thermolysin, Trypsin and Papain.

Sigma: Ampicillin (AMP) (100 mg/ml stock in dH_2O), Ammonium sulphate, ATP, ADP, AMPPNP ATPγS, BCIP/NBT, 2-β-mercaptoethanol, Carbenicillin (CB) (100 mg/ml stock in dH_2O), Chloroamphenicol (CM) (34 mg/ml in 100 % ethanol), Goat serum, L-glutamine, Lysozyme, MOPS, NaI, NP40, $RbCl_2$, Silica, Sucrose, Tris Base, Triton X-100, Tween 20, Thymidine, X-gal.

2.1.2. Enzymes and materials for molecular biology

Amersham Pharmacia: Taq DNA polymerase Ready-To-Go™ beads

Invitrogen: BL21 (DE3) Gold and of BL21 (DE3) Gold pLysS and DH5α strains

New England Biolabs (NEB): Restriction enzymes (*Nde*I, *Xho*I, *BamH*I, *EcoR*I, *Mlu*I, *Bgl*II, *Kpn*I and *Sma*I), T4 ligation kit, Quick ligase kit, CIP, T4 Polynucleotide kinase, Vent polymerase, BSA, ϕX174 virion ssDNA, pUC19 plasmid and1 kb DNA ladder with molecular weight markers of 10, 8, 6, 5, 4, 3, 2, 1.5, 1 and 0.5 kb

Novagen: pET21b+ plasmid, pET15b+ plasmid

Promega: pGEM® T easy plasmid and T4 rapid ligation kit

Qiagen: Plasmid Mini, Midi, and Maxi prep kits. Gel extraction and PCR purification kits

Sigma: Proteinase K

Sigma Genosys: All PCR and SDM, primers were ordered from here. They were purified by PAGE at a 0.05 μg scale.

Stratagene: Quick-change® site directed mutagenesis kit

Whatman: DE81 DEAE paper

pET30-β-catenin-His$_6$ construct (Kindly provided by Professor L.Pearl, Institute of cancer research, U.K)

2.1.3. Materials for protein chromatography/ techniques

Amersham Pharmacia: Mono Q FPLC, HiTrap SP sepharose, HiTrap Q sepharose, Superdex 200 HR FPLC

Bio-Rad: Hydroxyapatite resin, DEAE BioGel, Nitrocellulose membrane, PVDF membrane, Gel filtration molecular markers

Clontech BD: TALON™ (Talon) resin

Millipore: Amicon® Ultra-15 Centrifugal filters, Ultrafree®- 0.5 Centrifugal filters (protein concentrators)

NEB: Pre-stained protein markers (Broad range) with the following molecular masses: 175, 83, 62, 47.5, 32.5, 25, 16.5 and 6.5 kDa

Sigma: ssDNA cellulose, TLC PEI plates

The Ultra centrifuge used during protein purification was the Optima L-XP 100 preparative ultra centrifuge (Beckman)

RuvA and RuvB proteins (purified in the laboratory by C.Pryvezentsev (Privezentzev et al., 2004))

2.1.4. Antibodies

Anti-α-tubulin mouse monoclonal (Sigma), anti-β-catenin mouse monoclonal (BD Transduction Laboratories), Penta-His mouse monoclonal antibody (Qiagen), Anti-BAF53 rabbit polyclonal (Kindly provided by Professor M.D.Cole, Princeton university, (Park et al., 2002)), Anti-TIP49 W1B3 mouse monoclonal antibody, (Kindly provided by Professor L. Wagner Vienna University (Gartner et al., 2003)), Alexa Fluor 680-labelled goat anti-mouse IgG (Molecular Probes), IRDye 38-labelled goat anti-rabbit IgG (Rockland Immunochemicals), Alkaline phosphatase conjugated anti-Mouse IgG (Sigma), HRP conjugated anti-Rabbit IgG (Amersham), HRP conjugated anti-Mouse IgG (Amersham), TRITCH conjugated goat-anti-rabbit IgG and FITCH-conjugated goat-anti-mouse IgG (Molecular probes).

2.1.5. Buffers and media

ATPase running buffer: 1 M Formic acid and 0.5 M LiCl

ATPase reaction buffer: (10x) 500 mM Tris-HCl (pH 7.5), 500 mM NaCl and 20 mM $MgCl_2$

ATPase reaction buffer B: (10x) 500 mM Tris-HCl (pH 7.5), 500 mM NaCl, 100 mM DTT and 1 mg/ml BSA

ATPase reaction buffer C: (10x) 500 mM Tris-HCl (pH 7.0), 1 M of NaCl, 100 mM DTT and 1 mg/ml BSA

ATP binding buffer: 20 mM Tris-HCl (pH 7.5), 100 mM NaCl, BSA 25 μg/ml and 1 mM DTT

Blocking buffer: TBS-Tween with 5 % skimmed milk powder (Marvel)

Buffer A: 10 mM $RbCl_2$ and 10 mM MOPS (pH 7.0)

Buffer B: 10 mM $RbCl_2$, 10 mM MOPS (pH 6.8) and 50 mM $CaCl_2$

Buffer H: 10 mM Potassium phosphate (pH 6.8), 100 mM KCl, 1 mM DTT, 1 mM PMSF and 10 % glycerol

Buffer R: 20 mM Tris-HCl (pH 8.0), 100 mM NaCl, 10 % glycerol, 1 mM PMSF, 1 mM DTT and 1 mM EDTA

Buffer R_1: 20 mM Tris-HCl (pH 8.0), 100 mM NaCl, 10 % glycerol, 1 mM PMSF and 1 mM DTT

Buffer R_2: 20 mM Tris-HCl (pH 8.0), 300 mM NaCl, 10 % glycerol, 1 mM PMSF, 1 mM DTT and 1 mM EDTA

Coomassie brilliant blue: 0.25 g Coomassie brilliant blue, 10 ml isopropanol, 10 ml glacial acetic acid; made to 100 ml with dH_2O

Destain: 10 ml isopropanol and 10 ml glacial acetic acid; made to 100 ml with dH_2O

ddH_2O: Autoclaved distilled water

DNA loading Buffer: (6x): 0.25 % bromophenol blue, 0.25 % xylene cyanol FF and 30 % glycerol

Gene wash: 50 mM NaCl, 10 mM Tris-HCl (pH 7.5), 2.5 mM EDTA and 50 % ethanol

IF blocking buffer: 1 x PBS containing 10 % goat serum and 0.3 % BSA

LB media: 10 g tryptone, 5 g yeast extract, 10 g NaCl in 1litre dH_2O and autoclaved

LB agar: LB media plus 20 g of solid agar per litre: autoclaved

Lysis /Talon buffer: 20 mM Tris-HCl (pH 8.0), 300 mM NaCl, 10 % glycerol, 1 mM PMSF, 1 mM βME

PBS: 8 g NaCl, 0.2 g KCl, 1.44 g Na_2HPO_4, 0.24 g KH_2PO_4; made up to 1 litre with dH_2O

PBS-Tween: PBS with 0.05 % Tween 20

Protein loading buffer: 50 mM Tris-HCl (pH 6.8), 100 mM DTT, 4 % SDS, 0.1 % bromophenol blue and 40 % glycerol

RuvAB buffer: (10x) 500 mM Tris-HCl (pH 7.5), 500 mM NaCl and 150 mM $MgCl_2$

Running gel: 5 ml of 12 % SDS PAGE running gel: 1.6 ml dH_2O, 2 ml 30 % acrylamide mix (29:1), 1.3 ml 1.5 M Tris-HCl (pH 8.8), 50 µl 10 % SDS, 50 µl 10 % APS and 2 µl TEMED.

Stacking gel: 2 ml SDS PAGE stacking gel: 1.4 ml dH_2O, 0.33 ml 30 % acrylamide mix (29:1), 0.25 ml 1.0 M Tris-HCl (pH 6.8), 20 µl 10 % SDS, 20 µl 10 %APS and 2 µl TEMED.

Sucrose buffers (5 and 20 %): 10 mM Tris-HCl (pH 7.5), 1 M NaCl, 10 mM EDTA (pH 8.0) and 5 or 20 % sucrose

Silica and NaI: 1 g of silica, washed with 1 ml of PBS. It was centrifuged at 1500 *g* and the silica pellet was resuspended in 6 M NaI to give a concentration of 100 mg/ml. Stored at -20 °C.

SSC: (20x) 175.3 g NaCl, 27.6 g NaH_2PO_4, 7.4 g EDTA in 800 ml of H_2O: pH adjusted to 7.4 with NaOH; made up to 1 litre with dH_2O

Stop buffer: 100 mM Tris-HCl (pH 7.5), 200 mM EDTA, 2.5 % SDS and 10 mg/ml Proteinase K

TAE: (50x) 242 g Tris base, 57.1 ml glacial acetic acid, 100 ml 0.5 M EDTA (pH 8.0) and made up to 1 litre with dH_2O

TBE: (10x) 108 g Tris base, 55 g Boric acid, 40 ml 0.5 M EDTA pH 8.0; made up to 1 litre with dH_2O

TBE native gels: 20 ml, 6 % PAGE gel: 2 ml TBE, 4 ml acrylamide mix (19:1), 100 µl 10 % APS, 20 µl TEMED; made up 20 ml with ddH_2O. (For 8 % gels add 5.3 ml of acrylamide mix and then add other reagents and make up to 20 ml with dH_2O).

TBS: 20 mM Tris-HCl (pH 7.5), 137 mM NaCl

TBS-Tween: TBS with 0.05 % Tween 20

TE: 10 mM Tris (pH 7.5) and 1 mM EDTA (pH 8.0)

Transfer buffer: 39 mM glycine, 48 mM Tris-HCl (pH 7.5), 0.037 % SDS, 20 % methanol

Tris-Glycine buffer: 10x stock: 30.2 g Tris, 187.6 g glycine, 10 g SDS; made up to 1 litre with dH_2O.

METHODS

2.2. *E.coli* cell culture and DNA preparation

2.2.1. I.M.A.G.E clones

All I.M.A.G.E clones used in this thesis were obtained from the I.M.A.G.E. consortium. Fully sequenced, full-length clones for the human TIP48, TIP49 and BAF53 coding sequences were obtained and are shown below with their accession numbers:

Human *TIP49* clones:
2822960 (CM10-m09)
2823526 (CM12 d23)
2823568 (CM12-f17)
591284 (1430-b21)

Human *TIP48* clones:
22267 (71-ao3)
2819778 (CM2-h19)

Human *BAF53* clone:
13436-h02

Clones labelled as CM were streaked onto LB agar plates containing 34 μg/μl of chloroamphenicol and grown at 30 °C. Clones without the CM abbreviation were streaked on LB agar plates containing 100 μg/μl carbenicillin (CB) or ampicillin (AMP) and grown at 37 °C. Frozen stocks and DNA preparations of these clones were made as described below.

Frozen stocks

Single colonies were picked from the agar plates and inoculated into 5 ml of LB with the appropriate antibiotic. They were grown overnight at 30 °C (cultures containing CM) or 37 °C (cultures containing AMP or CB). One ml of each culture was transferred into a cryogenic vial along with 200 µl of 80 % glycerol. They were kept frozen at -80 °C.

2.2.2. Competent bacterial cells

All strains shown in Table 2.1 were prepared under the conditions described as follows: The cells were streaked out on an LB agar plates and incubated overnight at 37 °C. A single colony was inoculated into 5 ml of LB media and incubated at 37 °C overnight, with shaking at 200 rpm. From the overnight culture, 1.6 ml was inoculated into 100 ml of LB and grown for 3 h at 37 °C to an OD_{600} of 0.6. The cells were then centrifuged for 15 min at 3000 *g* and the resulting cell pellet was kept continuously on ice throughout the rest of the procedure. Following one wash with 34 ml of ice cold Buffer A, the suspension was centrifuged at 3000 *g* for 30 sec. To the washed cells 34 ml of Buffer B was added and the cells were incubated on ice for 90 min. These were then centrifuged at 3000 *g* for 30 sec at 4 °C. The cell pellet was resuspended gently in 10 ml of Buffer B, containing 10 % glycerol. Aliquots were prepared and stored at –80 °C.

2.2.3. Transformation of DNA

50 ng of plasmid DNA was incubated on ice with 100 µl of competent cells, for 30 min. The cells were heat shocked at 42 °C for 90 sec and then incubated on ice for 2 min. One ml of LB was added to each reaction and incubated at 37 °C for 1 h, with shaking. The cells were centrifuged at 1500 *g* for 5 min and the pellet was gently resuspended in 200 µl of LB. The cells were spread on agar plates, containing antibiotic, which were then incubated overnight at the appropriate temperature, to allow growth.

Table 2.1: *E.coli* strains used for cloning and protein expression

Strain	Application	Genotype
DH5α	**Cloning experiments**	F^- ϕ80*lacZ*ΔM15 Δ(*lacZYA-argF*)U169 *recA1* *endA1* *hsdR17*(rk^-, mk^+) *phoA* *sup*E44 *thi-1* *gyrA96* *relA1* λ^-
BL21 (DE3) Gold	**Protein expression** This strain is a lysogen of the bacteriophage λDE3 that carries a DNA fragment containing the *lacI* gene, the *lacUV5* promoter, and the gene for T7 RNA polymerase (Studier, 1991). *lacUV5* promoter directs transcription of the T7 RNA polymerase gene, after induction with IPTG.	*E.coli* B F^- *omp T* $hsdS_B$ (rB^- mB^-) dcm^+ Tetr gal (DE3) *endA Hte*
BL21 (DE3) Gold pLysS	**Protein expression** This strain is used to suppress basal expression of T7 RNA polymerase, prior to induction, thus stabilizing recombinants encoding toxic proteins.	*E. coli* B F^- *ompT* *hsdS*(rB^- mB^-) dcm+ Tetr gal (DE3) endA *Hte* [pLysS Camr][a]

2.2.4. Plasmid DNA purification

Cultures for plasmid mini-preps and midi/maxi-preps were grown and prepared as described in the protocols provided by the manufacturer (Qiagen). The plasmids were concentrated by Ethanol precipitation (see below), when necessary.

2.2.5. Ethanol precipitation

The DNA sample was made up with dH_2O to a minimum volume of 200 µl, when necessary. Sterile sodium acetate 3 M (pH 5.0) was added to the DNA, to a final concentration of 10 %, followed by an addition of 2-3 volumes of ice-cold 100 %

ethanol. This was incubated at -20 °C overnight, so that precipitation could occur effectively. The DNA was centrifuged at 20,000 *g*, for 30 min at 4 °C and the supernatant was removed carefully without dislodging the DNA pellet. One ml of 70 % ethanol was added and the DNA and was centrifuged at 20,000 *g* for 5 min, at 4 °C. The supernatant was taken out carefully (any residual ethanol was pipetted out with a fine tip) and the DNA pellet was allowed to air dry for 10 min. The required amount of ddH_2O was added, usually around 150-300 µl for midi/maxi preps, or 20-30 µl for mini-preps and other procedures (see following sections).

2.2.6. Determination of DNA concentration

The concentration of plasmid preps were measured in 1 cm quartz cuvettes. The absorbance was measured in a spectrophotometer at a wavelength of 260 nm. Concentration was calculated by the following formula:

DNA concentration = OD_{260} x 50 x dilution factor **Formula 1**

2.3. Primers and polymerase chain reaction

2.3.2 PCR primers for the TIP48 and TIP49 and BAF53 coding sequences

The primers shown in Tables 2.2, 2.3 and 2.4 were designed to amplify the TIP49, TIP48 and BAF53 coding sequences. Restriction enzymes were designed at the ends of the primer sequences, so that the amplified products could be digested with restriction enzymes shown and subsequently cloned into *E.coli* expression vectors (section 2.4.5).

Table 2.2. PCR primers for *TIP49*

Name[a]	Primer sequence and restriction sites	Primer set
IT250	5'-GAGACATATGAAGATTGAGGAGGTGAAGAGC-3' *Nde*I	SET 1
IT251	5'-GAGAGGATCCACTTCATGTACTTATCCTGCT-3' *BamH*I stop	
IT250	5'-GAGACATATGAAGATTGAGGAGGTGAAGAGC-3' *Nde*I	SET 2
IT252	5'-GAGAGGATCCCTTCATGTACTTATCCTGCTGGT-3' *BamH*I	

Table 2.3. PCR primers for *TIP48*

Name[a]	Primer sequence and restriction sites	Primer set
IT115	5'-ATATCTCGAGCATATGGCAACCGTTACAGCC-3' *Nde*I	SET 3
IT118	5'-ATATGAATTCAGGAGGTGTCCATGGTCTCGCC-3' *EcoR*I	
IT115	5'-ATATCTCGAGCATATGGCAACCGTTACAGCC-3' *Nde*I	SET 4
IT119	5'ATATGAATCTCGAGGGAGGTGTCCATGGTCTCGCC-3' Xho1	
IT115	5'-ATATCTCGAGCATATGGCAACCGTTACAGCC-3' *Nde*I	SET 5
IT292	5'-ATATGGATCCTCAGGAGGTGTCCATGGTCTC-3' *BamH*I stop	

Table 2.4. PCR primers for *BAF53*

Name[a]	Primer sequence and restriction sites	Primer set
IT309	5'-TAGACATATGAGCGGCGGCGTGTACGG-3' *Nde*I	SET 6
IT310X1	5'-GTAGCCTCGAGTCAAGGGCATTTTCTTTCTACACACTGCTTC-3' *Xho*I	
IT309	5'-TAGACATATGAGCGGCGGCGTGTACGG-3' *Nde*I	SET 7
IT310X2	5'-GTAGCCTCGAGAGGGCATTTTCTTTCTACACACTGCTTC-3' *Xho*I	

a The first primer of the set is the 5' primer and the second is the 3' primer

2.3.2. Polymerase chain reaction

PCR reactions with Taq DNA polymerase Ready-To-Go™ beads were carried out as described in protocols, provided by the manufacturer (Amersham). Reaction mixtures contained: 30 pmole 5' and 3' primers and 0.125-1 μg of DNA template.

For PCR reactions carried out with the VENT proofreading DNA polymerase, the reaction mixtures contained: 200 μM dNTPs mix, 2-8 mM $MgSO_4$, 2 units of VENT polymerase, 1x VENT buffer, 20 pmole of 5' and 3' primers and 0.0025-1 μg DNA template. Reactions were made up to a final volume of 50 μl with ddH_2O. All PCR reactions were carried out using the program shown in Table 2.5. The conditions for the PCR reactions with VENT and Taq polymerases are summarized in Table 2.6.

TABLE 2.5: Reaction program for PCR reactions

Temperature	Time	
95 °C	5 min	
95 °C	30 sec	25 cycles
Annealing temperature (see table 2)	30 sec	
72 °C	2 min	
4 °C	Overnight	

TABLE 2.6: Conditions for amplification of *TIP48*, *TIP49* and BAF53 by PCR

PCR product	Polymerase	Primers	[Template]	[$MgSO_4$]	Annealing temperature
TIP49	Taq	Set 1	CM12-f17 (0.175 µg)	-	65 °C
TIP49 (no stop codon)	Taq	Set 2	CM12-f17 (0.175 µg)	-	65 °C
TIP48	Taq	Set 3	CM2-H19 (0.135 µg)	-	67 °C
TIP48 (no stop codon)	Taq	Set 4	CM2-H19 (0.135 µg)	-	67 °C
TIP49	Vent	Set 1	CM10-mo9 (0.010 µg/ 0.0025 µg)	8-6 mM	65 °C
TIP49 (no stop codon)	Vent	Set 2	CM10-mo9 (0.0025 µg)	6 mM	65 °C
TIP48	Vent	Set 3	CM2-H19 (0.0675 µg)	8 mM	67 °C
TIP48 (no stop codon)	Vent	Set 4	CM2-H19 (0.0675 µg)	8 mM	67 °C
TIP48 (to give 3' BamH1 site)	Vent	Set 5	pET21b TIP48 (see below) (0.165 µg)	6 mM	67 °C
BAF53	Taq	Set 6	13436-h02 (0.25 µg)	-	68 °C
BAF53 (no stop codon)	Taq	Set 7	13436-h02 (0.25 µg)	-	68 °C

2.4. Cloning

2.4.1. Restriction digests and alkaline phosphatase treatment

Restriction enzyme digests were performed following the manufacturer's protocols (NEB). For *Nde*I digests, incubations were performed for at least 2 h. Fresh *Nde*I enzyme was replenished every hour.

Some restrictions enzymes, used in this work, were heat inactivated at the temperatures recommended by the manufacturer (NEB). CIP was added straight to the plasmid enzyme digestion reactions (0.5 units per μg of DNA). Incubations were carried out for 1 h at 37 °C.

2.4.2. Agarose gel electrophoresis and gel purification

0.5 % or 0.8 % agarose in 1x TAE buffer was melted by heating in a microwave and cooled to 50 °C before addition of ethidium bromide, to a final concentration of 0.5 μg/ml. Gels were cast in cleaned agarose gel trays and set with well combs. Samples were loaded in 1x DNA loading buffer. 1 μg of 1 kb DNA ladder was also loaded. The gels were run in 1x TAE running buffer at 7 V/cm for 45-60 min. DNA was visualized with a Gene Genius gel imaging system (Syngene).

The appropriate DNA band was sliced out of the gel and placed in an eppendorph tube. It was weighed and 2 volumes of 6 M NaI were added to the gel slice. The mixture was then incubated at 55 °C until the agarose was melted. 10 μl of silica/NaI suspension was added to the melted agarose/NaI mix and incubated at room temperature for 5 min. This mixture was then centrifuged at 18,000 *g* for 30 sec. To the silica bead pellet, 1 ml of Gene Wash was added and mixed gently so as not to shear the DNA. The mixture was then centrifuged at 18,000 *g* for 30 sec and the supernatant removed. This step was repeated once more. The residual buffer was carefully removed and the pellet was air dried for 5 min. The pellet was resuspended gently in the appropriate amount of ddH2O or TE buffer. The suspension was incubated at 55 °C for 20 min and then centrifuged at 18,000 g for 30 sec. The eluted DNA was transferred to a sterile tube and the last step was repeated. The second eluate was combined with the first and the DNA was used for ligations as described below.

2.4.3. Ligations reactions

Ligation reactions were carried out with the T4 ligation kit, the Quick ligation kit or the T4 rapid ligation kit (for cloning into pGEM®-T Easy vectors). These were set up with 50-100 ng of CIP treated vector DNA and the amount of insert DNA added was calculated using Formula 2. The insert to vector ratio normally used was from 3:1 up to 10:1. Reactions were supplemented with T4 ligase enzyme and buffer, as stated by the manufacturers' protocols (see Materials). Control reactions that contained only the CIP treated vector were also set up. Reactions were then incubated as described in the manufacturers' protocols.

$$\text{ng of insert} = \frac{\text{ng of vector x kb size of insert}}{\text{kb size of vector}} \times (\text{insert : vector molar ratio}) \qquad \textbf{Formula 2}$$

2.4.4. Cloning into the pGEM®-T Easy vector

Coding sequences for *TIP48, TIP49* and *BAF53* (section 2.3), amplified by PCR using Taq polymerase, were cloned into the pGEM®-T Easy vector (Figure 2.1). The PCR products were analyzed on a 0.8 % agarose gel and if necessary were excised from the gel and purified. Ligation reactions were set up using components from the T4 rapid ligation kit (Promega); the PCR amplified coding sequence; and the pGEM®-T Easy vector. 100 ng of the pGEM®-T Easy vector was used for all ligation reactions.

Ligation reactions were transformed as described in section 2.2.3 using a blue/white screening assay. Transformed cells were plated on LB/CB agar plates (containing 0.5 mM IPTG and 80 μg/ml X-Gal). Control transformations were also carried out in the absence of DNA or with 40 ng of pUC19 DNA. Selected white colonies were grown in 5 ml LB/CB overnight and plasmid DNA was purified by minipreps. Plasmids were screened by restriction digests, with *EcoR*I, and analyzed by agarose gel electrophoresis. The pGEM®-T Easy clones that were made in this project are summarized in Table 2.7.

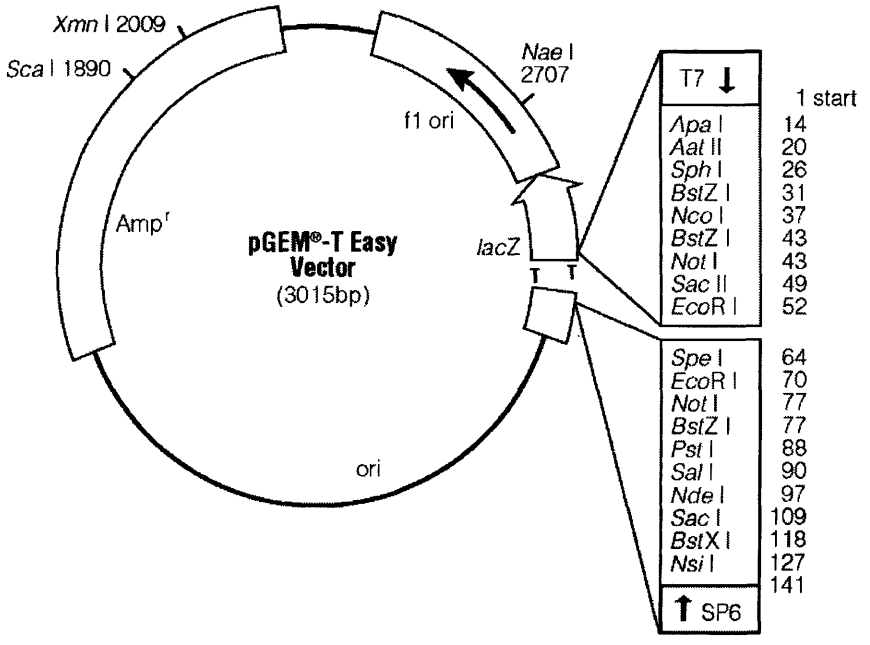

FIGURE 2.1: Restriction map of the pGEM® T-Easy cloning vector

Table 2.7: pGEM®-T Easy clones

Clone	PCR amplified product[a]	Orientation[b]
pGEM-TIP48 (4)	*TIP48* (SET 3)	From SP6 → T7
pGEM-TIP48 (2) (no stop codon)	*TIP48* (no stop codon, SET 4)	From T7 → SP6
pGEM-TIP48 (10)	*TIP48* (SET 5)	From T7 → SP6
pGEM-TIP49 (2)	*TIP49* (SET 1)	From T7 → SP6
pGEM -TIP49 (4) (no stop codon)	*TIP49* (no stop codon, SET 2)	From T7 → SP6
pGEM-TIP49 (3)[c]	SDM of pGEM-TIP49 (2)	From T7 → SP6
pGEM-BAF53 (8)	*BAF53* (SET 6)	From T7 → SP6
pGEM-BAF53 (12)	*BAF53* (no stop codon, SET 7)	From T7 → SP6

a PCR products are the same as those in Table 2.6. The primer sets used are also shown.

b Clones were sequenced (see section 2.4.8) and the orientation of the *TIP48*, *TIP49* or *BAF53* coding sequences in pGEM®-T Easy are indicated, in regards to the position of the T7 and SP6 primer sites (see Figure 2.1).

c pGEM-TIP49 (3) was corrected by site-directed mutagenesis (section 2.4.5) and does not contain a *BamH*1 site.

2.4.5. Cloning into *E.coli* expression vectors

The *TIP48*, *TIP49* and *BAF53* coding sequences were cloned into the *E.coli* expression vectors pET21b+ or pET15b+ vectors (Figures 2.2 and 2.3). The coding sequences were either obtained from the pGEM®-T Easy clones (Table 2.7) or the Vent-PCR amplified products (Table 2.6). The cloning of these constructs is summarized in Table 2.8.

Table 2.8: Cloning of *E.coli* expression constructs

Clone[a]	Source of insert	Restriction enzyme digest[b]	Screening[c]
pET21-TIP48 (16)	Vent amplified *TIP48* (SET 3)	*Nde*I and *EcoR*I	*Nde*I and *EcoR*I
pET21-TIP48-His_6 (12)	pGEM-TIP48 (2)	*Nde*I and *Xho*I	*Nde*I and *Xho*I
pET21-TIP48 (11)	pGEM-TIP48 (10)	*Nde*I and *BamH*I	*Nde*I and *BamH*I
pET21-TIP49 (13)	pGEM-TIP49 (2)	*Nde*I and *BamH*I	*Nde*I and *BamH*I
pET21-TIP49-His_6 (3)	pGEM -TIP49 (4)	*Nde*I and *BamH*I	*Nde*I and *BamH*I
pET21-TIP49 (1)[d]	SDM of pET21-TIP49 (13)	n.a	*Nde*I and *BamH*I
pET21-TIP49-His_6 (2)[d]	SDM of pET21-TIP49-His_6 (3)	n.a	*Nde*I, *BamH*I and *Kpn*I
pET15-His_6-TIP49 (1)	pET21-TIP49 (1)	*Nde*I and *Xho*I	*Nde*I and *Xho*I
pET15-His_6-TIP48 (5)	pET21-TIP48 (16)	*Nde*I and *Xho*I	*Nde*I and *Xho*I
pET21-BAF53	pGEM-BAF53 (8)	*Nde*I and *Xho*I	*Nde*I and *Xho*I
pET21-BAF53-His_6 (4)	pGEM-BAF53 (12)	*Nde*I and *Xho*I	*Nde*I and *Xho*I

a Constructs with pET21 and pET15 in front were cloned using the pET21b+ and pET15b+ vectors, respectively.

b The restriction enzymes shown were used to digest both the insert DNA and the vector DNA, which were then both separated on an agarose gel and purified. These were then used together in ligation reactions.

c The enzymes shown were used to screen purified plasmids from clones that had been selected from LB agar plates after the transformation of the ligation reactions.

d pET21-TIP49 (1) and pET21-TIP49-His_6 (2) were obtained after site-directed mutagenesis of the clones indicated (see table 2.8 and below) and do not contain a BamH1 site. pET21-TIP49-His6 (2) contains a *Kpn*1 site instead.

When pET21-TIP48-His_6 (12) was cloned, the pGEM-TIP48 (2) clone was digested with *Nde*I for 2 h before *Xho*I was added. As there were two *Xho*I sites, one on the 5' end and one on the 3' end of the fragment, cloned into pGEM®-T Easy vector, this digest would ensure that the 5' end was cut with *Nde*I enzyme first so that it could be cloned into pET21b+ that had also been digested with *Nde*I and *Xho*I.

The pET21-TIP49 (13), pET21-TIP49-His_6 (3) and pGEM-TIP49 (2) clones shown in Tables 2.7 and 2.8, were used for site directed mutagenesis to correct errors in primer design (primers IT251 and IT252) and produce new constructs, namely pET21-TIP49 (1), pET21-TIP49-His_6 (2) and pGEM-TIP49 (3). Mutagenic primers were designed using the guidelines from the QuikChange® Site-directed mutagenesis kit booklet (Stratagene) and are shown below.

Primers for pET21-TIP49

5'-CAGGATAAGTACATGAAG**TGA**ATCCGAATTCGAGCTC-3'

5'-GAGCTCGAATTCGGAT**TCA**CTTCATGTACTTATCCTG-3'

Primers for pET21-TIP49-His_6

5'-GCAGGATAAGTACATGAA**GGTACC**GAATTCGAGCTC-3'
*Kpn*I
5'-GAGCTCGAATTC**GGTACC**TTCATGTACTTATCCTGC-3'
*Kpn*I

Primers for pGEM®-T Easy-TIP49

5'-CAGGATAAGTACATGAAG**TGA**ATCCTCTCAATCACTAGTG-3'

5'-CACTAGTGATTGAGAGGAT**TCA**CTTCATGTACTTATCCTG-3'

The PCR reactions were carried out under the conditions shown in Table 2.9 along with a control reaction using the pWhitescript 4.5kb plasmid and control primers, under conditions that were described in the protocol (Stratagene). The plasmid DNA in the PCR reactions was digested with *Dpn*I for 1 h at 37 °C, to remove the parental

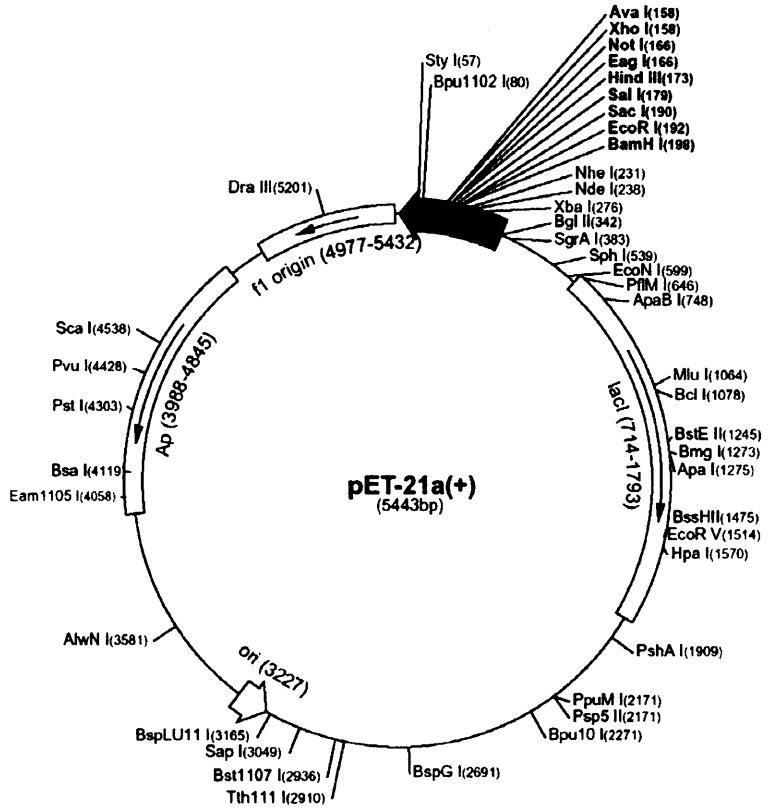

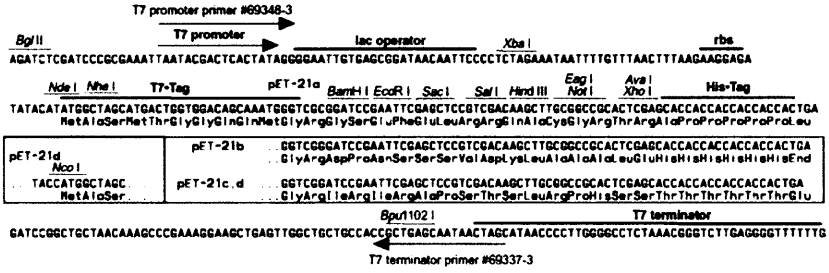

pET-21a-d(+) cloning/expression region

FIGURE 2.2: Restriction map of the pET21a-d+ *E.coli* expression vector

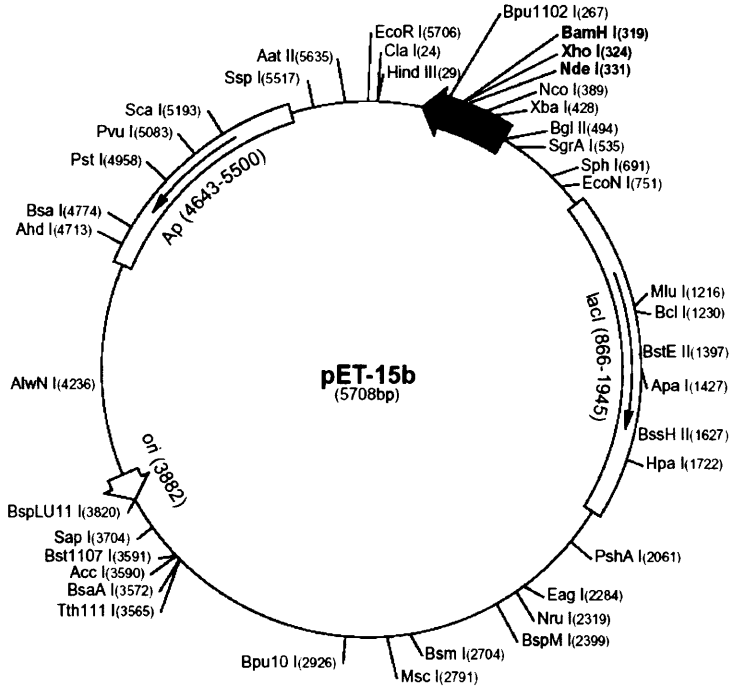

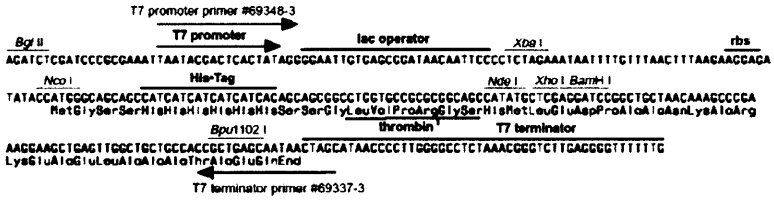

pET-15b cloning/expression region

FIGURE 2.3 : Restriction map of the pET15b+ *E.coli* expression vector

template DNA. 1 µl of the *Dpn*I-treated DNA was transformed into XL1-Blue cells as described by the manufacturers protocol (Stratagene). Colonies were selected from agar plates and the plasmids were purified and screened using restriction enzymes shown in Table 2.8. All three constructs had the *BamH*1 site removed after mutation. This helped identify mutated clones by restriction enzyme digests with *BamH*1.

Table 2.9: PCR reaction program for SDM of pET21-TIP49 and pGEM® T Easy-TIP49 clones

Temperature	Time	
95 °C	30sec	
95 °C	30sec	18 cycles
55 °C	1min	
68 °C	2 min/kb plasmid length (13 min 36sec)	
4 °C	Overnight	

2.4.6. Site-directed mutagenesis of *TIP48* and *TIP49* clones in the Walker B motifs

Primers were created to mutate the aspartic acid residue to an asparagine residue in the Walker B motifs of the TIP48 (aa 299) and TIP49 (aa 302) sequences, within the different constructs created. The TIP49 constructs that were mutated with the Quick® change site mutagenesis kit were: pET21-TIP49 (1); pET21-TIP49-His_6 (2) and pET15 His_6-TIP49 (1), with the first set of primers shown below. The pET21-TIP48-His_6 (12) construct was mutated with the second set of primers shown below. The conditions for the PCR reaction are shown in Table 2.10.

TIP49 SDM primers

5'-GTGCTGTTTGTTAATGAGGTCCACATGCTGGAC-3'

5'-GTCCAGCATGTGGACCTCATTAACAAACAGCAC-3'

TIP48 SDM primers
5'- GGAGTGCTGTTCATCAACGAGGTCCACATGCTGGAC-3'

5'-GTCCAGCATGTGGACCTCGTTGATGAACAGCACTCC-3'

TABLE 2.10: PCR reaction program for SDM of pET21/15 TIP48 and TIP49 constructs

Temperature	Time	
95 °C	30sec	
95 °C	30sec	12 cycles
65 °C	1min	
68 °C	6 min 48 sec	
4 °C	Overnight	

2.4.7. Cloning of pET21-TIP48/TIP49-His_6 dual expression plasmid

A pET21-TIP48/TIP49-His_6 dual expression plasmid was created to allow the co-expression of TIP48 and TIP49-His_6 in *E.coli*. A schematic for this cloning is shown in Figure 2.4. pET21-TIP48 (11) construct was digested with *Mlu*I and *BamH*I restriction enzymes. The pET21-TIP49-His_6 (2) construct was digested with the *Mlu*I and *Bgl*II enzymes. The fragments containing the TIP48 and TIP49 coding sequences were gel purified and ligation reactions were set up. Transformants were screened by restriction digestion that confirmed the presence of both TIP48 and TIP49 coding sequences.

2.4.8. Sequencing of TIP48 and TIP49 clones

For sequencing pGEM® T Easy clones the standard primers for the T7 promoter, SP6 promoter or the pUC/M13 forward and reverse sequences were used. For all pET21b+

and pET15+ clones the primers for the T7 promoter and terminator were used. The following internal primers for the *TIP49* and *TIP48* sequences were designed and also used:

TIP49

5'-AAGTCACAGAGCTAACTC-3'	IT261 (start at 401 bp)
5'-GAAGACAGAAATCACAGA-3'	IT262 (start at 801 bp)
5'-TCACATCTCCAGCTTCTA-3'	IT263 (start at 571 bp - reverse)

TIP48

5'-GAGACGGAGATCATCGAA-3'	IT264 (start at 401 bp)
5'-AGATCAAGTCAGAAGTCC-3'	IT265 (start at 801 bp)
5'-CCTTGTCGATGGTGATCA-3'	IT266 (start at 590 bp - reverse)
5'-CACAGAGATGGAGACCAT-3'	IT275 (start at 500 bp)
5'-ACGGTTGGTGGCCATGAT-3'	IT276 (start at 800 bp)
5'-GATGAACAGCACTCCAGG-3'	IT277 (start at 880 bp - reverse)

500 ng of DNA/6 µl of ddH_2O was sent for each sequencing reaction at the Wolfson Institute of Biomedical Research (UCL) with 2 pmols/µl of primer concentration, which gave efficient readings of 400-600 bases. Another company (MWG Biotech) was also used for which 1 µg of vacuum dried DNA was sent for each reaction. This sequencing gave readings >800bp. Sequences were checked against the published sequences of *TIP49* and *TIP48* from PubMed, using the BCM search launcher (http://searchlauncher.bcm.tmc.edu/).

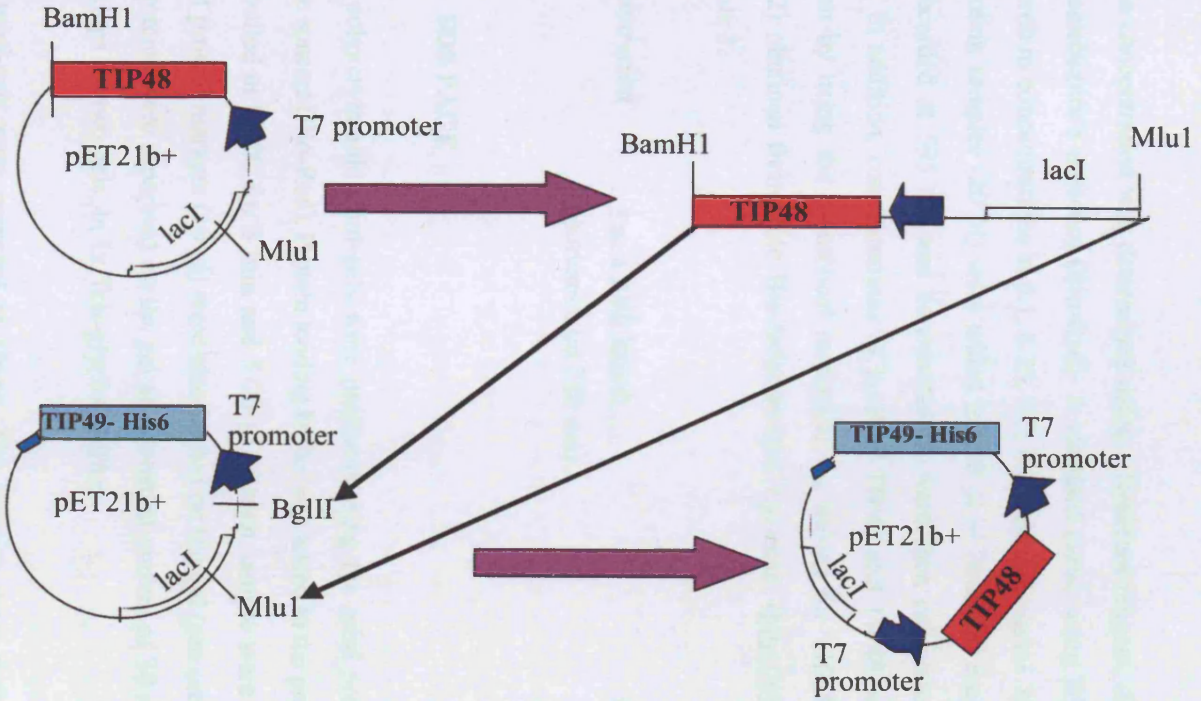

Figure 2.4: **Schematic representation of the cloning performed to obtain the pET21-TIP48/TIP49-His_6 dual expression plasmid**

2.5 Protein techniques

2.5.1 Protein concentration

Protein concentration was determined using a Bradford reagent, diluted as specified by the manufacture's protocol (Bio-Rad). A standard curve using BSA protein was made with protein concentrations at 0.1, 0.25, 0.5, 0.75 and 1.0 mg/ml. Either the standards or the protein samples (20 µl) were added to 980 µl of Bradford reagent. The absorbance was recorded at 595 nm and concentrations were then calculated using the standard curve. In addition, concentrations of purified TIP48 and TIP49 were also measured at 280 nm by using the theoretical molecular ε_{280} values for TIP48 (19424) and TIP49 (18432) obtained from Pole Bio-Informatique Lyonnais (http://pbil.univ-lyon1.fr) and Formula 3.

$$\text{Concentration} = \frac{\varepsilon_{280} \times \text{path length}}{\text{Absorbance (at 280 nm)}} \qquad \textbf{Formula 3}$$

2.5.2. SDS PAGE

12 % polyacrylamide mini-gels were prepared using the mini protean II gel cast with 0.7 mm spacers (Bio-Rad). Protein loading buffer was added to the protein samples. Samples were boiled at 98 °C for 3 min and 5-20 µl of each sample were loaded per well. Pre-stained protein markers (10 µl) were also loaded on the gel (see section 2.1.3, Materials). The proteins were separated on the gel at a constant current of 30 mA for single gels or 60 mAmps for two gels, in 1x Tris-glycine buffer.

18 % mini-gels were prepared as above. The proteins were separated overnight at a constant voltage of 44 V. The voltage was increased the next day to 150 V and the samples were separated for a further 4 h until the 48 and 62 kDa molecular mass markers had separated sufficiently.

Proteins on the gels were stained with Coomassie brilliant blue and destained with warmed destain solution for 2-3 h. Silver staining of gels was carried out using a silver staining kit (Sigma) as described in the manufacturers protocol.

2.5.3. Immunoblotting

Samples and pre-stained protein markers (10 µl) were separated by 12 % SDS PAGE. Gels were then incubated in transfer buffer for 20 min. Either PVDF or nitocellulose membranes were used for blotting and were also incubated in transfer buffer. Only PVDF membrane was soaked in methanol for 30 sec prior to incubation in transfer buffer. Proteins were transferred either using a wet transfer mini-blot apparatus (BioRad) or a semi-dry transfer apparatus (Bio-Rad). Wet transfers were carried out at 4 °C for 1.5 h at 20 V and semi-dry transfers were carried out at room temperature at 15 V for 30 min.

Following transfer, the membrane was incubated with blocking buffer for 1 h at room temperature, on a rotating platform. It was then washed with TBS-Tween for 30 min with frequent changes of buffer. It was then incubated with the primary antibody, either for 1 h at room temperature or overnight at 4 °C. The membrane was washed with TBS-Tween and incubated with specific secondary antibodies, at room temperature, for the times specified below.

Different types of secondary antibodies were used throughout the project and therefore membranes were developed by different techniques. Membranes incubated with secondary antibodies conjugated with alkaline phosphatase were developed with BCIP/NBT as specified by the manufacturer (Sigma). Secondary antibodies with horseradish peroxidase conjugates (HRP) were developed with ECL plus reagents as specified by the manufacturer (Amersham) and visualized with a LAS-1000 plus image analyzer (FUJI-FILM). Membranes that were to be visualized using the Odyssey Infrared Imaging system (LI-COR Biosciences) were incubated for 40 min with Alexa

Fluor 680-labelled goat anti-mouse IgG antibody or IRDye 38-labelled goat anti-rabbit IgG antibody, washed for 2-3 h with TBS-Tween and developed.

Antibody dilutions

Penta-His monoclonal mouse (1/1000). (This antibody was made up in PBS-Tween and all washes were also in PBS-Tween).
Anti-TIP48 rabbit polyclonal (1/1000) (section 2.10)
Anti-TIP49 rabbit polyclonal (1/750) (section 2.10)
Anti-TIP49 W1B3 mouse monoclonal antibody (1/1000)
Anti-BAF53 rabbit polyclonal (1/1000)
Anti-β-catenin mouse monoclonal (1/1000)
Alkaline Phosphatase conjugated anti-Mouse IgG (1/10,000)
HRP conjugated anti-Rabbit IgG (1/50,000)
HRP conjugated anti-Mouse IgG (1/25,000)
Alexa Fluor 680-labelled goat anti-mouse IgG antibody (1/10,000)
IRDye 38-labelled goat anti-rabbit IgG antibody (1/10,000)

2.5.4. Ammonium sulphate precipitation

Protein samples were mixed using a magnetic stirrer at 4 °C. Ammonium sulphate that had been ground finely was slowly added to the protein sample. Sometimes samples were left stirring, overnight at 4 °C, to allow efficient precipitation. For every gram of ammonium sulphate added, 10 μmoles of NaOH were added at the end of the procedure and the sample was mixed for a further 10 min at 4 °C. Samples were then centrifuged at 125,000 *g* for 1 h in a 45Ti rotor (Beckman ultracentrifuge), to pellet the precipitated protein.

2.6. Protein expression in E.coli

The pET (21/15) TIP48, TIP49 and BAF53 clones were transformed in *E.coli* BL21 (DE3) Gold or BL21 (DE3) Gold pLysS strains (section 2.22-2.2.3). Transformations with the BL21 Gold strain were carried out in the presence of 1 % glucose, included both during transformation and in the LB/CB agar plates. BL21 Gold pLysS transformed cells were plated on LB/CB agar plates that additionally contained CM at a final concentration of 25 μg/ml. Colonies grown overnight at 37 °C on LB agar plates, were used to prepare overnight cultures. BL21 Gold colonies were grown in LB media in the presence of 100 μg/ml CB and 1 % glucose. BL21 Gold pLysS colonies were grown in LB containing 100 μg/ml CB and 25 μg/ml CM.

Fresh culture was prepared by using the appropriate amount of the overnight culture to give a final OD_{600} of 0.1, as calculated by Formula 4. This culture was grown at 37 °C for 2-2.5 h until the OD_{600} reading was approximately 0.8. One ml aliquots were collected, before induction for analysis by SDS-PAGE. The remaining culture was then induced by addition of IPTG at 1 mM final concentration. The induction was carried out for 3-4 h and one ml aliquots were taken at 2, 3 and 4 h to check the level of induction. The samples collected were centrifuged at 1500 *g* for 4 min and the cell pellets were then resuspended in 200 μl of protein loading buffer. The remaining induced culture was sedimented at 3000 *g* for 15-25 min and the pellet was frozen at -20 °C.

$$\text{Volume to be inoculated} = \frac{0.1 \times \text{culture volume}}{\text{OD of overnight culture}} \qquad \textbf{Formula 4}$$

Inductions of TIP48, TIP49, BAF53 and TIP48/TIP49 co-expression were carried out in both strains at either 30 °C or 37 °C to test the optimum temperature for the protein expression and solubility (see below). Different concentrations of IPTG were also tested from 0.1-1 mM.

The pET30-β-catenin-Hi_6 construct, which contained the coding sequence for the mouse β-catenin protein but also contained a segment of the human β-catenin protein (cloned at the *Nco*I restriction enzyme site), was transformed into *E.coli* BL21 (DE3) Gold cells. Transformed cells were plated on LB agar plates containing 30 μg/ml of kannamycin and 1 % glucose. Colonies grown overnight on LB agar plates at 37 ℃, were used to prepare overnight LB cultures containing 30 μg/ml of kannamycin and 1 % glucose. Fresh culture was prepared by using the appropriate amount of the overnight culture, as described above. Cells were induced with IPTG at 1 mM final concentration and left to grow at 30 ℃ for 4 h. Inductions were analyzed and induced cells were harvested as described above.

2.7. Cell lysis and protein purification

2.7.1 Purification of TIP48-His_6 and TIP48D299N-His_6 under native conditions

The pET21-TIP48-His_6/ pET21-TIP48D299N-His_6 constructs were transformed into BL21 (DE3) Gold pLysS strain, as described in Sections 2.2.3 and 2.6. Transformed cells were induced with 1 mM IPTG at 30 °C for 4 h. Induced cells were pelleted, frozen overnight at -20 ℃ and thawed out in the presence of lysis buffer (25 ml per litre of induced cells). Protease inhibitor tablets (one per 25 ml of lysis buffer) and 0.2 % NP40 were added to the cell suspension. Cells were lysed following incubation for 90 min at 4 °C and soniciated three times for 10 sec at outputs ranging from 10-14 (Soniprep 150, MSE). Lysates were cleared by centrifugation at 70,000 *g* for 30 min, in a 45Ti rotor.

The cleared lysates were loaded onto a Talon column equilibrated in lysis/Talon buffer. One ml of talon resin was used per 5 ml of lysate. Non-specifically bound proteins were washed with 20 mM imidazole in Talon buffer. The bound His_6 tagged protein was eluted with a 20-500 mM imidazole gradient, in Talon buffer. Peak fractions were collected and dialysed overnight in Buffer R. The dialysed protein sample was loaded onto a MonoQ FPLC anion exchange column and the protein was eluted with a 0.1-1 M

NaCl gradient in Buffer R. The purified protein was then dialysed in buffer R and either fractionated further on a size exclusion chromatography column (Superdex 200 FPLC), or on a ssDNA cellulose column. Most of the protein was collected in the flow-through from the ssDNA cellulose column and any protein bound to the column was eluted with 1 M NaCl in Buffer R. The flow-through fraction was concentrated using an Amicon® Ultra-15 Centrifugal filter and fractionated further on a Superdex 200 FPLC column.

2.7.2 Purification of TIP48-His_6 under denaturing conditions

TIP48-His_6 was expressed in BL21 (DE3) Gold pLysS and cells were lysed as described in section 2.7.1. The pellets from the lysed cells were solubilized in lysis buffer containing 6 M urea. The urea-protein sample was then sonicated as described in section 2.7.1 and centrifuged at 66,000 *g* for 30 min in a 70Ti rotor. The supernatant was loaded onto a Talon column, pre-equlibriated with lysis/Talon buffer, containing 6 M urea. The bound protein was refolded by removing the urea using a step-gradient, from 6 M urea to 4 M, 2 M and then talon buffer containing no urea. The refolded protein was then eluted with 500 mM imidazole in Talon buffer. Fractions containing the protein were dialyzed into buffer R^2, concentrated as described in section 2.7.1 and fractionated further on a Superdex 200 FPLC column.

2.7.3 Purification of His_6-TIP49 and His_6-TIP49D302N under native conditions

The pET15 His_6-TIP49/ pET15 His_6-TIP49D302N constructs were transformed into BL21 (DE3) Gold cells, as described in Sections 2.2.3 and 2.6. Cells were induced for protein expression with 1 mM IPTG at 30 °C for 3 h. Induced cells were pelleted, frozen overnight at -20 °C and thawed out in the presence of lysis buffer (25 ml per litre of induced cells). Protease inhibitor tablets (one per 25 ml of lysis buffer), 0.5 % NP40 and 0.75 mg/ml lysozyme were added and the cells were lysed following incubation for 60 min at 4 °C and soniciated, as described in section 2.7.1. Lysates were then centrifuged at 70,000 *g* for 30 min in a 45Ti rotor.

The cleared lysate was loaded onto a Talon column, pre-equilibrated in lysis/Talon buffer. Non-specifically bound proteins were washed with 20 mM imidazole in Talon buffer. The bound His_6 tagged protein was eluted with a 20-500 mM imidazole gradient in Talon buffer. Peak fractions were collected and dialysed overnight, into Buffer H. The dialysed sample was fractionated further on a hydroxyapatite column. Bound proteins were eluted with a 10-600 mM potassium phosphate gradient in Buffer H. Peak fractions were dialysed into Buffer R and fractionated further on either (a) a Superdex 200 FPLC column or (b) a ssDNA cellulose column. The flow-through from the ssDNA cellulose column was concentrated as described in section 2.7.1 and fractionated further on a Superdex 200 FPLC column. Any remaining protein on the ssDNA cellulose column was eluted with 1 M NaCl in Buffer R.

2.7.4 Purification of TIP49-His_6 and TIP49D302N-His_6 under denaturing conditions

The pET21 TIP49-His_6 (2)/ pET21 TIP49D302N-His_6 constructs were transformed into BL21 (DE3) Gold cells (section 2.2.3 and 2.6) and cells were induced at 30 °C for 4 h with 1 mM IPTG. Induced cells were pelleted, frozen overnight at -20 °C and thawed out in the presence of lysis buffer (25 ml per litre of induced cells). Protease inhibitor tablets (one per 25 ml of lysis buffer), 0.1 % NP40 and 0.75 mg/ml lysozyme were added to the cell suspension. Soluble TIP49-His_6 and TIP49D302N-His_6 were obtained, after sonication and clarification of the cell extract by centrifugation as in section 2.7.1. However, neither protein bound to the Talon column. The insoluble pellet was therefore resuspended in lysis buffer containing 6 M urea, sonicated (section 2.7.1) and centrifuged at 66,000 *g* for 30 min in a 70Ti. The supernatant was loaded onto a Talon column pre-equilibriated with Talon buffer containing 6 M urea and bound His_6 protein was eluted with 500 mM imidazole in Talon buffer, containing 6M urea. The eluted protein was dialyzed by stepwise dialysis to remove the urea; using Buffer R^2 containing 4 M urea, which was changed to buffer R^2 containing 2 M urea and lastly the protein was dialyzed overnight in buffer R^2

containing no urea. The dialyzed protein sample was then centrifuged at 66,000 *g* for 30 min in a 70Ti to remove any insoluble protein after refolding. The soluble protein was concentrated (section 2.7.1) and fractionated further on a Superdex 200 FPLC column.

2.7.5 Purification of co-expressed TIP48 and TIP49-His_6 complex under denaturing conditions

The co-expression construct prepared as described in section 2.4.7. was transformed into BL21 (DE3) Gold pLysS cells (section 2.2.3 and 2.6) and protein expression was induced at 30 °C for 4 h with 1 mM IPTG. Induced cells were pelleted, frozen overnight at -20 °C and thawed out in the presence of lysis buffer (25 ml per litre of induced cells). Protease inhibitor tablets (one per 25 ml of lysis buffer) and 0.2 % APO128 were added to the cell suspension. Cells were lysed following incubation for 60 min at 4 °C and soniciated as described in section 2.7.1. Lysed cells were centrifuged at 66,000 *g* for 30 min in a 70Ti. However, no soluble TIP48 and TIP49-His_6 were obtained after lysis. The insoluble fraction was resuspended in lysis buffer containing 6 M urea, sonicated (section 2.7.1) and centrifuged at 66,000 *g* for 30 min in a 70Ti rotor. The soluble fraction was then put through a stepwise dialysis procedure (section 2.7.4) to remove the urea. The insoluble pellet from the last step was solubilized further by resuspension in lysis buffer containing 8 M urea. This was sonicated, clarified by centrifugation as above and refolded by stepwise dialysis (section 2.7.4).

The dialyzed samples of the refolded protein from 6 and 8 M urea were centrifuged at 66,000 g for 30 min in a 70Ti rotor for 30 min, and loaded onto Talon columns, pre-equlibriated with lysis/Talon buffer. Protein was eluted with a 20-500 mM imidazole gradient in lysis buffer. An equimolar complex was obtained, which was dialyzed in Buffer R^2 and fractionated further on a Superdex 200 column, pre-equilibrated with Buffer R^2 containing 0.05 % Triton X-100.

2.7.6 Purification of TIP48-His_6/TIP49 complex under native conditions

Partial purification of TIP49 was as follows: the pET21-TIP49 construct was transformed into BL21 (DE3) Gold cells (section 2.2.3 and 2.6). Cells were induced as described in section 2.7.4, pelleted, frozen overnight at -20 °C and thawed out in the presence of Buffer R^2 (12.5 ml per litre of induced cells). Protease inhibitor tablets (one per 25 ml of lysis buffer), 0.2 % NP40 and 0.75 mg/ml lysozyme were added to the cell suspension. Cells were lysed following incubation for 60 min at 4 °C and soniciated, as described in section 2.7.1. Lysed cells were centrifuged at 66,000 *g* for 30 min in a 70Ti rotor.

To remove cellular DNA the cleared lysate was loaded onto a DEAE column, pre-equilibrated in Buffer R^2. Protein did not bind to the column under these conditions, as shown by SDS PAGE, and was collected in the flow through fraction. DNA however, did bind to the column and the presence of DNA in the different fractions, were analyzed by adding ethidium bromide to 5 µl of each fraction to a final concentration of 0.1 µg/ml and visualizing the samples under a UV light. Very little bacterial DNA was present in the flow-through fraction, which was fractionated by 20 % ammonium sulphate precipitation followed by 70 % ammonium sulphate precipitation.

The 20-70 % ammonium sulphate pellet was resuspended and dialyzed in Buffer H. The soluble fraction was loaded onto a SP sepharose column, connected to a hydroxyapatite column. Once the sample was loaded and the columns washed with Buffer H, the SP sepharose column was removed and the protein was eluted from the hydroxyapatite column with a 10-600 mM potassium phosphate gradient in Buffer H. Fractions containing TIP49, analyzed by SDS-PAGE, were pooled and precipitated with 70 % ammonium sulphate.

The ammonium sulphate pellet was resuspended, dialyzed into lysis/Talon buffer and centrifuged at 61,000 *g* for 30 min in a 70.1 Ti rotor to remove insoluble protein. A fraction of the sample was visualized by SDS-PAGE. The amount of TIP49 in the

sample was quantified by measuring the protein concentration and then quantifying the percentage of TIP49 in the sample from the gel, using the gel quantification program Gene tools (Syngene). The TIP49 sample was then incubated with TIP48-His_6 that had been passed through a ssDNA cellulose column (section 2.7.1) and dialyzed into Talon buffer. TIP49 was incubated in a 2:1 ratio with the TIP48-His_6 protein on ice on for 30 min, and the mixture was loaded onto a Talon column, pre-equilibrated with Talon buffer. The column was washed with 10 mM imidazole in Talon buffer. The bound proteins were then eluted with a 10-500 mM imidazole gradient in Talon buffer. The presence of TIP49 and TIP48-His_6 in the eluted fractions was analyzed by 18 % SDS PAGE.

Fractions containing both TIP49 and TIP48-His_6 were dialyzed in Buffer R and loaded onto a ssDNA cellulose column. The flow through was collected, concentrated and fractionated further on a Superdex 200 FPLC column, which had been pre-equilibrated with Buffer R containing 0.05 % Triton X-100.

2.7.7 Purification of β-catenin-His_6

The β-cateinin expression construct was transformed into a BL21 Gold strain, as described in Sections 2.2.3 and 2.6. Cells were induced for protein expression with 1 mM IPTG at 30 °C for 4 h. Induced cells were pelleted, frozen overnight at -20 °C and thawed out in the presence of lysis buffer (25 ml per litre of induced cells). Protease inhibitor tablets (one per 25 ml of lysis buffer), 0.2 % NP40 and 0.75 mg/ml lysozyme were added to the cell suspension. Cells were lysed following incubation for 60 min at 4 °C and soniciated, as described in section 2.7.1. Lysed cells were centrifuged at 70,000 *g* for 30 min in a 45Ti rotor.

The cleared lysate was loaded onto a Talon column, pre-equilibrated in lysis/Talon buffer. Non-specifically bound proteins were washed with 20 mM imidazole in Talon buffer. The bound His_6 tagged protein was eluted with a 20-500 mM imidazole gradient

in Talon buffer. Peak fractions were collected and dialysed overnight into Buffer R. The dialysed sample was fractionated further on a MonoQ FPLC column. Bound proteins were eluted with a 0.1-1 M NaCl gradient in Buffer R. Peak fractions were dialysed back into Buffer R and fractionated further on a Superdex 200 FPLC column.

2.7.8 Size exclusion chromatography experiments

Purified protein obtained as described in the previous sections (2.7.1-2.7.7) were dialyzed in Buffer R and concentrated using Amicon® Ultra-15 Centrifugal filters to concentrations of 1 mg/ml or above. 500 µl of the sample was filtered using a 0.2 µM filter (Millipore) and loaded onto a Superdex 200 FPLC size exclusion chromatography column, pre-equilibrated in Buffer R or as otherwise stated (section 2.7.1-2.7.7).

For experiments with the purified His_6-TIP49 and TIP48-His_6 proteins in the presence of nucleotide cofactors, 200 µl of sample was used for each chromatography run. The column was pre-equilibrated with the Buffer R containing 0.1 mM adenine nucleotide, when possible. If the protein was incubated with $MgCl_2$ and adenine nucleotides then the column was pre-equlibriated with Buffer R^1 containing 2 mM $MgCl_2$ and 0.1 mM adenine nucleotide. The protein sample was supplemented with the adenine nucleotide at 1 mM final concentration (or 0.2 mM AMPPNP – see Chapter 5), and incubated for 5 min on ice. If $MgCl_2$ was to be used, then 2 mM of it was added after incubation with the adenine nucleotide and the sample was incubated for a further 5 min on ice. Samples were then filtered and fractionated on the Superdex 200 FPLC column.

Molecular size chromatography markers (Bio-Rad) were also fractionated on the Superdex 200 FPLC column after pre-equilibrating the column with buffer R. The protein markers were Thryoglobin (670 kDa), Gamma Globin (158 kDa), Ovalbumin (44 kDa), Myoglobin (17 kDa) and Vitamin B12 (3.5 kDa). After fractionation of the markers a K_{AV} value, for each marker was calculated using Formula 5:

$K_{AV} = (V_E - V_0) / (V_t - V_0)$ **Formula 5**

Where V_E = Elution volume (ml) of the marker
V_0 = Void volume of the column
and V_t = total volume of the column (24 ml for Superdex 200 HR)

The K_{AV} values were plotted against the log values of the molecular mass markers to obtain a calibration curve. The relative molecular masses of the proteins fractionated on the Superdex 200 FPLC, were then calculated from this calibration curve.

2.8. Biochemical assays

2.8.1 DNA substrates

ϕX174 virion ssDNA was used for preparing the helicase substrate and was used as a substrate in ATPase assays (sections 2.8.2 and 2.8.4). It was diluted in buffers/reactions as indicated for these experiments. Supercoiled pUC19 plasmid was prepared from *E.coli* cultures by Midi-preps. pUC19 was linearized by digestion with *EcoR*I. The linearized fragment was separated and purified from an agarose gel using a gel extraction kit (Qiagen). Both forms of pUC19 were used in ATPase assays (section 2.8.2).

Mobile Holliday junction was made with the following primers:

IT01 GACGCTGCCGAATTCTACCAGTGCCTTGCTAGGACATCTTTGCCCACCTGCAGGTTCACCC
IT07 TGGGTGAACCTGCAGGTGGGCAAAGATGTCCTAGCAATGTAATCGTCAAGCTTTATGCCGTT
IT08 CAACGGCATAAAGCTTGACGATTACATTGCTAGGACATGCTGTCTAGAGGATCCGACTATCGA
IT09 ATCGATAGTCGGATCCTCTAGACAGCATGTCCTAGCAAGGCACTGGTAGAATTCGGCAGCGT

The IT07 primer was labeled using an equimolar amount of [γ-^{32}P]-ATP. The reaction mixture contained 80 pmoles of IT07 oligo and 80 pmoles of [γ-^{32}P]-ATP, 1x T4 PNK buffer and 10 units of PNK. The final volume of the reaction was 20 µl made up with

ddH_2O and incubated at 37 °C for 1 h. The radioactive reaction was applied to a micro-spin column (Amersham) and centrifuged at 735 *g* for 2 min to remove unincorporated [γ-^{32}P]-ATP label. The labeled oligo was collected at the bottom of the tube. The annealing reaction was performed by adding 80 pmoles each of IT01, IT08 and IT09 oligos to the labeled IT07 oligo. The reaction included 1x SSC buffer and was made up to 50 µl with ddH_2O. Alongside this reaction, another annealing reaction was also set up that contained all the oligos including IT07 that had not been radioactively labeled. Both reactions were heated at 95 °C for 3 min and then the heat block was set to room temperature and allowed to cool overnight.

The four-way junction was purified by adding DNA loading buffer to the samples, supplemented with 0.2 % SDS. They were then loaded onto an 8 % mini native TBE acrylamide gel and the sample was separated at 8 V/cm for 2 h. To identify the band containing the junction the gels were exposed onto a Biomax TM MS double emulsion film (Kodak) for 0.5-2 min and developed. The radioactively labeled junction was sliced out of the gel as was the cold junction, which would have migrated in the same position as the labeled junction. DNA was electro-eluted from the gel in 0.5 M TBE (Schleicher and Schull, Biotrap Multi-kit) and then dialyzed in dH_2O overnight. Junctions were stored at 4 °C and used in ATPase and branch migration assays (sections 2.8.2 and 2.8.5).

2.8.2. ATPase assays

Master mixtures and single reactions

Master mixtures for 10 or 20 µl single reactions contained: 1x ATPase reaction buffer; BSA added to a final concentration of 0.1 mg/ml; DTT added to a final concentration of 1 mM; ATP added to a final concentration of 1 mM; and [α-^{32}P]-ATP added to a final concentration of 0.0025 µCi/µl. If DNA substrates were used then they were added to a final concentration of 5 ng/µl.

The master mixture was made up with ddH_2O to one ninth of the final volume, and 9 or 18 µl was then aliquoted into each tube. Protein was then added to each reaction tube to a final concentration, as stated in the results (normally 1 µM final concentration) and the reactions were then made up to 10 or 20 µl. A control reaction that did not include any protein was also prepared. Reactions were incubated for the specific time at 37 °C and stopped by adding 5 µl of 0.5 M EDTA (pH 8.0). Control reactions with RuvAB were also carried out, in RuvAB buffer with 0.64 µM of RuvA and 1.08 µM of RuvB and reactions carried out as described above.

Time courses

For time courses a master mixture was made with all the components as described above and was split into two, so that one was used as a control reaction. Both master mixtures were made up with ddH_2O to the final volume, minus the volume of the protein that was to be added. These reactions were pre-incubated at 37 ° C for 5 min. The protein was then added, (ddH_2O was added to the control reaction), mixed and then a 10 µl aliquot was taken from the reaction and added to a tube containing 2.5 µl of 0.5 M EDTA (pH 8.0). This was the 0 min time point of the reaction. The rest of the reaction was incubated at 37 °C and 10 µl aliquots were taken at specific time points and stopped by adding them to EDTA.

Optimizing of conditions and pre-incubation with DNA/β-catenin

For experiments in which $MgCl_2$/ATP concentrations were optimized (section 4.7), the protein was added to ATPase Reaction Buffer B. $MgCl_2$/ATP/[α-^{32}P]-ATP mixture was added to reactions, at various concentrations of $MgCl_2$ or ATP. To optimize pH or NaCl conditions, the protein was added to reaction buffer that had various concentrations of NaCl or various pH/buffer conditions. $MgCl_2$/ATP/[α-^{32}P]-ATP mixture was then added at the optimal concentrations. Reactions were incubated at 37 °C for 20 min and stopped as above.

For experiments in section 4.7, 1x ATPase Reaction Buffer C was used for incubation of the purified TIP48 and TIP49 proteins at various concentrations, either individually or

together. Reactions were incubated for 10 min on ice and then ATP/$MgCl_2$/[α^{32}P]-ATP mixture was added to each reaction to give a final concentration of 2 mM ATP and 5 mM $MgCl_2$. Reactions were incubated at 37 °C for 10 min after which, half the reaction was stopped with EDTA. The remaining reaction was incubated for a further 10 min, which was then stopped with EDTA.

For assays with DNA (section 4.7), TIP48 or TIP49 were pre-incubated with DNA (5 ng/µl) in ATPase Reaction buffer C. Reactions were incubated for 5 min on ice and then the other protein (TIP48 or TIP49) was added and the reaction was incubated for a further 5 min. ATP/$MgCl_2$/[α^{32}P]-ATP mixture was then added to each reaction to give a final concentration of 2 mM ATP and 5 mM $MgCl_2$ and reactions were incubated for 20 min at 37 °C and were stopped as described above.

For reactions with β-catenin, 1 µM of TIP48, TIP49 or the TIP48/49 complex were incubated with varying concentrations of β-catenin (see Chapter 4), in Reaction buffer B. Reactions were incubated on ice for 10 min. ATP/$MgCl_2$/[α^{32}P]-ATP mixture was then added to each reaction to give a final concentration of 1 mM ATP and 2 mM $MgCl_2$. Reactions were incubated for 20 min at 37 °C and were stopped as described above.

Developing and analyzing data

1 µl from each reaction was spotted onto TLC PEI plates, which were developed with ATPase running buffer for 2 h. Plates were then dried and exposed on a phosphorimager screen (FUJI-FILM) and developed with a FUJI-FILM FLA 2000 phosphorimager. Spots were quantified using the FUJI-FILM Image Gauge program. Briefly, the background signal from the control reaction was subtracted from all the other spots. Then, a value for the total amount of ATP in each reaction was obtained by adding the pixels from both the ATP and ADP spots, from each reaction spotted. The total amount of pixels from the ADP spot were then divided by the total amount of ATP (ATP + ADP spots) and a percentage of the amount of ATP hydrolyzed were obtained. This was

converted into moles of ATP hydrolyzed and then converted into moles of ATP hydrolyzed per mole of protein, as described below.

The molecular masses for TIP48 and TIP49 were approximately 50 kDa and this was used to calculate the concentration of protein added to reactions, and the amount of ATP hydrolyzed per mole of protein. The molecular mass of 50 kDa (monomeric mass) was used to calculate the concentration of the TIP48/TIP49 complex. The molecular mass of β-catenin is approximately 85 kDa and this was used to calculate the concentration of protein added to reactions.

2.8.3. ATP binding assays with [γ^{32}P]-2 azido-ATP

1-2 μg of protein was added to ATP binding buffer that contained 2 mM $MgCl_2$ and 1 μCi [γ^{32}P] 2 azido-ATP and the reaction was left at room temperature for 3 min. (Reactions were kept covered throughout the incubation to prevent exposure of [γ^{32}P]-2 azido-ATP to UV light). Reactions were pipetted into multi-well plates and exposed to UV light from 2 x 8 W lamps, which gave an intensity of 1800 μW/cm^2, at a distance of 15 cm. Samples were exposed for 30-60 sec. Reactions were then pipetted back into tubes and to each reaction 200 μl of 10 % TCA in 15mM Tris pH 7.5 buffer was added. Samples were left overnight at 4 °C to precipitate. Samples were centrifuged for 30 min at 6000 *g*. Supernatants were removed and 200 μl of ice cold acetone was added. The samples were then centrifuged for another 20-30 min at 6000 *g*. Supernatants were again removed and pellets were air dried. Protein loading buffer was added and proteins were separated by SDS-PAGE. Gels were stained by Coomassie brilliant blue or silver stain. They were then dried and exposed overnight on a phosphorimager screen and developed by FUJI-FILM FLA 2000 phosphorimager.

For adenine nucleotide competition experiments, a master mixture was made that included the protein in the ATP binding buffer. These master mixtures were made up to one ninth of the final volume (20 μl) and were aliquoted into each tube. To each tube a mixture of 10 μM [γ^{32}P] 2 azido-ATP, 2 mM $MgCl_2$ and the adenine nucleotide cofactor

was added. The adenine nucleotide cofactors used were; ATP, ADP, ATPγS and AMPPNP, which were added to final concentrations of 0.01, 0.1 or 0.5 mM. Reactions were again incubated at room temperature and exposed to UV light. Samples were then processed as above.

For [γ^{32}P]-2 azido-ATP hydrolysis time course experiments, a master mixture was set up in ATP binding buffer, 2 mM $MgCl_2$, 1 μCi [γ^{32}P]-2 azido-ATP (per reaction) and 1 μg protein (per reaction). The protein was cross-linked to the [γ^{32}P]-2 azido-ATP by exposure to UV light. A 10 μl aliquot was then taken as the zero point of the time course and the rest of the reaction was incubated at 37 °C. 10 μl aliquots were taken at specific time points and stopped with EDTA as in section 2.8.2. These reactions were then processed as above.

2.8.4. Helicase substrate and assays

Helicase substrate was prepared and assays were carried out in a similar way as described previously (Tsaneva et al., 1993). Briefly, 10 pmoles of the IT300 oligo (CAAAGTAAGAGCTTCTCGAGCTGCGCAAGGATAGGTCGAATTTTCTCATTTT) was labeled with [γ-^{32}P]-ATP, by using T4 PNK as described in section 2.8.1. Once labeled, the oligo was annealed with 10 pmoles (20 μg) of ϕX174 in annealing buffer at a final volume of 100 μl. Annealing was carried out at 95 °C for 3 min, 68 °C for 30 min and left to cool down at room temperature.

A 10.5 ml 5-20 % sucrose gradient, in sucrose buffer, was made in an SW41TI ultra centrifuge tube (Beckman). The annealing reaction was layered on top of the gradient, which was centrifuged at ~111,000 *g* (30,000 RPM) for 14.5 h. The gradient was fractionated into ten 1 ml fractions, from the bottom, using a microcapillary tube connected to a pump. These were analysed by electrophoresis on a 0.8 % agarose gel containing ethidium bromide and examined under a UV light. It was dried on Whatman DE81 paper, exposed on a phosphorimager screen for 1 h and developed

by FUJI-FILM FLA 2000 phosphorimager. Fractions containing the helicase substrate were dialysed in TE buffer and stored at 4 °C.

Helicase substrate was added into a master mixture containing 1x ATPase reaction buffer with ATP and DTT both at a final concentration of 1 mM, and BSA to a final concentration of 100 μg/ml. This was aliquoted into 20 μl reactions and protein was added to a final concentration of 1 μM, or as stated. Two control reactions without protein were also set up. A reaction containing RuvAB was made up in the same way, except that RuvAB buffer was used instead of ATPase reaction buffer. RuvA and RuvB concentrations were 100 nM and 190 nM, respectively. Reactions were incubated for 30 min at 37 °C and stopped with 5 μl of stop buffer. One of the control reactions was then heated at 100 °C for 3-5 min and quickly chilled on ice, to serve as a heat-denatured control. DNA loading buffer was added and the samples were separated by electrophoresis on a 1 % agarose gel. The gel was dried on DE81 paper, exposed on a phosphorimager screen overnight and developed by FUJI-FILM FLA 2000 phosphorimager.

2.8.5. Branch migration assays

Labeled ^{32}P Holliday junction (section 2.8.1) was added to a master mixture containing 1x ATPase reaction buffer with ATP and DTT both at a final concentration of 1 mM and BSA to a final concentration of 100 μg/ml. This was aliquoted into 20 μl reactions and protein was added to a final concentration of 1 μM, or as stated. A control reaction without protein was also set up. A reaction containing RuvAB was made up in the same way except that RuvAB buffer was used instead of ATPase reaction buffer. RuvA and B were added to final concentrations of 300 nM and 600 nM, respectively. Reactions were incubated for 30 min at 37 °C and stopped with 5 μl of stop buffer. DNA loading buffer was added to samples, which were separated on a 6 % polyacrylamide TBE gel at 6 V/cm, for 1 h in 1x TBE running buffer. The gel was then dried and exposed on a phosphorimager screen overnight and developed by FUJI-FILM FLA 2000 phosphorimager.

2.9. Electron microscopy by negative staining

The fraction of the TIP48/TIP49 complex that corresponded to a molecular mass of 650 kDa, by Superdex 200 size exclusion chromatography, was used for examination by electron microscopy by negative staining. The sample was diluted in a 1:10 ratio in buffer containing 0.1 M NaCl, 20 mM Tris (pH 7.5), 1 mM DTT and 5 % glycerol, to give a final concentration of ~63 μg/ml. 3 μl of the sample were placed on glow discharged ionized carbon coated copper grids, which were then stained with 2 % (wt/vol) uranyl acetate. Samples were imaged using a 120 kV transmission electron microscope (T12, Technai) and images were exposed onto Kodak EM film using low dose protocols (~10 $e^-/Å^2$). Micrographs were digitized using a Zeiss SCAI microdensitometer scanner at 14 μm/pixel. The magnification used was 42,000 therefore the pixel spacing on the scanned images was 3.3 Å/pixel. 2267 particles were selected using the program Ximdisp and extracted into 200 x 200 pixel boxes with LABEL. These were then band-pass filtered between 165 Å and 8,25Å using IMAGIC-5 (van Heel et al., 1996). The defocus was obtained by calculating the first Zero to a value of 12-20 Å and corrected for CTF using IMAGIC-5. Five rounds of translational and rotational alignment were carried out and the particles were aligned with a reference free approach and classified into classums using multivariate statistical analysis in IMAGIC-5. The low resolution, 3D map, was created by angular reconstitution in IMAGIC-5. It was then converted into a brix format and loaded into pymol so that different views and cross-sections could be obtained.

2.10. Anti-TIP48 and TIP49 polyclonal antibodies

Samples of the full length TIP48-His_6 and His_6-TIP49 recombinant proteins, purified as described sections 2.7.1 and 2.7.3 and sent to Genosphere Biotechnologies, were used to raise polyclonal antibodies in rabbits. The antibodies were affinity purified using Actigel ALD resin (Sterogene) coupled to the cognate protein, following the manufacturer's procedure. The purified antibodies were then tested by carrying out immunoblotting experiments.

2.11. Mammalian cell culture and immunofluoresence staining

2.11.1. HeLa cell culture

HeLa cells were grown in DMEM, supplemented with 5 % fetal bovine serum, 100 U/ml of penicillin/streptomycin and 1 % (v/v) L-glutamine. HeLa cells were synchronized at early S phase by treatment with 2 mM thymidine for 15 h, followed by 8 h release in fresh DMEM with 5 % fetal bovine serum. A repeat of the treatment with thymidine for 15 h was done, followed by 8 h release in order to obtain a population of cells enriched in M phase (Lu and Hunter, 1995).

2.11.2. Fibroblast cell culture

NIH3T3 mouse fibroblasts were grown in DMEM containing 10 % donor calf serum, 1 % Glutamine, 1 % penicillin/streptomycin. They were grown at 37 °C with 10 % CO_2. Once they were 70-80 % confluent they were split one in ten and left to grow on cover slips to the required confluency.

2.11.3. Immunofluorescence staining of cells

Hela cells were grown on cover slips to 50 % confluency. In some experiments, the cover slips were incubated with 1 % Triton X-100 in PBS for 10 min on ice prior to fixation. The cells were fixed with 2 % paraformaldehyde at room temperature for 5 min and were then permeablized twice with 0.3 % Tween 20, for 10 min. The cells were washed in ice-cold methanol and incubated with IF blocking buffer for 30 min at room temperature.

Fibroblast cells were fixed for 10 min with 2 % PFD containing 0.05 % glutaraldehyde, at room temperature. The cells were washed in ice-cold methanol and were

permeablized twice with 0.3 % Tween 20, for 10 min, without shaking. They were then incubated with IF blocking buffer for 30 min at room temperature.

Fixed cells were incubated with the primary antibodies in IF blocking buffer, overnight, at 4 °C. Cover slips were washed twice with IF blocking buffer and incubated with the respective secondary antibodies (TRITCH conjugated goat-anti-rabbit IgG or FITCH-conjugated goat anti-mouse IgG) for 1 h at room temperature. Cover slips were washed twice with IF blocking buffer for 10 min at room temperature and mounted in mounting solution (Vectashield, Vector Labs) containing DAPI stain. The samples were examined under a Zeiss Axiophot microscope. Images shown in Chapter 6 were gained using Pro-Image 4.5 and Adobe PhotoShop 7.0 software.

Antibody dilutions for immunofluorescence staining

Anti-TIP48 rabbit polyclonal (1/200)
Anti-TIP49 rabbit polyclonal (1/50)
Anti-BAF53 rabbit polyclonal (1/100)
Anti-β-catenin mouse monoclonal (1/400)
Anti-α-tubulin mouse monoclonal (1/400)
TRITCH conjugated goat-anti-rabbit IgG (1/400)
FITCH-conjugated goat-anti-mouse IgG (1/400)

CHAPTER 3

Expression, purification and characterisation of the recombinant TIP48 and TIP49 proteins

3.1. Introduction

TIP48 and TIP49 have been compared to RuvB because of their homology to the bacterial RuvB sequence (Kanemaki et al., 1997; Putnam et al., 2001; Qiu et al., 1998). In addition, one group who purified the two recombinant proteins from *E. coli*, have reported that they are both DNA helicases, with opposite polarities of unwinding (Kanemaki et al., 1999; Makino et al., 1999). However, other groups that purified the proteins from *E. coli* or insect cells detected traces of ATPase activity only, and did not observe helicase activity (Ikura et al., 2000; Qiu et al., 1998).

Due to the disagreement in the literature about the intrinsic activities of TIP48 and TIP49, it is still unknown whether they are functional homologues of RuvB. Therefore the coding sequences for the two proteins were cloned and both were expressed and purified from *E. coli*. Catalytically inactive mutants of the proteins were also expressed and purified. They were used to determine conclusively, whether both proteins exhibit DNA-dependent ATPase and helicase activities. Understanding the intrinsic activities of the two proteins *in vitro* will help to gain an insight into their roles *in vivo*.

3.2. Cloning and expression of recombinant TIP49 in *E.coli*

The coding sequence for the human TIP49 protein was amplified by PCR using a cDNA library I.M.A.G.E clone as a template (Accession No. 2823568), and primers, set 1 and 2 (with or without stop codon, respectively, see Materials and Methods, section 2.3.1). The PCR products were cloned into pGEM®-T Easy vectors. The TIP49 coding sequences were then sub-cloned into the pET21b+ *E. coli* vector to make two expression constructs for TIP49; with or without a C-terminal His_6 tag. Errors arising from incorrect design of the primers were corrected by site-directed mutagenesis. The primers used for the mutagenesis are shown in Materials and Methods (Section 2.4.6). All clones were fully sequenced and shown to be correct. The TIP49 coding sequence was then sub-

cloned from the pET21-TIP49 clone into a pET15b+ vector to produce a construct, which would express an N-terminal His_6-tagged TIP49 protein.

TABLE 3.1: Experimental conditions for obtaining optimal expression and lysis of TIP49 protein from *E. coli* BL21 (DE3) Gold expressing cells

Expression plasmid[a]	Lysis conditions	Amount of soluble TIP49[b]
pET15-His_6-TIP49	0.75 mg/ml lysozyme, 0.5 % Nonidet P40, sonication.	50 %
pET15-His_6-TIP49D302N		40 %
pET21b-TIP49-His_6	0.75 mg/ml lysozyme, 0.1 % Nonidet P40, sonication	50 %
pET21-TIP49D302N-His_6		
pET21- TIP49		60 %
pET21- TIP49D302N		

a All inductions were carried out at 30 °C for 3-4 h, with shaking.

b The amount of soluble and insoluble TIP49 protein was estimated from the intensities of the TIP49 band on the SDS-PAGE gel (Gene tools, Syngene). The amount of soluble protein was expressed as a percentage from the total amount of induced protein.

A mutation was introduced in the pET21-TIP49 constructs, substituting the aspartate residue at position 302 of the amino acid sequence for TIP49, for an aspargine (D302N). The same mutation was introduced in the pET15-TIP49 construct. This mutation is in the Walker B motif of the protein, and the residue mutated is thought to be important for ATP hydrolysis (Ogura and Wilkinson, 2001). The mutation was shown to inactivate TIP49 in *vivo* (Dugan et al., 2002; Feng et al., 2003; Wood et al., 2000), and was also shown to inactivate RuvB *in vivo* and *in vitro* (Mezard et al., 1997). The mutation in all the constructs was verified by sequencing.

The pET21-TIP49 and pET15-TIP49 constructs were checked for expression in both BL21 (DE3) Gold and BL21 (DE3) Gold pLysS *E. coli* strains. The cells were grown, and IPTG was added to induce the expression of the recombinant TIP49 protein. Expression was checked by SDS-PAGE and staining with Coomassie Brilliant Blue (BB). All constructs showed induced expression of a protein with a molecular mass of approximately 55 kDa (Figure 3.1). The presence of a His_6 tag in the induced protein was checked, where applicable, by immnoblotting using anti-His_6 antibody. All the constructs expressed TIP49 considerably well in BL21 Gold cells, but expression in BL21 Gold pLysS was low.

The solubility of the recombinant TIP49 proteins was tested under different extraction conditions, and the optimal conditions for induction and lysis of the cells are summarised in Table 3.1. The expression and solubility of the TIP49 with N-terminal or C-terminal His_6 tag are shown in Figure 3.1a and 3.1b, respectively. The gels also give representative pictures for the induction and solubility levels of the respective TIP49D302N mutants.

The His_6-TIP49 protein and its D302N mutant were used for characterization of the ATPase activity as will be described in the next sections. The pET21-TIP49-His_6 construct was used to express and purify TIP49-His_6 under denaturing conditions so that its activity could be compared to the TIP49-His_6/TIP48 complex obtained after refolding

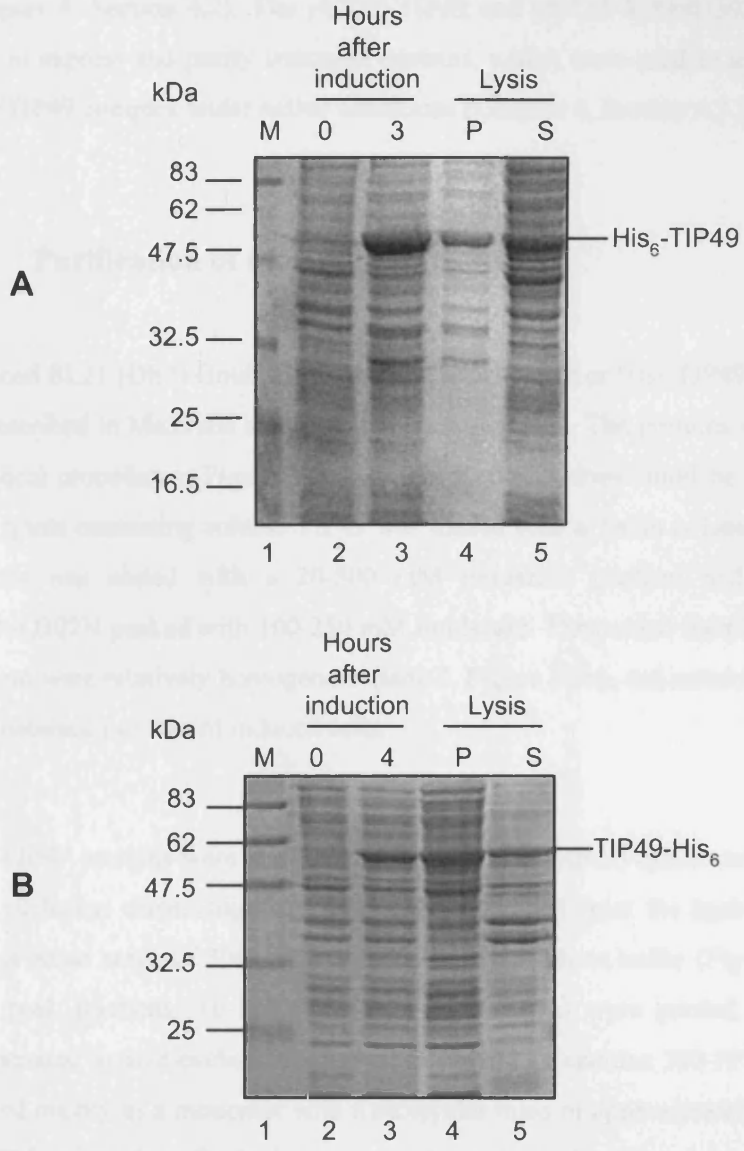

FIGURE 3.1: Induction and solubility of TIP49 expressed in *E.coli*

(A) 12 % SDS-PAGE of BL21 Gold cells transformed with pET15-His_6-TIP49 expression plasmid before (0) and 3 h after induction with IPTG (lanes 2 and 3). Soluble proteins (S) and insoluble pellet (P) after lysis of the induced cells are indicated, (lanes 4 and 5). The gel was stained with Coomassie brilliant blue. (B) 12 % SDS-PAGE of BL21 Gold cells transformed with pET21-TIP49-His_6 expression plasmid before (0) and 4 h after induction with IPTG (lanes 2 and 3). Soluble proteins (S) and insoluble pellet (P) after lysis of the induced cells are indicated (lanes 4 and 5). The gel was stained with Coomassie brilliant blue. Expression and lysis conditions for cells expressing these plasmids are described in Materials and Methods and Table 3.1.

(Chapter 4, Section 4.2). The pET21-TIP49 and pET21-TIP49D302N constructs were used to express and purify untagged proteins, which were used to assemble the TIP48-His_6/TIP49 complex under native conditions (Chapter 4, Section 4.3.).

3.3. Purification of recombinant TIP49

Induced BL21 (DE3) Gold cells expressing His_6-TIP49 or His_6-TIP49D302N were lysed as described in Materials and Methods (section 2.7.3). The proteins were purified using identical procedures (Figure 3.2a), so that their activities could be compared directly. The lysate containing soluble TIP49 was loaded onto a Talon column. The His_6-tagged protein was eluted with a 20-500 mM imidazole gradient and both TIP49 and TIP49D302N peaked with 100-250 mM imidazole. The pooled fractions from the Talon column were relatively homogenous (lane 3, Figure 3.2b), and around 2-3 mg of protein was obtained per litre of induced cells.

The TIP49 proteins were fractionated further on a hydroxyapatite column, followed by size exclusion chromatography. Both proteins eluted from the hydroxyapatite column with a broad range of 300-600 mM potassium phosphate buffer (Figure 3.2a and 3.3a). The peak fractions, 10-13 (lanes 2-5, Figure 3.3a) were pooled, concentrated and fractionated by size exclusion chromatography on a Superdex 200 FPLC column. TIP49 peaked mainly as a monomer with a molecular mass of approximately 55 kDa. The side TIP49 fractions from the hydroxyapatite chromatography (lanes 6-10, Figure 3.3a), were pooled separately and concentrated for ATPase assays (see below). Figure 3.2 shows a summary of the purification procedure and the SDS PAGE gel of the fractions from each step.

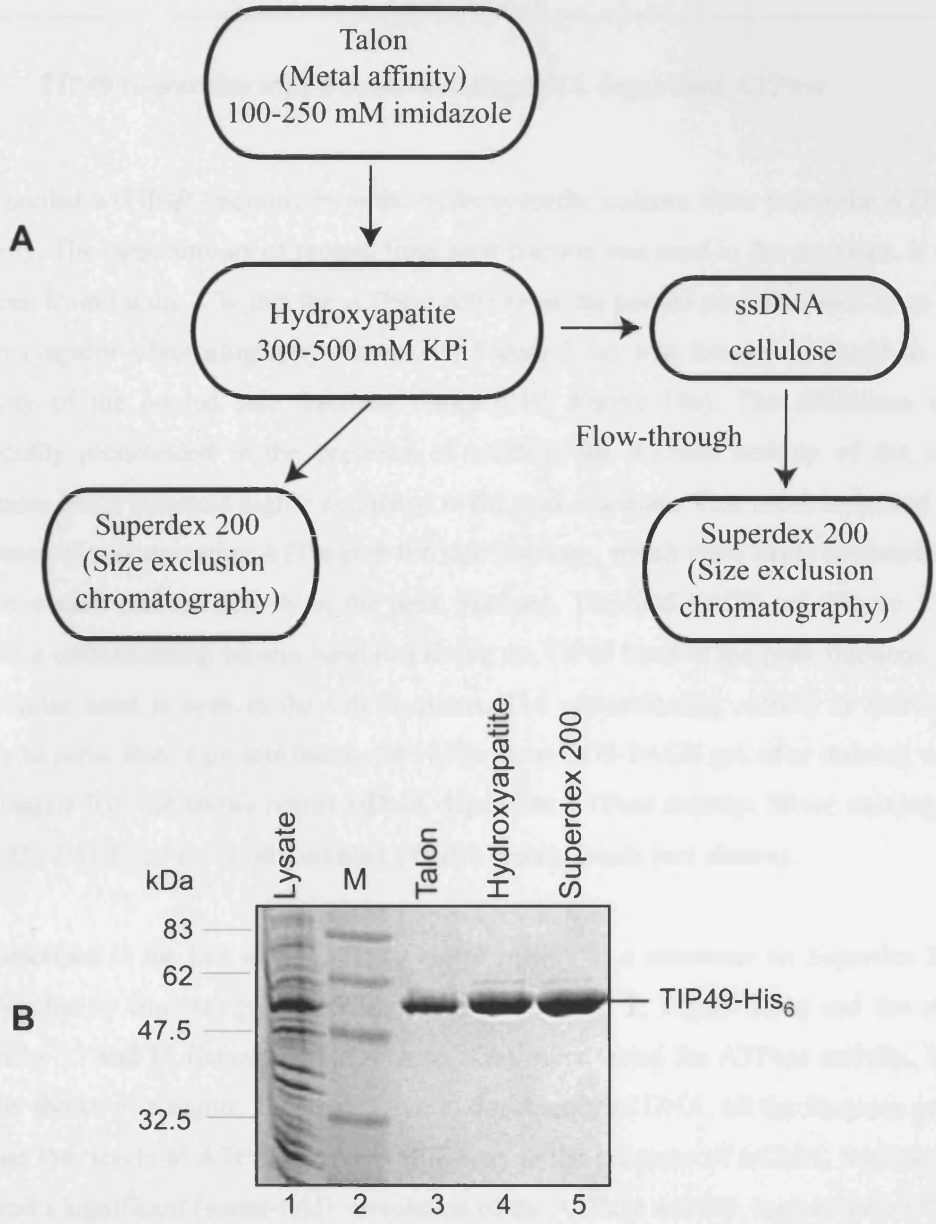

FIGURE 3.2: Purification of His_6-TIP49

(A) Purification scheme for His_6-TIP49. (B) 12 % SDS-PAGE of the TIP49 fractions collected from each step of the purification. Lane 1: crude lysate loaded onto the Talon column; lane 2: molecular mass markers; lane 3: pooled peak fractions, eluted from the Talon column; lane 4: pooled peak fractions, eluted from the hydroxyapatite column; lane 5: peak fraction, eluted from the Superdex 200 column. Approximately 2 µg of TIP49 from each sample were loaded on the SDS-PAGE gel, which was stained with Coomassie brilliant blue.

3.4. TIP49 co-purifies with a contaminating DNA dependent ATPase

The pooled wtTIP49 fractions from the hydroxyapatite column were tested for ATPase activity. The same amount of protein from each fraction was used in the reactions. It can be seen from Figure 3.3a that the ATPase activity of the pooled peak fractions from the hydroxyapatite chromatography (lanes 2-5, Figure 3.3a) was lower, compared to the activity of the pooled side fractions (lanes 6-10, Figure 14a). The difference was especially pronounced in the presence of ssDNA; the ATPase activity of the side fractions being threefold higher compared to the peak fractions. This result indicated the presence of contaminating ATPases in the side fractions, which were likely to contribute to the overall ATPase activity of the peak fractions. The SDS-PAGE gel (Figure 3.3a) shows a contaminating protein band just above the TIP49 band in the peak fractions but no similar band is seen in the side fractions. The contaminating activity is therefore likely to come from a protein that is not visible on an SDS-PAGE gel, after staining with Coomassie BB; but shows robust ssDNA-dependent ATPase activity. Silver staining of the SDS-PAGE gel revealed a number of extra protein bands (not shown).

As described in the last section, TIP49 eluted mainly as a monomer on Superdex 200 size exclusion chromatography. The peak fraction (lane 2, Figure 3.3b) and the side fractions 13 and 15 (lanes 1 and 3, Figure 3.3b), were tested for ATPase activity. The results shown in a Figure 3.3b reveal that in the absence of DNA, all the fractions gave similar low levels of ATPase activity. However, in the presence of ssDNA, fraction 13 showed a significant (seven-fold) stimulation of the ATPase activity, typical for a DNA helicase. The peak fraction (fraction 14) and side fraction (fraction 15), did not exhibit such a high stimulation of ATPase activity, in the presence of ssDNA. This result confirms that the peak fractions from the hydroxyapatite column contained a contaminating ssDNA-dependent ATPase, which could be separated from TIP49 by size exclusion chromatography. However, it is likely that some contaminating activity is still present in the TIP49 peak (fraction 14), contributing to the slight stimulation of the ATPase activity that is seen in the presence of ssDNA.

A

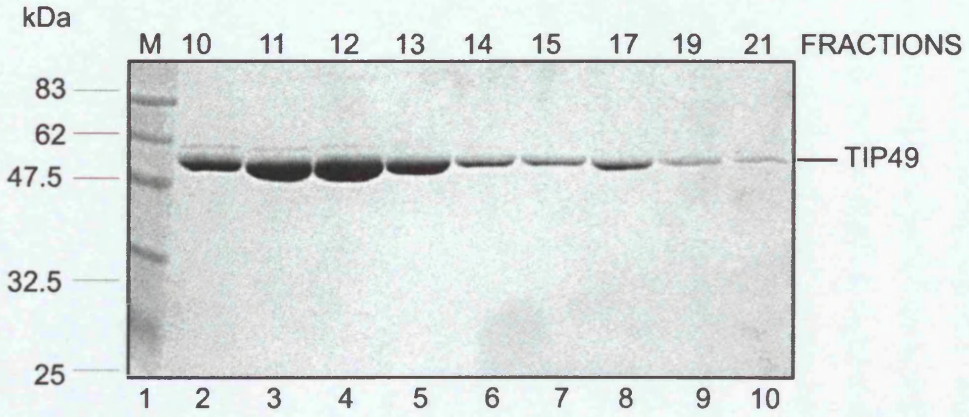
kDa
M 10 11 12 13 14 15 17 19 21 FRACTIONS
83
62
47.5
32.5
25
TIP49
1 2 3 4 5 6 7 8 9 10

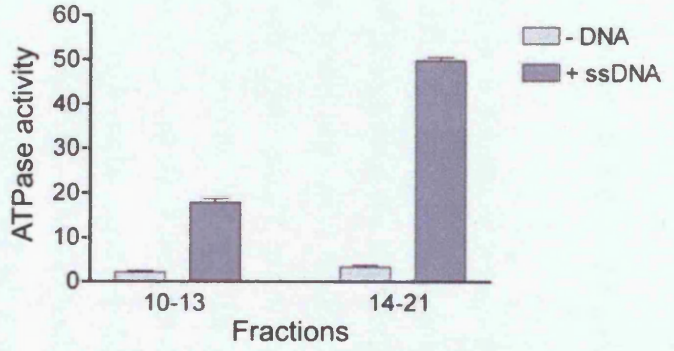
ATPase activity
60
50
40
30
20
10
0
- DNA
+ ssDNA
10-13
14-21
Fractions

B

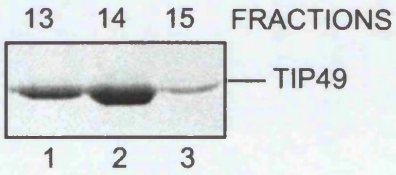
13 14 15 FRACTIONS
TIP49
1 2 3

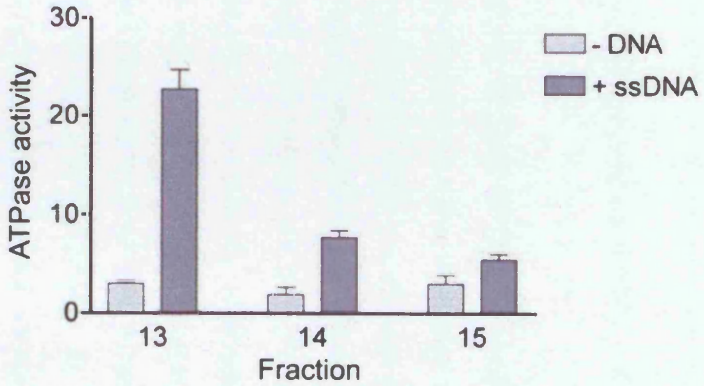
ATPase activity
30
20
10
0
- DNA
+ ssDNA
13
14
15
Fraction

FIGURE 3.3: Chromatography fractions of TIP49 and their ATPase activity

(A) TIP49 fractions obtained from hydroxyapatite chromatography were analyzed by 12 % SDS-PAGE (left). 10 µl of each eluted fraction, before concentration, were loaded and the gel was stained with Coomassie brilliant blue. The peak fractions 10-13 (lanes 2-5) and side fractions 14-21 (lanes 6-10) were pooled separately, concentrated and used at a final concentration of 1 µM per ATPase reaction, with or without ϕX174 ssDNA (5 ng/µl) (right). Reactions were incubated at 37 °C for 30 min.

(B) TIP49 fractions obtained from size exclusion chromatography, analyzed by 12 % SDS-PAGE (left). 10 µl of each eluted fraction, before concentration, were loaded and the gel was stained with Coomassie brilliant blue. Each fraction was concentrated and added to a final concentration of 1 µM per ATPase reaction, with or without ϕX174 ssDNA (5 ng/µl) (right). Reactions were incubated at 37 °C for 30 min. ATPase activity is expressed in moles of ATP hydrolyzed per mole of TIP49 monomer.

The TIP49D302N mutant, purified alongside TIP49, peaked at the same positions on hydroxyapatite and size exclusion chromatography as the wild-type protein. The ATPase activity however, did not peak with this protein, similar to was seen with wtTIP49 (Figure 3.3); and in all fractions the ATPase activity was higher than what was seen with the wild-type protein. This confirmed that both proteins co-purified with contaminants as the mutant was not expected to hydrolyze ATP. In view of the controversy surrounding published data on the DNA helicase activity of TIP49 and the observed ATPase activity of the D302N mutant, an additional purification step on ssDNA cellulose was introduced. The hydroxyapatite fractions of both proteins were pooled and loaded onto ssDNA cellulose columns. Around 90 % of TIP49 and about 99 % of the TIP49D302N mutant flowed through the column (Table 3.2). The material captured on the ssDNA column was eluted with buffer containing 1 M NaCl. All fractions were tested in ATPase assays, both in the absence and presence of ssDNA, and the results obtained are shown in Table 3.2.

The ON fractions of both TIP49 and mutant TIP49D302N showed approximately a five-fold stimulation of the ATPase activity in the presence of ssDNA. When the flow-through from both preps was tested, the stimulation of the ATPase activity in the presence of ssDNA was no longer detected. This proved conclusively that the ssDNA-dependent ATPase activity was not intrinsic to TIP49, but was due to contaminants, which could be separated away using ssDNA cellulose chromatography. Indeed, it can be seen that the fractions, which eluted from the column, contained this ssDNA stimulated activity (Table 3.2).

A DNA helicase assay was also carried out with TIP49 and TIP49D302N before and after ssDNA cellulose chromatography. Figure 3.4 demonstrates that the ON fractions of both wild type TIP49 and the mutant TIP49D302N displayed DNA helicase activities. The helicase activity was no longer present in the flow-through fractions from the ssDNA cellulose column. This confirmed that a contaminant displaying this

TABLE 3.2: ATPase activities of TIP49 and TIP49D302N purified after ssDNA cellulose chromatography.

Fraction	TIP49			TIP49D302N		
	% protein[a]	ATPase activity[b,c]		% protein[a]	ATPase activity[b,c]	
		- DNA	+ DNA		- DNA	+ DNA
ON	100	0.154 ± 0.016	0.718 ± 0.040	100	0.267 ± 0.027	1.460 ± 0.201
FT	95	0.087 ± 0.001	0.104 ± 0.003	99	0.320 ± 0.043	0.381 ± 0.068
Eluate	5	0.442 ± 0.1414	3.361 ± 0.410	1	0.118 ± 0.018	0.274 ± 0.050

a The percentages of TIP49/TIP49D302N in the flow-through and eluted fractions were estimated from quantifying bands on SDS-PAGE gels, using the program Gene tools (Syngene), and measuring protein concentration of samples by a Bradford assay.

b 1 μM of TIP49/TIP49D302N from the ON and flow-through fractions were used per (10 μl) ATPase reaction. 2 μl of the eluted fractions, which had been previously concentrated up to 500 fold, were added to 10 μl reactions.

c The units for the ATPase activities is in nmoles of ATP hydrolysed. Reactions contained 1 mM of ATP.

ssDNA-dependent ATPase activity was also a DNA helicase and was separated away from TIP49 by chromatography on ssDNA cellulose. The salt-eluted fractions had ssDNA-dependent ATPase activity but also contained nuclease activities which

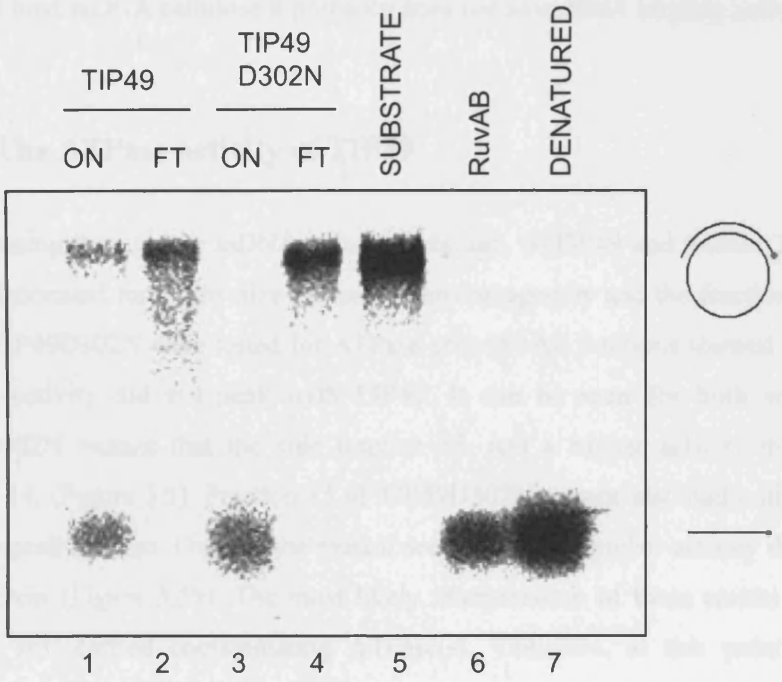

FIGURE 3.4: Helicase assays with TIP49 and TIP49D302N

Helicase assays were carried out with wtTIP49 or TIP49D302N fractions from the ssDNA cellulose column. Reactions were carried out as described in Materials and Methods (Section 2.8.4) . Lanes 1 and 3 show the reactions with the ON fractions. Lanes 2 and 4 show the reactions with the flow-through (FT) fractions. Control reactions contained helicase substrate alone (lane 5); *E.coli* RuvAB (lane 6); and the substrate that was heat denatured at 100 ° C (lane 7).

obscured any helicase activity (not shown). Therefore these results show that TIP49 does not have ssDNA-dependent ATPase activity or DNA helicase activity. Also, since TIP49 does not bind ssDNA cellulose it probably does not have DNA binding activities either.

3.5. The ATPase activity of TIP49

After passing through the ssDNA cellulose column, wtTIP49 and mutant TIP49D302N were fractionated further by size exclusion chromatography and the fractions containing TIP49/TIP49D302N were tested for ATPase activity. All fractions showed low activity, but the activity did not peak with TIP49. It can be seen for both wtTIP49 and TIP49D302N mutant that the side fraction 13, had a higher activity than the peak fraction 14, (Figure 3.5). Fraction 15 of TIP49D302N mutant also had a higher activity than the peak fraction. Overall, the mutant seemed to have higher activity than the wild-type protein (Figure 3.5b). The most likely interpretation of these results is that both proteins still carried contaminating ATPase(s). Therefore, at this point it was not possible to compare the intrinsic ATPase activities of TIP49 and the TIP49D302 mutant. However, these results indicate that the ATPase activity of TIP49 is likely to be very low and does not include DNA helicase activity. It may be that the recombinant TIP49 was not folded correctly and was unable to bind ATP. Hence ATP binding by wild type and mutant TIP49 was tested as described below.

3.6 TIP49 binds ATP

The TIP49 and TIP49D302N proteins were used in binding experiments with the ATP analogue, [γ^{32}P] 2 azido-ATP, to investigate whether the proteins bind ATP. This analogue can cross-link easily to residues in the ATP binding pocket of the protein after UV irradiation, via the azido group, which is on the second position on the purine ring of the ATP molecule (Melese and Boyer, 1985). Figure 3.6 demonstrates that TIP49 binds this analogue, whereas TIP49D302N does not. This binding to TIP49 was specific to the ATP binding pocket of the protein, as shown by a competition experiment with unlabelled ATP (Chapter 5, Figure 5.5). ATP was added to the protein at the same time

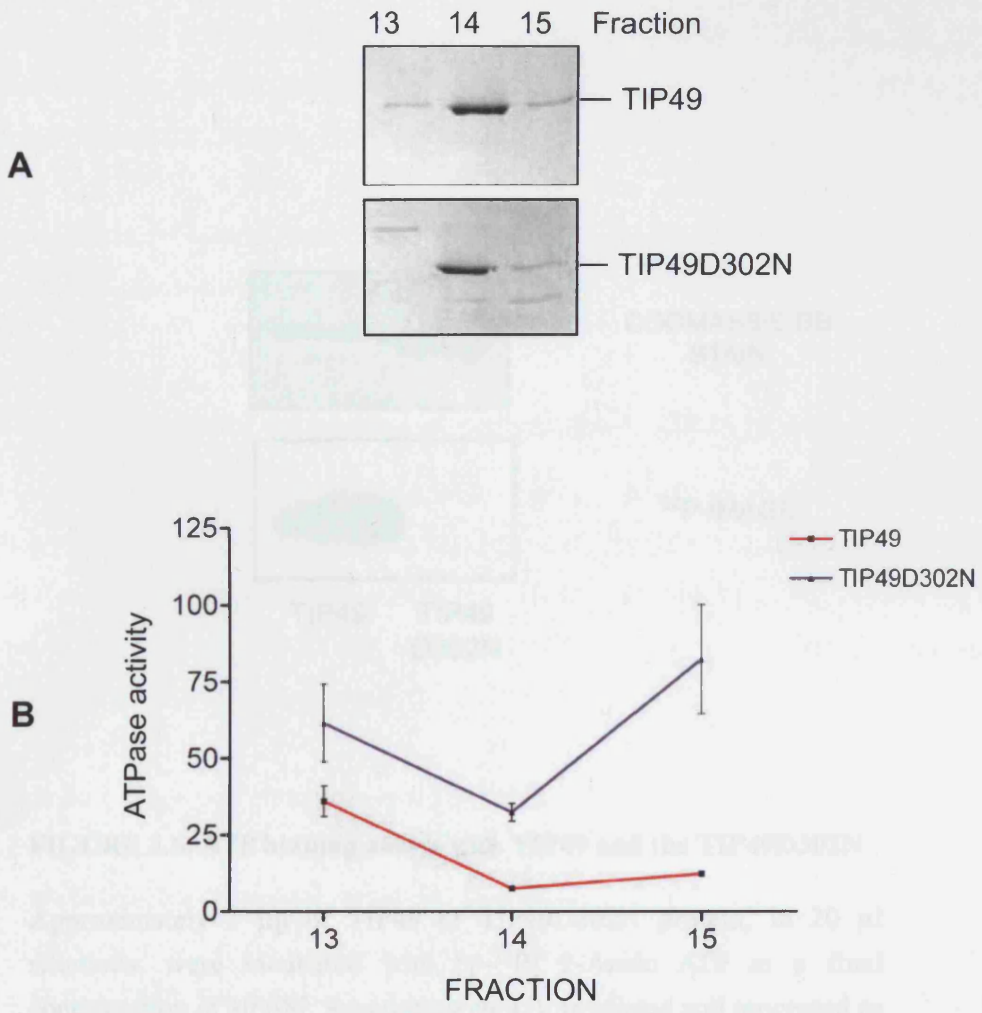

FIGURE 3.5: The ATPase activity of TIP49 and TIP49D302N after size exclusion chromatography

(A) 12 % SDS-PAGE of the Superdex 200 size exclusion chromatography fractions of TIP49 and TIP49D302N. 10 µl of each fraction, before concentration, were loaded on the gels, which were stained with Coomassie brilliant blue. (B) ATPase activities of the size exclusion chromatography fractions of TIP49 and TIP49D302N. Protein from each fraction was added to a final concentration of 1 µM, per ATPase reaction. ATP was added to a final concentration of 1 mM, per reaction. Reactions were then incubated at 37 ºC for 20 min. ATPase activity is expressed in moles of ATP hydrolysed per mole of protein monomer.

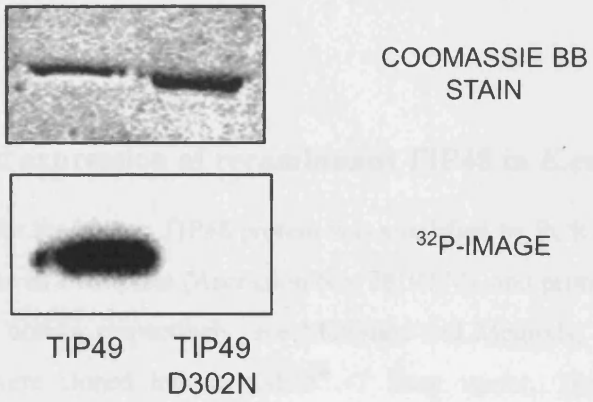

FIGURE 3.6: ATP binding assays with TIP49 and the TIP49D302N

Approximately 1 µg of TIP49 or TIP49D302N protein, in 20 µl reactions, were incubated with [γ–^{32}P] 2-Azido ATP at a final concentration of 10 µM. Reactions were UV irradiated and processed as described in Materials and Methods (section 2.8.3). The protein was separated by 12 % SDS-PAGE. The gel was stained with Coomassie brilliant blue, dried and exposed on a phosphorimager screen and developed by FUJI-FILM FLA 2000 phosphorimager.

as the [γ^{32}P] 2 azido-ATP, and it was shown that the signal from [γ^{32}P] 2 azido-ATP was lost when the ATP was also present. This confirms that TIP49 is a bona fide ATP-binding protein. The fact that TIP49D302N is unable to bind [γ^{32}P] 2 azido-ATP is quite an important result, as it confirms conclusively that the higher ATPase activity obtained from the TIP49D302N is coming exclusively from contaminants. Therefore this confirms that the activity from TIP49 is very low and it may even be that on its own, it is unable to hydrolyse any ATP.

3.7. Cloning and expression of recombinant TIP48 in *E.coli*

The coding sequence for the human TIP48 protein was amplified by PCR using a cDNA library I.M.A.G.E clone as a template (Accession No. 2819778), and primer sets 3 and 4 (with or without stop codon, respectively, see Materials and Methods, section 2.3.1). The PCR products were cloned into a pGEM® -T Easy vector. The clones were sequenced and shown to be correct.

The coding sequences excised from pGEM®-T Easy, or from PCR products amplified by VENT polymerase, were cloned into the pET21b+ *E. coli* expression vector (see Materials and Methods, section 2.4.5). Two constructs were made for expression of TIP48; with or without a C-terminal His_6 tag. A point mutation was also engineered in the pET21-TIP48-His_6 construct substituting the aspartate residue at position 299 of the amino acid sequence of TIP48 for an asparagine (D299N). This is the same mutation that was made in the Walker B motif of TIP49 (Section 3.2), D302N, which did not bind ATP (Figure 3.6). This mutation was predicted to inhibit the ATPase activity of TIP48 and the yeast homologue carrying this mutation was inactive *in vivo* (King et al., 2001).

The three constructs were transformed into BL21 (DE3) Gold and BL21 (DE3) Gold pLysS *E. coli* strains. The cells were grown and IPTG was added to induce expression of the recombinant TIP48 protein. Expression was checked by SDS-PAGE and gels were stained with Coomassie BB, which showed induction of a protein with a molecular mass of approximately 52 kDa (Figure 3.7). The presence of the His_6 tag in the induced band

of TIP48-His_6 was verified by immunoblotting using anti-His_6 antibody. All three constructs expressed TIP48 reasonably well, three to four hours after induction in both *E. coli* strains.

The solubility of the three recombinant proteins was checked under different extraction conditions. Table 3.3 summarises the optimal conditions of induction and lysis to gain soluble recombinant TIP48 / TIP48D299N protein. Figure 3.7 shows the induction and solubility of TIP48-His_6. The D299N mutant and the non-tagged TIP48 showed very similar levels of induction and solubility (not shown).

TABLE 3.3: Experimental conditions for obtaining optimal expression and lysis of TIP48 protein from *E. coli* BL21 (DE3) Gold pLysS expressing cells

Expression plasmid[a]	Lysis conditions	Amount of soluble TIP48[b]
pET21-TIP48	0.2 % Nonidet P40, sonication	50 %
pET21- TIP48-His_6	0.2 % Nonidet P40, 90 min, sonication	
pET21-TIP48D299N-His_6		

a All inductions were carried out at 30 °C for 4 h, with shaking.

b The amount of soluble and insoluble TIP48 protein was estimated from the intensities of the TIP48 band on the SDS-PAGE gel (Gene tools, Syngene). The amount of soluble protein was expressed as a percentage from the total amount of induced protein.

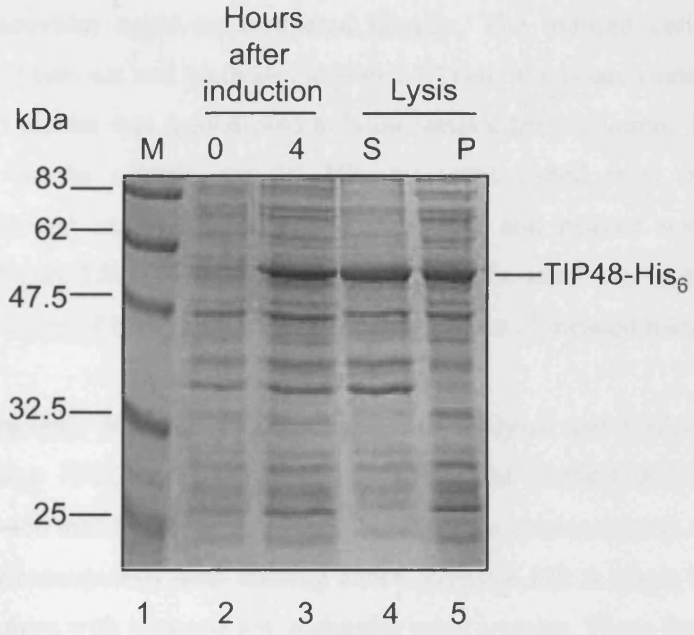

FIGURE 3.7: Expression and solubility of TIP48-His_6 in *E. coli*

12 % SDS-PAGE of BL21 Gold pLysS cells transformed with pET21-TIP48-His_6 expression plasmid before (0) and 4 h after induction with IPTG (lanes 2 and 3). Soluble proteins (S) and insoluble pellet (P) after lysis of the induced cells are indicated (lanes 4 and 5). Expression and lysis conditions are described in Materials and Methods and Table 3.3. The gel was stained with Coomassie brilliant blue.

3.8 Purification of recombinant TIP48

TIP48-His_6 and mutant TIP48D299N-His_6 were purified using identical procedures so that their activities could be compared directly. The induced cells were lysed as described in Materials and Methods (section 2.7.1) and the lysate containing the soluble recombinant protein was loaded onto a Talon metal affinity column. TIP48 that bound specifically to the column, via its His_6 tag, was eluted from the column with concentrations of imidazole between 50-500 mM and peaked with 150-200 mM imidazole (Figure 3.8a). TIP48D299N-His_6 behaved the same way on the Talon column and around 10 mg of each protein was obtained per litre of induced bacterial cells.

The peak fractions from the Talon column were dialysed and loaded onto a MonoQ anion-exchange FPLC column. Both TIP48-His_6 and TIP48D299N-His_6 eluted as a peak at 300-400 mM NaCl (Figure 3.8a). The fractions obtained (lanes 4-6, Figure 3.8b) showed near homogeneity after staining with Coomassie BB. A single band can be seen in these fractions with traces of low molecular mass proteins. These fractions were used in some of the experiments described below and for experiments described in Chapters 4, 5 and 6. However, the peak fraction from the Mono Q column (lane 5, Figure 3.8b) was further fractionated by size exclusion chromatography on Superdex 200 FPLC. The peak fractions of TIP48, at around 70 kDa, corresponded to a monomer/dimer equilibrium. These fractions were pooled together to give the Superdex 200-eluted protein fraction shown in Figure 3.8b (lane 7). The TIP48D299N mutant behaved differently on size exclusion chromatography, as most of the protein eluted with a molecular mass of 400 kDa, which would correspond to an octamer of TIP48, as will be shown and discussed in the next section.

The fractions of the TIP48 and TIP48D299N mutant corresponding to the monomer/dimer equilibrium of TIP48 were used in ATPase assays. ATPase activity was observed with TIP48; however, a similar level of activity was seen with the TIP48D299N mutant. This finding was unexpected and suggested that ATPase

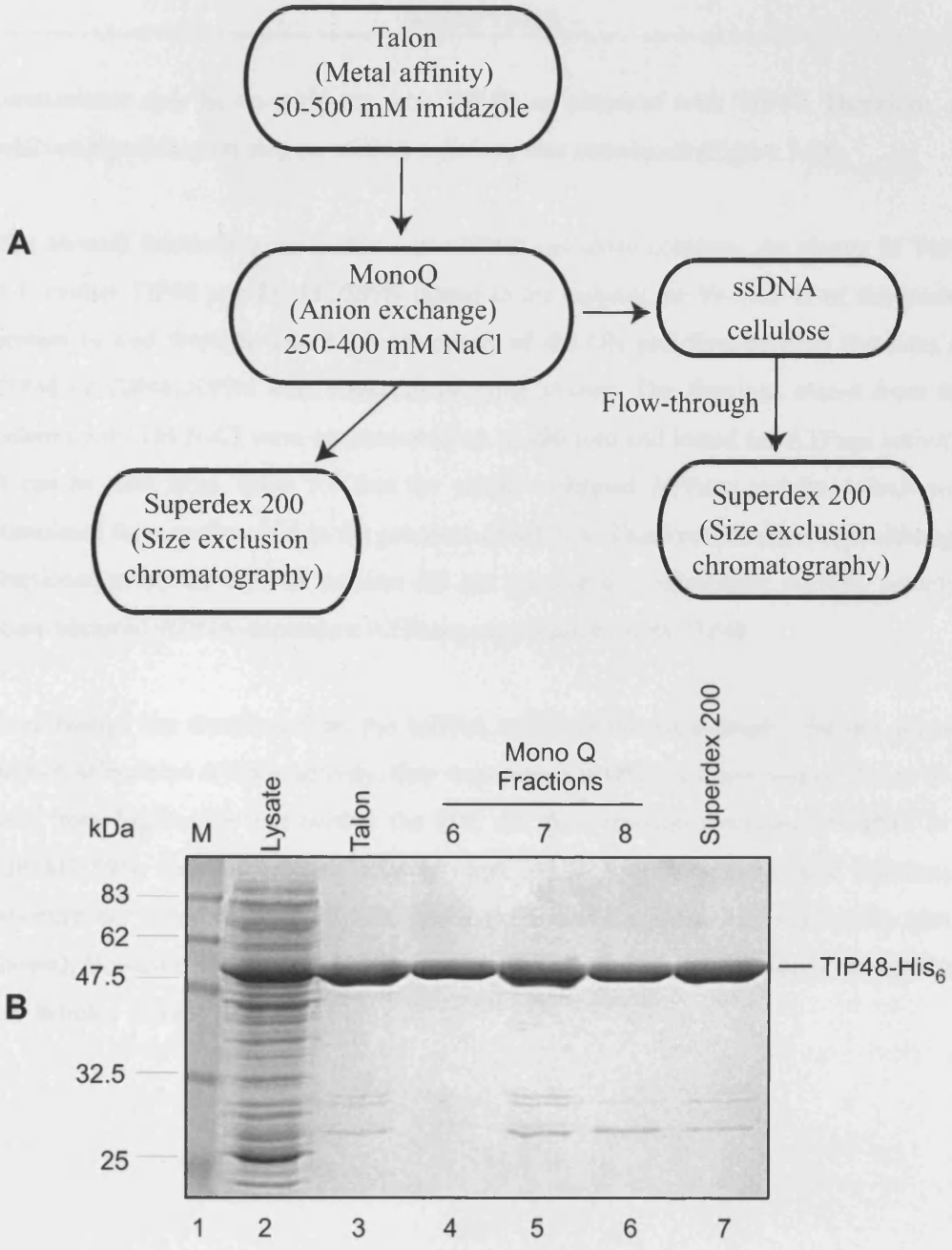

FIGURE 3.8: Purification of TIP48-His_6

(A) Purification scheme for TIP48-His_6. (B) 12 % SDS-PAGE showing the fractions collected from each step of the purification. Lane 1: molecular mass markers; lane 2: crude lysate loaded onto the Talon column; lane 3: pooled peak fractions, eluted from the Talon column; lanes 4-6: peak fractions, eluted from the MonoQ column; lane 7: pooled peak fractions, eluted from the Superdex 200 column. Approximately 2 µg of TIP48 from each sample were loaded on the SDS-PAGE gel, which was stained with Coomassie brilliant blue.

contaminant may be co-purifying with TIP48, as observed with TIP49. Therefore, an additional purification step on ssDNA cellulose was introduced (Figure 3.8a).

The MonoQ fractions were loaded onto ssDNA cellulose columns. As shown in Table 3.4, neither TIP48 nor TIP48D299N bound to the column, as 99-99.5 % of the loaded protein flowed through. The ATPase activity of the ON and flow-through fractions of TIP48 or TIP48D299N were found to be quite similar. The fractions eluted from the column with 1M NaCl were concentrated up to 500 fold and tested for ATPase activity. It can be seen from Table 3.4 that the eluate contained ATPase activity, which was stimulated three to five-fold in the presence of ssDNA. These results show that although fractionation on the ssDNA column did not remove any significant ATPase activity, some bacterial ssDNA-dependent ATPases can co-purify with TIP48.

Even though the fractions from the ssDNA cellulose chromatography did not show ssDNA-stimulated ATPase activity, they were tested in DNA helicase assays. It can be seen from Figure 3.9 that neither the ON, nor flow-through fractions of TIP48 or TIP48D299N, showed helicase activity (lane 1-4, Figure 3.9). The eluate fractions however, contained nucleases, which precluded analysis of DNA helicase activity (not shown). However, the results shown in Figure 3.9 confirm that TIP48 does not exhibit any helicase activity

TABLE 3.4: ATPase activities of TIP48 and TIP48D299N purified after ssDNA cellulose chromatography

Fraction	TIP48			TIP48D299N		
	% protein[a]	ATPase activity[b,c]		% protein[a]	ATPase activity[b,c]	
		- DNA	+ DNA		- DNA	+ DNA
ON	100	0.131 ± 0.064	0.113 ± 0.064	100	0.132 ± 0.075	0.116 ± 0.047
FT	99	0.129 ± 0.080	0.111 ± 0.052	99.5	0.118 ± 0.064	0.112 ± 0.077
Eluate	1	0.252 ± 0.042	1.056 ± 0.094	0.5	0.319 ± 0.086	0.871 ± 0.042

a The percentages of TIP48/TIP48D299N in the flow-through and eluted fractions were estimated from quantifying bands on SDS-PAGE gels, using the program Gene tools (Syngene), and measuring protein concentration of samples by a Bradford assay.

b 1 μM of TIP48/TIP48D299N from the ON and flow-through fractions were used per (10 μl) ATPase reaction. 2 μl of the eluted fractions, which had been previously concentrated up to 500 fold, were added to 10 μl reactions.

c The units for the ATPase activities is in nmoles of ATP hydrolysed. Reactions contained 1 mM of ATP.

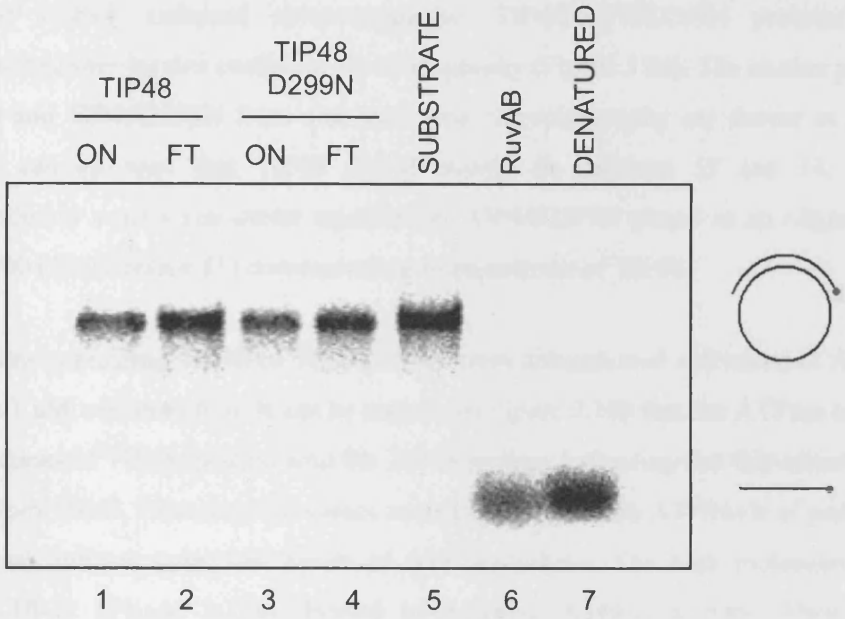

FIGURE 3.9: Helicase assays with TIP48 and TIP48D299N

Helicase assays were carried out with wtTIP48 or TIP48D299N fractions from the ssDNA cellulose column. Reactions were set up and carried out as described in Materials and Methods (section 2.8.4) . Lanes 1 and 3 show the reactions with the ON fractions. Lanes 2 and 4 show the reactions with the flow-through (FT) fractions. Control reactions contained helicase substrate alone (lane 5); *E.coli* RuvAB (lane 6); and the substrate that was heat denatured at 100 ° C (lane 7).

3.9. ATPase activity of TIP48

After the ssDNA cellulose chromatography, TIP48/TIP48D299N proteins were fractionated further by size exclusion chromatography (Figure 3.8a). The elution profiles of TIP48 and TIP48D299N from size exclusion chromatography are shown in Figure 3.10a. It can be seen that TIP48 eluted mainly in fractions 13 and 14, which corresponded to a monomer/dimer equilibrium. TIP48D299N eluted as an oligomer of about ~ 400 kDa (fraction 11) corresponding to an octamer of TIP48.

All fractions containing TIP48 or TIP48D299N were concentrated and tested in ATPase assays, at 1 μM concentration. It can be seen from Figure 3.10b that the ATPase activity of the fractions of TIP48, peaked with the TIP48 protein, indicating that this activity was coming from TIP48. However, the values measured (6-13 moles ATP/mole of protein in 20 minutes) indicate quite low levels of ATP hydrolysis. The high molecular mass fractions 10-12 (Figure 3.10a) showed even lower ATPase activity. These high molecular mass oligomers represented a small fraction of the protein and could be misfolded aggregates, but they could also be an inactive form of the enzyme.

Experiments presented in Chapter 5 showed that TIP48 oligomerized in the presence of ADP/ATP and $MgCl_2$. However, no increase of the ATPase activity was seen with these oligomers. Therefore the monomer/dimer form may be in the best conformation to hydrolyze ATP.

Time course experiments using the monomer/dimer fractions of TIP48 revealed that ATP hydrolysis occurred in the first minute, but was very slow and remained nearly constant at around 5-7 moles ATP/mole of protein during the rest of the 20 min time-course (not shown). As the levels are so close to background kinetic experiments were difficult to perform accurately and were not pursued.

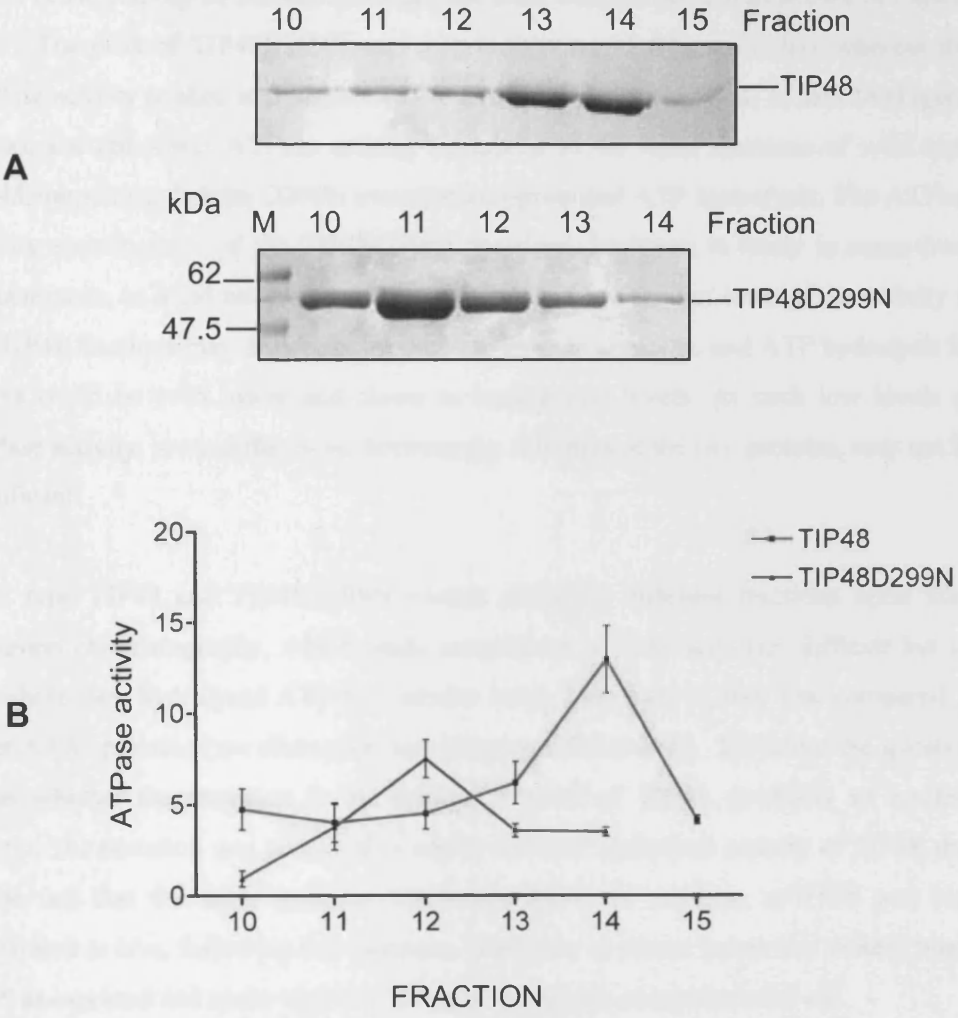

FIGURE 3.10: The ATPase activity of TIP48 and TIP48D299N after size exclusion chromatography

(A) 12 % SDS-PAGE of the Superdex 200 size exclusion chromatography fractions of TIP48 and TIP48D299N. 10 µl of each fraction, before concentration, were loaded on the gels, which were stained with Coomassie brilliant blue. (B) ATPase activities of the size exclusion chromatography fractions of TIP48 and TIP48D299N. Protein from each fraction was added to a final concentration of 1 µM, per ATPase reaction. ATP was added to a final concentration of 1 mM, per reaction. Reactions were then incubated at 37 ºC for 20 min. ATPase activity is expressed in moles of ATP hydrolysed per mole of protein monomer.

The ATPase activity of TIP48D299N did not peak with the protein as shown in Figure 3.10b. The peak of TIP48D299N was seen in fraction 11 (Figure 3.10a), whereas the ATPase activity peaked in fraction 12. The monomer/dimer fractions, 13 and 14 (Figure 3.10a), showed lower ATPase activity compared to the same fractions of wild type TIP48 suggesting that the D299N mutation compromised ATP hydrolysis. The ATPase activity seen in some of the TIP48D299N fractions, however, is likely to come from contaminants, as it did not peak with the protein. This means that some of the activity in the TIP48 fractions may also be contributed to by contaminants, and ATP hydrolysis by TIP48 could be even lower and closer to background levels. At such low levels of ATPase activity, some differences, between the activities of the two proteins, may not be significant.

Wild type TIP48 and TIP48D299N mutant eluted in different fractions upon size-exclusion chromatography, which made comparison of their activities difficult but on the whole they hydrolysed ATP to a similar level. This level is very low compared to other AAA^+ proteins (see discussion and Chapter 4 discussion). Therefore the question arises whether the mutation in the Walker B motif of TIP48, produces an inactive protein. The mutation was predicted to inhibit the ATP hydrolysis activity of TIP48, due to the fact that the same mutation inactivates RuvB. In addition, *sc*TIP48 was also inactivated *in vivo,* following this mutation. However, as shown below this mutant binds ATP, as expected and some very low levels of hydrolysis cannot be ruled out.

3.10. TIP48 and TIP48D299N mutant bind ATP

As the ATPase assays did not show a significant difference in activity between wild type and mutant TIP48, ATP binding experiments were carried out to see if the mutation, which should only effect ATP hydrolysis (Mezard et al., 1997; Ogura and Wilkinson, 2001), affected ATP binding. A binding assay was carried involving [γ_{32}P] 2 azido-ATP. Figure 3.11 shows that both TIP48 and TIP48D299N bind [γ^{32}P] 2 azido-ATP quite efficiently, as the ^{32}P signals correspond well to the Coomassie BB stained bands, shown on the SDS-PAGE gel.

This binding was shown to be specific to the ATP binding pocket of the proteins, by competition experiment with unlabelled ATP (Chapter 5, Figure 5.2 and 5.3). Excess ATP competed out the [γ^{32}P] 2 azido-ATP, confirming that the proteins bind ATP specifically. The fact that TIP48D299N is able to bind ATP indicates that the mutation still allows the protein to bind ATP, but is unlikely to allow the protein to hydrolyse ATP, to a similar level as TIP48, which supports the data shown above (Figure 3.10).

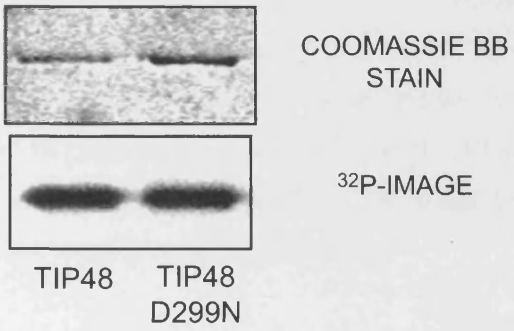

FIGURE 3.11: ATP binding assays with TIP48 and the TIP48D299N

Approximately 1 µg of TIP48 or TIP48D299N protein, in 20 µl reactions, were incubated with [γ–^{32}P] 2-Azido ATP at a final concentration of 10 µM. Reactions were UV irradiated and processed as described in Materials and Methods (section 2.8.3). The protein was separated by 12 % SDS-PAGE. The gel was stained with Coomassie brilliant blue, dried and exposed on a phosphorimager screen and developed by FUJI-FILM FLA 2000 phosphorimager.

3.11. Discussion

In summary, recombinant TIP48 and TIP49 do not display DNA helicase activities and their ATPase activities are not stimulated by DNA. They both have very low ATPase activities and are likely, even after ssDNA cellulose chromatography, to carry some ATPase contaminations that contribute to the overall low ATPase activity seen in the ATPase assays. However, both proteins bind ATP, which indicates they are folded correctly. The catalytically inactive mutants of both proteins behave differently from each other, both on size exclusion chromatography and in ATP binding. This signifies that the mutation made in the Walker B motif affects TIP48 and TIP49 in different ways. These findings will be discussed in more detail below.

The results presented here demonstrate directly, that the ssDNA stimulated ATPase activity seen with TIP49 and TIP49D302N was a contaminant, as it was removed using a ssDNA cellulose column, and that TIP49, on its own, is not a DNA helicase. However, it seems unlikely that ssDNA cellulose chromatography removed all contaminating bacterial ATPases. Size exclusion chromatography fractions of purified TIP49 and TIP49D302N showed activities that did not peak with the proteins, and some TIP49D302N fractions showed higher activity than wtTIP49. As the TIP49D302N mutant did not bind ATP, it would be unable to hydrolyze ATP. Clearly, the ATPase activity in the TIP49D302N fractions was coming from co-purifying contaminants. Also as the peak of activity in the TIP49D302N fractions was similar to the peak of activity in the TIP49 fractions, it is also likely that most of the activity in the TIP49 fractions was due to contaminants. The overall ATPase activity of TIP49 is therefore likely to be as low as the background of the enzyme assay.

Our data do not confirm the results for TIP49 published by (Makino et al., 1999), showing robust DNA helicase activity and ATPase activity, which were stimulated more than ten-fold in the presence of ssDNA. Our results, however, are in agreement with the data published by other groups, who showed that recombinant TIP49 had very low, or

no ATPase and no helicase activities (Ikura et al., 2000; Qiu et al., 1998). Therefore we suggest that the DNA helicase activity reported by (Makino et al., 1999) could have been due to contaminating bacterial helicases/ATPases. Significantly, the same authors reported no such activities in proteins expressed in insect cells. Hence, TIP49 has no intrinsic DNA helicase activity.

Our results show that recombinant TIP48 does not have ssDNA dependent ATPase or DNA helicase activity (Table 3.4 and Figure 3.9). The data shown in this chapter were obtained using a single batch of TIP48, but other TIP48 preparations made in the course of this project were in agreement with the results presented. Various other preparations showed similar low levels of ATPase activities but varied slightly, and in some cases a two-fold increase in ATPase activity in the presence of ssDNA was observed. This stimulation was very low compared to DNA/RNA helicases, which typically show 10- to 100- fold increase in ATPase activity, in the presence of DNA/RNA (Patel and Picha, 2000). All these data indicate that the DNA-dependent ATPase activity was due to a co-purifying contaminant and not an intrinsic property of TIP48.

These findings are in stark contrast with the data presented by (Kanemaki et al., 1999), who showed that the ATPase activity, which was ten times higher than the activity shown here in the absence of DNA, was stimulated approximately 44-fold in the presence of ssDNA. They also showed that TIP48 had helicase activity. The results presented here are however in agreement with those presented by (Ikura et al., 2000), who showed low ATPase activities with values similar to those shown in Figure 3.10b. They were also unable to demonstrate DNA helicase activity with the recombinant TIP48 protein. The discrepancies between the three studies could be due to differences in the way the TIP48 protein was purified resulting in different levels of contamination carried in the preps. Hence, we propose that TIP48 is not a DNA helicase as it did not bind to a ssDNA cellulose column and consistently did not show helicase activity in our hands, or in those of another group (Ikura et al., 2000). Moreover, co-purifying ssDNA dependent ATPases were successfully separated from TIP48 using ssDNA column. As TIP49 has a tendency to co-purify with robust DNA-helicases, from *E. coli*, it is likely

that a similar occurrence took place when TIP48 was purified by (Kanemaki et al., 1999).

The results presented show that TIP49 may have a strong tendency to associate with DNA helicases in *E. coli*. Other proteins purified in the lab using similar protocols, such as β-catenin-His_6, (described in Materials and Methods and Chapter 4) did not co-purify with DNA helicases, indicating that this event is characteristic of TIP49 and, to an extent, TIP48. It has been shown that both TIP48 and TIP49 bind specifically to the p400 protein, which is believed to have helicase activity (Fuchs et al., 2001). It may be that TIP49 and TIP48 interact with conserved DNA helicase motifs but, nevertheless, our experiments demonstrate convincingly that recombinant TIP48 and TIP49 do not have DNA helicase activity *in vitro*.

To evaluate the ATPase activity of TIP48 we compared the activity of TIP48 and TIP48D299N mutant. Differences in oligomeric state between the two proteins made this comparison complicated. The activity of the TIP48 monomeric/dimeric fractions was higher than the activity of the equivalent TIP48D299N fractions, so it is likely that TIP48 hydrolysed some ATP while the mutant did not. However, our experiments showed some ATPase activity associated with the monomeric/dimeric fractions of mutant TIP48D299N (Figure 3.10a lanes 5 and 6 and Figure 3.10b). The expectation that TIP48D299N would not hydrolyse ATP was based on the evidence that the same mutation made in the yeast homologue, (*sc*TIP48D296N), was inactive (King et al., 2001). The same mutation made in TIP49 also produces a dominant negative effect on the function of certain transcription activators (Dugan et al., 2002; Feng et al., 2003; Wood et al., 2000). Bacterial RuvB also exhibited a dominant negative phenotype when the same conserved residue in the Walker B motif was mutated (Iwasaki et al., 2000; Mezard et al., 1997) and additionally the ATPase activity of the RuvBD113N mutant was severely affected (Mezard et al., 1997).

Even though we cannot rule out the possibility that the TIP48D299N mutation could still hydrolyse some ATP, it is more likely that our results indicate the presence of

contaminants. To clarify this further it can be seen from Figure 3.10 that the ATPase activity peaked with the TIP48 protein, whereas is it did not peak with TIP48D299N, which mainly eluted with a molecular mass of approximately 400 kDa. This demonstrates that TIP48D299N fractions clearly contained some contaminating ATPases. Therefore a low level of contaminating activity may be associated with the equivalent wtTIP48 fractions (Figure 3.10b). The time course experiments indicated that as a whole TIP48 hydrolysed very little ATP, with almost all the hydrolysis occurring during the first minute of incubation (not shown). Therefore, TIP48, like TIP49, is an inefficient ATPase *in vitro* and is likely to have a very low ATP turnover number. The activities of TIP48 and TIP49 could be similar to the *A. fulgidus* clamp loader subunits and MCM proteins 2-6.

It was shown that both TIP48 and TIP48D299N bind ATP (Figure 3.11), but the level of binding has not been quantified here. The RuvBD113N mutant was also able to bind ATP, although the level of binding was 80 % of that observed with the wild-type protein (Mezard et al., 1997). The RuvB mutant, however, showed a 17-fold reduction in the k_{cat} value compared to the wild-type protein, indicating that this mutation does not affect ATP binding but does affect ATP hydrolysis. It is believed that this residue is involved in Mg^{2+} coordination for ATP hydrolysis by AAA^{+} proteins (Ogura and Wilkinson, 2001). The residue next to it, a conserved glutamate, which is believed to be the catalytic base in AAA^{+} proteins, was mutated in other studies and showed unquestionably that ATP hydrolysis was affected, whereas ATP binding was not (Seybert and Wigley, 2004). The residue mutated in our study (D299N), is less well characterized than the conserved glutamate residue, therefore the effect of mutating this residue in a protein such as TIP48, would not be obvious.

In the presence of ATP and $MgCl_2$ or $MgCl_2$ alone, RuvB forms hexamers (Mitchell and West, 1994). As will be shown in Chapter 5, TIP48 also forms oligomers in the presence of adenine nucleotides and $MgCl_2$. The RuvBD113N mutant was shown to form hexamers in the absence of $MgCl_2$, whereas the wild-type protein formed mainly dimeric and tetrameric species (Mezard et al., 1997). This showed that RuvBD113N had lost its dependence on divalent metal ions for formation of stable

hexamers. A similar observation was made for TIP48D299N, as it eluted from the size exclusion chromatography with a molecular mass of 400 kDa, which corresponds to an octamer but could well be is most likely a hexamer. These data show that there are similarities between TIP48 and RuvB as predicted. The adenine nucleotide binding and oligomerization properties of TIP48 will be described and discussed further in Chapter 5.

TIP49D302N on the other hand did not bind ATP, unlike TIP48D299N and RuvBD113N. Although this residue is not directly involved in the binding of ATP by AAA^+ proteins, the mutation obviously had a different effect on TIP49. Other data have shown that this mutation inactivates the function of TIP49 *in vivo* (Dugan et al., 2002; Feng et al., 2003; Wood et al., 2000). However, it is not known whether the loss of function *in vivo* is due to a defect in ATP binding alone, or whether ATP binding and hydrolysis are required for the functions of TIP49. Furthermore, this mutation did not affect the subunit organization of TIP49 as TIP49D302N still eluted as a monomer. Hence, this confirms that the mutation affects TIP49 in a different way compared to TIP48 and RuvB.

Although the activity of both TIP48 and TIP49 are low, the proteins are not inactive. They could both bind ATP and significantly, a higher activity was observed when the two proteins were mixed to form a complex (see Chapter 4). This may be similar to the observation made about the yeast MCM AAA^+ proteins, which show very low ATPase activities on their own but higher activities when put together in certain combinations or when they are part of the final functional complex (Davey et al., 2003).

This chapter has tried to demonstrate the intrinsic enzymatic properties of TIP48 and TIP49, as contradictions exist in the literature about their biochemical activities. In Chapter 4 more data has been presented, which shows that neither TIP48, nor TIP49 ATPase activities are stimulated by other forms of DNA (Table 4.1). Therefore, on their own, *in vitro*, they do not seem to do very much, as their ATPase activities are so low and, as reported by other groups, not stimulated by DNA. This does not mean

that they do not modify DNA or chromatin in some way, *in vivo*, but they may require accessory factors or as will be investigated in Chapter 4, they may need to form a complex. The effect on the ATPase activity of TIP48/49 complex formation and interaction with β-catenin will be presented and discussed in the next chapter.

CHAPTER 4

Purification and characterization of the TIP48/TIP49 complex

4.1. Introduction

There is a great deal of evidence in the literature that TIP48 and TIP49 form a complex *in vivo* (Bauer et al., 2000; Gohshi et al., 1999; Kanemaki et al., 1999; Wood et al., 2000) and it has also been demonstrated that they form a complex *in vitro* (Bauer et al., 2000; Ikura et al., 2000; Kanemaki et al., 1999). These findings have been supported recently with more solid evidence that they work together as a complex, for the function of the INO80 complex in yeast (Jonsson et al., 2004).

In Chapter 3 we have shown that TIP48 and TIP49 had very low ATPase activities on their own, which were not stimulated in the presence of ssDNA. These findings support those of one group, who also showed that TIP48 and TIP49 had low ATPase activities (Ikura et al., 2000). In addition, they also found that the TIP48/TIP49 complex showed a synergistic increase in ATPase activity. Therefore it was decided to purify this complex and examine its enzymatic activities. Moreover, mutant complexes were made to show the effect of Walker B mutations on the ATPase activity of the complex and to see whether both components of the complex hydrolyse ATP. Lastly, an investigation was carried out into whether an interacting partner of TIP48 and TIP49, β-catenin, would affect the ATPase activities of the individual proteins and the complex

4.2.1. A stoichiometric TIP48/TIP49 complex assembles upon refolding from urea

A dual expression cassette, containing the coding sequences of TIP49-His_6 and TIP48, was made for the co-expression of the two proteins in *E. coli,* as described in Materials and Methods (section 2.4.7). As shown schematically in Figure 2.4, each protein was expressed from a separate T7 promoter. Only the TIP49 protein was constructed with a His_6 tag so that a TIP48/TIP49 complex could be captured specifically, by metal affinity chromatography.

The construct was transformed into BL21 (DE3) Gold and BL21 (DE3) Gold pLysS strains and expression was verified 4 h after induction. Expression of TIP49 and TIP48

was low in the BL21 Gold strain, but a higher expression of both proteins was achieved in the BL21 Gold pLysS strain. Induced cells, from both strains, were lysed under different conditions, but the two proteins remained completely insoluble.

Since co-expression of TIP48 and TIP49 in the cells did not produce a soluble complex, it was decided to try and obtain a complex by refolding the proteins after denaturation. The pellets of lysed cells containing the two proteins were solubilized in 6 M and/or 8 M urea, as described in Materials and Methods (section 2.7.5). Almost equal amounts of the two proteins were solubilized by this process and were subjected to stepwise dialyses until all the urea had been removed (see Materials and Methods, section 2.7.5).

Almost all of the TIP48 and TIP49 proteins remained soluble after dialysis. Significantly, both proteins bound to the Talon column specifically, via TIP49-His_6, and therefore, had formed a complex. Some TIP48 was seen to flow through the column and may have been in excess over TIP49-His_6. However, most of the complex that eluted in the imidazole gradient fractions contained an equimolar TIP49:TIP48 ratio (Figure 4.1a, lane 4). The positions of TIP48 and TIP49-His_6 on the SDS-PAGE gel were identified by immunoblotting the proteins, using an anti-His antibody. Purified TIP49-His_6 protein (see below) was used as a control. This experiment showed that a stable stoichiometric TIP49/TIP48 complex could be assembled upon refolding.

In order to compare the ATPase activity of this complex with the individual proteins, both TIP48 and TIP49 were purified under denaturing conditions and refolded, as described in Materials and Methods (sections 2.7.2 and 2.7.4). TIP48-His_6 was loaded on the Talon column in 6 M urea, refolded on the column and eluted in the absence of urea. TIP49-His_6 was loaded and eluted from the Talon column in the presence of 6 M urea and the purified protein was refolded in solution, by step dialysis. The CD spectra of both proteins showed pronounced, mainly α-helical, secondary structure (not shown)

FIGURE 4.1: Purified fractions and ATPase activity of the refolded TIP48/TIP49 complex and the individual proteins

(A) 12 % SDS-PAGE of the refolded TIP49 (lane 2), TIP48 (lane 3) and TIP49-His_6/TIP48 complex (lane 4), purified by Talon metal affinity chromatography as described in Material and Methods (sections 2.7.2, 2.7.4 and 2.7.5). Approximately 2 μg of TIP48 or TIP49 and 0.5 μg of the complex were loaded on the gel, so that both bands could be seen separated clearly. The position of the TIP49-His_6 and TIP48 proteins were verified by immunoblotting and are indicated on the gel. The gel was stained with Coomassie brilliant blue.

(B) 12 % SDS-PAGE of the Superdex 200 size exclusion chromatography fractions of the refolded complex. 2 μg of each fraction were loaded, where possible. The positions of TIP49-His_6 and TIP48 were verified by immunoblotting and are indicated on the gel. The gel was stained with Coomassie brilliant blue.

(C) ATPase activity of refolded TIP49, TIP48 and TIP49-His_6/TIP48 complex. Reactions containing 1 μM of TIP48, TIP49 and the TIP48/TIP49 complex, with or without 5 ng/μl of ϕX174 (ssDNA) and 1 mM ATP were incubated at 37 °C for 30 min. The concentration of the complex was expressed in terms of TIP48/TIP49 monomers (see Materials and Methods, section 2.8.2). ATPase activity is expressed as moles of ATP hydrolyzed per mole of protein monomer.

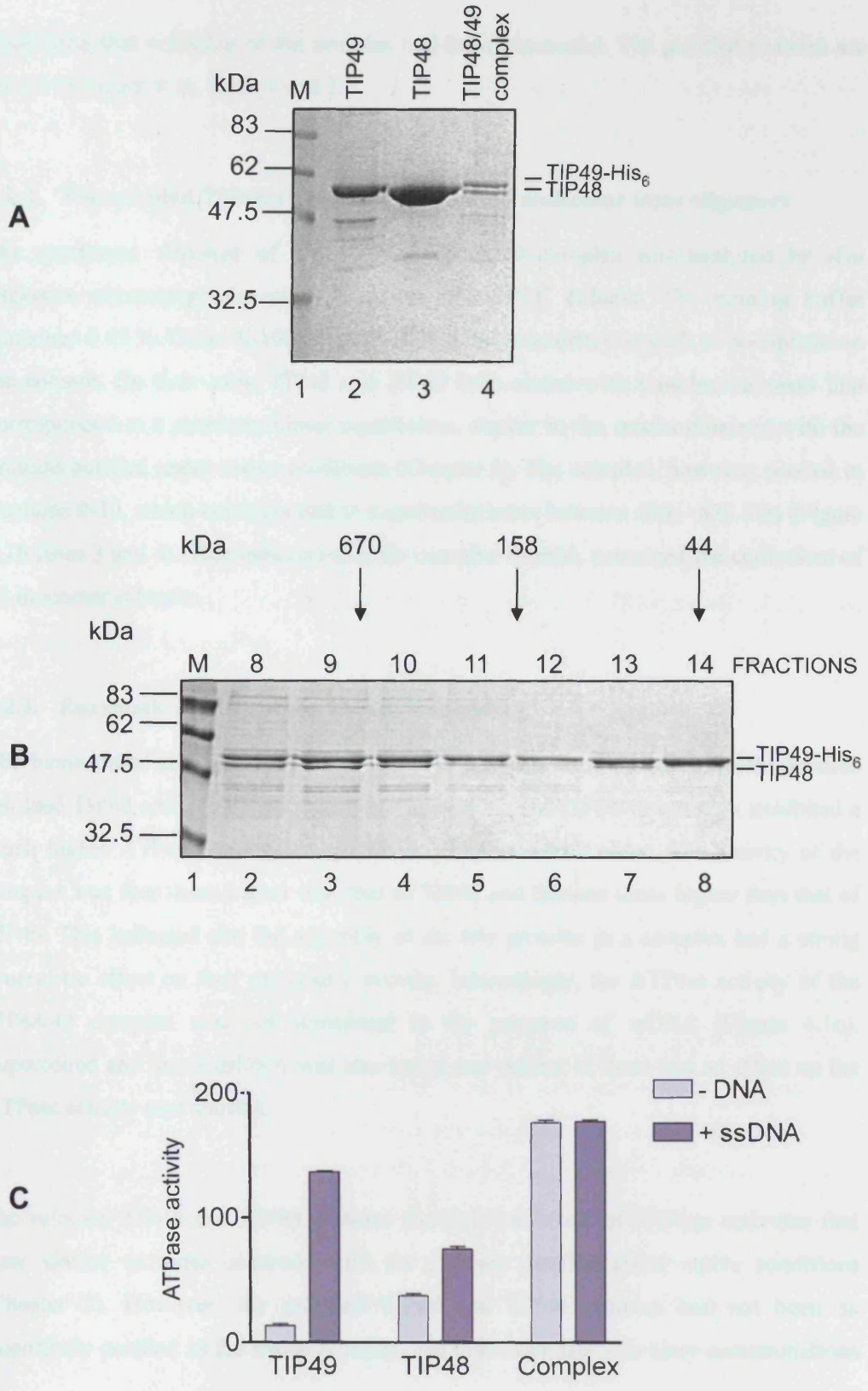
A
kDa
M
TIP49
TIP48
TIP48/49 complex
83
62
47.5
32.5
TIP49-His6
TIP48
1 2 3 4
B
kDa
670
158
44
kDa
M 8 9 10 11 12 13 14 FRACTIONS
83
62
47.5
32.5
TIP49-His6
TIP48
1 2 3 4 5 6 7 8
C
200
100
0
ATPase activity
- DNA
+ ssDNA
TIP49
TIP48
Complex

indicating that refolding of the proteins had been successful. The purified proteins are shown in Figure 4.1a, lanes 2 and 3.

4.2.2. The refolded TIP48/49 complex forms high molecular mass oligomers

The quaternary structure of the refolded TIP48/49 complex was analysed by size exclusion chromatography on a Superdex 200 FPLC column. The running buffer contained 0.05 % Triton X-100, as the complex had a tendency to stick or precipitate on the column. On their own, TIP48 and TIP49 both eluted with a molecular mass that corresponded to a monomer/dimer equilibrium, similar to the results obtained with the proteins purified under native conditions (Chapter 3). The complex, however, peaked in fractions 9-10, which corresponded to a molecular mass between 600 – 670 kDa (Figure 4.1b lanes 3 and 4). This indicates that the complex formed, contained the equivalent of 12 monomer subunits.

4.2.3. Enzymatic activity of the TIP48/49 complex

The biochemical activities of the TIP48/TIP49 complex were tested alongside purified refolded TIP48 and TIP49. As shown in Figure 4.1c, the TIP48/49 complex exhibited a much higher ATPase activity compared to TIP48 or TIP49 alone. The activity of the complex was four times higher than that of TIP48 and thirteen times higher than that of TIP49. This indicated that the assembly of the two proteins in a complex had a strong synergistic effect on their enzymatic activity. Interestingly, the ATPase activity of the TIP48/49 complex was not stimulated in the presence of ssDNA (Figure 4.1c). Supercoiled and linear dsDNA was also tested and neither of these had an effect on the ATPase activity (not shown).

The refolded TIP48 and TIP49 proteins showed low levels of ATPase activities that were similar to those observed with the proteins purified under native conditions (Chapter 3). However, the refolded TIP48 and TIP49 proteins had not been as extensively purified as the native proteins, and both were likely to carry contaminations

from bacterial ATPase(s). TIP49-His_6 in particular, showed a high stimulation (10-fold) of ATPase activity in the presence of ssDNA. The same activity was seen with the TIP49D302N-His_6 mutant, purified under identical conditions (not shown), and was therefore likely to be a contaminant. Hence, due to the presence of contaminating ATPases with the individual proteins, the increase in ATPase activity seen upon the formation of the TIP48/TIP49 complex was likely to be even higher than estimated from the results shown in Figure 4.1c.

While we cannot rule out the presence of contaminating ATPase activities in the refolded TIP48/49 complex, it is clear that the complex did not co-purify with the DNA-dependent ATPase(s), as seen with TIP48 and particularly, TIP49. These results are very similar to the results obtained with the native TIP48/49 complex, as described below. Since a number of minor protein bands could be seen in this complex by SDS-PAGE, and other contaminating ATPases may have been present, its biochemical activity was not characterized any further.

4.3. Assembly and purification of TIP48/TIP49 complex under native conditions

To assemble the TIP48/49 complex under native conditions it was decided to use purified TIP48-His_6, which gave high yields during purification (Chapter 3), and untagged TIP49. Untagged TIP49 was partially purified as described in Materials and Methods (section 2.7.6). Briefly, the bulk of the bacterial DNA was removed from the crude lysate by passage through a DEAE column in buffer containing 0.3 M NaCl, and the proteins were fractionated by ammonium sulphate precipitation, ion-exchange and hydroxyapatite chromatography. TIP48-His_6 was purified by chromatography on Talon, MonoQ and ssDNA cellulose columns, as described in Chapter 3 (Section 3.8). The TIP48/49 complex was assembled by mixing the two proteins in a 2:1 ratio of TIP49:TIP48-His_6, in Talon buffer. After incubation on ice for 30 min, the mixture was applied to a Talon metal affinity column. A TIP49/TIP48-His_6 complex specifically bound to the Talon column and was eluted with 150-400 mM imidazole (Figure 4.2b,

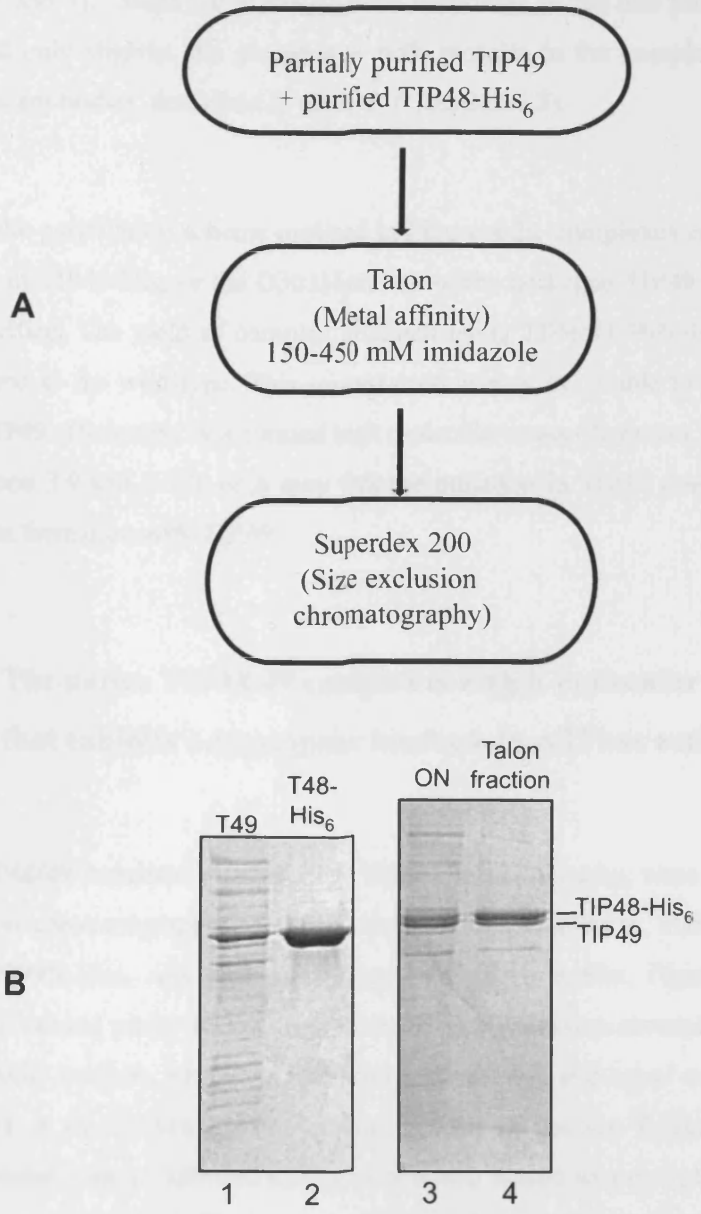

FIGURE 4.2: Purification of TIP48-His_6/TIP49 complex under native conditions

(A) Purification scheme of the TIP48-His_6/TIP49 complex under native conditions. (B) 18 % SDS-PAGE of the fractions collected from the purification of the TIP48-His_6/TIP49 complex. Lane 1: partially purified TIP49; lane 2: purified TIP48-His_6; lane 3: the mixture of the two before loading on the Talon column (the ON fraction); and lane 4: the Talon purified TIP48-His_6/TIP49 complex. The gels were stained with Coomassie brilliant blue.

lanes 3 and 4). Since the electrophoretic mobilities of the two proteins on SDS PAGE differed only slightly, the presence of both proteins in the complex was verified using specific antibodies, described in Chapter 6 (section 6.2).

Using the purification scheme outlined in Figure 4.2a, complexes containing the D299N mutant of TIP48-His_6 or the D302N mutant of the untagged TIP49 were also assembled and purified. The yield of complex obtained using TIP48D299N-His_6 was much lower compared to the wild-type. This mutant protein may be unable to assemble a complex with TIP49 efficiently, as it formed high molecular mass oligomers, as shown in Chapter 3 (Section 3.9 and 3.10), or it may that the mutation in TIP48 does not allow efficient complex formation with TIP49.

4.4. The native TIP48/49 complex is a high molecular mass oligomer that exhibits a synergistic increase in ATPase activity

The TIP48/49 complexes, purified by Talon chromatography, were fractionated by size exclusion chromatography on a Superdex 200 FPLC column, and free TIP48-His_6 or TIP48D299N-His_6, was separated away from the complex. Figure 4.3a shows the composition and purity of fractions from the size exclusion chromatography, following SDS PAGE analysis. Fractions had been concentrated and equal amounts were loaded (~ 2 μg). A stochiometric complex can be seen in fraction 9 (lane 3), corresponding to molecular mass of 850-650 kDa, which would equate to a complex made up of 12 to 16 monomers of TIP48/TIP49 protein. Fraction 8, which also contained similar amounts of each protein, formed part of the void volume for the column, in which high molecular mass aggregates are likely to elute.

It can be seen from fraction 10 onwards (Figure 4.3a, lanes 4-8), that the amount of TIP49 (lower band) decreased, and in fraction 13 only TIP48-His_6 (upper band) remained,

FIGURE 4.3: Size exclusion chromatography fractions of the TIP48-His_6/TIP49 complex and their ATPase activities

(A) 18 % SDS-PAGE of the TIP48-His_6/TIP49 complex size exclusion chromatography fractions, which was captured beforehand on the Talon column (ON fraction, lane 1). 2 μg of each sample were loaded on the gel, which was stained with Coomassie brilliant blue. The position of the TIP48-His_6 and TIP49 proteins were verified by immunoblotting and are indicated on the gel. Molecular mass markers for the Superdex 200 size exclusion chromatography column are shown above the gel.
(B) Bar graph showing the ATPase activities of the size exclusion chromatography fractions that are shown in (A) and the purified TIP48 and TIP49 proteins (see Chapter 3). Protein was added to the reactions at a final concentration of 1 μM, in terms of TIP48/TIP49 monomers. Reactions were incubated at 37 °C for a total of 30 min. ATPase activity is expressed as moles of ATP hydrolyzed per mole of TIP48/TIP49 monomer.

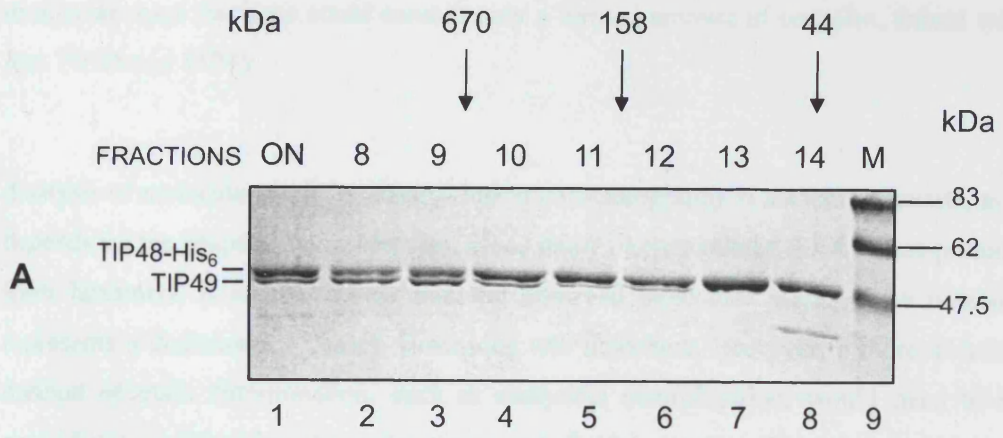
kDa
670
158
44
kDa
FRACTIONS ON 8 9 10 11 12 13 14 M
A
TIP48-His6
TIP49
83
62
47.5
1 2 3 4 5 6 7 8 9

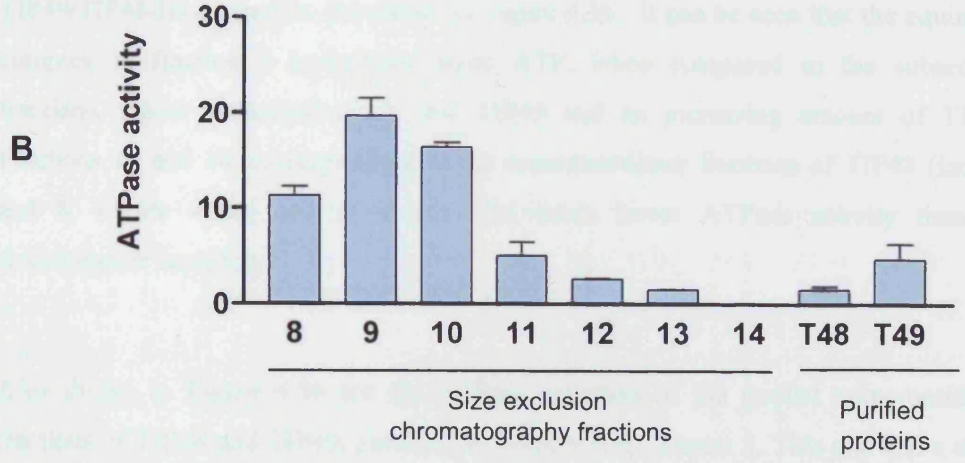
B
ATPase activity
30
20
10
0
8 9 10 11 12 13 14 T48 T49
Size exclusion chromatography fractions
Purified proteins

as determined by immunoblotting using anti-TIP48 and anti-TIP49 antibodies (Chapter 6). Therefore, the complex exists mainly as a high molecular mass oligomer. Lower molecular mass fractions could contain only a limited amount of complex, mixed with free TIP48 and TIP49.

Analysis of molecular mass by size exclusion chromatography is not very accurate, as it depends on the shape of the molecules. Since many closely related AAA^+ class proteins form hexamers, it is most likely that the observed molecular mass of the complex represents a dodecamer (12mer), containing two hexamers. However, a more accurate method of mass determination, such as analytical centrifugation, would need to be carried out to determine the molecular mass of this complex. To determine if these proteins form hexamers *in vitro*, a more in depth study was necessary, and was carried out using electron microscopy, which is presented in Chapter 5.

The ATPase activities of the fractions from the size exclusion chromatography of the TIP49/TIP48-His_6 complex are shown in Figure 4.3b. It can be seen that the equimolar complex in fraction 9 hydrolysed more ATP, when compared to the subsequent fractions, which contained much less TIP49 and an increasing amount of TIP48. Fractions 13 and 14, corresponding to the monomer/dimer fractions of TIP48 (lanes 7 and 8, Figure 4.3a), had more than ten times lower ATPase activity than the stochiometric complex.

Also shown in Figure 4.3b are the ATPase activities of the pooled monomer/dimer fractions of TIP48 and TIP49, purified, as described in Chapter 3. This allowed a direct comparison of the ATPase activity of TIP48 and TIP49 with the TIP48/TIP49 complex. It can be seen that the activity of the TIP48 fraction is similar to that of fraction 13 (Figure 4.3a, lane 7), which contained free TIP48. The activity of purified TIP49 is around five times less than the equimolar complex. These data confirm that the complex

has a higher activity than TIP48 and TIP49 alone, and that the two proteins have a synergistic effect on each other for the ATPase activity of the complex.

4.5. Both TIP48 and TIP49 bind and hydrolyse ATP within the complex

As a synergistic increase in activity was seen when TIP48 and TIP49 formed a complex, it was important to address whether both components of the complex bound and hydrolysed ATP. The complex was incubated with the ATP analogue [γ^{32}P] 2 azido-ATP and UV-irradiated to test if it cross-linked to the complex. Figure 4.4 shows the Coomassie BB stained gel of the complex and the phosphorimage of the same gel. It can be seen that both TIP48 and TIP49 within the complex bind the ATP analogue. The ^{32}P signal from both bands appears almost equivalent, suggesting that the two proteins bind the same amount of ATP. However, an experiment that gives actual quantities of ATP bound to the proteins would need to be carried out to determine if both components do indeed, bind an equal amount of ATP. Nevertheless, as both components of the complex bind ATP, it is very likely that both also hydrolyse ATP within the complex.

In order to investigate this hypothesis, a time course of the ATPase activity of the wtTIP48/TIP49 complex was first carried out. Figure 4.5 shows an increase in ATP hydrolysis over time by the TIP48/TIP49 complex. This demonstrates that unlike the individual proteins (Chapter 3), the complex was able to hydrolyse a steady amount of ATP over time *in vitro*. An approximation was made for the turnover number by the complex, by looking at the rate from the whole 20 min time course, which gave a value of 0.48 moles ATP/mole protein/min. However, to get a more accurate value for the turnover number, initial rates for the complex would have to be calculated at different substrate concentrations. This turnover number for the complex is quite low, compared to the turnover numbers of some other AAA$^+$ proteins, as discussed later.

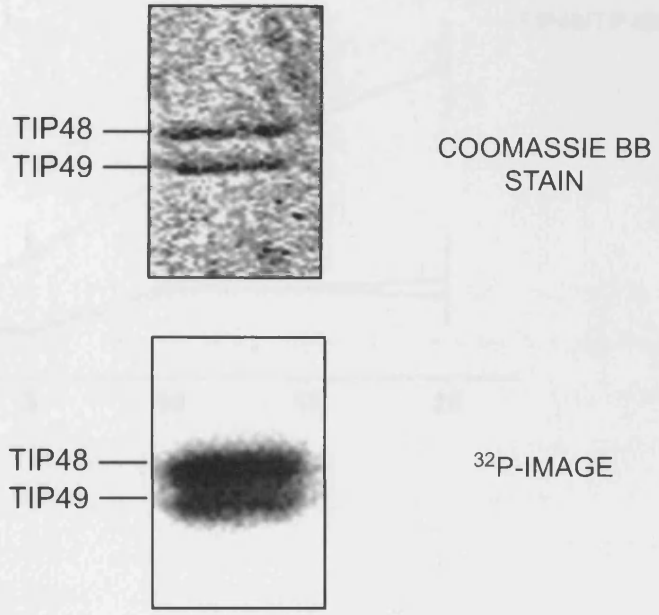

FIGURE 4.4: ATP binding assay with the TIP48/TIP49 complex

Approximately 1 µg of the TIP48/TIP49 complex, in 20 µl reactions, were incubated with [γ–^{32}P] 2-Azido ATP at a final concentration of 10 µM. Reactions were irradiated with UV light and processed as described in Materials and Methods (section 4.8.3). The proteins were separated by 18 % SDS-PAGE. The gel was stained with Coomassie brilliant blue, dried and exposed on a phosphorimager screen and developed by FUJI-FILM FLA 2000 phosphorimager.

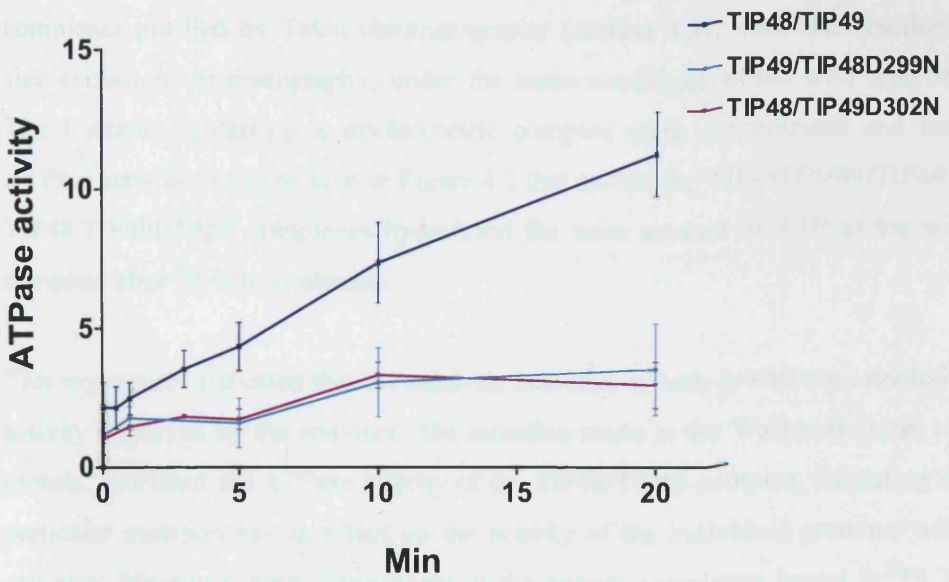

FIGURE 4.5: Effect of Walker B mutations on the ATPase activity of the TIP48/TIP49 complex

Time courses of ATP hydrolysis by the TIP48/TIP49, TIP49/TIP48D299N and TIP48/TIP49D302N complexes. Reactions contained 1 μM complex in terms of TIP48/TIP49 monomers. The reactions were incubated at 37 °C and 10 μl aliquots were taken and stopped at the specific time-points indicated. ATPase activity is expressed in terms of moles of ATP hydrolysed per mole of protein monomer.

To see whether both proteins are required for the activity of the complex, the two mutant complexes purified by Talon chromatography (section 4.3), were also fractionated by size exclusion chromatography, under the same conditions as the wild type complex. The fractions containing a stochiometric complex were concentrated and tested for ATPase activity. It can be seen in Figure 4.5 that neither the TIP48D299N/TIP49 nor the TIP48/TIP49D302N complexes hydrolysed the same amount of ATP as the wild type complex, after 20 min incubation.

This experiment indicated that the catalytic activities of both proteins are needed for the activity displayed by the complex. The mutation made in the Walker B motif, of either protein, abolished the ATPase activity of the TIP48/TIP49 complex, indicating that this particular mutation has an effect on the activity of the individual proteins, within the complex. Moreover, both components of the mutant complexes bound [γ^{32}P] 2 azido-ATP (not shown), indicating that the mutation affected ATPase activity but not ATP binding by the two proteins, as expected (discussed in Chapter 3). These experiments therefore confirm that the two proteins facilitate each other to hydrolyse ATP as a complex, and that ATP hydrolysis, by both proteins, is essential for this activity.

4.6. The ATPase activity of the complex is not stimulated by DNA

ATPase assays were carried out with the native wtTIP48/TIP49 complex, both in the absence and presence of different forms of DNA. The DNAs used were ϕX174 ssDNA, pUC19 supercoiled dsDNA, linearised pUC19 dsDNA, and a synthetic four-way Holliday junction. The results in Figure 4.6a show time courses of ATP hydrolysis by the complex, in the absence or presence of ssDNA. Figure 4.6b displays the ATP hydrolyzed by the complex, in the presence of all the DNA forms, at the 20 min time point. It can be observed from these results that no significant stimulation of the ATPase

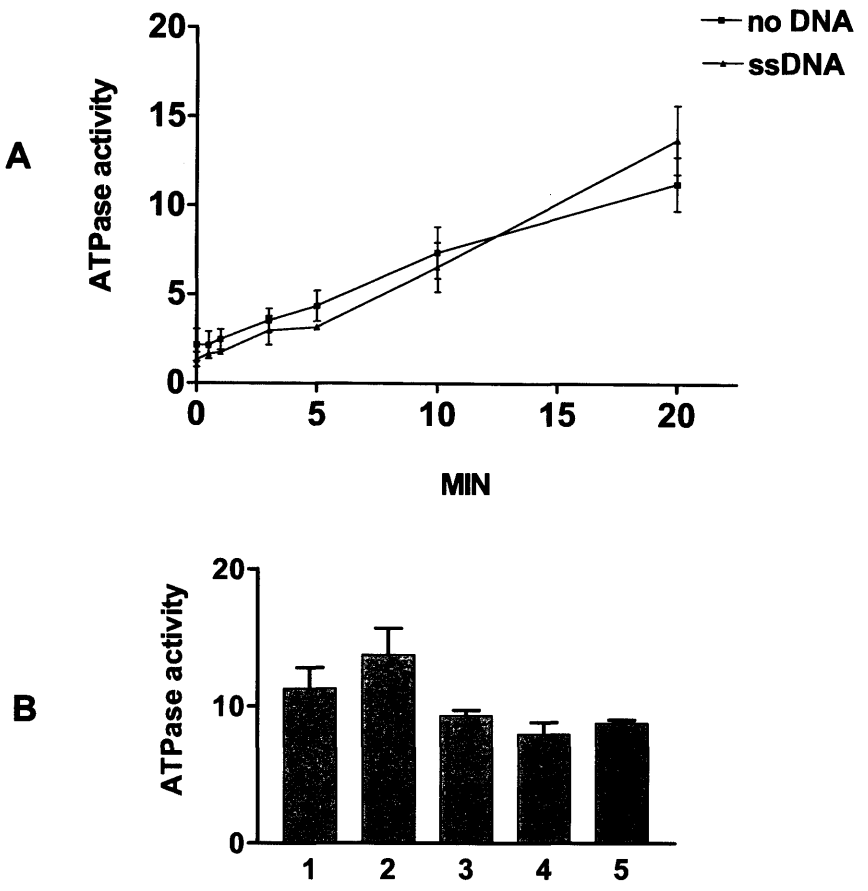

FIGURE 4.6: Effect of DNA on the ATPase activity of the TIP48/TIP49 complex

(A) Time courses of ATP hydrolysis by the TIP48/TIP49 complex, in the presence and absence of ϕX174 ssDNA (5 ng/μl). The complex was added to reactions at a final concentration of 1 μM, in terms of TIP48/TIP49 monomers. ATPase activity is expressed in moles of ATP hydrolyzed per mole of protein monomer. (B) Bar graph representing the ATPase activity of the TIP48/TIP49 complex in the presence of different DNA substrates: (1) No DNA; (2) ϕX174 ssDNA; (3) pUC19 super-coiled dsDNA; (4) pUC19 linearised dsDNA; (5) Synthetic Holliday junction. DNA was added to a final concentration of 5 ng/μl. Reactions containing 1 μM of complex, in terms of TIP48/TIP49 monomers, were incubated for 20 min in total, at 37 °C. ATPase activity is expressed in terms of moles of ATP hydrolyzed per mole of protein monomer.

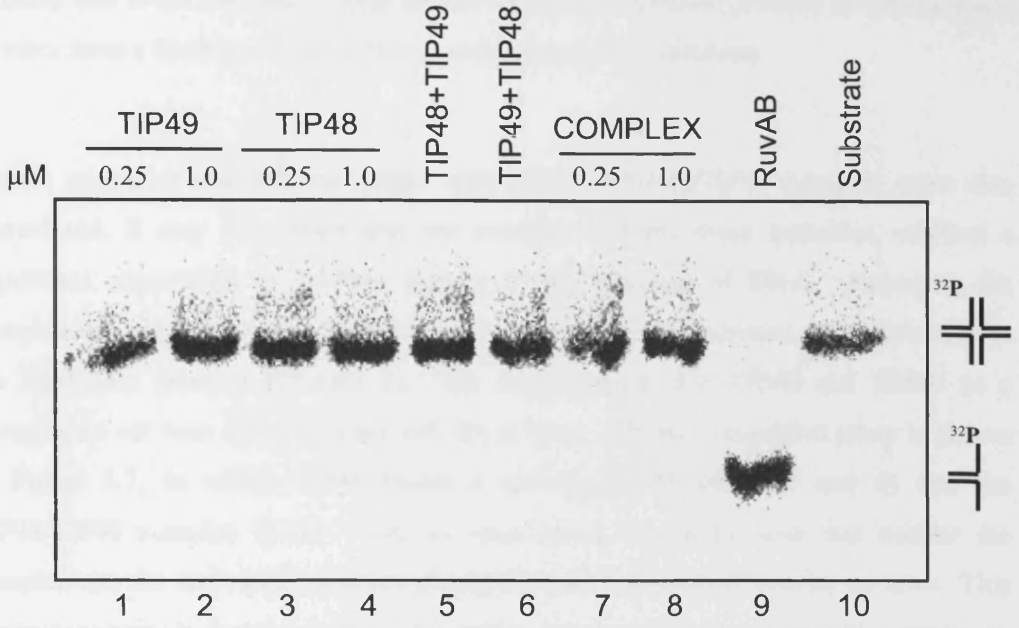

FIGURE 4.7: Assays for branch migration with TIP48, TIP49 and the TIP48/TIP49 complex

Branch migration assays with increasing concentrations of purified TIP49 (lanes 1 and 2), TIP48 (lanes 3 and 4) and TIP48/TIP49 complex (lanes 7 and 8). Lane 5 shows a reaction that was carried out by pre-incubating the Holliday junction with TIP48 before adding TIP49. Lane 6 shows a reaction that was carried out by pre-incubating the Holliday junction with TIP49 before adding TIP48 (concentrations of 1.0 μM were used for both proteins in each reaction). Lane 9: control reaction with *E. coli* RuvAB; and lane 10: control reaction with labelled Holliday junction alone.

activity of the native TIP48/TIP49 complex occurred in the presence of any of these DNA forms, as seen with the refolded TIP48/TIP49 complex (section 4.2). It is therefore unlikely that in the absence of other factors either the individual proteins or the complex, *in vitro,* have a function on DNA that is coupled to ATP hydrolysis.

Branch migration and helicase assays with native wtTIP48/TIP49 complex were also carried out. It may have been that the complex exhibits these activities, without a significant stimulation of ATPase activity in the presence of DNA. However, the complex did not exhibit any DNA helicase activity (data not shown), as observed with the individual proteins (Chapter 3). This demonstrated that TIP48 and TIP49 as a complex do not have DNA helicase activity *in vitro*. A branch migration assay is shown in Figure 4.7, in which TIP48 (lanes 1 and 2), TIP49 (lanes 3 and 4) and the TIP48/TIP49 complex (lanes 7 and 8) were tested. It can be seen that neither the complex nor the individual proteins displayed branch migration activity *in vitro*. This shows conclusively that the preformed complex does not show any detectable activity on DNA *in vitro*.

4.7. Reconstituting the complex in the presence of DNA has no effect on the ATPase activity of the complex

The fact that the ATPase activity of the complex was not stimulated in the presence of different DNA forms, and it did not exhibit DNA helicase or branch migration activities, may have been because the complex was preformed and unable to load onto DNA. Therefore, it was decided to assemble the complex by mixing the individual proteins in the presence of DNA and then observe if there was any effect on the ATPase activity.

TIP48 and TIP49, purified as described in Chapter 3, were incubated together and their ATPase activity was compared to that of the pre-formed TIP48/TIP49 complex. Equal

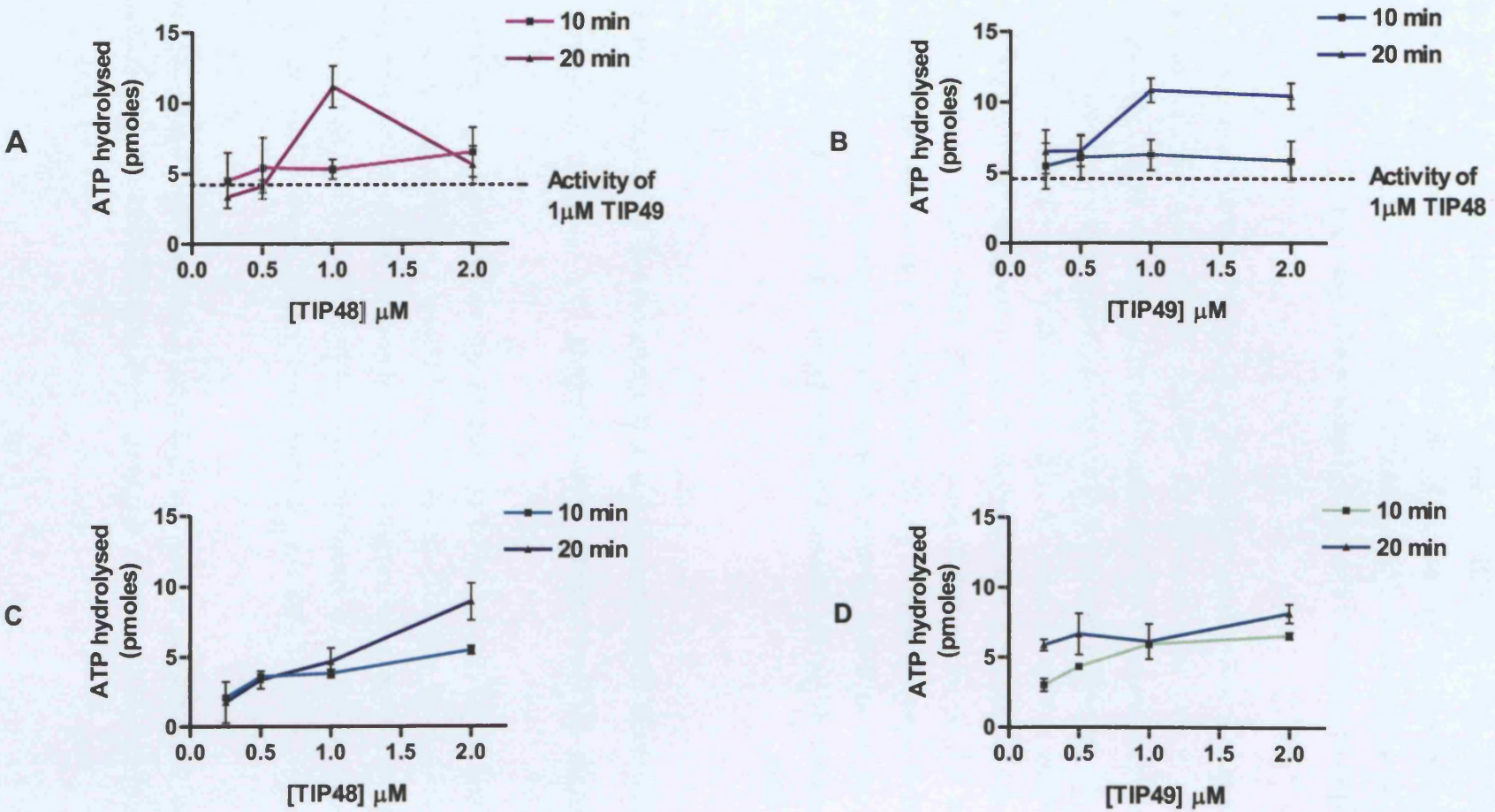
A
ATP hydrolysed (pmoles)
15
10
5
0
0.0
0.5
1.0
1.5
2.0
[TIP48] μM
10 min
20 min
Activity of 1μM TIP49
B
ATP hydrolysed (pmoles)
[TIP49] μM
10 min
20 min
Activity of 1μM TIP48
C
ATP hydrolysed (pmoles)
[TIP48] μM
10 min
20 min
D
ATP hydrolyzed (pmoles)
[TIP49] μM
10 min
20 min

FIGURE 4.8: The ATPase activity of the complex formed at different concentrations of TIP48 and TIP49

(A) Reactions containing 1 μM of TIP49 in reaction buffer C (Materials and Methods, section 2.8.2), were pre-incubated on ice for 10 min with increasing concentrations of TIP48, as indicated. ATP/$MgCl_2$/[α^{32}P]-ATP mixture was added to each reaction to give a final concentration of 2 mM ATP and 5 mM $MgCl_2$ and reactions were incubated at 37 °C. Reactions were stopped at 10 min and 20 min.
(B) Reactions containing 1 μM of TIP48 in reaction buffer C, were pre-incubated on ice for 10 min with increasing concentrations of TIP49, as indicated. Reactions were then carried out as described in (A). The dashed lines (in A and B) represent the activity of 1 μM of TIP49 or TIP48 proteins, on their own, after a 20 min incubation.
(C and D) show the control reactions with the individual proteins at the different concentrations. Reactions were set up as in A and B and stopped at 10 and 20 min.

amounts of the two proteins were used and they were pre-incubated in the presence or absence of ATP. A 50 % increase of the ATPase activity was seen compared to TIP48 and TIP49 alone, when the proteins were pre-mixed, both in the presence and absence of ATP (not shown). However, the activity observed was approximately 50 % lower than the activity of the purified complex. Therefore, although there was a clear increase in ATPase activity when TIP48 and TIP49 were mixed, conditions for the assembly of the complex had to be optimized.

The effect of NaCl, $MgCl_2$, ATP and pH on the ATPase activity of the complex formed from the individual proteins, was tested (not shown). The level of effect seen with each variable, when concentration or pH was changed was between 5-40 %. It was found that 100 mM of NaCl, 5 mM of $MgCl_2$ and 2 mM of ATP were optimum. The effects of buffers with different pH values were also tested and it was shown that potassium phosphate buffer (pH 6.8) had an inhibitory effect on the activity. The optimum was pH 7.0 in Tris-HCl buffer. These conditions were used for the subsequent assays, described below. Although these conditions were optimal, it is still unlikely that all the TIP48 and TIP49 molecules would engaged in complex formation, because as shown earlier, not all of the TIP48-His_6 molecules were involved in the formation of the complex, even with an excess of TIP49, as some of it eluted as a monomer/dimer after size exclusion chromatography (Section 4.4).

Different ratios of the two proteins were used to determine the optimal stoichiometry of complex assembly. Firstly, different concentrations of TIP48 or TIP49 were tested alone, and the ATPase activity determined at 10 and 20 min (Figure 4.8c and d). Figure 4.8c shows an increase in ATP hydrolysis as TIP48 concentration increased. Reactions with 2 μM of TIP48 showed a slight difference in activity between the 10 and 20 min time points, which suggest that there was an increase in ATP hydrolysis over time when higher concentrations of TIP48 were used. Figure 4.8d shows the ATPase activity of TIP49 at different concentrations and illustrates that although there was a slight increase in activity as TIP49 concentration was increased, the activity remained low and close to background levels. Moreover, not much difference was seen in the ATPase activities

between the 10 and 20 min time points, demonstrating that TIP49 hydrolyses very little ATP.

Figure 4.8a and 4.8b show the ATPase activities when increasing concentrations of TIP48 (Figure 4.8a) or TIP49 (Figure 4.8b) were added to a constant concentration (1 μM) of TIP49, or TIP48, respectively. The dashed lines in Figures 4.8a and b represent the activities of 1 μM of TIP48 or TIP49 alone after 20 min incubation. It can be seen that a significant increase in activity was gained, after 20 min, when 1 μM of TIP48 was added to 1 μM of TIP49 (Figure 4.8a). However, at other concentrations of TIP48, this stimulation was not seen. It is also shown that when 1 μM of TIP49 was added to 1 μM of TIP48 (Figure 4.8b), this stimulation of activity was again seen and even when 2 μM of TIP49 is added, the activity remains the same. On the other hand, when 2 μM of TIP48 was added to TIP49 the activity dropped (Figure 4.8a). The reason for this difference is unknown; nonetheless these results indicate that a one to one ratio of TIP48 to TIP49 was optimal.

Little increase in ATPase activity could be detected after a 10 min incubation of reactions containing an equimolar ratio of TIP48 to TIP49. Interestingly, incubation for a further 10 min resulted in a clear stimulation of ATP hydrolysis. This indicates that although a one to one TIP48 to TIP49 ratio was optimal, some time was required for the effect of complex assembly to be seen.

Once the conditions for assembling the complex from the individual proteins were optimized, TIP48 or TIP49 were incubated with different forms of DNA. The other component (TIP48 or TIP49) was then added, so that the complex could be assembled in the presence of DNA. ATPase assays were carried out to test for any stimulation of the ATPase activity, when the complex was formed in the presence of DNA. The results presented in Table 4.1 show that neither combination with any of the DNA forms tested,

caused a stimulation of the ATPase activity. Therefore, it is unlikely that the ATPase activity of the complex is coupled to an activity on DNA.

TABLE 4.1: Tabulated data of ATP hydrolyzed by the TIP48/TIP49 complex, formed in the presence of DNA[a]

	-DNA[b]	ssDNA	Supercoiled dsDNA	Linear dsDNA	Synthetic Holliday junction
TIP48	3.94 ± 0.560	2.24 ± 0.34	1.64 ± 0.38	1.30 ± 0.56	1.9 ± 0.44
TIP49	4.50 ± 0.40	2.04 ± 0.42	1.74 ± 0.36	2.78 ± 0.56	2.32 ± 0.42
TIP48 followed by TIP49	6.50 ± 0.66	6.58 ± 0.80	7.16 ± 1.00	7.24 ± 0.72	7.24 ± 0.84
TIP49 followed by TIP48	7.44 ± 1.28	6.44 ± 1.12	6.96 ± 0.72	9.10 ± 2.18	6.86 ± 0.76

a 1 μM of TIP48 or TIP49 were pre-incubated on ice for 5 min in Reaction buffer C (Materials and Methods, section 2.8.2), in the presence of different DNA forms (5 ng/μl), as shown. The other protein (TIP48 or TIP49) was then added to the reactions, which were incubated on ice for a further 5 min. Control reactions with the individual proteins were also set up. ATP/$MgCl_2$/[α^{32}P]-ATP mixture was added to each reaction to give a final concentrations of 2 mM ATP and 5 mM $MgCl_2$ and the reactions were incubated for 20 min at 37 °C.

b Units are in moles ATP/mole of protein, determined as described in Materials and Methods, section 2.8.2.

As control reactions, the individual proteins were incubated with the different DNA forms. It can be seen from Table 4.1 that the ATPase activities of TIP48 and TIP49 were not stimulated by DNA. However, a slight inhibition was seen with all DNA forms. This

inhibition was not seen before (Chapter 3) and has not been reported previously. It is likely that this was a non-specific effect that occurred under the conditions used in this experiment. A very slight inhibition with ssDNA was also seen in the assays where the two proteins were mixed but not with the other forms of DNA and not to the extent shown with the individual proteins. Again this could be due to non-specific effects due to conditions in the reactions.

Branch migration reactions were also carried out by incubating either TIP48 or TIP49 with radio-labelled Holliday junction and then adding the other subunit of the complex, before carrying out the branch migration reaction. It can be seen from Figure 4.7 in lanes 5 and 6, that no branch migration activity could be detected with either combinations of TIP48 or TIP49. The results in Figure 4.7 therefore confirm that the recombinant TIP48 and TIP49 proteins cannot promote branch migration of Holliday junctions, either on their own or as a complex.

4.8. The effect of β-catenin on the ATPase activity of TIP48 and TIP49 and the complex

The function of TIP48 and TIP49 is linked to interactions with an array of other proteins. It may be that TIP48 and TIP49, or their complex, have some type of chaperone activity on proteins they interact with, so the full extent of their ATPase activity would not be observed unless interacting partners were present.

Two candidate proteins, BAF53 and β-catenin, which have been shown to interact with TIP48 and TIP49 *in vitro* or *in vivo*, were chosen as they have important roles in the cell, but have differing functions. The coding sequence of BAF53 was cloned into a pET21b+ vector to yield BAF53 with a C-terminal His_6 tag and the protein was expressed both in BL21 (DE3) Gold and BL21 (DE3) Gold pLysS *E.coli* cells at a range of temperatures

and with a range of IPTG concentrations. However, the recombinant BAF53 was completely insoluble, and could not be solubilized under all the conditions tested and purified BAF53 could not be obtained.

β-catenin protein was expressed from a construct, which contained a hybrid of the coding sequences for the mouse and human β-catenin protein, fused to a C-terminal His_6 tag. The TIP48 and TIP49 proteins are highly conserved between humans and mice (99 % identity), so slight differences between mouse and human β-catenin should not affect interactions with TIP48 or TIP49. The protein expressed in BL21 (DE3) Gold cells was soluble and could be purified on a Talon column, followed by a Mono Q anion exchange column and size exclusion chromatography (Superdex 200 FPLC column). The purified β-catenin did not show any detectable ATPase contaminants and, therefore, could be tested with TIP48 and TIP49.

Figure 4.9a shows the ATPase activity of TIP48 on its own with different concentrations of the purified β-catenin, added to give ratios of TIP48 to β-catenin, as shown. At a one to one molar ratio β-catenin had an inhibitory effect on the ATPase activity of TIP48. However, as the amount of β-catenin decreased, this inhibition was reduced. Therefore, this experiment shows quite clearly that β-catenin inhibits the activity of TIP48 at equimolar concentrations, and at lower concentrations, β-catenin had no effect on the ATPase activity of TIP48. Similar results were obtained when TIP49 was tested in the presence of different concentrations of β-catenin as shown in Figure 4.9b. The ATPase activity of TIP49 was inhibited at a one to one ratio with β-catenin. When β-catenin was reduced this inhibition was also reduced.

Figure 4.9c shows the ATP hydrolyzed when the TIP48/TIP49 complex was incubated with different concentrations of β-catenin. At a one to one ratio of TIP48/TIP49 complex to β-catenin (in terms of monomers for the complex), inhibition of the ATPase activity was seen. As the amount of β-catenin was decreased, from a 1:1 to a 6:1 ratio of

complex to β-catenin, this inhibitory effect decreased, but only slightly. However, at a ratio of twelve to one, the ATPase activity reached control level. A slight increase in ATP hydrolyses seen with this reaction falls within the error of the measurement.

In summary, these experiments show that at high concentrations, β-catenin had an inhibitory effect on the ATPase activity of the TIP48/TIP49 proteins, rather than a stimulatory effect. This suggests that β-catenin interacts with the proteins. At high concentrations of β-catenin, which gave an equal ratio of β-catenin to the TIP48/TIP49 proteins or their complex, this interaction was very obvious as it inhibited the ATPase activities by almost 50 %. However, at lower concentrations, especially when a ratio of 6:1 was used with the individual proteins and 12:1 with the complex, this inhibition was not observed. Therefore, β-catenin does not really seem to have a significant effect on the ATPase activities of these proteins.

FIGURE 4.9: ATPase activity of TIP48, TIP49 and TIP48/TIP49 complex in the presence of β-catenin

(A and B) Reactions contained 1 μM TIP48 or TIP49 in reaction buffer B (Materials and Methods, section 2.8.2). Varying amounts of purified β-catenin were added to give the indicated molar ratios of TIP48 or TIP49 to β-catenin. Reactions were pre-incubated for 10 min on ice. ATP/$MgCl_2$/[α^{32}P]-ATP mixture was added to each reaction to give a final concentration of 1 mM ATP and 2 mM $MgCl_2$. Reactions were then incubated at 37 °C for 20 min. ATPase activity is expressed in terms of moles of ATP hydrolyzed per mole of protein monomer.

(C) Reactions containing 1 μM TIP48/TIP49 complex in reaction buffer B, were pre-incubated with varying amounts of β-catenin, to give the indicated molar ratios of TIP48/TIP49 complex to β-catenin. The concentration of the complex was expressed in moles of TIP48/TIP49 monomers. Reactions were pre-incubated for 10 min on ice. ATP/$MgCl_2$/[α_{32}P]-ATP mixture was added to each reaction to final concentrations as stated in (A and B). Reactions were then incubated at 37 °C for 20 min. ATPase activity is expressed in terms of moles of ATP hydrolyzed per mole of TIP48/TIP49 monomer.

A

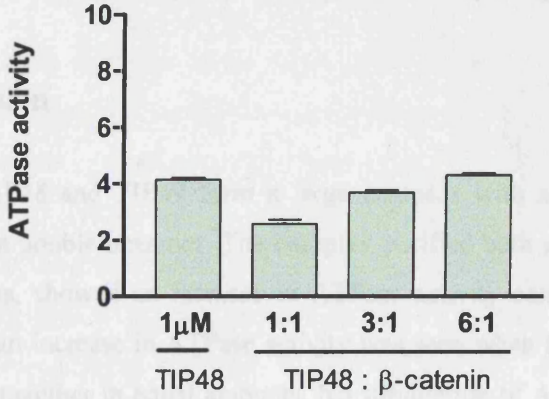
ATPase activity
10
8
6
4
2
0
1μM
1:1
3:1
6:1
TIP48
TIP48 : β-catenin

B

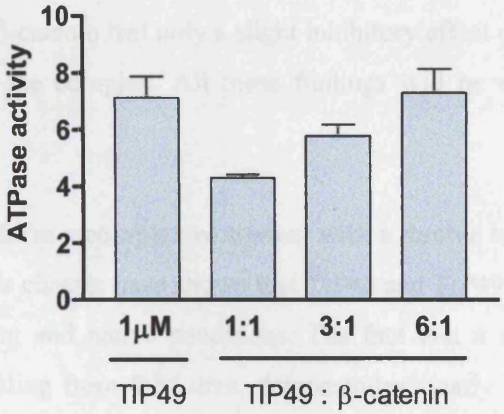
ATPase activity
10
8
6
4
2
0
1μM
1:1
3:1
6:1
TIP49
TIP49 : β-catenin

C

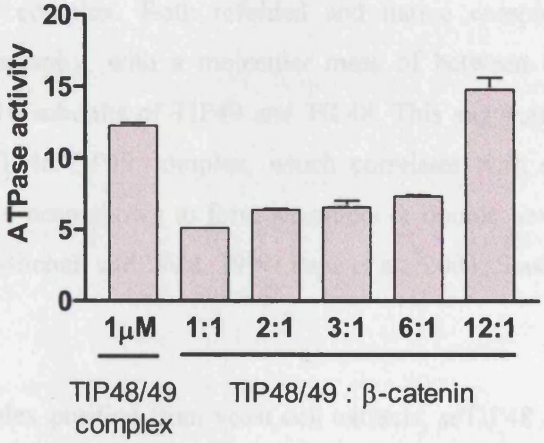
ATPase activity
20
15
10
5
0
1μM
1:1
2:1
3:1
6:1
12:1
TIP48/49 complex
TIP48/49 : β-catenin

4.10. Discussion

In summary, TIP48 and TIP49 form a large complex with a molecular mass that is consistent with a double hexamer. The complex purified both after refolding and under native conditions, showed an increase in ATPase activity compared to the individual subunits. Also, an increase in ATPase activity was seen when the two purified proteins were incubated together in equal amounts. No stimulation of ATPase activity was seen in the presence of DNA, even when the complex was pre-formed in the presence of DNA. The complex, like the individual proteins, did not exhibit helicase activity and neither the individual proteins, nor the complex, showed branch migration activities. An interacting partner β-catenin had only a slight inhibitory effect on the ATPase activity of TIP48, TIP49 and the complex. All these findings will be discussed in more detail below.

TIP48 and TIP49 form a complex consistent with a double hexamer

The results from this chapter have shown that TIP48 and TIP49 form a complex *in vitro*, both under refolding and native conditions. The fact that a stable complex could be obtained after refolding from 8 M urea, demonstrates clearly that specific interactions exist between the two proteins, as the majority of the proteins were insoluble but remained soluble after refolding from urea. Therefore, it is likely that the proteins facilitate each other during refolding, so the correct conformation is obtained to form this stable soluble complex. Both refolded and native complex eluted from size exclusion chromatography, with a molecular mass of between 600-800 kDa, which corresponds to 12-16 subunits of TIP49 and TIP48. This suggests a double hexameric structure for the TIP48/TIP49 complex, which correlates with data on other AAA^+ proteins, which have been shown to form hexamers or double hexamers (Chong et al., 2000; King, 2000; Mitchell and West, 1994; Pape et al., 2003; Stasiak et al., 1994; Valle et al., 2000).

In the INO80 complex purified from yeast cell extracts, *sc*TIP48 and *sc*TIP49 have an equal ratio to each other but both have approximately a six to one ratio compared to

other subunits of the complex (Shen et al., 2000). This indicated a double hexamer TIP48/TIP49 core complex, within this larger complex. Other groups have also shown that the two recombinant proteins purified from either *E. coli* (Ikura et al., 2000) or insect cells (Jonsson et al., 2004), form a large complex with a molecular mass containing approximately six subunits of each protein. These results confirm a general property of the TIP48/TIP49 complex, which forms a high molecular mass oligomer *in vivo* as well as *in vitro*. This occurs, as observed in the present study, without the help of any cofactors or interacting proteins, demonstrating that the complex formation must be very important for the function of TIP48 and TIP49. They most probably form this complex independently of other cellular complexes or interacting partners. In fact, it was shown recently that when *sc*TIP48 was depleted from cells, the INO80 complex lost both *sc*TIP48 and *sc*TIP49, even though *sc*TIP49 was still abundant in the cell (Jonsson et al., 2004). This suggested that both proteins have to associate with each other before either is incorporated into the INO80 complex.

When TIP48 and TIP49 were mixed in solution under native conditions, not all the molecules assembled in the complex. Although TIP49 was in excess of TIP48-His_6 before loading onto the Talon column, a significant amount of TIP48-His_6 did not assemble with TIP49 to form the complex, and upon size exclusion chromatography eluted in the monomer/dimer fractions. This may be due to limitations of the experiment. Other factors such as adenine nucleotides or interacting proteins may be required to facilitate complex formation with a greater efficiency *in vitro*.

A synergistic increase in ATPase activity is seen when TIP48 and TIP49 form a complex

An important observation made about the TIP48/TIP49 complex, was that its ATPase activity was much greater than the individual proteins. Both proteins formed a stable complex and modulated each other within the complex, so that a synergistic increase in ATPase activity was seen. The experiments presented here clearly demonstrate that the two proteins require each other in order to hydrolyse ATP *in vitro*. A similar result was

published by (Ikura et al., 2000), who reported ATPase activity for the complex at values similar to what has been shown here.

When the two purified proteins were mixed in solution, the highest ATPase activity was achieved at a one to one ratio of TIP48 and TIP49, at concentrations of 1 μM of protein or above (Figure 4.7). High concentrations of protein are probably required for cooperative assembly of the complex and the experiment again showed that the two proteins contribute equally to the formation of the complex. Both TIP48 and TIP49 bound ATP in the complex to almost an equal extent, and both components of the complex were required for the full ATPase activity of the complex, as shown by experiments using mutant complexes containing TIP48D299N or TIP49D302N

The mutation made in the two proteins, as mentioned in Chapter 3, should only affect ATP hydrolysis. However, as shown in Chapter 3, TIP49D302N was unable to bind ATP, whereas in the TIP48/TIP49D302N complex, both components bound ATP, as did both components of the TIP49/TIP48D299N complex (results not shown). This demonstrated that although TIP49D302N did not bind ATP on its own, it had the ability to bind ATP within the complex, suggesting that when part of the TIP48/TIP49 complex the mutation only affected the ATPase activity, not the ATP binding ability of TIP49. This perhaps suggests that TIP49 is in a functional conformation within the TIP48/TIP49 complex, but not on its own, which will be discussed further in Chapter 5.

Some other AAA^+ proteins show little or no ATPase activity, on their own, but when they are part of a functional complex with related AAA^+ proteins, they show a synergistic increase in ATPase activity *in vitro*, similar to TIP48 and TIP49. One example is provided by the MCM proteins from eukaryotes. The *S. cerevisiae* Mcm2-7 complex, when reconstituted *in vitro* (Davey et al., 2003), showed significantly more ATPase activity than the individual subunits, which showed little or no ATPase activity. The complex was shown to have an ATPase activity of 30 pmol/μg/min, whereas Mcm7 showed an ATPase activity of 7 pmol/μg/min (0.7 moles ATP/moles protein/min) and the activities from the other subunits were undetectable. It is unknown, as stated by the

authors of this study, whether the activity from the heterohexamer complex was in fact a property of the entire complex or the result of contaminating pair wise complexes of the MCM proteins, which show higher ATPase activities compared to the individual proteins.

The Mcm3/7 pair produced the most active ATPase, which hydrolyzed approximately 44 moles ATP/mole protein/min. The same level of ATPase activity by this MCM pair was also observed by another group (Schwacha and Bell, 2001). The Mcm4/7 pair also showed a high ATPase activity of approximately 20.8 moles ATP/mole protein/min. Other groups have also shown that certain complexes of the mouse MCM proteins are DNA helicases. Mcm467 was shown to have ATPase activity (153 pmols/μg in 60min) and DNA helicase activity but in the presence of Mcm2 this activity was inhibited (Ishimi, 1997; You et al., 2002). The heterohexamer has also been shown to lack helicase activity *in vitro* (Lee and Hurwitz, 2000). It was therefore suggested that Mcm467 forms the catalytic core, whereas Mcm235 negatively regulates the complex. This was demonstrated by mutational analysis of the yeast homologues, which showed that Mcm 4, 6 and 7 contribute the Walker A motifs involved in ATP hydrolysis and Mcm 2, 3 and 5 regulate this activity (Schwacha and Bell, 2001). Another study also showed that the yeast Mcm7 provides the Walker A motif and binds ATP whereas Mcm3 within this active pair provides the catalytic arginine required to regulate the ATPase activity (Davey et al., 2003). This leads to models of a ringed structure with the MCM proteins arranged in a specific way (Davey et al., 2003; Schwacha and Bell, 2001). The data from these studies, however, indicate clearly that a complex or sub-complexes of the MCM proteins are required to see a synergistic increase in ATPase activity compared to the individual proteins, which do little or nothing on their own, when tested *in vitro*.

It has also been shown that another sub-family of AAA^+ proteins, the RFC clamp loader proteins from eukaryotes and archaea, must also assemble into a complex or sub-complexes, before significant ATPase activity is seen. It was shown that the *sc*RFC2 recombinant protein, expressed and purified from *E.coli,* lacked ATPase activity both in

authors of this study, whether the activity from the heterohexamer complex was in fact a property of the entire complex or the result of contaminating pair wise complexes of the MCM proteins, which show higher ATPase activities compared to the individual proteins.

The Mcm3/7 pair produced the most active ATPase, which hydrolyzed approximately 44 moles ATP/mole protein/min. The same level of ATPase activity by this MCM pair was also observed by another group (Schwacha and Bell, 2001). The Mcm4/7 pair also showed a high ATPase activity of approximately 20.8 moles ATP/mole protein/min. Other groups have also shown that certain complexes of the mouse MCM proteins are DNA helicases. Mcm467 was shown to have ATPase activity (153 pmols/μg in 60min) and DNA helicase activity but in the presence of Mcm2 this activity was inhibited (Ishimi, 1997; You et al., 2002). The heterohexamer has also been shown to lack helicase activity *in vitro* (Lee and Hurwitz, 2000). It was therefore suggested that Mcm467 forms the catalytic core, whereas Mcm235 negatively regulates the complex. This was demonstrated by mutational analysis of the yeast homologues, which showed that Mcm 4, 6 and 7 contribute the Walker A motifs involved in ATP hydrolysis and Mcm 2, 3 and 5 regulate this activity (Schwacha and Bell, 2001). Another study also showed that the yeast Mcm7 provides the Walker A motif and binds ATP whereas Mcm3 within this active pair provides the catalytic arginine required to regulate the ATPase activity (Davey et al., 2003). This leads to models of a ringed structure with the MCM proteins arranged in a specific way (Davey et al., 2003; Schwacha and Bell, 2001). The data from these studies, however, indicate clearly that a complex or sub-complexes of the MCM proteins are required to see a synergistic increase in ATPase activity compared to the individual proteins, which do little or nothing on their own, when tested *in vitro*.

It has also been shown that another sub-family of AAA^+ proteins, the RFC clamp loader proteins from eukaryotes and archaea, must also assemble into a complex or sub-complexes, before significant ATPase activity is seen. It was shown that the *sc*RFC2 recombinant protein, expressed and purified from *E.coli,* lacked ATPase activity both in

the absence and presence of DNA (Yao et al., 2003). Neither *sc*RFC3 nor *sc*RFC4 could be obtained as soluble proteins however, the scRFC3/4 co-expressed complex displayed ssDNA stimulated ATPase activity. When *sc*RFC2 was added to the *sc*RFC3/4 complex a 4-fold stimulation of activity was seen, indicating that a complex of two or more of these paralogues is required for a stimulation of the ATPase activity; similar to TIP48 and TIP49. It was demonstrated that when the arginine finger, common to many AAA^+ proteins (Neuwald et al., 1999), in the SRF/C motif of *sc*RFC3, was mutated, the ssDNA dependent ATPase activity was lost, but when the same mutation was made in *sc*RFC4 the complex remained active. This indicated that, as with other AAA^+ oligomers, one subunit provides the ATP binding function by using its Walker A motif, and the other subunit provides the arginine finger, which is thought to be needed for catalysis (Ogura and Wilkinson, 2001). ATP hydrolysis sites are found at the subunit interface of many AAA^+ complexes, such as the *sc*RFC clamp loader complex, the *sc*MCM complex and the *E.coli* clamp loader complex (Davey et al., 2002; Johnson and O'Donnell, 2003). This suggests that when the individual subunits are not part of a complex an efficient ATPase site is not formed. This is probably why the individual TIP48 and TIP49 proteins hydrolyse very little or no ATP, but a synergistic increase is seen when they form a complex.

The observed ATPase activity of the TIP48/TIP49 complex is very low (estimated ~ 0.48 moles ATP/moles protein/min) compared to some of the values for the AAA+ protein complexes stated above. A similar turnover is seen with the *A. fulgidus* RFC complex (Seybert et al., 2002), which is made up of two related AAA^+ proteins. However, the ATPase activity of this complex was shown to be stimulated both by DNA and an interacting protein, namely PCNA. A 50-fold increase was seen in the k_{cat} of the *Af*RFC complex, in the presence of different DNA substrates, and this was increased a further 2-3 fold in the presence of PCNA. As discussed below, no stimulation of ATPase activity of the TIP48/TIP49 complex was detected in the presence of DNA. However, the low ATPase activity of the complex suggests that other cofactors are required for the full extent of the ATP hydrolysing activities of the TIP48/TIP49 complex.

The ATPase activity of TIP48/TIP49 complex is not stimulated by DNA

It was shown that, similar to the individual proteins, there was no stimulation of the ATPase activity of the TIP48/TIP49 complex in the presence of ssDNA, dsDNA, as well as synthetic Holliday junction. This demonstrated that, like the individual proteins, the complex on its own is unlikely to be a DNA helicase. A DNA helicase assay confirmed this directly (not shown). Also, branch migration activity was not observed by the individual proteins; the preformed complex; or when the complex was formed in the presence of radio-labelled Holliday junction. Therefore, these results confirmed that neither the individual proteins nor the complex has the ability to branch migrate Holliday junctions. However, accessory proteins may be needed to observe branch migration or helicase functions *in vitro*, as is required for the bacterial RuvB protein, which is an efficient DNA helicase in the presence of RuvA (Tsaneva et al., 1993) and only shows branch migration activities in the absence of RuvA, under certain conditions (Tsaneva et al., 1992).

It was shown by another group that neither TIP48, TIP49 or the complex bound different DNA forms, but the TIP60 complex as a whole could (Ikura et al., 2000). This confirmed that these proteins cannot work on DNA on their own, as they do not have any means of interacting with DNA. Results published recently show that the *sc*TIP48/TIP49 complex does not have chromatin remodelling activity (Jonsson et al., 2004), whereas the INO80 complex does (Jonsson et al., 2004; Shen et al., 2000). It was also shown in the same study that both proteins are required for the chromatin remodelling activity of the INO80 complex but it is the Ino80 protein, which is the catalytic subunit of the complex (Jonsson et al., 2004; Shen et al., 2000). These results indicate that if TIP48 and TIP49 do have functions on DNA, then they require other factors to display these activities. However, as will be discussed in Chapter 7, TIP48 and TIP49 are more likely to have a more general role in the assembly of large complexes, than to function directly on DNA.

The ATPase activity of the TIP48/TIP49 complex is not stimulated by an interacting partner, β-catenin

It was hypothesised that a stimulation of ATPase activity may be seen with proteins that are known to interact with TIP48 and TIP49. The results obtained here, demonstrated that there was no stimulation of the ATPase activity of TIP48; TIP49; or their complex, in the presence of β-catenin. Instead, at high concentrations of β-catenin (one to one ratio) a slight inhibition of activity was seen. This suggests an interaction between TIP48 and TIP49 with β-catenin. Also as inhibition of ATP hydrolysis was seen, it is likely that TIP48, TIP49 and the complex were binding ATP in the presence of β-catenin, but not hydrolysing it. Other proteins may then be required, such as components of the TIP60 complex, for TIP48/TIP49 to be able to hydrolyse the bound ATP. This hypothesis is based on the fact that the *sc*TIP48E297G mutant, which is able to bind ATP but not hydrolyse it, assembled a functional INO80 complex *in vivo* (Jonsson et al., 2004). Hence ATP hydrolysis by *sc*TIP48 was not required for this function. Because the situation *in vitro* is very different from that *in vivo*, by using individual interacting proteins, a stimulation of ATPase activity by TIP48 and TIP49 may not be seen and other types of experiments will have to be carried out to show the functions of TIP48 and TIP49 in chromatin remodelling and transcriptional activation.

Chapter 5

Investigation into the subunit organization of TIP48, TIP49 and their complex

5.1. Introduction

Proteins from the AAA^+ superfamily tend to form oligomers which are typically hexamers (Chong et al., 2000; Stasiak et al., 1994; Valle et al., 2000). Some of these AAA^+ proteins, such as RuvB, require adenine nucleotide cofactors for oligomerization (Mitchell and West, 1994). In Chapter 3, the purified TIP48 and TIP49 proteins peaked as monomer/dimers during size exclusion chromatography. However, some batches of purified TIP48 contained a significant population of oligomers with a molecular mass of 400 kDa (not shown). This suggests that TIP48 oligomerizes but these oligomers could be more stable in the presence of adenine nucleotide cofactors. Hence, a more detailed investigation into the nucleotide dependent oligomerization and adenine nucleotide binding, by TIP48 and TIP49, will be presented in this chapter.

In Chapter 4 it was shown that the TIP48/TIP49 complex existed as a high molecular mass oligomer that had a mass consistent with a double hexamer of the two proteins. The structure of the TIP48/TIP49 complex will also be shown. This was determined by electron microscopy by negative staining and processing with single particle analysis in IMAGIC (van Heel et al., 1996) to yield a low resolution model.

5.2. Oligomerization of TIP48 in the presence of adenine nucleotide cofactors

The oligomeric state of TIP48 was determined by size exclusion chromatography. TIP48 was purified to homogeneity on a MonoQ FPLC column as described in Chapter 3 (Figure 3.8). Samples were loaded onto a Superdex 200 FPLC column in the absence or presence of adenine nucleotide cofactors. The chromatographs obtained are shown in Figure 5.1.

Figure 5.1(a-c) shows that in the absence of cofactors TIP48 eluted with a mass of 70 kDa, which corresponds to a monomer/dimer equilibrium for the protein, which has a molecular mass of approximately 50 kDa. Another much smaller peak was also seen, corresponding to a mass of approximately 180 kDa. This peak could correspond to a trimer/tetramer of TIP48. In the presence of ATP alone, a small shift in the subunit organisation was observed, as a very small peak was seen corresponding to a mass of approximately 400 kDa (Figure 5.1a). However, when the protein was incubated with both ATP and $MgCl_2$ a substantial shift to 400 kDa was observed. About 80 % of the protein eluted in these high molecular mass fractions. This result indicates that the protein requires both ATP and $MgCl_2$ to form high molecular mass oligomers. The molecular mass calculated indicates that this oligomer could be between a hexamer and an octamer, but would be too small to be a dodecamer of TIP48. SDS-PAGE of the fractions confirmed that TIP48 was present in all the peaks seen in the chromatographs.

The effect of ADP on TIP48 quaternary structure is shown in Figure 5.1b. When the protein was incubated with ADP in the absence of $MgCl_2$, 40 % of the protein formed a high molecular mass oligomer. When the protein was incubated with both ADP and $MgCl_2$ more oligomerization was seen and about 65 % of the protein formed these oligomers. Therefore, $MgCl_2$ facilitates oligomerization with both ADP and ATP.

The results in Figure 5.1a and b show that even in the absence of $MgCl_2$ some of the molecules can oligomerize with ADP and to an extent ATP. This indicates that nucleotide cofactors alone, affect the equilibrium between the monomeric/dimeric state and the oligomeric state of TIP48 and this shift in the equilibrium is particularly prominent in the presence of ADP. When $MgCl_2$ is added this oligomeric state is probably stabilized further, therefore an increase in the amount of oligomers is seen. However, no oligomerization of TIP48 was seen when the protein was incubated with $MgCl_2$ alone (Figure 5.1c). Even at higher concentrations of $MgCl_2$ (10 mM), the protein did not oligomerize (not shown). This demonstrated that oligomerization by TIP48 requires adenine nucleotide cofactors.

FIGURE 5.1: Size exclusion chromatography of TIP48 in the presence of adenine nucleotides

Samples of purified TIP48 protein, supplemented with cofactors as indicated, were analysed by Superdex 200 FPLC size exclusion chromatography as described in Materials and Methods (section 2.7.8). First the adenine nucleotide was added to the protein and incubated on ice. $MgCl_2$ was added next, if used, and the samples were incubated on ice for a further 10 min before applying to the column. Samples contained: (A) No cofactors; ATP; ATP + $MgCl_2$: (B) No cofactors; ADP; ADP + $MgCl_2$: (C) No cofactors; ATPγS + $MgCl_2$; AMPPNP + $MgCl_2$; $MgCl_2$.

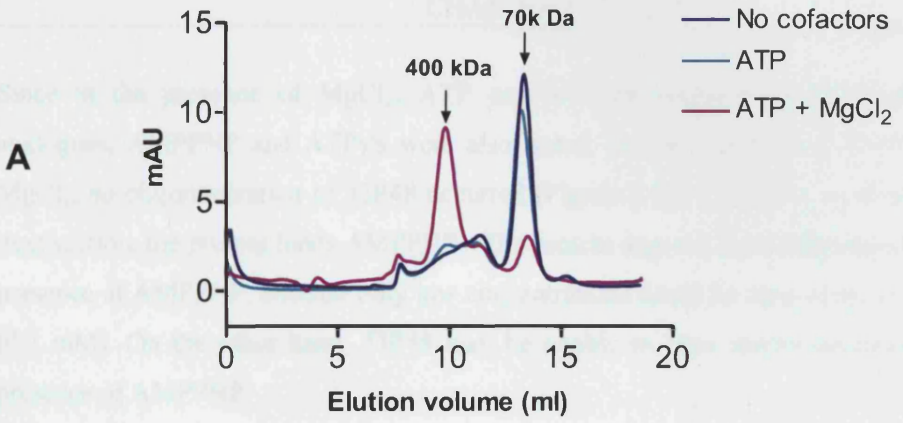
A
mAU
15
10
5
0
0
5
10
15
20
Elution volume (ml)
400 kDa
70k Da
No cofactors
ATP
ATP + MgCl2

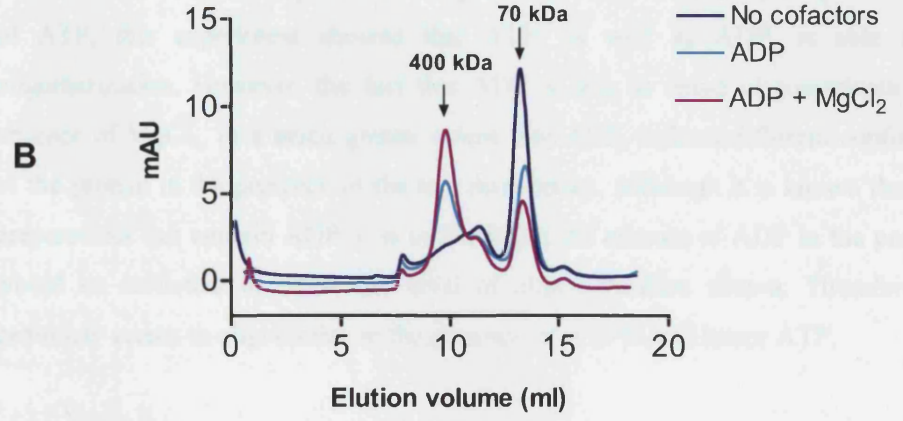
B
mAU
15
10
5
0
0
5
10
15
20
Elution volume (ml)
400 kDa
70 kDa
No cofactors
ADP
ADP + MgCl2

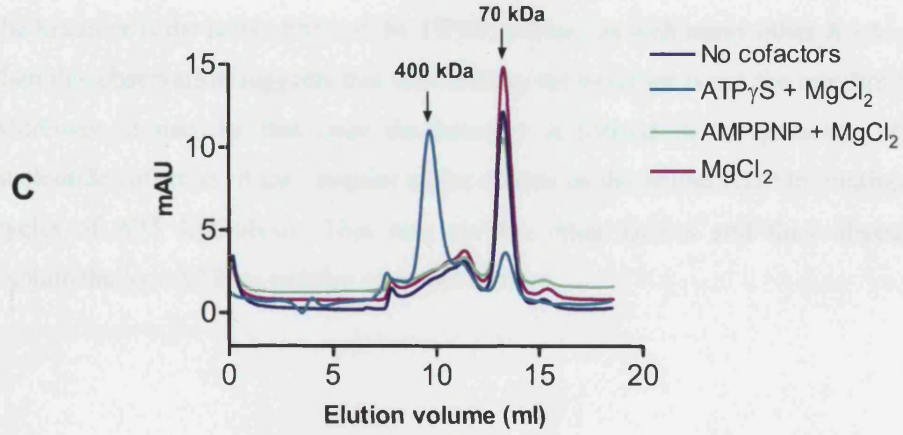
C
mAU
15
10
5
0
0
5
10
15
20
Elution volume (ml)
400 kDa
70 kDa
No cofactors
ATPγS + MgCl2
AMPPNP + MgCl2
MgCl2

Since in the presence of $MgCl_2$, ATP can be hydrolysed, non-hydrolysable ATP analogues, AMPPNP and ATPγS were also tested. In the presence of AMPPNP and $MgCl_2$, no oligomerization of TIP48 occurred (Figure 5.1c). However, as shown in the next section, the protein binds AMPPNP. The protein may not have oligomerized in the presence of AMPPNP, because only low concentrations could be used in the experiment (0.2 mM). On the other hand, TIP48 may be unable to form stable oligomers in the presence of AMPPNP.

With ATPγS and $MgCl_2$, TIP48 formed the same high molecular mass oligomers, seen with ATP and ADP in the presence of $MgCl_2$. As ATPγS is a non-hydrolysable analogue of ATP, this experiment showed that ATP, as well as ADP, is able to cause oligomerization. However, the fact that ADP is able to cause oligomerization in the absence of $MgCl_2$, to a much greater extent than ATP, reflects different conformations of the protein in the presence of the two nucleotides. Although it is known that ATPγS preparations can contain ADP, it is unlikely that the amount of ADP in the preparation would be sufficient to cause the level of oligomerization shown. Therefore TIP48 genuinely seems to oligomerize in the presence of ATPγS and hence ATP.

The fractions obtained from size exclusion chromatography in the presence of ATP and $MgCl_2$, were also tested for ATPase activity (not shown). It was observed that these high molecular mass oligomers had a lower activity than the monomeric/dimeric fractions. If the hexamer is the active form of the TIP48 ATPase, as with many other AAA^+ proteins, then this observation suggests that pre-forming the hexamer is not the rate-limiting step. Moreover, it may be that once the hexamer is formed in the presence of adenine nucleotide cofactors, it may require active release of the bound ADP to continue further cycles of ATP hydrolysis. This may involve other factors and their absence could explain the low ATPase activity observed *in vitro*.

5.3. Binding of adenine nucleotide cofactors by TIP48

As TIP48 was shown to oligomerize, in the presence of some adenine nucleotide cofactors, under specific conditions, further experiments were carried out to confirm that TIP48 binds these nucleotide cofactors. The experiments were carried out under the same conditions, as those used in the experiments described above. Binding with AMPPNP had to be checked in particular, as the protein was unable to oligomerize in the presence of this ATP analogue. The effect of $MgCl_2$ on ATP binding was also investigated.

It was shown in Chapter 3, section 3.6, that TIP48 and its D299N mutant bind [γ^{32}P] 2-azido ATP. To see whether TIP48 also binds ADP and the ATP analogues, AMPPNP and ATPγS, binding assays with [γ^{32}P] 2-azido ATP were carried out using these adenine nucleotides as competitors. It can be seen in Figure 5.2a (lane 2), that TIP48 binds the analogue in the absence of ATP, as shown in Chapter 3. When ATP was added at an equal concentration of 10 μM, the ^{32}P signal was decreased to approximately half. The signal decreased even more as increasing concentrations of ATP (up to 0.5 mM) were added. This experiment therefore showed that TIP48 binds this analogue specifically at the ATP binding site, as the analogue was competed out by increasing concentrations of ATP.

It was shown by similar experiments that TIP48 binds ADP. It can be seen in Figure 5.2b (lane 3), that when equal amounts of ADP and [γ32P] 2-azido ATP were added, the ^{32}P signal was significantly reduced. Increasing the ADP concentration up to 0.5 mM of ADP caused the signal to be reduced even further. This result indicates that TIP48 may have a higher affinity for ADP compared to ATP (compare lanes 3 Figure 5.2a and 5.2b) and the fact that ADP causes oligomerization in the absence of $MgCl_2$, whereas ATP does not, supports this observation. However, to show this directly, binding constants for the two nucleotide cofactors would need to be obtained.

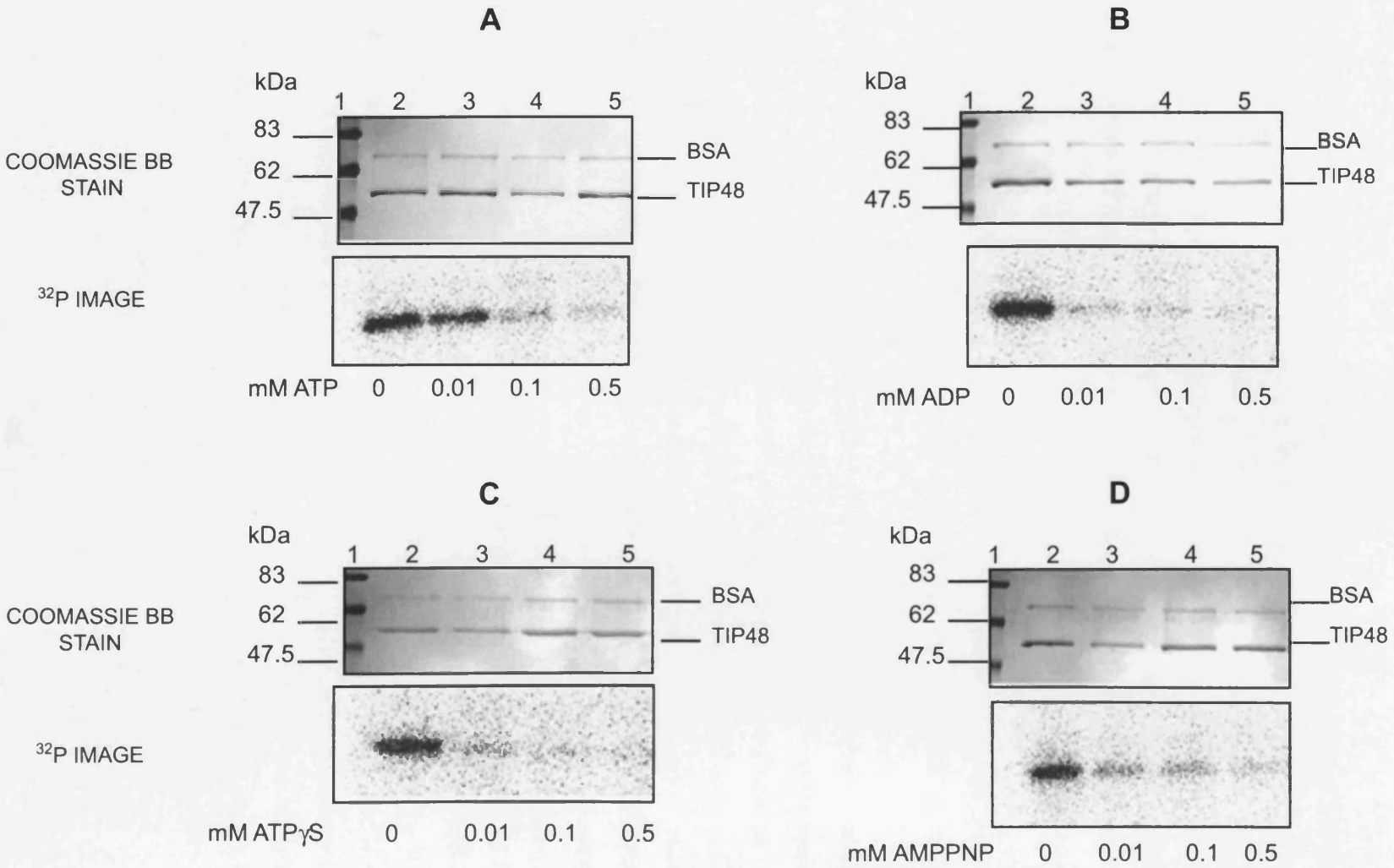
A
kDa
1 2 3 4 5
83
62
47.5
BSA
TIP48
COOMASSIE BB STAIN
32P IMAGE
mM ATP 0 0.01 0.1 0.5
B
kDa
1 2 3 4 5
83
62
47.5
BSA
TIP48
mM ADP 0 0.01 0.1 0.5
C
kDa
1 2 3 4 5
83
62
47.5
BSA
TIP48
COOMASSIE BB STAIN
32P IMAGE
mM ATPγS 0 0.01 0.1 0.5
D
kDa
1 2 3 4 5
83
62
47.5
BSA
TIP48
mM AMPPNP 0 0.01 0.1 0.5

FIGURE 5.2: Binding experiments of TIP48 with adenine nucleotide cofactors

Reactions were set up containing 1 μg of TIP48. $MgCl_2$ was added to a final concentration of 2 mM and at the same time [γ-^{32}P] 2-Azido ATP was added to a final concentration of 10 μM, along with either, (A) ATP, (B) ADP, (C) ATPγS or (D) AMPPNP, at final concentrations from 0 to 0.5 mM, as shown. Reactions were incubated for 3 min at room temperature and then irradiated for 1 min with UV light. The protein was precipitated overnight with 10 % TCA (see Materials and Methods, section 2.8.3). Protein pellets were resuspended in 1x SDS-loading buffer, separated by 12 % SDS-PAGE and the gels stained with Coomassie brilliant blue. Gels were dried and exposed on a phosphorimager screen overnight and developed by FUJI-FILM FLA-2000 phosphorimager. The BSA used in the binding buffer can be seen on the stained gel, as indicated.

Similar competition experiments were carried out by increasing the concentration of ATPγS (Figure 5.2c) and AMPNP (Figure 5.2d) in the presence of [γ^{32}P] 2-azido ATP. As the figures show, TIP48 binds both these analogues, as the ^{32}P signal from [γ^{32}P] 2-azido ATP decreased when increasing amounts of both analogues were added to the reaction. TIP48 seems to have a higher affinity for ATPγS compared to ATP (compare lanes 3 Figure 5.2a and 5.2c). However, as mentioned earlier, the ATPγS stock could contain ADP, hence a greater decrease in the signal is seen when ATPγS is used compared to ATP. Nevertheless, it is unlikely that there would be a large population of ADP molecules in the ATPγS preparation; therefore this experiment shows that TIP48 does bind ATPγS, probably to a similar level as ATP.

AMPPNP can be seen to bind less efficiently than ATPγS (compare lanes 3 and 4, Figure 5.2c and d). However, the fact that TIP48 binds AMPPNP indicates that if used at higher concentrations in the size exclusion chromatography experiment, it may cause TIP48 to oligomerize, like the other adenine nucleotide. Commercially available AMPPNP did not allow such experiments to be performed.

The [γ^{32}P] 2-azido ATP substrate, used in these experiments, can be hydrolysed. ATP hydrolysis was tested after cross-linking TIP48 to the substrate and then incubating it up to 60 min at 37 °C, but no loss of signal was observed (not shown). This could indicate that TIP48 is an inefficient ATPase, as shown in Chapter 3, but it may be that it is unable to hydrolyse this analogue when cross-linked. Nevertheless, the fact that ATPγS and AMPPNP could compete out [γ^{32}P] 2-azido ATP, confirms that the protein can stably bind ATP. These results confirm that TIP48 oligomerizes in the presence of ATP, rather than ADP produced by hydrolysis. Therefore, as TIP48 binds both ATP and ADP it is likely to have different conformational states within the hexamer, one that is an ATP-bound state and one that is an ADP-bound state. These different conformational states and their functional significance can probably be investigated by structural studies.

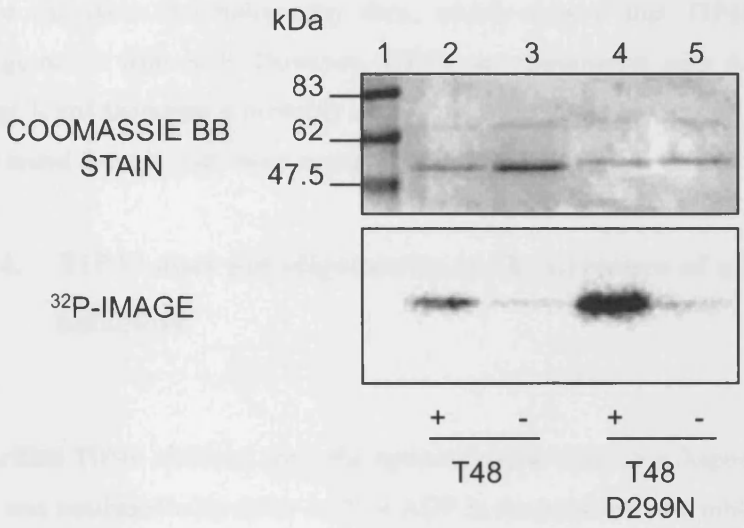

FIGURE 5.3: The effect of $MgCl_2$ on TIP48 and TIP48D299N ATP binding

1 µg of TIP48 (lanes 2 and 3) or TIP48D299N (lanes 4 and 5) in 20 µl reactions, were incubated with [γ–^{32}P] 2-Azido ATP at a final concentration of 10 µM. Reactions were set up with (+) or without (-) 2 mM $MgCl_2$ and processed as described in Figure 5.2 and Materials and Methods (section 2.8.3). Proteins were separated by 12 % SDS-PAGE. Gels were stained with Coomassie brilliant blue, dried and exposed on a phosphorimager screen overnight and developed by FUJI-FILM FLA-2000 phosphorimager.

Another experiment was carried out to see whether $MgCl_2$ is needed for binding of the [γ^{32}P] 2-azido ATP. TIP48 and TIP48D299N were incubated with [γ^{32}P] 2-azido ATP in the presence or absence of $MgCl_2$. It can be seen from Figure 5.3 that both TIP48 and TIP48D299N require $MgCl_2$ to bind [γ^{32}P] 2-azido ATP. This is in agreement with the size exclusion chromatography data, which showed that TIP48 required $MgCl_2$ to oligomerize with ATP. However, TIP48 can oligomerize with ADP in the absence of $MgCl_2$ and therefore it probably also binds ADP in the absence of $MgCl_2$. This needs to be tested though, with more experiments.

5.4. TIP49 does not oligomerize in the presence of adenine nucleotide cofactors

Purified TIP49 obtained from the hydroxyapatite column (Chapter 3, Figure 3.2b; lane 4) was incubated with either ATP or ADP in the presence of 2 mM $MgCl_2$, and analysed by size exclusion chromatography (Superdex 200 column). Oligomerization was not observed under these conditions and the protein remained as a monomer (Figure 5.4). Even at a higher $MgCl_2$ concentration of 10 mM, no oligomerization was seen in the presence of ATP. Therefore, it seems that TIP49 is unable to form stable oligomers in the presence of adenine nucleotide cofactors. It may require other factors to oligomerize, and as shown in Chapter 4, TIP49 did form a high molecular mass oligomer with TIP48. Therefore although TIP49 has the ability to oligomerize *in vitro*, it appears to require TIP48 rather than nucleotide cofactors.

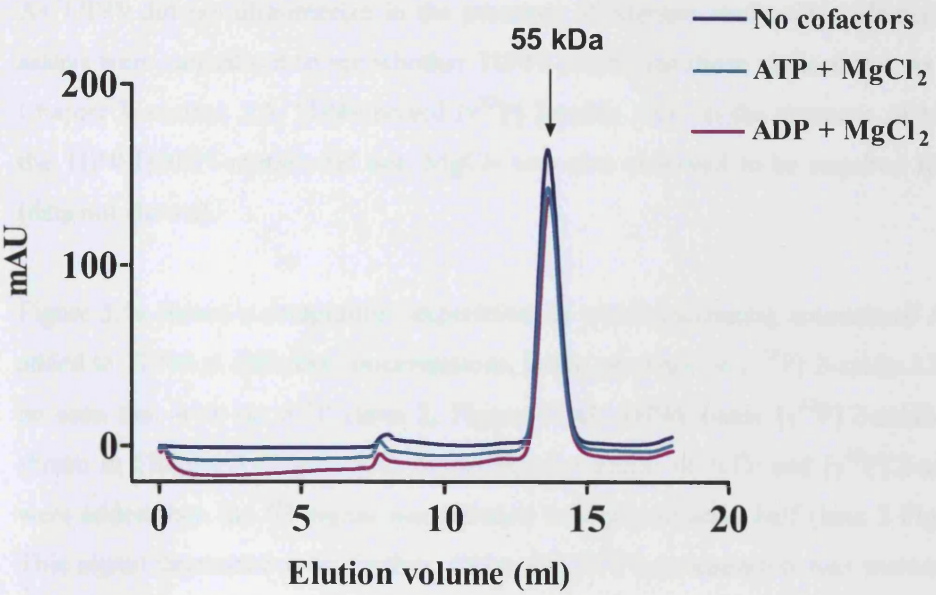

FIGURE 5.4: Size exclusion chromatography of TIP49 in the presence of adenine nucleotides

Samples of the purified TIP49 protein, prepared as described in Materials and Methods (section 2.8.3), were supplemented with ATP or ADP, as indicated, and analysed by Superdex 200 FPLC size exclusion chromatography. The adenine nucleotide was added first to the protein and incubated on ice, followed by addition of $MgCl_2$ and incubation for another 10 min on ice. The concentration of nucleotides was 1 mM.

5.5 Binding of adenine nucleotide cofactors by TIP49

As TIP49 did not oligomerize in the presence of adenine nucleotide cofactors, binding assays were carried out to see whether TIP49 could bind these nucleotides. As shown in Chapter 3, section 3.5, TIP49 bound [γ^{32}P] 2-azido ATP, in the presence of $MgCl_2$, but the TIP49D302N mutant did not. $MgCl_2$ was also observed to be required for binding (data not shown).

Figure 5.5a shows a competition experiment in which increasing amounts of ATP were added to TIP49 at different concentrations, in the presence of [γ^{32}P] 2-azido ATP. It can be seen that with no ATP (lane 2, Figure 5.5a), TIP49 binds [γ^{32}P] 2-azido ATP, as shown in Chapter 3 (Figure 3.6). When equal amounts of ATP and [γ^{32}P] 2-azido ATP were added then the ^{32}P signal was reduced to approximately half (lane 3 Figure 5.5a). This signal decreased even further, when the ATP concentration was increased up to 0.5 mM. The experiment therefore shows that TIP49 binds this analogue specifically at the ATP binding site, as it is competed out by adding increasing amounts of ATP.

Similar experiments showed that TIP49 bound ADP specifically, as the ^{32}P signal from [γ^{32}P] 2-azido ATP was reduced when increasing amounts of ADP were added (Figure 5.5b). Also, when equal amounts of ADP and [γ^{32}P] 2-azido ATP were added to the reaction, the ^{32}P signal was hardly detectable, whereas when an equal amount of ATP was added, the signal was just reduced to half (compare lanes 3, Figure 5.5a and 5.5b). These results indicate that TIP49 probably has a higher affinity of binding to ADP, compared to ATP. However, binding constants for both nucleotides would have to be obtained to confirm this observation.

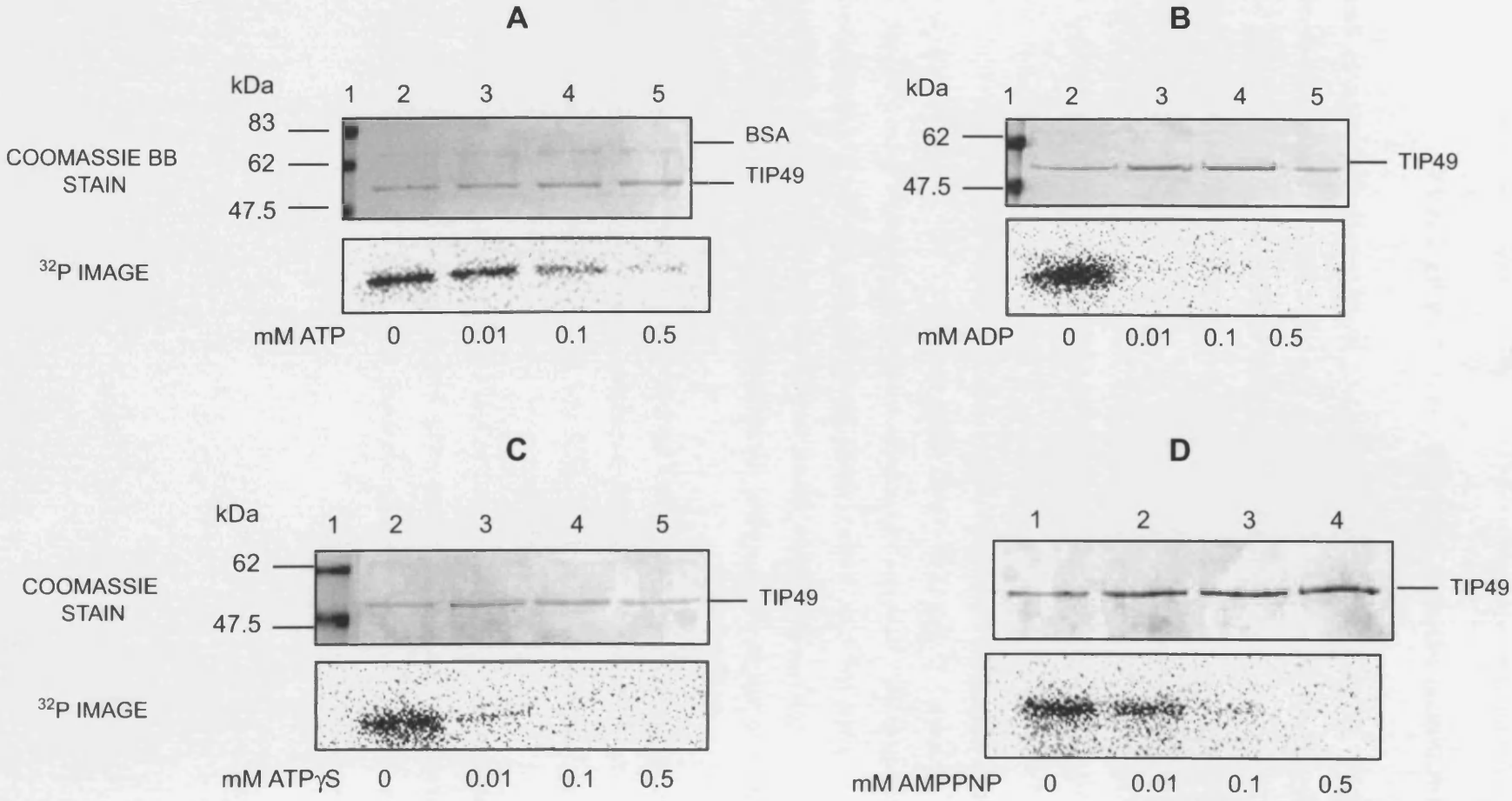
A
kDa
1 2 3 4 5
83
62
47.5
BSA
TIP49
COOMASSIE BB STAIN
32P IMAGE
mM ATP 0 0.01 0.1 0.5
B
kDa
1 2 3 4 5
62
47.5
TIP49
mM ADP 0 0.01 0.1 0.5
C
kDa
1 2 3 4 5
62
47.5
TIP49
COOMASSIE STAIN
32P IMAGE
mM ATPγS 0 0.01 0.1 0.5
D
1 2 3 4
TIP49
mM AMPPNP 0 0.01 0.1 0.5

FIGURE 5.5: Binding experiments of TIP49 with adenine nucleotide cofactors

Reactions were set up containing 1 μg of TIP49. $MgCl_2$ was added to a final concentration of 2 mM and at the same time [γ-^{32}P] 2-Azido ATP was added to a final concentration of 10 μM, along with either, (A) ATP, (B) ADP, (C) ATPγS or (D) AMPPNP, at final concentrations from 0 to 0.5 mM, as shown. Reactions were processed as described in Figure 5.2 and Materials and Methods (section 2.8.3). Proteins were separated by 12 % SDS-PAGE. Gels were stained with Coomassie brilliant blue, dried and exposed on a phosphorimager screen overnight and developed by FUJI-FILM FLA-2000 phosphorimager. The BSA used in the binding buffer can be seen on the stained gel, as indicated.

The protein also bound the ATP analogues ATPγS and AMPPNP, specifically (Figures 5.5c and 5.5d, respectively). The results also show that the protein may have a higher affinity for ATPγS over AMPPNP, as the [γ^{32}P] 2-azido ATP label is competed out with low concentrations of ATPγS, compared to AMPPNP (compare lanes 3, Figure 5.5c and 5.5d). It can also been seen that TIP49 may have a higher affinity for ATPγS over ATP (compare lanes 3, Figure 5.5a and 5.5c). However, as mentioned in section 5.3, there may be a sub-population of ADP in the ATPγS stock and therefore it competes out the [γ^{32}P] 2-azido ATP, better than ATP.

An experiment was carried out to see if TIP49 could hydrolyse [γ^{32}P] 2-azido ATP and hence hydrolyse ATP. However, after cross-linking TIP49 to the substrate, and then incubating it for up to 60 min at 37 °C, no loss of signal was observed (not shown). This indicates that the protein can bind ATP but hydrolyses none or very little of it. It may be that the cross-linking of the analogue affects the catalytic site of TIP49 so it is unable to hydrolyse it, but it has already been shown in Chapter 3 that TIP49 hydrolyses virtually no ATP. Nevertheless, TIP49 can bind ATP as well as ADP, which suggests that it is folded correctly and is likely to have different conformational states, one that is an ATP-bound and one that is an ADP-bound. Moreover, as TIP49 can bind these adenine nucleotides, this strengthens the finding that TIP49 is unable to form stable oligomers in the presence of adenine nucleotides.

5.6. Electron microscopy of the TIP48/TIP49 complex

Many AAA^+ proteins have been shown, by electron microscopy, to form ringed hexamers or double hexamers (Chen et al., 2002; Ogura and Wilkinson, 2001; Pape et al., 2003). In most cases this hexameric form signifies the functional state of these proteins. In relation to this it was shown in Chapter 4, that the multimeric TIP48/TIP49 complex was most likely to be a functional form of the two proteins, as it hydrolyzed more ATP than the individual proteins. The equimolar complex eluted from the size exclusion chromatography column with a molecular mass between 850-650 kDa. As this corresponds to complexes containing 12 to 16 subunits of TIP48 and TIP49, it was likely

that similar to other AAA^+ proteins, the complex exists as a double hexamer. A fraction corresponding to a molecular mass of 650 kDa (~ 13mer) was examined by electron microscopy using negative staining and images were processed using single particle analysis in IMAGIC-5[1] (van Heel et al., 1996).

The samples were prepared for electron microscopy as described in Materials and Methods (section 2.9). They were then placed onto glow discharged carbon coated copper grids, stained twice with 2 % uranyl acetate and viewed using a Technai T12 electron microscope, operated at an accelerating voltage of 120 kV. The micrographs obtained (Figure 5.6a) were digitised using a SCAI microdensitometer with a pixel size of 14 μm. The magnification was 42,000 therefore the pixel spacing obtained was 3.3 Å/pixel. 2267 particles were selected in Ximdisp and extracted into 200 x 200 boxes with LABEL. By determining the spatial frequencies at which the first zero in the contrast transfer function (CTF) occurred, in the rotationally averaged power spectra, the defocus was estimated on each micrograph. CTF correction was done with IMAGIC-5 and a defocus range between 380-1015 nM was obtained.

The box size was reduced to 140 x 140 pixels and the images were band-pass filtered between 165 and 8.25 Å using IMAGIC-5. In five rounds of translational and rotational alignment the particles were aligned with a reference free approach and classified into 110 classums, each containing approximately 20 images of the particle in a particular orientation using multivariate statistical analysis. Figure 5.6b shows some of these class averages with top (or end) and side views of the complex indicated. An initial reconstruction was created by angular reconstitution in IMAGIC-5, applying C6 symmetry. This map was used as a starting model for refinement.

Eigen image analysis of the end views (top and bottom) was then carried out to obtain the symmetry of the complex. The eigen image analysis gave no clear rotational symmetry for the complex but by studying the classums it can clearly be seen that there are six TIP48/TIP49 monomers arranged around a six-fold symmetry (Figure 5.6b).

[1] This work was carried by P.Wendler, Birkbeck school of crystallography

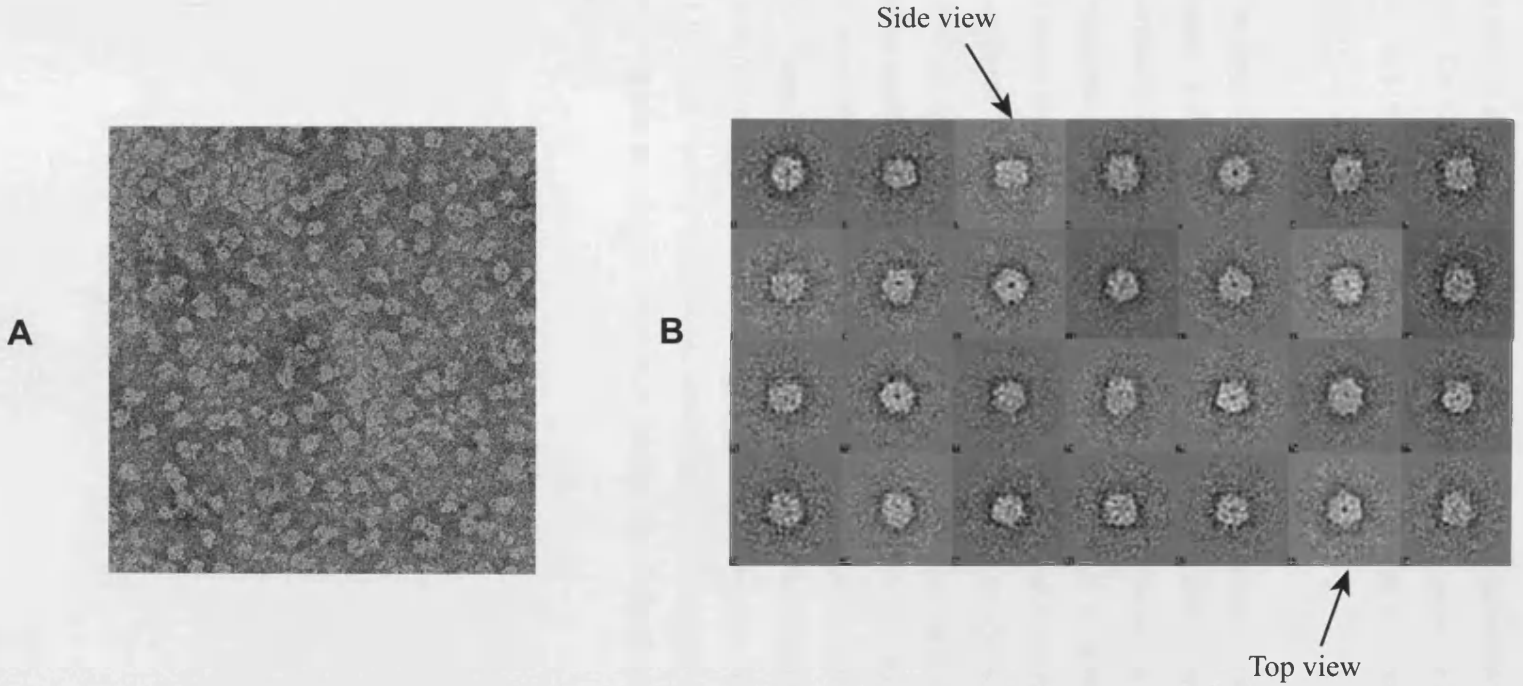

Figure 5.6: Electron microscopy of the TIP48/TIP49 complrx by negative staining

A A portion of a micrograph showing particles of the TIP48/TIP49 complex, which were stained with 2 % uranyl acetate on carbon coated grids. Photographs were taken with with a 120 kV transmission electron microscope and the developed films were digitised by scanning with a resolution of 14 µm/pixel. **B** A representation of some of the classums obtained after processing with single particle analysis in IMAGIC. Five rounds of alignment and subsequent rounds of multi-reference alignment were carried out to obtain 110 classums, each showing a certain orientation of the TIP48/TIP49 complex molecule. There were around 20 images per classum. Classums showing a side view and a top view of the TIP48/TIP49 complex, are pointed out.

3D models of the complex using the classums were built by angular reconstitution in IMAGIC-5. The model was first constructed using the 110 classums obtained, as described above. Extra rounds of multi reference alignment were then carried out, which gave 220 classums containing approximately 10 images per classum. These were used in the later steps for the 3D model refinement. The low resolution model is shown in Figure 5.7.

The diameter of the particle from side to side is approximately 145Å. The height of the double layer (the side view) is approximately 110Å. The top and bottom views are noticeably different, indicating that there are differences in the compositions of the two hexameric rings. From the model there also seems to quite a large interaction surface between the two rings. Such a solid interaction between the two hexamers suggests a functional significance of this double hexamer structure. A central channel is also observed running through the particle with a size of approximately 10 Å, which would be too small to accommodate dsDNA but may allow the passage of ssDNA. However, as no interaction was seen by the complex with DNA (Chapter 4 and (Ikura et al., 2000)) this channel may have a different function, from the translocation of DNA. This model gives preliminary data about the structure of the complex. To confirm the measurements of this low resolution structure, cryo-electron microscopy could be employed to solve the structure to a higher resolution. Hence, more detail about this complex would be obtained.

FIGURE 5.7: Low resolution 3D model of the TIP48/TIP49 complex

Using the classums shown in Figure 5.6b, a low resolution 3D map of the complex was created by angular reconstitution in IMAGIC-5. Extra rounds of model refinement and multi reference alignment were carried out to improve the 3D model (see Materials and Methods, section 2.9). The model was loaded into pymol, which allowed rotation and cross-sections of the particle model. (A) Different views of the 3D model. Top row shows the top and bottom views. The model was then rotated 45 ° in each case (middle row). It was then rotated another 45 ° so that two side views are seen (bottom row).
(B) Cross-sections of the TIP48/TIP49 complex model. One view shows a cross-section of the model when it was cut through the middle from top to bottom (top left) and one view shows a cross-section of the model when it was cut through the middle from one side to the other (bottom right).

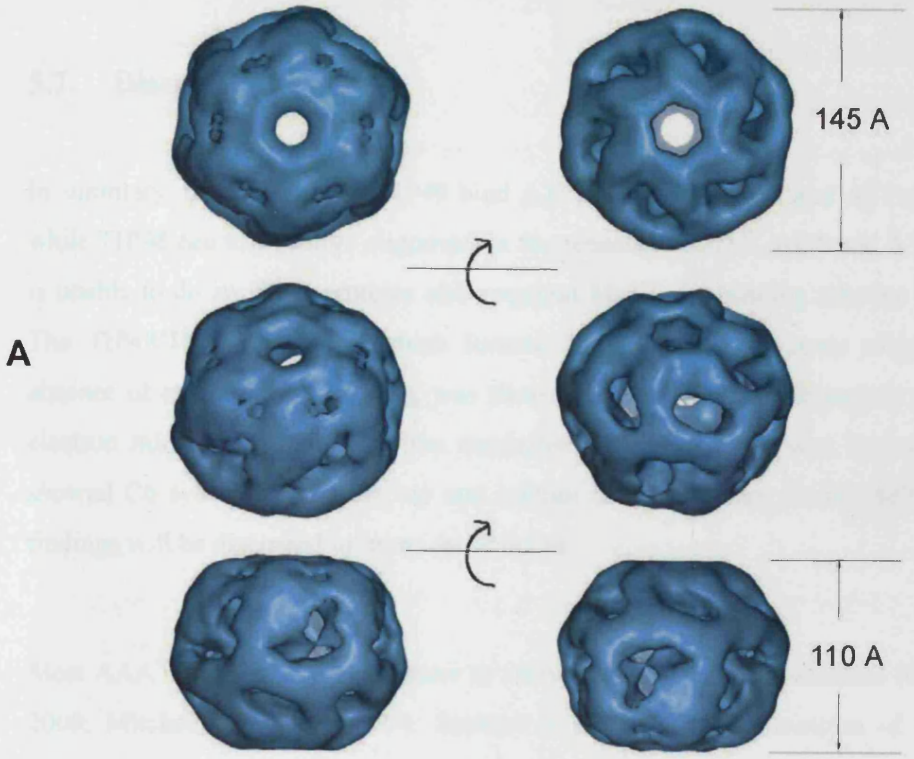
A
145 A
110 A

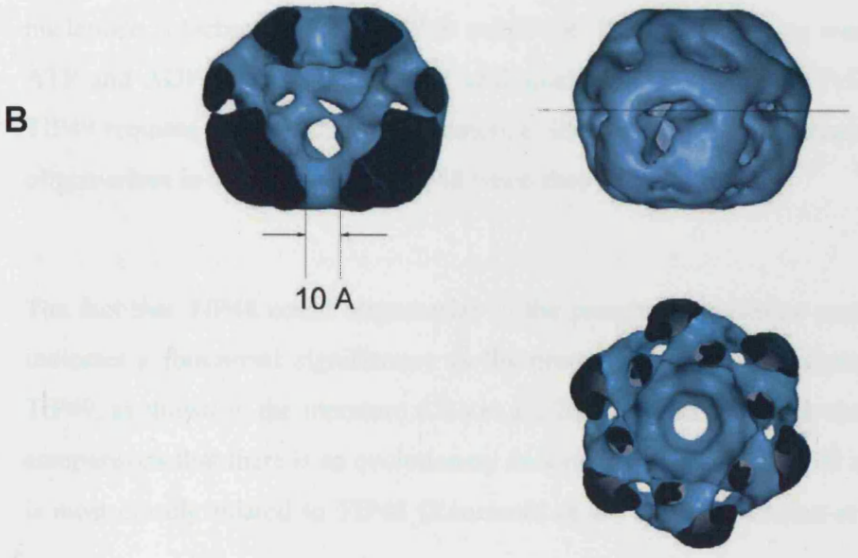
B
10 A

5.7. Discussion

In summary, both TIP48 and TIP49 bind ATP, ADP, AMPPNP and ATPγS. However, while TIP48 can form stable oligomers in the presence of ATP, ADP and ATPγS, TIP49 is unable to do so. Both proteins also required $MgCl_2$ for binding adenine nucleotides. The TIP48/TIP49 complex, which formed a high molecular mass oligomer in the absence of cofactors (Chapter 4), was shown to have a double hexameric structure by electron microscopy. Although the resolution of the structure was low, the complex showed C6 symmetry and the top and bottom hexamers were clearly different. These findings will be discussed in more detail below.

Most AAA^+ proteins form oligomers to carry out their specific functions (Chong et al., 2000; Mitchell and West, 1994; Seybert et al., 2002). The location of the adenine nucleotide binding pocket at the subunit interface has made this oligomerization nucleotide dependent for some AAA+ proteins (Lupas and Martin, 2002; Mitchell and West, 1994; Stasiak et al., 1994; Valle et al., 2000). Therefore it was likely that nucleotide binding would affect oligomerization of TIP48 and TIP49. However, the results presented here show that TIP48 could oligomerize in the presence of adenine nucleotide cofactors, whereas TIP49 could not. Yet, both proteins were shown to bind ATP and ADP as well as the ATP analogues, AMPPNP and ATPγS. It may be that TIP49 requires other factors to oligomerize. In fact, as shown in Chapter 4, TIP49 only oligomerizes in the presence of TIP48 when they form a complex.

The fact that TIP48 could oligomerize in the presence of adenine nucleotide cofactors indicates a functional significance as the protein may have functions independent of TIP49, as shown in the literature (Cho et al., 2001). It has also been shown by sequence comparisons that there is an evolutionary ancestor of TIP48 and TIP49 in archaea, which is most closely related to TIP48 (Kanemaki et al., 1999) (Newman et al., 2000). This

suggests that TIP49 may have arisen through evolution by gene duplication of the TIP48 gene. However, in eukaryotes both proteins have essential and non-redundant functions (Kanemaki et al., 1999; Lim et al., 2000; Qiu et al., 1998) and it is most likely that it is the complex of the two, which provides this essential function rather than functions of the individual proteins. Nevertheless, due to its evolutionary links, and that fact that TIP48 formed stable oligomers in the presence of nucleotide cofactors, it is likely that TIP48 also plays some important roles on its own.

TIP48 also oligomerized with ADP in the absence of $MgCl_2$ and appears to have a higher affinity for ADP over ATP. On a few occasions, when TIP48 was purified from *E. coli*, half of the protein was seen as oligomers in the absence of cofactors, on size exclusion chromatography (not shown). This suggested that on these occasions TIP48 co-purified with $MgCl_2$ and adenine nucleotides from *E. coli*. Interestingly, most of the TIP48D299N mutant eluted as a high molecular mass oligomer, which suggests that the mutation may have caused the protein to lose its dependence on $MgCl_2$ and adenine nucleotides for oligomerization. A similar observation was reported for the RuvBD113N mutant (Mezard et al., 1997). This shows that this mutation stabilizes oligomer formation of TIP48 and RuvB in the absence of adenine nucleotides. Therefore, these data confirm that TIP48 has a strong tendency to form oligomers.

The fact that TIP48 and TIP49 can form a double hexameric complex in the absence of nucleotide cofactors is very interesting. Some other AAA^+ proteins have also been shown to form oligomers in the absence of nucleotide cofactors, such as the MCM proteins from archaea and eukaryotes (Chong et al., 2000; Davey et al., 2003; Pape et al., 2003). As TIP48 and TIP49 form a complex in the absence of cofactors, it is unknown whether the two form hetero-hexamers or homo-hexamers, as TIP48 formed oligomers in the presence of nucleotide cofactors and TIP49 did not seem to form stable oligomers on its own. However, the electron microscopy data and the 3D model, although at low resolution, suggests two different hexamers come together to form the complex. The top and bottom views of the complex are very different, and as TIP48 has a tendency to form oligomers on its own, it is likely that two homo-hexamers are

formed, when the two proteins come into contact. How this occurs for the TIP48/TIP49 complex, without using the nucleotide binding energy, would be an interesting phenomenon to investigate. Moreover, the large interaction surface between the two hexamers that is seen in the model indicates a very strong interaction and hence functional significance of this double hexamer complex.

It has been shown in Chapter 4 that the TIP48/TIP49 complex hydrolyses ATP *in vitro* even though the activity is quite low. However, TIP48 and TIP49 have been shown to hydrolyse little or no ATP on their own (Chapter 3). By looking at the subunit organization of TIP49 this is probably expected because it is unable to form stable hexamers *in vitro*. TIP48 on the other hand does form hexamers but does not seem to hydrolyse ATP. This may be because once TIP48 has hydrolysed one round of ATP it is unable to exchange the bound ADP for free ATP. TIP48 also appears to have a higher affinity for ADP over ATP; hence bound ADP is likely to inhibit the function of TIP48 *in vitro* as it cannot be removed.

Many AAA^+ proteins need to form oligomers to hydrolyse ATP. This is because the ATPase site is at the interface between subunits, and the conserved arginine finger, found in many of these proteins, act to cause conformational changes in adjacent subunits so that bound ADP can be exchanged for ATP (Davey et al., 2003; Hishida et al., 2004; Johnson and O'Donnell, 2003; Neuwald et al., 1999; Ogura and Wilkinson, 2001; Yao et al., 2003). Therefore, it is likely that although TIP48 forms oligomers *in vitro*, it does not have the correct factors to release bound ADP for subsequent rounds of ATP hydrolysis. The TIP48/TIP49 complex, on the other hand, seems to be able to hydrolyse ATP independently of other interacting proteins. The subunits within this complex are probably in the correct conformation to allow the exchange of bound-ADP for free ATP and hence multiple rounds of ATP hydrolysis can occur. However, the complex can probably hydrolyse much more ATP when it is within the right environment, such as chromatin modifying complexes and this remains to be seen.

Chapter 6

Localization of TIP48 and TIP49 in mammalian cells by immunofluorescence microscopy

6.1 Introduction

The localization of TIP48 and TIP49 in cells may give clues about their functions *in vivo*. Therefore polyclonal antibodies were raised against the two proteins and used for localization studies in HeLa and fibroblast cells, by immunofluorescence microscopy. Comparison of the localization with other proteins that have been previously identified in TIP48/TIP49 containing complexes, was also carried out.

6.2. Characterization of the TIP48 and TIP49 polyclonal antibodies

Polyclonal antibodies of TIP48 and TIP49 were raised in rabbits, immunised with TIP48-His_6 and His_6-TIP49 proteins, purified as described in Materials and Methods (sections 2.7.1 and 2.7.3). The specificities of the affinity purified antibodies were tested by immunoblotting using purified recombinant TIP48 and TIP49 proteins. Figure 6.1 shows that the anti-TIP48 antibody immunostained the recombinant TIP48-His_6 protein (lane 1). Moreover, the antibody did not cross react with purified recombinant His_6-TIP49 protein (lane 2). The anti-TIP49 antibody immunostained the recombinant His_6-TIP49 protein (lane 3) and did not cross-react with the recombinant TIP48-His_6 protein (lane 4). Both antibodies also detected endogenous TIP48 or TIP49 from HeLa extracts (Sigala et al., 2005); with only a single protein band showing up in each case, after Western blot analysis. These antibodies were subsequently used for immunofluorescence microscopy studies, as described below. Other antibodies that were also used for the immunolocalization studies were obtained commercially or as gifts, as specified in Materials and Methods (Section 2.1.4), and included anti-BAF53, anti-β-catenin and anti-α-tubulin antibodies.

6.3 TIP48 and TIP49 are mainly nuclear proteins

The anti-TIP48 and anti-TIP49 antibodies were used to visualize TIP48 and TIP49 in HeLa cells by indirect immunofluorescence microscopy. Asynchronous cells were grown on cover slips (as described in Materials and Methods, section 2.11.3) and

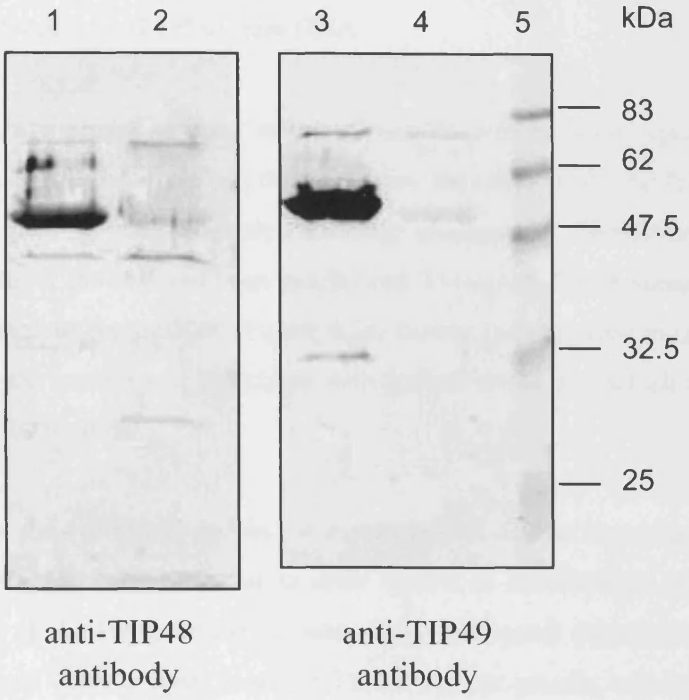

FIGURE 6.1: Immunoblotting with the anti-TIP48 and anti-TIP49 polyclonal antibodies

Polyclonal antibodies were raised in rabbits against the recombinant TIP48-His_6 and His_6-TIP49 proteins, as described in Materials and Methods (sections 2.10). 2 µg of each of the recombinant proteins were separated by 12 % SDS-PAGE and transferred onto nitrocellulose membranes. Lane 1, TIP48-His_6; lane 2, His_6-TIP49; lane 3, His_6-TIP49; lane 4, TIP48-His_6 and lane 5, markers. The membrane on the left was immunoblotted with the anti-TIP48 antibody and the membrane on the right was immunblotted with anti-TIP49 antibody. Membranes were developed using IRDye 38-labelled goat anti-rabbit IgG antibody and visualised by an Odyssey Infrared Imaging system

some were treated with 0.1 % Triton-X100 before fixation, to remove soluble cytoplasmic and nuclear components. Cells were fixed and immunostained with anti-TIP48 or anti-TIP49 antibodies simultaneously with anti-α-tubulin antibody, followed by incubation with fluorescently labeled secondary species-specific anti-IgG antibodies. Lastly samples were incubated with DAPI to stain DNA.

TIP48 showed strong staining in the nucleus as well as some signal in the cytoplasm (Figure 6.2a, top panel). When the cells were treated with 0.1 % Triton X-100, prior to fixation, most of the α-tubulin staining disappeared, indicating that cytoplasmic components of the cell had been solubilized. However, TIP48 staining remained strong and localized in the nucleus (Figure 6.2a, bottom panel). This indicated that TIP48 is mainly in the nucleus and associated with nuclear structures, which are not disrupted by Triton X-100 treatment.

TIP49 also showed strong staining in the nucleus as well as some signal in the cytoplasm (Figure 6.2a, top panel), similar to other reports in the literature (Gartner et al., 2003; Holzmann et al., 1998). It can be seen within this panel that staining with anti-TIP49 showed some definite areas in which TIP49 was not present, which could represent the nucleoli. When the cells were treated with 0.1 % Triton X-100, prior to fixation, again most of the α-tubulin staining disappeared. The staining of TIP49 was not as strong in the Triton X-100 treated cells, however, it can clearly be seen that TIP49 was in the nucleus, indicating that like TIP48, TIP49 remained associated with nuclear structures after Triton X-100 treatment (Figure 6.2b, bottom panel).

Similar experiments were done to investigate the localization of the BAF53 protein in HeLa cells. BAF53 and its homologue in yeast, Arp4, has been shown to be part of many complexes that also include TIP48 and TIP49 (Fuchs et al., 2001; Ikura et al., 2000; Park et al., 2002; Shen et al., 2000). Some localization studies of BAF53/Arp4 have been carried out previously (Weber et al., 1995; Zhao et al., 1998), but the experiments here were carried out to compare BAF53 localization to that of TIP48 and TIP49, under the same experimental conditions. BAF53 staining was much stronger,

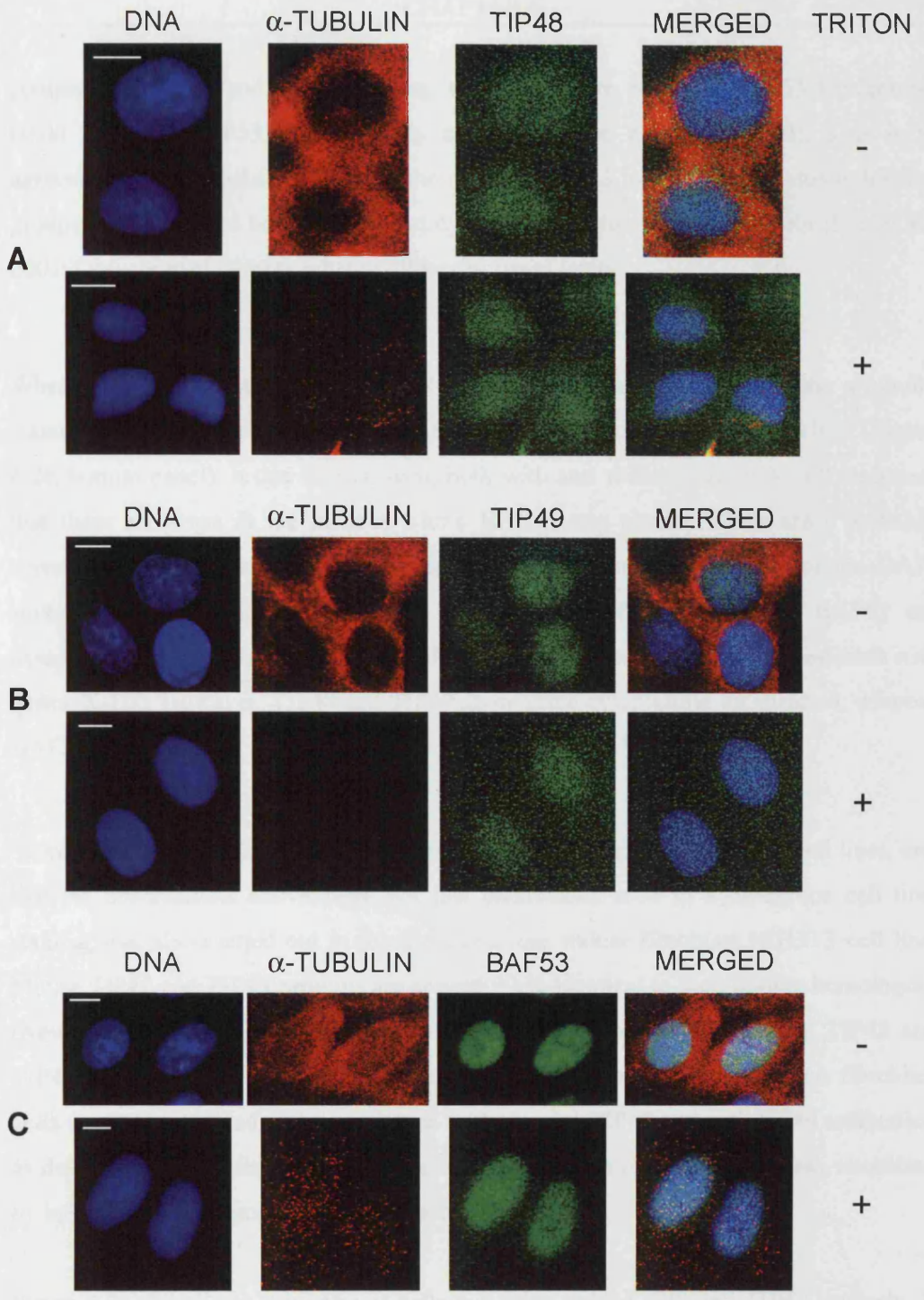

FIGURE 6.2: Localization of TIP48, TIP49 and BAF53 in HeLa cells

Co-localization of (A) TIP48, (B) TIP49 and (C) BAF53 (green) with α-tubulin (red) in asynchronous HeLa cells. The nucleus/DNA is also shown, which was stained with DAPI stain (blue). Cells were either treated (+) or not treated (-) with 0.1 % Triton X-100 before fixation with 2 % PFD. Bar represents 10 μm.

compared to TIP48 and TIP49 staining; therefore, more detail on BAF53 localization could be seen. BAF53 is exclusively nuclear (Figure 6.2c, top panel). This is in agreement with published data about the roles of BAF53 in the nucleus, although some groups have observed both nuclear and cytoplasmic staining of this protein (Lee et al., 2003; Ohfuchi et al., 2002), which will be discussed later.

When the cells were treated with 0.1 % Triton X-100 prior to fixation, the α-tubulin staining disappeared but staining of BAF53 remained strong and in the nucleus (Figure 6.2c, bottom panel). It can also be seen, both with and without Triton X-100 treatment that there are areas in the nucleus where BAF53 was absent. These areas probably correspond to the nucleoli, as the same dark patches are seen in some of the DAPI stained nuclei. These results clearly indicate that TIP48, TIP49 and BAF53 are associated with nuclear structures in HeLa cells that are not disrupted by treatment with Triton X-100. However, TIP48 and TIP49 show some cytoplasmic localization, whereas BAF53 does not.

To confirm whether TIP48 and TIP49 are indeed nuclear proteins in other cell lines, and that the observations above were not just phenomena seen in a cancerous cell line, staining was also carried out in the non-cancerous mouse fibroblast NIH3T3 cell line. Mouse TIP48 and TIP49 proteins are around 99 % identical to their human homologues (Newman et al., 2000) and therefore comparisons of the localizations of TIP48 and TIP49 proteins between the different cell lines, could be made. Asynchronous fibroblast cells were grown, fixed and then stained with the anti-TIP48 and anti-TIP49 antibodies, as described in Materials and Methods. The localization of the proteins was visualized by indirect immunofluorescence microscopy.

Figure 6.3a shows two examples of cells that were stained with anti-TIP48 antibody. It can be seen that TIP48 is localized in the nucleus but there is also significant staining in the cytoplasm. There is slightly more staining of the cytoplasm, which overlaps with the α-tubulin staining in the fibroblasts, compared to HeLa cells. However, the staining of

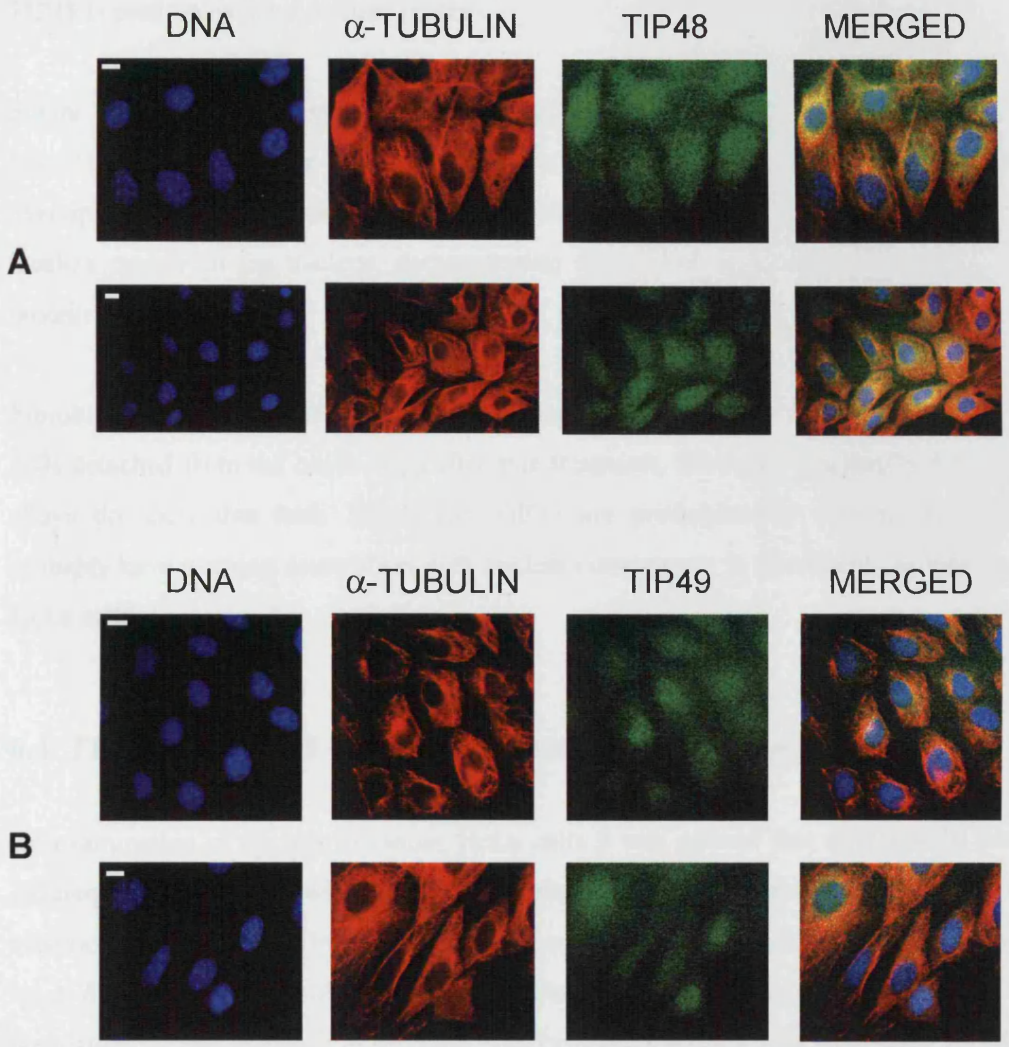

FIGURE 6.3: Localization of TIP48 and TIP49 in fibroblasts

Fluoresence staining of asynchronous NIH3T3 mouse fibroblast cells. Cells were stained with DAPI (blue) and immunostained with: anti-α-tubulin (red) antibody and (A) anti-TIP48; (B) anti-TIP49 (green) antibodies. Bar represents 10 μm.

TIP48 does seem to be predominantly in the nucleus supporting the observation that TIP48 is predominantly a nuclear protein.

Figure 6.3b shows two examples of cells that were stained with anti-TIP49 antibody. Like TIP48, TIP49 is seen both in the nucleus and the cytoplasm as the TIP49 staining overlaps with both DNA and the α-tubulin staining. Also, like TIP48, TIP49 seems to localize mainly in the nucleus, demonstrating that TIP49 is predominantly a nuclear protein.

Fibroblast cells treated with Triton X-100 before fixation could not be examined, as the cells detached from the cover slips after this treatment. However, the results described above do show that both TIP48 and TIP49 are predominantly nuclear and hence probably have a strong association with nuclear components in fibroblasts, as they do in HeLa cells.

6.4. TIP48 and TIP49 localize differently during mitosis

On examination of the asynchronous HeLa cells it was noticed that mitotic cells had a different pattern of TIP48 and TIP49 localization. To examine more carefully the behavior of TIP48 and TIP49 in mitosis, HeLa cells were synchronized at early S-phase by a double thymidine block and then released for 8 hours in order to obtain a population of cells enriched in M phase. The cells were stained with either anti-TIP48 or anti-TIP49 antibodies, along with anti-α-tubulin as described in Materials and Methods and Figures 6.4 to 6.5. Localization of the proteins was examined by indirect immunofluoresence microscopy.

Figure 6.4 shows panels of cells in different stages of mitosis, stained with anti-TIP48 and anti-α-tubulin antibodies, and DAPI. In the metaphase cell, (Figure 6.4a) the α-tubulin can be seen to have formed the bipolar spindles surrounding the condensed chromatin. As shown in Figure 6.2, TIP48 usually associates with chromatin in

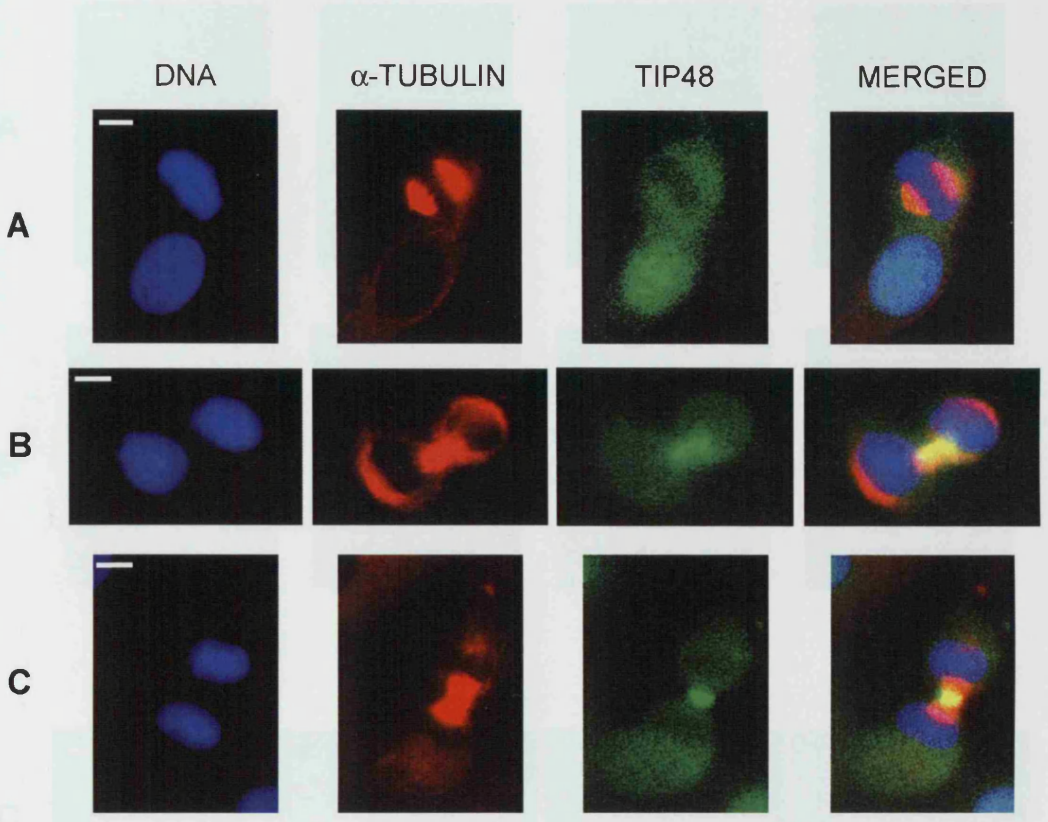

FIGURE 6.4: Localization of TIP48 during mitosis

HeLa cells were synchronized at early S phase following a double thymidine block protocol and immunostained 8 h after release from the block. Cells were stained with DAPI (blue) and immunostained with anti-α-tubulin (red) and anti-TIP48 (green) antibodies. They were then examined by fluorescence microscopy. Panels show cells in: (A) interphase and metaphase stages; (B) and (C) cytokinesis. Bar represents 10 μm.

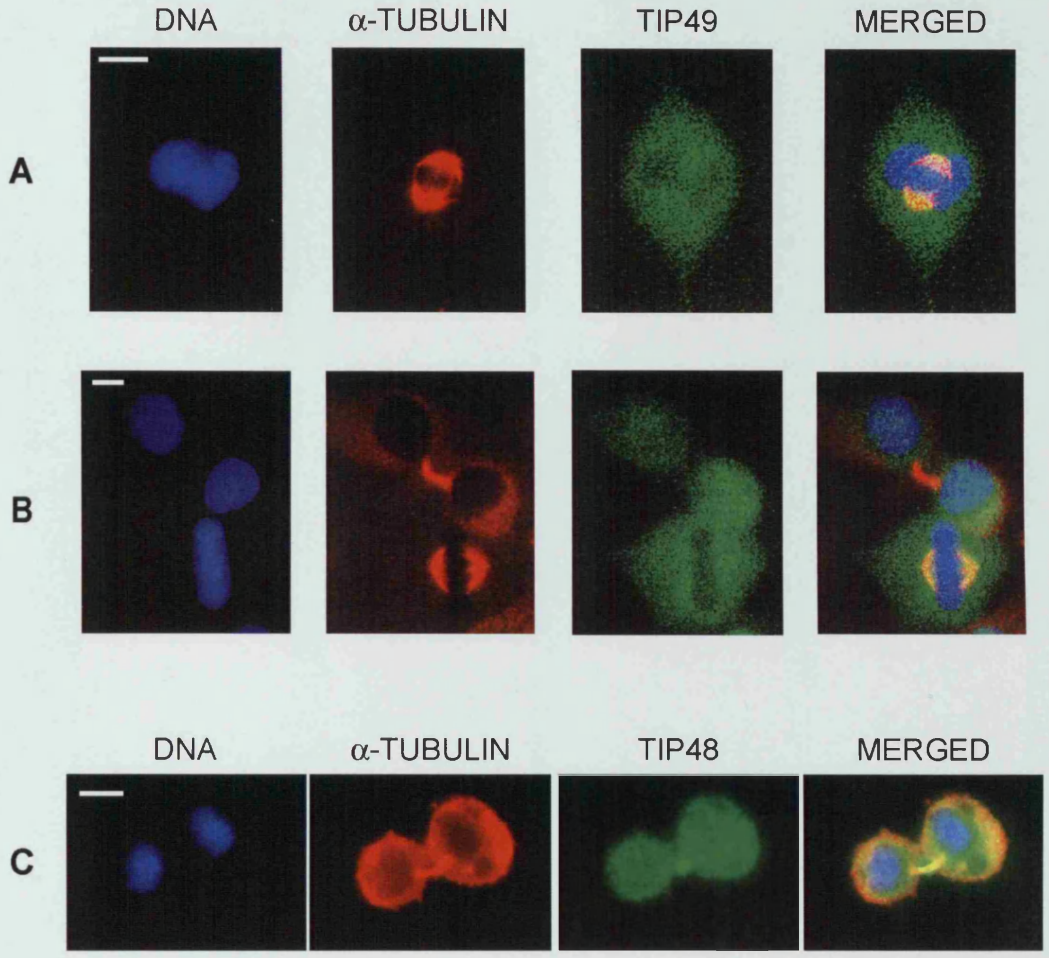

FIGURE 6.5: Localization of TIP49 during mitosis

HeLa cells were synchronized at early S phase, following a double thymidine block protocol and immunostained 8 h after release from the block. Cells were stained with DAPI (blue) and immunostained with α-tubulin (red), anti-TIP49 (A and B) and anti-TIP48 (C) (green) antibodies. They were then examined by fluorescence microscopy. Panels show cells in: (A) metaphase; (B) cytokinesis and metaphase. Panel (C) shows the localization of TIP48 during cytokinesis. The experiment in (C) was carried out under similar conditions as in (A and B) but using another set of synchronized HeLa cells. Bar represents 10 μm.

interphase cells however, during metaphase it no longer associates with the chromatin (Figure 6.4a), but is seen to associate with the α-tubulin and the surrounding areas.

Figure 6.4b and 6.4c show cells, which are undergoing cytokinesis. It can be seen that α-tubulin is present in the midbody within the area of constriction between the two daughter cells, as well as surrounding the chromatin of the newly formed daughter cells. TIP48 is seen diffusely where the two daughter nuclei are. However, there is also strong staining of TIP48 in the midbody where α-tubulin is also seen. By comparing Figures 6.4b with 6.4c, it can be seen that the staining of TIP48 in the midbody becomes much more concentrated as cytokinesis is brought to a close (Figure 6.4c) and appears dot-like, while staining in other parts of the daughter cells is not as concentrated. Although not shown here, this concentration of TIP48 in the midbody is a progression of earlier accumulation of TIP48 in the midzone during the anaphase and telophase stages. This staining then becomes much more concentrated, as the midbody is formed during cytokinesis and hence this dot-like structure is seen (Sigala et al., 2005).

Figure 6.5a and b shows panels of cells, in different stages of mitosis, stained with anti-TIP49 and anti-α-tubulin antibodies and DAPI. In metaphase cells, shown in Figures 6.5a and 6.5b, staining with α-tubulin reveals the bipolar spindles. TIP49 in these cells is excluded from the chromatin and is localized with the α-tubulin and surrounding areas. Similar observations of TIP49 localization during metaphase have been reported (Gartner et al., 2003).

Figure 6.5b also shows a cell that is undergoing cytokinesis. It can be seen that TIP49 is re-associated with the two daughter nuclei at this stage, similar to what has been observed previously (Gartner et al., 2003). There is no staining of the midbody and by comparing this figure to Figure 6.5c, which shows localization of TIP48 during cytokinesis, it can be seen that there is a distinct difference in the localization of the two proteins at this stage. These experiments therefore show that TIP48 and TIP49 have different localization patterns during the later stages of mitosis, especially during

cytokinesis. This suggests that they may have different roles during this stage of the cell cycle and hence are unlikely to work as a complex at this stage.

6.5. Distribution of TIP48 and TIP49 interacting proteins BAF53 and β-catenin during mitosis

Localization studies of cells in mitosis using antibodies against BAF53 and β-catenin were carried out. As mentioned in section 6.2, BAF53 is found in TIP48/TIP49-containing complexes, such as the TIP60, p400 and c-Myc complexes. β-catenin, on the other hand, interacts with both TIP48 and TIP49, which are both required for the transcription of genes by LEF/TCF transcription factors. However, the proteins have been shown to have opposite effects on β-catenin mediated transcription (Bauer et al., 2000; Rottbauer et al., 2002). As TIP48 and TIP49 seem to separate during the later stages of mitosis it was quite interesting to investigate how BAF53 and β-catenin, which form complexes with TIP48 and TIP49, would distribute during mitosis. Also, as there have been some recent reports in the literature of a mitotic function of β-catenin (Kaplan et al., 2004) and the *S. pombe* homolog of BAF53 (Minoda et al., 2005), these localization studies may give a clue about the function of TIP48 and TIP49 during mitosis.

Figure 6.6 shows panels of cells in different stages of mitosis, which were stained with anti-BAF53 and anti-α-tubulin antibodies, and DAPI stain. It can be seen in Figure 6.6a that BAF53 is distributed throughout the cell but excluded from the condensed chromatin during metaphase. Like TIP48 and TIP49, an accumulation of BAF53 at the mitotic spindle is seen. This suggests that like TIP49, BAF53 probably associates with α-tubulin (Gartner et al., 2003). Although during interphase, BAF53 was shown to be exclusively nuclear (Figure 6.2) and its homologue in yeast is shown to interact with core histones, (Galarneau et al., 2000; Harata et al., 1999); during metaphase it does not seem to associate with chromatin. It was recently reported by (Minoda et al., 2005) that

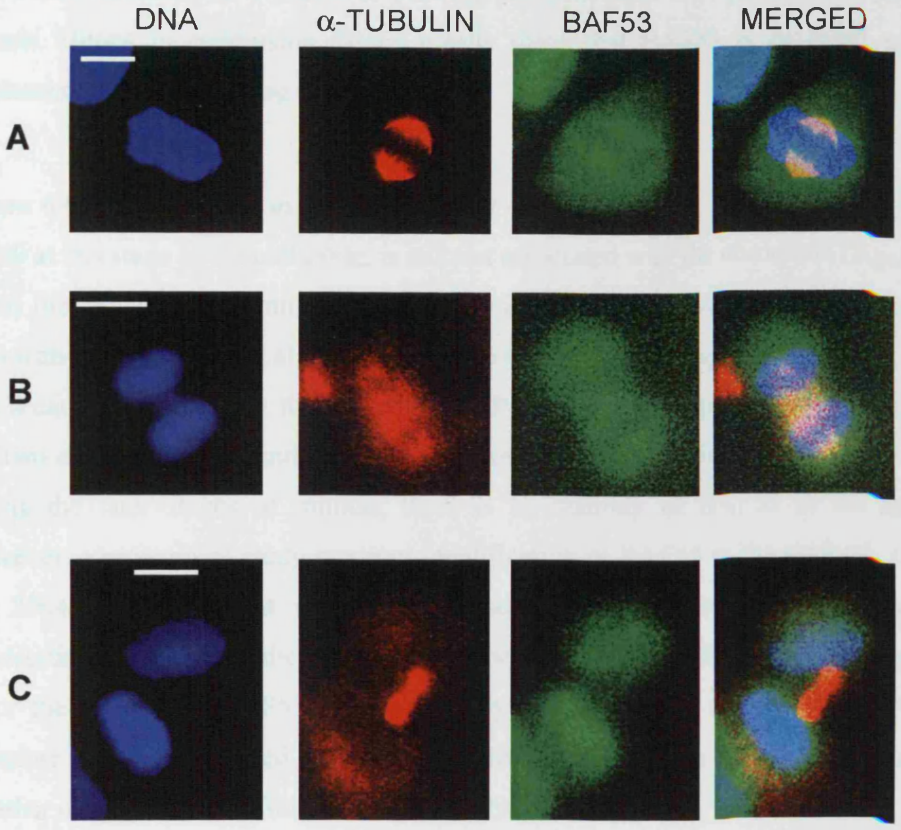

FIGURE 6.6: Localization of BAF53 during mitosis

HeLa cells were synchronized at early S phase following a double thymidine block protocol and immunostained 8 h after release from the block. Cells were stained with DAPI (blue) and immunostained with α-tubulin (red) and anti-BAF53 (green) antibodies. They were then examined by fluorescence microscopy. Panels show cells in: (A) metaphase; (B) telophase and (C) cytokinesis. Bar represents 10 μm.

the *S. pombe* homolog of BAF53 (Alp5), is required for kinetechore attachment to the mitotic spindle but it stayed associated with chromatin during all stages of the cell cycle. There may however be differences between the functions of Alp5 and BAF53 during mitosis. Hence in conclusion theses results show that BAF53 is excluded from the condensed chromatin during metaphase.

Figure 6.6b shows a cell in telophase and it can be seen that BAF53, like TIP48 and TIP49 at this stage of the cell cycle, is still not associated with the chromatin (Sigala et al., 2005) (not shown). Accumulation of BAF53 in the midzone was not as pronounced as seen with TIP48 (Sigala et al., 2005). Figure 6.6c shows two daughter cells in cytokinesis and it can be seen that by this stage, like TIP49, BAF53 completely re-associates with the two daughter nuclei and cytoplasmic staining is very limited. Also, unlike TIP48, during the later stages of mitosis, there is no staining of BAF53 in the midbody. However, a proteomics study reported identification of BAF53 in the midbody (Skop et al., 2004). The fact that the antibody used in these experiments, did not show localization of BAF53 in the midbody, may be because the antibody itself did not detect it, or the amount of BAF53 in the midbody may be small, compared to TIP48 and therefore was not detected. Confocal microscopy may have to be used to confirm whether or not BAF53 is found at the midbody.

HeLa cells that were synchronized to contain a high population of cells undergoing mitosis, were incubated with either anti-TIP48 or anti-TIP49 antibodies alongside anti-β-catenin antibody (Figures 6.7 and 6.8). In interphase cells, β-catenin is shown to be present both in the nucleus and cytoplasm but is concentrated at the periphery of the nuclei of HeLa cells (Figure 6.7a and 6.8a). TIP48 and TIP49 in these cells were shown to be predominantly nuclear, as before (Figure 6.2a and b).

In the metaphase cell (Figure 6.7b), it can be seen that like TIP48, β-catenin is excluded from the condensed chromatin. Figure 6.7c shows that both TIP48 and β-catenin are excluded from the chromatin, so it is likely, that this stage is telophase. However, in

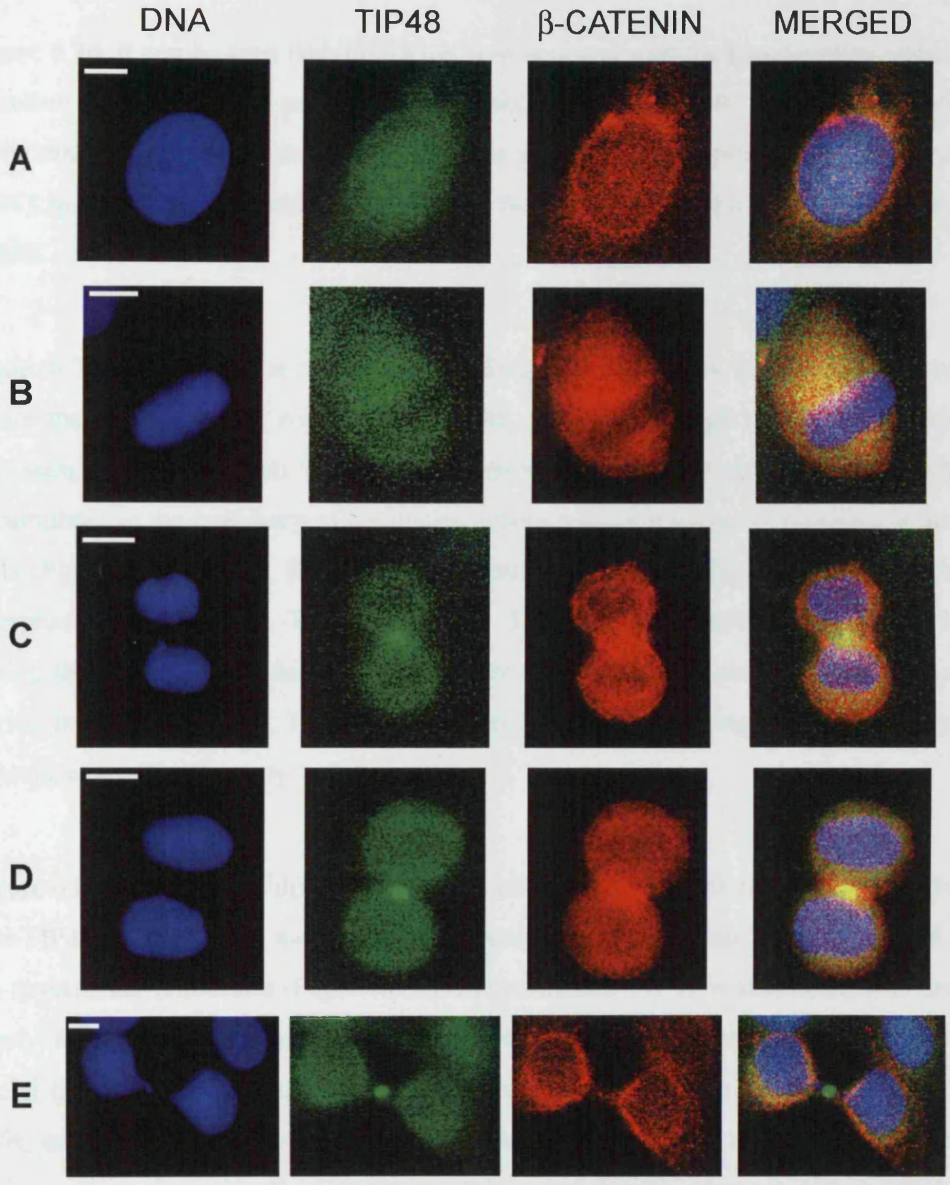

FIGURE 6.7: Co-localization of β-catenin and TIP48 during mitosis

HeLa cells were synchronized at early S phase following a double thymidine block protocol and immunostained 8 h after release from the block. Cells were stained with DAPI (blue) and immunostained with anti-TIP48 (green) and β-catenin (red) antibodies. They were then examined by fluorescence microscopy. Panels show cells in: (A) interphase; (B) metaphase; (C) telophase; (D) cytokinesis; (E) nascent cells in cytokinesis. Bar represents 10 μm.

Figure 6.7d, it can be seen that TIP48 has re-associated with the two daughter nuclei and therefore these cells have progressed to cytokinesis. In both cells TIP48 is concentrated at the midbody. β-catenin accumulates in this area, as reported previously (Kaplan et al., 2004), but is more dispersed in the midbody rather than forming a dot-like structure, like TIP48.

Figure 6.7e, shows nascent cells that are undergoing cytokinesis. It can be seen from this figure that TIP48 is still concentrated in the midbody although nuclear localization is also seen. However, at this late stage β-catenin is no longer present in the midbody but accumulates at the periphery of the nuclei, where α-tubulin normally localizes in nascent cells (Figure 6.4b and c). β-catenin also localizes at the periphery of the nuclei during interphase (Figure 6.7a). Therefore, while TIP48 remains localized at the midbody during the late stages of mitosis, β-catenin re-localizes to regions it is usually found at during interphase. Hence, TIP48 and β-catenin co-localize during most of the stages of mitosis, except for the very last stage.

Figure 6.8 shows cells in different stages of mitosis stained with both anti-β-catenin and anti-TIP49 antibodies. In metaphase both β-catenin and TIP49 are clearly excluded from the condensing chromatin (Figure 6.8b). In cytokinesis TIP49 is associated with the two newly formed daughter nuclei, although there is still significant staining around the nuclei (Figure 6.8c). There is very little staining of β-catenin in the two nuclei of these cells, and it is localized mainly on the nuclear periphery and also in the cytoplasmic region, where there is also significant staining of TIP49. There is also a substantial concentration of β-catenin in the midbody, which is not seen with TIP49. This shows that this localization of β-catenin and TIP48 to the midbody is a unique property of these proteins, which does not apply to TIP49. In conclusion, BAF53 and β-catenin show specific localizations that are similar to TIP48 and TIP49, at some stages of mitosis but also differ at other stages.

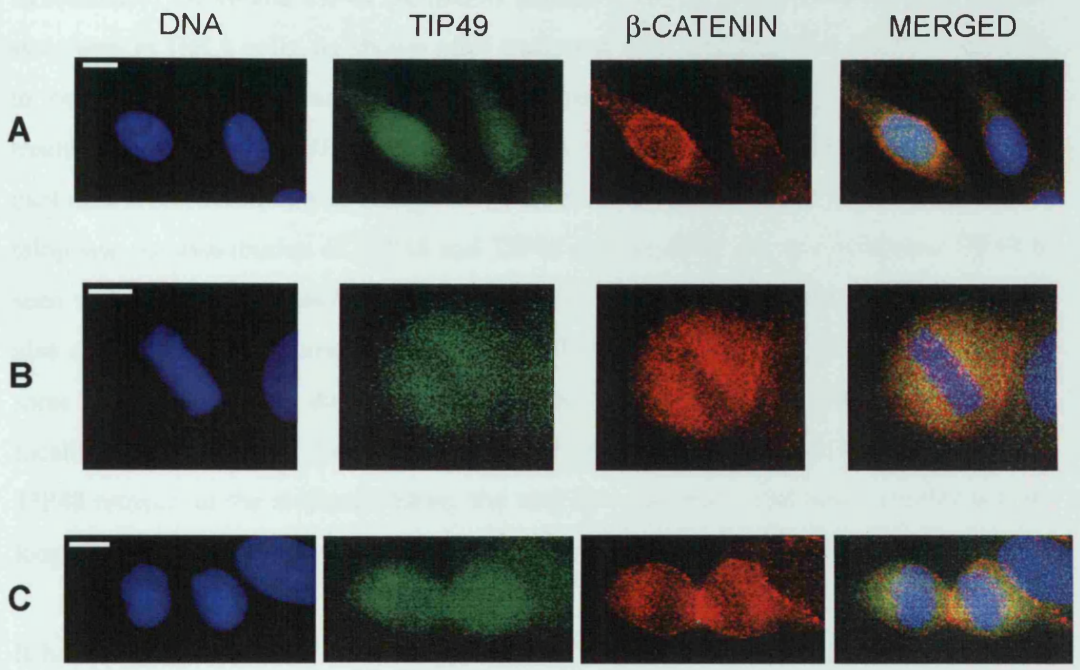

FIGURE 6.8: **Co-localization of β-catenin and TIP49 during mitosis**

HeLa cells were synchronized at early S phase following a double thymidine block protocol and immunostained 8 h after release from the block. Cells were stained with DAPI (blue) and immunostained with anti-TIP49 (green) and anti-β-catenin (red) antibodies. They were then examined by fluorescence microscopy. Panels show cells in: (A) interphase; (B) metaphase; and (C) cytokinesis. Bar represents 10 μm.

6.6 Discussion

In summary, TIP48 and TIP49 are mainly nuclear proteins, which associate with nuclear structures in HeLa cells, as shown after treatment with Triton X-100. BAF53 was seen to be exclusively nuclear and its localization was not disrupted by Triton X-100 treatment. TIP48 and TIP49 showed specific localizations during mitosis. Both are excluded from chromatin at metaphase. However, as cells progress from metaphase to telophase the distribution of TIP48 and TIP49 start to differ and at cytokinesis TIP48 is seen to localize at the midbody, whereas TIP49 is not. Both BAF53 and β-catenin are also excluded from chromatin at metaphase. However, while BAF53 distributes in the same fashion as TIP49 during the subsequent stages of mitosis, β-catenin is seen to localize at the midbody during telophase and cytokinesis, similar to TIP48. Yet, while TIP48 remains at the midbody during the very last stages of cytokinesis, β-catenin is no longer localized at this region. These findings will be discussed in more detail below.

It has been demonstrated here using immunofluorescence microscopy, that TIP48 and TIP49 predominantly localize in the nuclei, similar to what has been published by other groups (Bauer et al., 1998; Gartner et al., 2003; Holzmann et al., 1998; King et al., 2001; Lim et al., 2000; Makino et al., 1998; Newman et al., 2000). Some cytoplasmic staining of TIP48 and TIP49 was also seen, which has also been observed by some groups (Gartner et al., 2003; Salzer et al., 1999). Two different cell types were examined, a cancerous cell line and non-cancerous cell line. Although slightly more cytoplasmic localization was seen in the non-cancerous fibroblast cells, the two proteins do have a tight association with the nuclei from HeLa cells, as they were not solubilized by Triton X-100 treatment. Fractionation experiments showed that a major fraction of the TIP48 and TIP49 proteins were part of the nuclear matrix (Sigala et al., 2005). Similar observations have been made by (Gohshi et al., 1999; Holzmann et al., 1998; Kikuchi et al., 1999). These results are in agreement with what is already known about the function of TIP48 and TIP49 in the nucleus as part of chromatin modifying complexes. Nevertheless, cytoplasmic staining of the proteins suggests that they may also be involved in important functions in the cytoplasm.

Another protein, BAF53, was also examined within the same experiment and showed exclusively nuclear localization. This is in agreement with previously published data, which have shown that BAF53 is part of chromatin modifying complexes such as the SWI/SNF related BAF complex (Zhao et al., 1998), TIP60 complex (Ikura et al., 2000), p400 complex (Fuchs et al., 2001) and its homologue in yeast is also part of the INO80, Swr1 and NuA4 complexes (Galarneau et al., 2000; Kobor et al., 2004; Shen et al., 2000). The yeast homolog Arp4 has been shown to interact with core histones and nucleosomes and may have a role in maintenance or reconfiguration of chromatin structure (Galarneau et al., 2000; Harata et al., 1999) Arp4 also has important roles in transcription and DNA DSB repair (Bird et al., 2002; Downs et al., 2004; Galarneau et al., 2000; Harata et al., 2002).

A role in nuclear processes, suggests that BAF53 only localizes in the nucleus. However, like TIP48 and TIP49, cytoplasmic localization of the protein has been reported (Lee et al., 2003; Ohfuchi et al., 2002) and BAF53 was thought to shuttle between the nucleus and cytoplasm (Lee et al., 2003). However, it was shown that a splice product, which lacks the 42 amino-terminal amino acids of BAF53, was localized mainly in the cytoplasm of HeLa cells, whereas BAF53 was localized to the nucleus (Ohfuchi et al., 2002). This splice product still contains putative nuclear localization signals. Therefore, it is thought that protein-protein interactions are probably responsible for the sub-cellular localization of this splice product (Ohfuchi et al., 2002). Hence BAF53 is likely, as we have seen here, to be exclusively nuclear but its splice product may not be.

The data presented here show that both TIP48 and TIP49 accumulate at the mitotic apparatus when cells were in metaphase. Similar observations by confocal microscopy showed that TIP49 accumulated at the centrosomes and sites of tubulin polymerization (Gartner et al., 2003). In our experiments by confocal microscopy, TIP48 was also seen to accumulate at the centrosome and astral microtubles of the mitotic spindle (Sigala et al., 2005). Association of BAF53 at the mitotic spindle during metaphase is also quite

prominent (Figure 6.6a). TIP49 has been shown to directly interact with α-tubulin (Gartner et al., 2003) and it would be interesting to see whether TIP48 and BAF53 form complexes with α-tubulin, which would confirm that they interact with the mitotic spindle.

β-catenin has been shown to participate in the establishment of the bipolar spindle (Kaplan et al., 2004). It co-localized with β-tubulin in the centrosome regions, similar to what has been observed here. It was reported that by depleting β-catenin from cells, using RNAi, a marked increase in monoastral spindles occurred (Kaplan et al., 2004). This indicated a failure of centrosomes to segregate. In confirmation to this, these monoastral spindles exhibited two puncta of γ-tubulin, suggesting that the centrosomes had duplicated but were not properly separated. By introducing *Xenopus* β-catenin into HeLa cells that had been depleted of endogenous β-catenin, this mitotic defect was rescued. These results indicate a role for β-catenin in centrosome separation. As TIP48, TIP49 and BAF53 all seem to localize at the mitotic spindle they may also have a role in the establishment of the bipolar spindle in conjunction with β-catenin.

There is however evidence that BAF53 may have an important role in mitosis, at a slightly different stage. Its homologue in *S. pombe*, known as Alp5, was shown to be required for kinetechore spindle attachment (Minoda et al., 2005). The temperature-sensitive mutant *alp5-1134* displayed mitotic phenotypes, including chromosome condensation and mis-segregation. The study showed that Alp5 was crucial for the establishment of the bipolar attachment of the kinetochore to the spindle. It was also shown to be required for transcriptional silencing at the centromere. These data suggest that BAF53 may play a role in the attachment of kinetchores to the spindle. Then again it is unknown whether this function would be conserved in humans, through the BAF53 protein, due to differences in the mechanism of mitosis from *S. pombe* to humans.

It was also shown in *S. cerevisiae* that mutations in Htz1 histone, and the Swr1 and NuA4 complexes caused defects in chromosome segregation (Krogan et al., 2004). Genetic analysis suggested that all these components work together. Spindle checkpoint

mutants are hypersensitive to the microtubule destabilizing drug benomyl, as are some mutants of the NuA4 complex and Δ*htz1* and Δ*swr1* strains. Therefore these complexes are likely to have an important role in chromosome segregation. It has been shown that the Swr1 complex recruits Htz1 to regions of the genome (Krogan et al., 2003) and it was also shown that it recruits Htz1 to the centromere (Krogan et al., 2004). Recruitment of Htz1 to the centromere was Swr1 dependent but did not require the NuA4 complex. Therefore, NuA4 is not needed for the recruitment of Htz1 but could play a role after recruitment. As *sc*TIP48, *sc*TIP49 and Arp4 are part of the Swr1 complex and Arp4 is also part of the NuA4 complex, these proteins are also likely to have an important role in chromosome segregation and, for Arp4 at least, this may involve a function in kinetechore attachment.

Another observation made in our experiments was that TIP48 localized at the midbody whereas TIP49 did not. This clearly suggests a separate role for TIP48 away from TIP49, during cytokinesis. Like TIP49, BAF53 was not visualized at the midbody in this study. However, another group has identified BAF53, in a proteomics study, as part of the midbody, in Chinese hamster ovary cells (Skop et al., 2004). The functional role of the same midbody proteins, including BAF53 was examined in *C. elegans*. RNAi against BAF53 and 171 other homologues in *C. elegans* revealed that BAF53 plays an important role in cytokinesis. Depletion of BAF53 caused early cytokinesis defects, sterility and mitotic defects, including spindle assembly and cell cycle defects. TIP48 was also identified in the midbody, but its effects on cytokinesis were not studied. The midbody has no clear function but contains proteins that are indispensable for cytokinesis, asymmetric cell division and chromosome segregation. In fact it was shown by depleting these 172 homologs, by RNAi, that 58 % displayed defects in cleavage furrow formation or completion of germline cytokinesis (Skop et al., 2004). Therefore, it is likely that TIP48 has an important role in cytokinesis and this is currently being investigated in the lab, by the use of RNAi.

TIP48 and TIP49 obviously have roles in mitosis as they accumulate at the mitotic spindle during metaphase. However, the functions of these two proteins at the mitotic

spindle remain to be seen. BAF53 may also work in conjunction with TIP48 and TIP49 but as yet a direct interaction between these proteins still remains to be shown. Hence, TIP48 and TIP49 may be functioning within a larger complex that includes BAF53, therefore further experiments may be carried out to see if other components of TIP48, TIP49 and BAF53 containing complexes such as the TIP60 and p400 complexes, co-localize with these proteins at the mitotic spindle. It may be that the three proteins function with β-catenin in the establishment of the mitotic spindle, as TIP48 and TIP49 have direct interaction with β-catenin but again more experiments need to be done to determine this. Our experiments also showed that TIP48 and TIP49 have different localization patterns during the late stages of mitosis. It is likely that TIP48 has roles of its own away from the TIP48/TIP49 complex and this is discussed further in the next chapter.

CHAPTER 7

General Discussion

In this thesis I have shown the ATP binding and hydrolysis activities of two related human AAA^+ proteins, TIP48, TIP49 and their complex. The oligomeric states of these two proteins were also investigated and it was shown that TIP48 could form stable oligomers in the presence of adenine nucleotide factors and $MgCl_2$, whereas TIP49 could not. However, the two proteins formed a double hexameric complex together, which showed enhanced ATPase activity, compared to the individual proteins. The proteins did not show stimulation of ATPase activity in the presence of DNA and it seems unlikely, as discussed below, that they act on DNA. Hence they are probably not functional homologues of the bacterial RuvB protein. As well as functioning as a complex, there are indications from observations made in this study, and in the literature, that the two proteins have individual functions, which will also be discussed below.

7.1 TIP48 and TIP49 complex formation

TIP48 and TIP49 were shown to form a double hexameric complex. The complex hydrolyzed ATP and both subunits were shown to be required for this activity. Both subunits were also shown to bind ATP. It is clear that complex formation stimulates the ATPase activity of these two proteins, as neither seems to hydrolyze significant amounts of ATP, on their own. A similar observation has been made with other AAA^+ proteins and often complex formation is crucial because the ATPase site is at the interface between two subunits. Most AAA^+ protein contain a conserved arginine in the conserved region known as box VII (Neuwald et al., 1999), (Figure 7.1), which is important for ATP hydrolysis. This residue often functions as an 'arginine finger' in "intermolecular catalysis mechanism" (Ogura and Wilkinson, 2001). This arginine finger is thought to transduce ATP hydrolysis into conformational changes in the neighboring subunit of the hexamer. Hence, this would explain why the ATPase activities of most AAA^+ proteins is observed, when they are in an oliogomeric form.

Some AAA^+ proteins, such as the eukaryotic MCM and RFC proteins and the bacterial $\gamma_3\delta_1\delta'_1$ DNA polymerase III clamp loader complex, form hetero-oligomers, with a

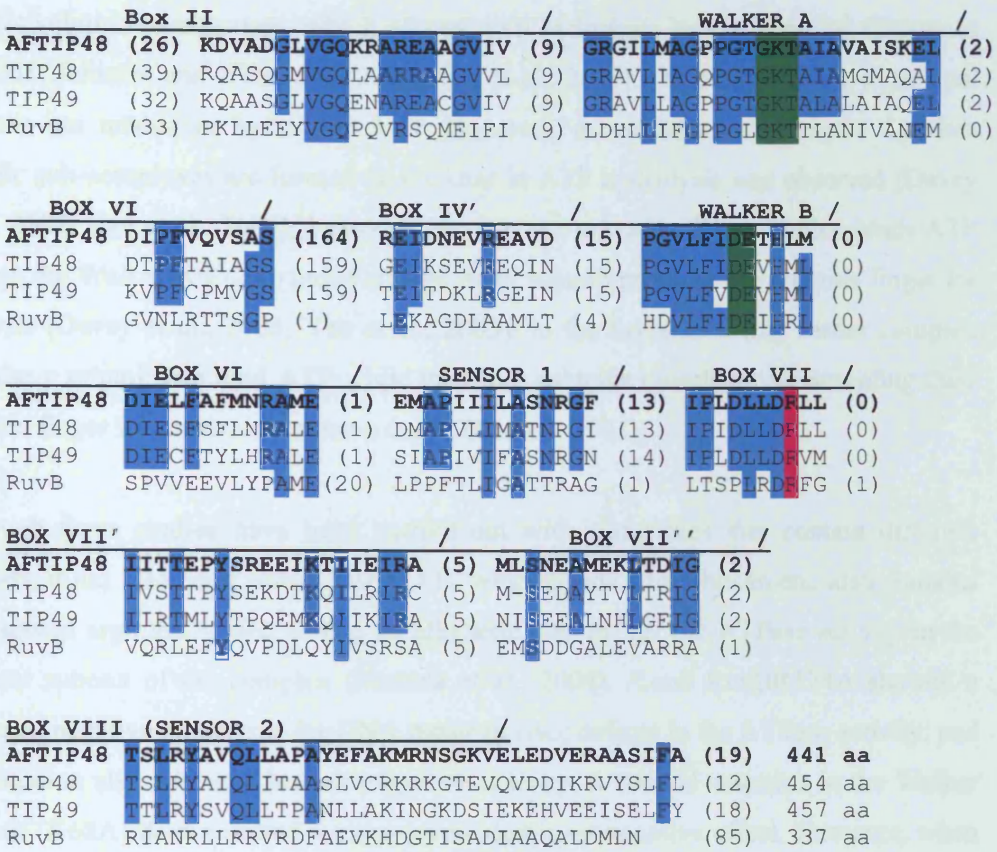

FIGURE 7.1: Sequence alignment of TIP48 and TIP49 showing the AAA$^+$ motifs within the amino acid sequences of the two proteins

Human TIP48 and TIP49 amino acid sequences were aligned with the sequences of the *A. fulgidus* TIP48 and *E.coli* RuvB AAA$^+$ proteins that were used previously in alignments by Newald et al. 1999, who defined the AAA$^+$ class of proteins (Chapter 1). TIP48 and TIP49 were aligned with the sequence of *Af*TIP48 using the pairwise alignment tool from the BCM search launcher (http://searchlauncher.bcm.tmc.edu). Residues highlighted in blue are conserved in TIP48, TIP49 *Af*TIP48 and occasionally *in E. coli* RuvB. Residues highlighted in green are conserved residues in all four proteins within the Walker A and B motifs. The residue highlighted in pink across all four proteins is the conserved arginine finger.

specific subunit arrangement, which allows ATP hydrolysis by the complex (Davey et al., 2003; Johnson and O'Donnell, 2003; Yao et al., 2003). On their own, the individual subunits are unable to hydrolyze ATP. However, as explained in Chapter 4, when specific sub-complexes are formed an increase in ATP hydrolysis was observed (Davey et al., 2003; Yao et al., 2003). It was shown that one subunit of the complex binds ATP through the Walker A/P-loop motif and the other subunit provides the arginine finger for catalysis (Davey et al., 2003; Yao et al., 2003). In the bacterial clamp loader complex only the γ subunit can bind ATP while the other subunits contribute by providing their arginine finger for catalysis (Johnson and O'Donnell, 2003).

Although these studies have been carried out with complexes that contain different subunits, it has also been shown that RuvB, which forms homo-hexamers; also contains a conserved arginine, which acts as an allosteric effector for the ATPase activity in the adjacent subunit of the complex (Hishida et al., 2004). *E.coli* RuvBR174A showed a dominant negative phenotype for DNA repair *in vivo*; defects in the ATPase activity; and the mutation also inhibited branch migration activity. A second mutation in the Walker A motif (K68A) demonstrated a more severe dominant negative effect. However, when K68A and R174A single mutants were mixed, ATPase activity was partially restored. Figure 7.2a shows a possible mechanism of how the ATPase activity was restored when the two single mutants were mixed. The mutants compliment each other's deficiencies. These results and other data (Marrione and Cox, 1995; Putnam et al., 2001; Yamada et al., 2002) suggest that the RuvB hexamer includes nonequivalent active sites that equates to functional asymmetry of the hexamer.

A model for the hydrolytic cycle of RuvB is shown in Figure 7.2b, which shows a hexamer, composed of a pair each of ATP-bound, ADP-bound and nucleotide-free monomers (Hishida et al., 2004). It is speculated, as demonstrated by the model, that when ATP binds to a nucleotide-free site (A), this causes a conformational change so that Arg174 repositions close to the nucleotide phosphate in the adjacent subunit (B), causing ATP hydrolysis. Release of ADP by RuvB was predicted to be the rate-limiting step. It was speculated that ATP hydrolysis in one subunit (B) and its conformational

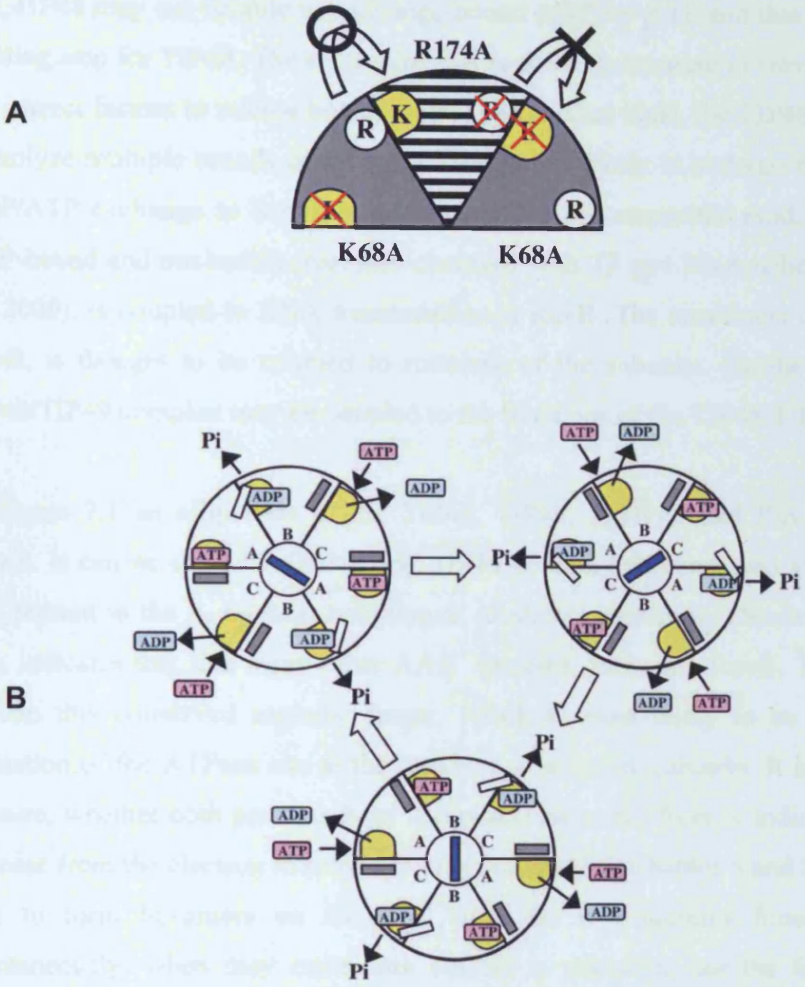

FIGURE 7.2: Assymetric binding of adenine nucleotides in RuvB hexamers

(A) A model for the mechanism of how ATPase activity is restored in RuvB when K68A and R174A mutants are mixed. (B) A model of the hydrolylytic cycle of RuvB. Paired subunits are labeled A, B and C. Gray and white bars indicate inactive and active forms of Arg174, respectively. The yellow box indicates the ATPase site. The blue bar indicates dsDNA. (Both Figures A and B are taken from Hishida. et al. 2004)

change, induces ADP release in the next subunit (C). As described in Chapter 5, it seems that TIP48 may not be able to exchange bound ADP for ATP and this could be the rate limiting step for TIP48. The reason for this is probably because *in vitro* it does not have the correct factors to release bound ADP. On the other hand, the TIP48/49 complex can hydrolyze multiple rounds of ATP and therefore is likely to undergo the same cycle of ADP/ATP exchange as RuvB. It is believed that this sequential model of ATP-bound, ADP-bound and nucleotide free, also observed with T7 gp4 DNA helicase (Singleton et al., 2000), is coupled to DNA translocation in RuvB. The movement of DNA, through RuvB, is thought to be coupled to rotations of the subunits. Similar rotations in the TIP48/TIP49 complex may be coupled to the functions of the TIP48/TIP49 complex.

In Figure 7.1 an alignment of the TIP48, TIP49, *Af*TIP48 and RuvB sequences are shown. It can be seen that TIP48 and TIP49 contain this conserved arginine, which is also present in the *A. fulgidus* homologue, as shown previously (Neuwald et al., 1999). This indicates that like many other AAA^+ proteins, including RuvB, TIP48 and TIP49 contain this conserved arginine finger, which is most likely to be involved in the formation of the ATPase site at the interface of adjacent subunits. It is still not known for sure, whether both proteins form homo-hexamers, but there is indication that this is the case from the electron microscopy data presented in Chapter 5 and because TIP48 is able to form hexamers on its own. How the two proteins form two hexamers spontaneously, when they come into contact is unknown, but the fact that they do underscores the significant interactions between them. The biological function of the core TIP48/TIP49 complex will be discussed below.

7.2. The function of the TIP48/TIP49 complex in cellular complexes

TIP48 and TIP49 and their homologues in yeast are part of a number of chromatin modifying complexes, which have direct and important roles in both transcription and DNA DSB repair (Chapter 1). TIP48 and TIP49 are required for the transcription of over 5 % of genes in yeast (Jonsson et al., 2001) and have also been shown to interact with a

number of transcription-activating proteins that recruit the TIP60 complex, in higher eukaryotes. This has prompted speculations that the two proteins may somehow modify DNA to facilitate the function of transcription activating proteins such as c-Myc, β-catenin, E2F1 and TBP. However, there was no evidence in this study that the two proteins, on their own or as a complex, promoted activities on DNA such as helicase or branch migration activities, in agreement with other studies (Ikura et al., 2000; Qiu et al., 1998). This does not rule out, however, that they have activities on chromatin and they may require accessory factors to act on DNA.

Recently, a report in the literature has confirmed that TIP48 and TIP49 are unlikely to have roles on DNA. It was shown by (Jonsson et al., 2004) that *sc*TIP48 and *sc*TIP49 did not associate with some of the promoters they regulate (*PHO5* and *PHO84*), whereas Ino80p, which also regulates these promoters, did. Yet, TIP48 and TIP49 have been shown to interact with TBP (Bauer et al., 2000; Bauer et al., 1998; Ohdate et al., 2003), which was also shown to be present on these two promoters, during transcription (Jonsson et al., 2004). TIP49 has also been shown to associate with TCF sites in the *ITF-2* promoter along with other components of the TIP60 complex (Feng et al., 2003). This indicates that TIP48 and TIP49 must interact with promoters they regulate, but this interaction is probably transient and therefore prolonged modifying activities on DNA by the proteins would not occur.

It has been suggested that the *sc*TIP48 and *sc*TIP49 proteins do not have a catalytic role in chromatin remodelling in the INO80 complex but are in fact required for the correct assembly of this complex (Jonsson et al., 2004). INO80 complexes, purified from cells that had been depleted of *sc*TIP48 also lacked *sc*TIP49 and Arp5, and were deficient in chromatin remodelling activities (Jonsson et al., 2004). The INO80 (*Δarp5*) mutant complex, which included all other representative INO80 subunits, was also deficient in ATPase, chromatin remodelling and DNA binding activities (Shen et al., 2003). These data implied that the loss in activity of the INO80 (*Δarp5*) complex was due to the missing Arp5 subunit. As *sc*TIP48/TIP49 proteins were still present in the INO80

(*Δarp5*) complex, it was speculated that these proteins do not have a chromatin remodelling activity in the INO80 complex, but instead are involved in the assembly of the complex (Jonsson et al., 2004; Shen et al., 2003). Addition of purified recombinant *sc*TIP48/TIP49 core complex to the mutant INO80 (*ΔscTIP48*) complex did not restore the activity of the INO80 complex (Jonsson et al., 2004). However, when *sc*TIP48 was expressed *in vivo*, in cells that had been depleted of *sc*TIP48, an active INO80 complex was obtained, which contained Arp5 (Jonsson et al., 2004), demonstrating that the Arp5 subunit and the correct assembly of the complex was required for the activity of the INO80 complex.

A mutant *sc*TIP48 was expressed in the same cells that had been depleted of *sc*TIP48 (Jonsson et al., 2004). This mutant contained a mutation at the conserved glutamic acid residue (E297G) of the Walker B motif, which has been predicted to allow binding but not hydrolysis of ATP by AAA^+ proteins (Ogura and Wilkinson, 2001; Seybert and Wigley, 2004). Arp5 was assembled into the INO80 complex by this mutant, demonstrating that Arp5 recruitment by *sc*TIP48 did not require ATP hydrolysis (Jonsson et al., 2004). The INO80 complex containing *sc*TIP48E297G also exhibited chromatin remodelling activity *in vitro*, which indicated that the ATPase activity of *sc*TIP48 was not required for chromatin remodelling. Moreover, when recombinant, purified His_6-Arp5 protein was incubated with a yeast lysate, a stable association with *sc*TIP48 was seen in the presence of ATPγS, but not in its absence and much more weakly in the presence of ATP. INO80 was also required for this interaction between scTIP48 and Arp5 (Jonsson et al., 2004).

These results, therefore, showed that TIP48 and TIP49 are indeed required for the assembly of the INO80 complex. Moreover, the complex was able to function in the presence of *sc*TIP48E297G, which showed conclusively that the action of TIP48 and TIP49 in the assembly of the complex, does not requires ATP hydrolysis by *sc*TIP48. To have a catalytic role in the INO80 complex, the ATPase activity of the *sc*TIP48/TIP49 complex would be necessary. ATP hydrolysis is probably important for the release of the *sc*TIP48/TIP49 complex from INO80 complex, as suggested by

the authors (Jonsson et al., 2004). It has been estimated that there are 1900 *sc*TIP49 molecules per cell, which would regulate 6200 molecules of Ino80p that are in the cell (Ghaemmaghami et al., 2003). Therefore the interaction of the *sc*TIP48/TIP49 with the INO80 complex must be transient to explain the large difference between the number of molecules of *sc*TIP49 and Ino80p in cells.

The fact that TIP48 and TIP49 are part of many other large cellular complexes indicates they may have a similar role in the assembly of these complexes. TIP49 was shown to be important for the histone acetylation of promoter regions by the TIP60 complex (Feng et al., 2003). Accumulation of both of both C/D and H/ACA snoRNAs was also shown to be dependent on ATP binding by *sc*TIP48 (King et al., 2001). As both these processes involve the function of large complexes, it is likely that TIP48 and TIP49 are involved in assembling functional complexes. Disruption of the ATP binding and hydrolysis activities of TIP48 and TIP49, render these complexes inactive. Also the association of TIP48 and TIP49 with various complexes seems to be dependent on protein-protein interactions. For example, it was shown that the recruitment of the proteins to snoRNAs was not directly through the conserved stems I and II of a C/D snoRNA but through an interacting protein Nop58 (Watkins et al., 2002). Moreover, as both proteins interact with c-Myc and β-catenin it is likely that they themselves recruit the TIP60 complex to promoters (Feng et al., 2003; Frank et al., 2003). Therefore the TIP48/TIP49 complex may play a role in the remodeling of protein-protein interactions.

In fact it was suggested in a recent study that snoRNP-associated proteins cause a restructuring event, which leads to the stabilization of the core box C/D complex before it enters the nucleous (Watkins et al., 2004). It was speculated that TIP48 and TIP49 could cause this restructuring by functioning as molecular motors within the complex. Therefore a similar event in other large complexes such as INO80, TIP60 and p400, is also possible. As discussed by (Neuwald et al., 1999) the AAA^+ class of proteins contains a group of chaperone-like ATPases that are involved in the assembly, operation and disassembly of a variety of protein complexes. The TIP48/TIP49 complex probably employs similar mechanisms as other AAA^+

proteins, for the correct assembly of a variety of nuclear complexes. The same mechanisms may extend to complexes or processes in the cytoplasm or at cell membranes (Hawley et al., 2001; Salzer et al., 1999). Furthermore, TIP49 interacts with tubulin (Gartner et al., 2003) and TIP48 and TIP49 were shown to localize with the mitotic apparatus (Gartner et al., 2003; Sigala et el., 2005) and Chapter 6). This indicates that they have roles during mitosis, which may be to facilitate the assembly of the mitotic apparatus or drive some function at the sites of tubulin polymerization.

As well as being involved in the assembly of complexes, TIP48 and TIP49 could be involved in moving around large complexes. They were shown to be required for the localization of snoRNPs to the nucleolus (King et al., 2001). They are also associated with the nuclear matrix (Gohshi et al., 1999; Holzmann et al., 1998; Kikuchi et al., 1999; Sigala et al., 2005). Such a tight association indicates that they may interact with nuclear lamins and may function to transport chromatin remodeling complexes, once assembled, to chromatin. A likely candidate to facilitate this process would be BAF53 as its homologue in yeast has been shown to interact with core histones and nucleosomes (Galarneau et al., 2000; Harata et al., 1999) and hence may be a factor that recruits TIP48/TIP49 containing complexes to chromatin. The connection between BAF53 and TIP48/TIP49 would be interesting to investigate as it may lead to a better understanding of the roles of TIP48 and TIP49 in chromatin modifying complexes.

7.3. Individual roles of TIP48 and TIP49

TIP48 seems to behave in a similar way to the bacterial RuvB protein, *in vitro,* as it forms oligomers in the presence of adenine nucleotides and $MgCl_2$ (Chapter 5, (Mezard et al., 1997; Mitchell and West, 1994)). Also the TIP48D299N mutant bound ATP and formed oligomers in the absence of cofactors, in a similar way as the RuvB mutant ((Mezard et al., 1997) and Chapters 3 and 5). These results indicate that TIP48 has features that are common to RuvB, which have been well conserved throughout evolution. Although TIP48 may not have similar functions to RuvB, it

obviously shares structural properties with RuvB, and hence probably functions with similar mechanisms to RuvB and other closely related AAA+ proteins. TIP49, on the other hand, behaves differently from the two proteins and seems to require TIP48 for its function. It is likely that TIP48 has roles of its own in the cell away from TIP49, for which evidence is starting to emerge (see below). However, TIP49 may also have roles of its own but more evidence for this is still required.

TIP48 was shown to interact with, and affect the transcriptional activities of ATF2, whereas TIP49 did not (Cho et al., 2001). However, it was shown that the C-terminal region that did not contain the Walker A or B motifs of TIP48 was capable of attenuating ATF2 transcription, indicating that this function by TIP48 did not require ATP binding or hydrolysis activities by the protein. Nevertheless, this study did show a function of TIP48 in the absence of TIP49. It has also been shown in Chapter 6 that TIP48 probably has a role in cytokinesis, as it was localized at the midbody. TIP49 was not found in the midbody indicating that if TIP48 has a function in the midbody, it operates without TIP49. A recent study has also shown that both TIP48 and TIP49 interact with the precursor form of a snoRNP, U3, whereas TIP49 was also associated with the mature form of the snoRNP (Watkins et al., 2004). From this observation it was suggested that TIP48 associates with the pre-snoRNP prior to TIP49. Therefore it is likely that TIP48 has the ability to function independently of TIP49 and also can recruit TIP49 for certain functions in the cell.

The most interesting observation in the literature, indicating separate functions for TIP48 and TIP49, is that they have been shown to act as antagonistic regulators of the Wnt-signalling pathway. Using reporter gene assays, it was demonstrated that the proteins antagonistically influenced the transactivation poteintial of the β-catenin-TCF complex (Bauer et al., 2000). They were also shown to regulate wing development in *Drosophila* (Bauer et al., 2000) and heart growth in zebrafish embryos (Rottbauer et al., 2002), by functioning in opposite directions to each other. Therefore, although they are both present during the same process of β-catenin mediated transcription, they do not seem to be working together as part of a complex to exert the same effects on promoters.

A recent study has shed more light on how these two proteins act as antagonistic regulators of certain promoters (Kim et al., 2005). It was shown that the metastasis suppressor gene *KAI1* is down-regulated in prostate cancer cells by the inhibitory actions of β-catenin and TIP48. β-catenin and TIP48 were shown to antagonize the function of TIP60 and TIP49, which are required for activation of the gene. In non-metastatic cells TIP60 and TIP49 were recruited to the promoter but TIP48 was not. However, in metastatic cells β-catenin and TIP48 were recruited to the promoter but TIP49 was not. It was also shown that TIP48 binds the histone deacetylase HDAC1, and it was demonstrated that the repression function of β-catenin-TIP48 was partly due to HDAC1 activity. The results from that study confirm that TIP48 and TIP49 participate in the same cellular pathway but they work antagonistically. Whether TIP48 and TIP49 only behave in this way in the Wnt/β-catenin pathway, remains to be seen. Nevertheless, in this case the proteins seem to function on their own, rather than as a TIP48/TIP49 complex.

7.4 Future directions

Below are a number of investigations that could be carried out, using constructs and reagents that have been generated throughout the course of this study and based on information that has been presented in this thesis.

Investigate interactions of TIP48/TIP49 with BAF53

The aim of this would be to see if BAF53 is capable of recruiting TIP48/TIP49 to nucleosomes/histones. Another question would be whether BAF53 has an effect on TIP48/TIP49 ATPase activity.

Electron microscopy to investigate the structure of TIP48/TIP49 complex in the presence of interacting proteins

Further electron microscopy studies of the TIP48/TIP49 complex need to be carried out, using cryo electron microscopy to obtain a higher resolution structure. These studies

could be used to investigate conformational states of the TIP48/TIP49 complex in the presence of adenine nucleotides. More proteins could be added, such as β-catenin (see below), TIP60, or/and BAF53 to see how the conformation of the complex is changed on the addition of these proteins. Further studies could then be carried out to investigate how the TIP48/TIP49 complex relates within a large complex. This may give a clue of how the TIP48/TIP49 functions within cellular complexes.

Investigate by size exclusion chromatography the complexes formed by TIP48, TIP49 or the TIP48/TIP49 complex with β-catenin

This may show whether TIP48 and TIP49 form hexamers in the presence of β-catenin and whether the TIP48/TIP49 complex is stable in the presence of β-catenin. These experiments may shed light on how TIP48 and TIP49 act as antagonistic regulators of the Wnt/ β-catenin pathway

Investigate interactions of TIP48/TIP49 with the nuclear matrix and nuclear lamins

The aim of this would be to see how TIP48 and TIP49 associate with the nuclear matrix. Interactions between BAF53 and the nuclear matrix could be investigated. Physical and functional interactions with lamins could also be investigated, such as ATPase activity of TIP48/TIP49 in the presence of purified lamins.

Function of TIP48, TIP49 and BAF53 during mitosis and cytokinesis

Investigations into the function of these proteins at the mitotic apparatus could be carried out. The function of TIP48 in the midbody may be revealed, using RNAi (already being carried out in the lab) and other techniques. This would demonstrate whether TIP48 plays an important role during cytokinesis.

Broader aims

In general this study should be a starting point for much broader aims that would be of interest to a number of people, as well as groups working directly in this field.

Understand the mechanistic functions of TIP48/TIP49 complex in large complexes

The proteins obviously function in chromatin modifying complexes to exert their effects on transcription activators and most probably also DNA damage repair. To elucidate the mechanisms of their functions, within these complexes, would give a much better idea of how chromatin modifying complexes can function directly in these particular nuclear functions. Hence this would give a much better idea how these processes are regulated in the cell.

Investigate the opposing functions of TIP48 and TIP49 on β-catenin-mediated transcription to generate drug inhibitors for either TIP48 or TIP49 that may stop the onset of cancer through β-catenin and c-Myc

TIP48 and TIP49 are cofactors for oncogenic transformation by β-catenin and c-Myc. Hence, if the mechanisms of these two proteins within in these transformation pathways are understood, this would inevitably lead to further studies about whether the processes can be affected by inhibiting TIP48 and/or TIP49. As the two proteins are likely to be essential in humans as they are in yeast and *Drosophila*, these essential functions need to be identified, before designing drugs to inhibit the protein.

Bibliography

Aberle, H., Schwartz, H. and Kemler, R. (1996) Cadherin-catenin complex: protein interactions and their implications for cadherin function. *J Cell Biochem*, 61, 514-523.

Allard, S., Utley, R.T., Savard, J., Clarke, A., Grant, P., Brandl, C.J., Pillus, L., Workman, J.L. and Cote, J. (1999) NuA4, an essential transcription adaptor/histone H4 acetyltransferase complex containing Esa1p and the ATM-related cofactor Tra1p. *Embo J*, 18, 5108-5119.

Amati, B., Brooks, M.W., Levy, N., Littlewood, T.D., Evan, G.I. and Land, H. (1993) Oncogenic activity of the c-Myc protein requires dimerization with Max. *Cell*, 72, 233-245.

Bauer, A., Chauvet, S., Huber, O., Usseglio, F., Rothbacher, U., Aragnol, D., Kemler, R. and Pradel, J. (2000) Pontin52 and Reptin52 function as antagonistic regulators of beta-catenin signalling activity. *EMBO*, 19, 6121-6130.

Bauer, A., Huber, O. and Kemler, R. (1998) Pontin52, an interaction partner of beta-catenin, binds to the TATA box binding protein. *Proc.Natl.Acad.Sci*, 95, 14787-14792.

Baumann, P. and West, S.C. (1998) Role of human Rad51 protein in homologous recombination and double-stranded-break repair. *Trends Biochem Sci*, 23, 247-251.

Bennett, R.J., Dunderdale, H.J. and West, S.C. (1993) Resolution of Holliday junctions by RuvC resolvase: cleavage specificity and DNA distortion. *Cell*, 74, 1021-1031.

Beyer, A. (1997) Sequence analysis of the AAA protein family. *Protein Sci*, 6, 2043-2058.

Bhoumik, A., Ivanov, V. and Ronai, Z. (2001) Activating transcription factor 2-derived peptides alter resistance of human tumor cell lines to ultraviolet irradiation and chemical treatment. *Clin Cancer Res*, 7, 331-342.

Bird, A.W., Yu, D.Y., Pray-Grant, M.G., Qiu, Q., Harmon, K.E., Megee, P.C., Grant, P.A., Smith, M.M. and Christman, M.F. (2002) Acetylation of histone H4 by Esa1 is required for DNA double-strand break repair. *Nature*, 419, 411-415.

Bochtler, M., Hartmann, C., Song, H.K., Bourenkov, G.P., Bartunik, H.D. and Huber, R. (2000) The structures of HsIU and the ATP-dependent protease HsIU-HsIV. *Nature*, 403, 800-805.

Brough, D.E., Hofmann, T.J., Ellwood, K.B., Townley, R.A. and Cole, M.D. (1995) An essential domain of the c-myc protein interacts with a nuclear factor that is also required for E1A-mediated transformation. *Mol Cell Biol*, 15, 1536-1544.

Cairns, B.R. (2004) Around the world of DNA damage INO80 days. *Cell*, 119, 733-735.

Chen, Y.J., Yu, X. and Egelman, E.H. (2002) The hexameric ring structure of the Escherichia coli RuvB branch migration protein. *J Mol Biol*, 319, 587-591.
Cho, S.G., Bhoumik, A., Broday, L., Ivanov, V., Rosenstein, B. and Ronai, Z. (2001) TIP49b, a regulator of activating transcription factor 2 response to stress and DNA damage. *Mol Cell Biol*, 21, 8398-8413.
Chong, J.P., Hayashi, M.K., Simon, M.N., Xu, R.M. and Stillman, B. (2000) A double-hexamer archaeal minichromosome maintenance protein is an ATP-dependent DNA helicase. *Proc Natl Acad Sci U S A*, 97, 1530-1535.
Clarke, A.S., Lowell, J.E., Jacobson, S.J. and Pillus, L. (1999) Esa1p is an essential histone acetyltransferase required for cell cycle progression. *Mol Cell Biol*, 19, 2515-2526.
Cole, M.D. (1986) Activation of the c-myc oncogene. *Basic Life Sci*, 38, 399-406.
Confalonieri, F. and Duguet, M. (1995) A 200-amino acid ATPase module in search of a basic function. *Bioessays*, 17, 639-650.
Connolly, B., Parsons, C.A., Benson, F.E., Dunderdale, H.J., Sharples, G.J., Lloyd, R.G. and West, S.C. (1991) Resolution of Holliday junctions in vitro requires the Escherichia coli ruvC gene product. *Proc Natl Acad Sci U S A*, 88, 6063-6067.
D'Atri, S., Tentori, L., Lacal, P.M., Graziani, G., Pagani, E., Benincasa, E., Zambruno, G., Bonmassar, E. and Jiricny, J. (1998) Involvement of the mismatch repair system in temozolomide-induced apoptosis. *Mol Pharmacol*, 54, 334-341.
Davey, M.J., Indiani, C. and O'Donnell, M. (2003) Reconstitution of the Mcm2-7p heterohexamer, subunit arrangement, and ATP site architecture. *J Biol Chem*, 278, 4491-4499.
Davey, M.J., Jeruzalmi, D., Kuriyan, J. and O'Donnell, M. (2002) Motors and switches: AAA+ machines within the replisome. *Nat Rev Mol Cell Biol*, 3, 826-835.
Downs, J.A., Allard, S., Jobin-Robitaille, O., Javaheri, A., Auger, A., Bouchard, N., Kron, S.J., Jackson, S.P. and Cote, J. (2004) Binding of chromatin-modifying activities to phosphorylated histone H2A at DNA damage sites. *Mol Cell*, 16, 979-990.
Downs, J.A., Lowndes, N.F. and Jackson, S.P. (2000) A role for Saccharomyces cerevisiae histone H2A in DNA repair. *Nature*, 408, 1001-1004.
Doyon, Y., Selleck, W., Lane, W.S., Tan, S. and Cote, J. (2004) Structural and functional conservation of the NuA4 histone acetyltransferase complex from yeast to humans. *Mol Cell Biol*, 24, 1884-1896.
Dudas, A. and Chovanec, M. (2004) DNA double-strand break repair by homologous recombination. *Mutat Res*, 566, 131-167.
Dugan, K.A., Wood, M.A. and Cole, M.D. (2002) TIP49, but not TRRAP, modulates c-Myc and E2F1 dependent apoptosis. *Oncogene*, 21, 5835-5843.
Dyson, N. (1998) The regulation of E2F by pRB-family proteins. *Genes Dev*, 12, 2245-2262.
Ebbert, R., Birkmann, A. and Schuller, H.J. (1999) The product of the SNF2/SWI2 paralogue INO80 of Saccharomyces cerevisiae required for efficient

expression of various yeast structural genes is part of a high-molecular-weight protein complex. *Mol Microbiol*, 32, 741-751.

Elliott, B. and Jasin, M. (2002) Double-strand breaks and translocations in cancer. *Cell Mol Life Sci*, 59, 373-385.

Etard, C., Wedlich, D., Bauer, A., Huber, O. and Kuhl, M. (2000) Expression of xenopus homologs of the beta-catenin binding protein pontin52. *Mechanisms of development*, 94, 219-222.

Feng, Y., Lee, N. and Fearon, E.R. (2003) TIP49 regulates beta-catenin-mediated neoplastic transformation and T-cell factor target gene induction via effects on chromatin remodeling. *Cancer Res*, 63, 8726-8734.

Filipowicz, W., Pelczar, P., Pogacic, V. and Dragon, F. (1999) Structure and biogenesis of small nucleolar RNAs acting as guides for ribosomal RNA modification. *Acta Biochim Pol*, 46, 377-389.

Frank, S.R., Parisi, T., Taubert, S., Fernandez, P., Fuchs, M., Chan, H.M., Livingston, D.M. and Amati, B. (2003) MYC recruits the TIP60 histone acetyltransferase complex to chromatin. *EMBO Rep*, 4, 575-580.

Fritsch, O., Benvenuto, G., Bowler, C., Molinier, J. and Hohn, B. (2004) The INO80 protein controls homologous recombination in Arabidopsis thaliana. *Mol Cell*, 16, 479-485.

Fuchs, M., Gerber, J., Drapkin, R., Sif, S., Ikura, T., Ogryzko, V., Lane, W.S., Nakatani, Y. and Livingston, D.M. (2001) The p400 complex is an essential E1A transformation target. *Cell*, 106, 297-307.

Galarneau, L., Nourani, A., Boudreault, A.A., Zhang, Y., Heliot, L., Allard, S., Savard, J., Lane, W.S., Stillman, D.J. and Cote, J. (2000) Multiple links between the NuA4 histone acetyltransferase complex and epigenetic control of transcription. *Mol Cell*, 5, 927-937.

Gartner, W., Rossbacher, J., Zierhut, B., Daneva, T., Base, W., Weissel, M., Waldhausl, W., Pasternack, M.S. and Wagner, L. (2003) The ATP-dependent helicase RUVBL1/TIP49a associates with tubulin during mitosis. *Cell Motil Cytoskeleton*, 56, 79-93.

Ghaemmaghami, S., Huh, W.K., Bower, K., Howson, R.W., Belle, A., Dephoure, N., O'Shea, E.K. and Weissman, J.S. (2003) Global analysis of protein expression in yeast. *Nature*, 425, 737-741.

Gohshi, T., Shimada, M., Kawahire, S., Imai, N., Ichimura, T., Omata, S. and Horigome, T. (1999) Molecular cloning of mouse p47, a second group mammalian RuvB DNA helicase-like protein: homology with those from human and Saccharomyces cerevisiae. *J Biochem (Tokyo)*, 125, 939-946.

Grant, P.A., Schieltz, D., Pray-Grant, M.G., Yates, J.R., 3rd and Workman, J.L. (1998) The ATM-related cofactor Tra1 is a component of the purified SAGA complex. *Mol Cell*, 2, 863-867.

Guenther, B., Onrust, R., Sali, A., O'Donnell, M. and Kuriyan, J. (1997) Crystal structure of the delta' subunit of the clamp-loader complex of E. coli DNA polymerase III. *Cell*, 91, 335-345.

Harata, M., Oma, Y., Mizuno, S., Jiang, Y.W., Stillman, D.J. and Wintersberger, U. (1999) The nuclear actin-related protein of Saccharomyces cerevisiae, Act3p/Arp4, interacts with core histones. *Mol Biol Cell*, 10, 2595-2605.

Harata, M., Zhang, Y., Stillman, D.J., Matsui, D., Oma, Y., Nishimori, K. and Mochizuki, R. (2002) Correlation between chromatin association and transcriptional regulation for the Act3p/Arp4 nuclear actin-related protein of Saccharomyces cerevisiae. *Nucleic Acids Res*, 30, 1743-1750.

Hawley, S.B., Tamura, T.-a. and Miles, L.A. (2001) Purification, cloning and characterization of profibrinolytic plasminogen-binding protein TIP49a. *Journal of biological chemistry*, 276, 179-186.

Helleday, T. (2003) Pathways for mitotic homologous recombination in mammalian cells. *Mutat Res*, 532, 103-115.

Henriksson, M. and Luscher, B. (1996) Proteins of the Myc network: essential regulators of cell growth and differentiation. *Adv Cancer Res*, 68, 109-182.

Hishida, T., Han, Y.W., Fujimoto, S., Iwasaki, H. and Shinagawa, H. (2004) Direct evidence that a conserved arginine in RuvB AAA+ ATPase acts as an allosteric effector for the ATPase activity of the adjacent subunit in a hexamer. *Proc Natl Acad Sci U S A*, 101, 9573-9577.

Holliday, R. (1964) The Induction Of Mitotic Recombination By Mitomycin C In Ustilago And Saccharomyces. *Genetics*, 50, 323-335.

Holzmann, K., Gerner, C., Korosec, T., Poltl, A., Grimm, R. and Sauermann, G. (1998) Identification and characterization of the ubiquitously occuring nuclear matrix protein NMP 238. *Biochem Biophys Res Commun*, 252, 39-45.

Hsieh, J.K., Fredersdorf, S., Kouzarides, T., Martin, K. and Lu, X. (1997) E2F1-induced apoptosis requires DNA binding but not transactivation and is inhibited by the retinoblastoma protein through direct interaction. *Genes Dev*, 11, 1840-1852.

Ikura, T., Ogryzko, V.V., Grigoriev, M., Groisman, R., Wang, J., Horikoshi, M., Scully, R., Qin, J. and Nakatani, Y. (2000) Involvement of the TIP60 histone acetylase complex in DNA repair and apoptosis. *Cell*, 102, 463-473.

Ishimi, Y. (1997) A DNA helicase activity is associated with an MCM4, -6, and -7 protein complex. *J Biol Chem*, 272, 24508-24513.

Iwasaki, H., Han, Y.W., Okamoto, T., Ohnishi, T., Yoshikawa, M., Yamada, K., Toh, H., Daiyasu, H., Ogura, T. and Shinagawa, H. (2000) Mutational analysis of the functional motifs of RuvB, an AAA+ class helicase and motor protein for holliday junction branch migration. *Mol Microbiol*, 36, 528-538.

Iwasaki, H., Takahagi, M., Nakata, A. and Shinagawa, H. (1992) Escherichia coli RuvA and RuvB proteins specifically interact with Holliday junctions and promote branch migration. *Genes Dev*, 6, 2214-2220.

Johnson, A. and O'Donnell, M. (2003) Ordered ATP hydrolysis in the gamma complex clamp loader AAA+ machine. *J Biol Chem*, 278, 14406-14413.

Johnson, R.D. and Jasin, M. (2001) Double-strand-break-induced homologous recombination in mammalian cells. *Biochem Soc Trans*, 29, 196-201.

Jonsson, Z.O., Dhar, S.K., Narlikar, G.J., Auty, R., Wagle, N., Pellman, D., Pratt, R.E., Kingston, R. and Dutta, A. (2001) Rvb1p and Rvb2p are essential components of a chromatin remodeling complex that regulates transcription of over 5% of yeast genes. *J Biol Chem*, 276, 16279-16288.

Jonsson, Z.O., Jha, S., Wohlschlegel, J.A. and Dutta, A. (2004) Rvb1p/Rvb2p recruit Arp5p and assemble a functional Ino80 chromatin remodeling complex. *Mol Cell*, 16, 465-477.

Kamine, J., Elangovan, B., Subramanian, T., Coleman, D. and Chinnadurai, G. (1996) Identification of a cellular protein that specifically interacts with the essential cysteine region of the HIV-1 Tat transactivator. *Virology*, 216, 357-366.

Kanemaki, M., Kurokawa, Y., Matsu-ura, T., Makino, Y., Masani, A., Okazaki, K., Morishita, T. and Tamura, T.A. (1999) TIP49b, a new RuvB-like DNA helicase, is included in a complex together with another RuvB-like DNA helicase, TIP49a. *J Biol Chem*, 274, 22437-22444.

Kanemaki, M., Makino, Y., Yoshida, T., Kishimoto, T., Koga, A., Yamamoto, K., Yamamoto, M., Moncollin, V., Egly, J.M., Muramatsu, M. and Tamura, T. (1997) Molecular cloning of a rat 49-kDa TBP-interacting protein (TIP49) that is highly homologous to the bacterial RuvB. *Biochem Biophys Res Commun*, 235, 64-68.

Kaplan, D.D., Meigs, T.E., Kelly, P. and Casey, P.J. (2004) Identification of a role for beta-catenin in the establishment of a bipolar mitotic spindle. *J Biol Chem*, 279, 10829-10832.

Kikuchi, N., Gohshi, T., Kawahire, S., Tachibana, T., Yoneda, Y., Isobe, T., Lim, C.R., Kohno, K., Ichimura, T., Omata, S. and Horigome, T. (1999) Molecular shape and ATP binding activity of rat p50, a putative mammalian homologue of RuvB DNA helicase. *J Biochem (Tokyo)*, 125, 487-494.

Kim, J.H., Kim, B., Cai, L., Choi, H.J., Ohgi, K.A., Tran, C., Chen, C., Chung, C.H., Huber, O., Rose, D.W., Sawyers, C.L., Rosenfeld, M.G. and Baek, S.H. (2005) Transcriptional regulation of a metastasis suppressor gene by Tip60 and beta-catenin complexes. *Nature*, 434, 921-926.

King, S.M. (2000) AAA domains and organization of the dynein motor unit. *J Cell Sci*, 113 (Pt 14), 2521-2526.

King, T.H., Decatur, W.A., Bertrand, E., Maxwell, E.S. and Fournier, M.J. (2001) A well-connected and conserved nucleoplasmic helicase is required for production of box C/D and H/ACA snoRNAs and localization of snoRNP proteins. *Mol Cell Biol*, 21, 7731-7746.

Kobor, M.S., Venkatasubrahmanyam, S., Meneghini, M.D., Gin, J.W., Jennings, J.L., Link, A.J., Madhani, H.D. and Rine, J. (2004) A protein complex containing the conserved Swi2/Snf2-related ATPase Swr1p deposits histone variant H2A.Z into euchromatin. *PLoS Biol*, 2, E131.

Kolligs, F.T., Hu, G., Dang, C.V. and Fearon, E.R. (1999) Neoplastic transformation of RK3E by mutant beta-catenin requires deregulation of Tcf/Lef transcription but not activation of c-myc expression. *Mol Cell Biol*, 19, 5696-5706.

Koonin, E.V. (1993a) A common set of conserved motifs in a vast variety of putative nucleic acid-dependent ATPases including MCM proteins involved in the initiation of eukaryotic DNA replication. *Nucleic Acids Res*, 21, 2541-2547.

Koonin, E.V. (1993b) A superfamily of ATPases with diverse functions containing either classical or deviant ATP-binding motif. *J Mol Biol*, 229, 1165-1174.

Krogan, N.J., Baetz, K., Keogh, M.C., Datta, N., Sawa, C., Kwok, T.C., Thompson, N.J., Davey, M.G., Pootoolal, J., Hughes, T.R., Emili, A., Buratowski, S., Hieter, P. and Greenblatt, J.F. (2004) Regulation of chromosome stability by the histone H2A variant Htz1, the Swr1 chromatin remodeling complex, and the histone acetyltransferase NuA4. *Proc Natl Acad Sci U S A*, 101, 13513-13518.

Krogan, N.J., Keogh, M.C., Datta, N., Sawa, C., Ryan, O.W., Ding, H., Haw, R.A., Pootoolal, J., Tong, A., Canadien, V., Richards, D.P., Wu, X., Emili, A., Hughes, T.R., Buratowski, S. and Greenblatt, J.F. (2003) A Snf2 family ATPase complex required for recruitment of the histone H2A variant Htz1. *Mol Cell*, 12, 1565-1576.

Kusch, T., Florens, L., Macdonald, W.H., Swanson, S.K., Glaser, R.L., Yates, J.R., 3rd, Abmayr, S.M., Washburn, M.P. and Workman, J.L. (2004) Acetylation by Tip60 is required for selective histone variant exchange at DNA lesions. *Science*, 306, 2084-2087.

Lafontaine, D.L. and Tollervey, D. (2001) The function and synthesis of ribosomes. *Nat Rev Mol Cell Biol*, 2, 514-520.

Lee, J.H., Chang, S.H., Shim, J.H., Lee, J.Y., Yoshida, M. and Kwon, H. (2003) Cytoplasmic localization and nucleo-cytoplasmic shuttling of BAF53, a component of chromatin-modifying complexes. *Mol Cells*, 16, 78-83.

Lee, J.K. and Hurwitz, J. (2000) Isolation and characterization of various complexes of the minichromosome maintenance proteins of Schizosaccharomyces pombe. *J Biol Chem*, 275, 18871-18878.

Lenzen, C.U., Steinmann, D., Whiteheart, S.W. and Weis, W.I. (1998) Crystal structure of the hexamerization domain of N-ethylmaleimide-sensitive fusion protein. *Cell*, 94, 525-536.

Lim, C.R., Kimata, Y., Ohdate, H., Kokubo, T., Kikuchi, N., Horigome, T. and Kohno, K. (2000) The Saccharomyces cerevisiae RuvB-like protein, Tih2p, is required for cell cycle progression and RNA polymerase II-directed transcription. *J Biol Chem*, 275, 22409-22417.

Lu, K.P. and Hunter, T. (1995) Evidence for a NIMA-like mitotic pathway in vertebrate cells. *Cell*, 81, 413-424.

Lupas, A.N. and Martin, J. (2002) AAA proteins. *Curr Opin Struct Biol*, 12, 746-753.

Madigan, J.P., Chotkowski, H.L. and Glaser, R.L. (2002) DNA double-strand break-induced phosphorylation of Drosophila histone variant H2Av helps prevent radiation-induced apoptosis. *Nucleic Acids Res*, 30, 3698-3705.

Majka, J. and Burgers, P.M. (2004) The PCNA-RFC families of DNA clamps and clamp loaders. *Prog Nucleic Acid Res Mol Biol*, 78, 227-260.

Makino, Y., Kanemaki, M., Kurokawa, Y., Koji, T. and Tamura, T. (1999) A rat RuvB-like protein, TIP49a, is a germ cell-enriched novel DNA helicase. *J Biol Chem*, 274, 15329-15335.

Makino, Y., Mimori, T., Koike, C., Kanemaki, M., Kurokawa, Y., Inoue, S., Kishimoto, T. and Tamura, T. (1998) TIP49, homologous to the bacterial

DNA helicase RuvB, acts as an autoantigen in human. *Biochem Biophys Res Commun*, 245, 819-823.

Maldonado, E., Shiekhattar, R., Sheldon, M., Cho, H., Drapkin, R., Rickert, P., Lees, E., Anderson, C.W., Linn, S. and Reinberg, D. (1996) A human RNA polymerase II complex associated with SRB and DNA-repair proteins. *Nature*, 381, 86-89.

Marrione, P.E. and Cox, M.M. (1995) RuvB protein-mediated ATP hydrolysis: functional asymmetry in the RuvB hexamer. *Biochemistry*, 34, 9809-9818.

Marrione, P.E. and Cox, M.M. (1996) Allosteric effects of RuvA protein, ATP, and DNA on RuvB protein-mediated ATP hydrolysis. *Biochemistry*, 35, 11228-11238.

McMahon, S.B., Van Buskirk, H.A., Dugan, K.A., Copeland, T.D. and Cole, M.D. (1998) The novel ATM-related protein TRRAP is an essential cofactor for the c-Myc and E2F oncoproteins. *Cell*, 94, 363-374.

McMahon, S.B., Wood, M.A. and Cole, M.D. (2000) The essential cofactor TRRAP recruits the histone acetyltransferase hGCN5 to c-Myc. *Mol Cell Biol*, 20, 556-562.

Melese, T. and Boyer, P.D. (1985) Derivatization of the catalytic subunits of the chloroplast ATPase by 2-azido-ATP and dicyclohexylcarbodiimide. Evidence for catalytically induced interchange of the subunits. *J Biol Chem*, 260, 15398-15401.

Meneghini, M.D., Wu, M. and Madhani, H.D. (2003) Conserved histone variant H2A.Z protects euchromatin from the ectopic spread of silent heterochromatin. *Cell*, 112, 725-736.

Mezard, C., Davies, A.A., Stasiak, A. and West, S.C. (1997) Biochemical properties of RuvBD113N: a mutation in helicase motif II of the RuvB hexamer affects DNA binding and ATPase activities. *J Mol Biol*, 271, 704-717.

Minoda, A., Saitoh, S., Takahashi, K. and Toda, T. (2005) BAF53/Arp4 homolog Alp5 in fission yeast is required for histone H4 acetylation, kinetochore-spindle attachment, and gene silencing at centromere. *Mol Biol Cell*, 16, 316-327.

Mitchell, A.H. and West, S.C. (1994) Hexameric rings of Escherichia coli RuvB protein. Cooperative assembly, processivity and ATPase activity. *J Mol Biol*, 243, 208-215.

Miyata, T., Yamada, K., Iwasaki, H., Shinagawa, H., Morikawa, K. and Mayanagi, K. (2000) Two different oligomeric states of the RuvB branch migration motor protein as revealed by electron microscopy. *J Struct Biol*, 131, 83-89.

Mizuguchi, G., Shen, X., Landry, J., Wu, W.H., Sen, S. and Wu, C. (2004) ATP-driven exchange of histone H2AZ variant catalyzed by SWR1 chromatin remodeling complex. *Science*, 303, 343-348.

Morrison, A.J., Highland, J., Krogan, N.J., Arbel-Eden, A., Greenblatt, J.F., Haber, J.E. and Shen, X. (2004) INO80 and gamma-H2AX interaction links ATP-dependent chromatin remodeling to DNA damage repair. *Cell*, 119, 767-775.

Muller, B., Tsaneva, I.R. and West, S.C. (1993) Branch migration of Holliday junctions promoted by the Escherichia coli RuvA and RuvB proteins. I.

Comparison of RuvAB- and RuvB-mediated reactions. *J Biol Chem*, 268, 17179-17184.

Neuwald, A.F., Aravind, L., Spouge, J.L. and Koonin, E.V. (1999) AAA+: A class of chaperone-like ATPases associated with the assembly, operation, and disassembly of protein complexes. *Genome Res*, 9, 27-43.

Nevins, J.R. (1995) Adenovirus E1A: transcription regulation and alteration of cell growth control. *Curr Top Microbiol Immunol*, 199 (Pt 3), 25-32.

Newman, D.R., Kuhn, J.F., Shanab, G.M. and Maxwell, E.S. (2000) Box C/D snoRNA-associated proteins: two pairs of evolutionarily ancient proteins and possible links to replication and transcription. *Rna*, 6, 861-879.

Nourani, A., Utley, R.T., Allard, S. and Cote, J. (2004) Recruitment of the NuA4 complex poises the PHO5 promoter for chromatin remodeling and activation. *Embo J*, 23, 2597-2607.

Ogryzko, V. (2000) Mammalian histone acetyltransferase complexes. *Medicina (B Aires)*, 60 Suppl 2, 21-26.

Ogura, T. and Wilkinson, A.J. (2001) AAA+ superfamily ATPases: common structure--diverse function. *Genes Cells*, 6, 575-597.

Ohdate, H., Lim, C.R., Kokubo, T., Matsubara, K., Kimata, Y. and Kohno, K. (2003) Impairment of the DNA binding activity of the TATA-binding protein renders the transcriptional function of Rvb2p/Tih2p, the yeast RuvB-like protein, essential for cell growth. *J Biol Chem*, 278, 14647-14656.

Ohfuchi, E., Nishimori, K. and Harata, M. (2002) Alternative splicing products of the gene for a human nuclear actin-related protein, hArpNbeta/Baf53, that encode a protein isoform, hArpNbetaS, in the cytoplasm. *Biosci Biotechnol Biochem*, 66, 1740-1743.

Osman, F. and Subramani, S. (1998) Double-strand break-induced recombination in eukaryotes. *Prog Nucleic Acid Res Mol Biol*, 58, 263-299.

Pape, T., Meka, H., Chen, S., Vicentini, G., van Heel, M. and Onesti, S. (2003) Hexameric ring structure of the full-length archaeal MCM protein complex. *EMBO Rep*, 4, 1079-1083.

Parfait, B., Giovangrandi, Y., Asheuer, M., Laurendeau, I., Olivi, M., Vodovar, N., Vidaud, D., Vidaud, M. and Bieche, I. (2000) Human TIP49b/RUVBL2 gene: genomic structure, expression pattern, physical link to the human CGB/LHB gene cluster on chromosome 19q13.3. *Ann Genet*, 43, 69-74.

Park, J., Wood, M.A. and Cole, M.D. (2002) BAF53 forms distinct nuclear complexes and functions as a critical c-Myc-interacting nuclear cofactor for oncogenic transformation. *Molecular and cellular biology*, 22, 1307-1316.

Parsons, C.A., Stasiak, A., Bennett, R.J. and West, S.C. (1995a) Structure of a multisubunit complex that promotes DNA branch migration. *Nature*, 374, 375-378.

Parsons, C.A., Stasiak, A. and West, S.C. (1995b) The E.coli RuvAB proteins branch migrate Holliday junctions through heterologous DNA sequences in a reaction facilitated by SSB. *Embo J*, 14, 5736-5744.

Parsons, C.A., Tsaneva, I., Lloyd, R.G. and West, S.C. (1992) Interaction of Escherichia coli RuvA and RuvB proteins with synthetic Holliday junctions. *Proc Natl Acad Sci U S A*, 89, 5452-5456.

Parsons, C.A. and West, S.C. (1993) Formation of a RuvAB-Holliday junction complex in vitro. *J Mol Biol*, 232, 397-405.

Patel, S. and Latterich, M. (1998) The AAA team: related ATPases with diverse functions. *Trends in cell biology*, 8, 65-71.

Patel, S.S. and Picha, K.M. (2000) Structure and function of hexameric helicases. *Annu Rev Biochem*, 69, 651-697.

Peterson, C.L. (1996) Multiple SWItches to turn on chromatin? *Curr Opin Genet Dev*, 6, 171-175.

Pfeiffer, P., Goedecke, W. and Obe, G. (2000) Mechanisms of DNA double-strand break repair and their potential to induce chromosomal aberrations. *Mutagenesis*, 15, 289-302.

Poch, O. and Winsor, B. (1997) Who's who among the Saccharomyces cerevisiae actin-related proteins? A classification and nomenclature proposal for a large family. *Yeast*, 13, 1053-1058.

Privezentzev, C.V., Keeley, A., Sigala, B. and Tsaneva, I.R. (2004) The role of RuvA octamerisation for RuvAB function in vitro and in vivo. *J Biol Chem.*

Putnam, C.D., Clancy, S.B., Tsuruta, H., Gonzalez, S., Wetmur, J.G. and Tainer, J.A. (2001) Structure and mechanism of the RuvB Holliday junction branch migration motor. *J Mol Biol*, 311, 297-310.

Qin, X.Q., Livingston, D.M., Kaelin, W.G., Jr. and Adams, P.D. (1994) Deregulated transcription factor E2F-1 expression leads to S-phase entry and p53-mediated apoptosis. *Proc Natl Acad Sci U S A*, 91, 10918-10922.

Qiu, X.B., Lin, Y.L., Thome, K.C., Pian, P., Schlegel, B.P., Weremowicz, S., Parvin, J.D. and Dutta, A. (1998) An eukaryotic RuvB-like protein (RUVBL1) essential for growth. *J Biol Chem*, 273, 27786-27793.

Rafferty, J.B., Sedelnikova, S.E., Hargreaves, D., Artymiuk, P.J., Baker, P.J., Sharples, G.J., Mahdi, A.A., Lloyd, R.G. and Rice, D.W. (1996) Crystal structure of DNA recombination protein RuvA and a model for its binding to the Holliday junction. *Science*, 274, 415-421.

Redon, C., Pilch, D., Rogakou, E., Sedelnikova, O., Newrock, K. and Bonner, W. (2002) Histone H2A variants H2AX and H2AZ. *Curr Opin Genet Dev*, 12, 162-169.

Rottbauer, W., Saurin, A.J., Lickert, H., Shen, X., Burns, C.G., Wo, Z.G., Kemler, R., Kingston, R., Wu, C. and Fishman, M. (2002) Reptin and pontin antagonistically regulate heart growth in zebrafish embryos. *Cell*, 111, 661-672.

Rynditch, A., Pekarsky, Y., Schnittger, S. and Gardiner, K. (1997) Leukemia breakpoint region in 3q21 is gene rich. *Gene*, 193, 49-57.

Salzer, U., Kubicek, M. and Prohaska, R. (1999) Isolation, molecular characterization, and tissue-specific expression of ECP-51 and ECP-54 (TIP49), two homologous, interacting erythroid cytosolic proteins. *Biochim Biophys Acta*, 1446, 365-370.

Schwacha, A. and Bell, S.P. (2001) Interactions between two catalytically distinct MCM subgroups are essential for coordinated ATP hydrolysis and DNA replication. *Mol Cell*, 8, 1093-1104.

Seybert, A., Scott, D.J., Scaife, S., Singleton, M.R. and Wigley, D.B. (2002) Biochemical characterisation of the clamp/clamp loader proteins from the euryarchaeon Archaeoglobus fulgidus. *Nucleic Acids Res*, 30, 4329-4338.

Seybert, A. and Wigley, D.B. (2004) Distinct roles for ATP binding and hydrolysis at individual subunits of an archaeal clamp loader. *Embo J*, 23, 1360-1371.

Shah, R., Bennett, R.J. and West, S.C. (1994) Genetic recombination in E. coli: RuvC protein cleaves Holliday junctions at resolution hotspots in vitro. *Cell*, 79, 853-864.

Shen, X., Mizuguchi, G., Hamiche, A. and Wu, C. (2000) A chromatin remodelling complex involved in transcription and DNA processing. *Nature*, 406, 541-544.

Shen, X., Ranallo, R., Choi, E. and Wu, C. (2003) Involvement of actin-related proteins in ATP-dependent chromatin remodeling. *Mol Cell*, 12, 147-155.

Sigala, B., Edwards, M., Puri, T., Tsaneva, I. (2005) Relocalisation of human chromatin remodelling co-factor TIP48 in mitosis. *Experimental cell research* 310, 357-369.

Singleton, M.R., Sawaya, M.R., Ellenberger, T. and Wigley, D.B. (2000) Crystal structure of T7 gene 4 ring helicase indicates a mechanism for sequential hydrolysis of nucleotides. *Cell*, 101, 589-600.

Skop, A.R., Liu, H., Yates, J., 3rd, Meyer, B.J. and Heald, R. (2004) Dissection of the mammalian midbody proteome reveals conserved cytokinesis mechanisms. *Science*, 305, 61-66.

Smith, E.R., Eisen, A., Gu, W., Sattah, M., Pannuti, A., Zhou, J., Cook, R.G., Lucchesi, J.C. and Allis, C.D. (1998) ESA1 is a histone acetyltransferase that is essential for growth in yeast. *Proc Natl Acad Sci U S A*, 95, 3561-3565.

Stasiak, A., Tsaneva, I.R., West, S.C., Benson, C.J., Yu, X. and Egelman, E.H. (1994) The Escherichia coli RuvB branch migration protein forms double hexameric rings around DNA. *Proc Natl Acad Sci U S A*, 91, 7618-7622.

Steger, D.J., Haswell, E.S., Miller, A.L., Wente, S.R. and O'Shea, E.K. (2003) Regulation of chromatin remodeling by inositol polyphosphates. *Science*, 299, 114-116.

Stillman, B. (1992) Initiation of chromosome replication in eukaryotic cells. *Harvey Lect*, 88, 115-140.

Stone, J., de Lange, T., Ramsay, G., Jakobovits, E., Bishop, J.M., Varmus, H. and Lee, W. (1987) Definition of regions in human c-myc that are involved in transformation and nuclear localization. *Mol Cell Biol*, 7, 1697-1709.

Studier, F.W. (1991) Use of bacteriophage T7 lysozyme to improve an inducible T7 expression system. *J Mol Biol*, 219, 37-44.

Taubert, S., Gorrini, C., Frank, S.R., Parisi, T., Fuchs, M., Chan, H.M., Livingston, D.M. and Amati, B. (2004) E2F-dependent histone acetylation and recruitment of the Tip60 acetyltransferase complex to chromatin in late G1. *Mol Cell Biol*, 24, 4546-4556.

Terns, M.P. and Terns, R.M. (2002) Small nucleolar RNAs: versatile trans-acting molecules of ancient evolutionary origin. *Gene Expr*, 10, 17-39.

Tsaneva, I., Muller, B. and West, S.C. (1993) RuvA and RuvB proteins of Escherichia coli exhibit DNA helicase activity in vitro. *Proc Natl Acad Sci U S A*, 90, 1315-1319.

Tsaneva, I.R., Muller, B. and West, S.C. (1992) ATP-dependent branch migration of Holliday junctions promoted by the RuvA and RuvB proteins of E. coli. *Cell*, 69, 1171-1180.

Tsukiyama, T., Palmer, J., Landel, C.C., Shiloach, J. and Wu, C. (1999) Characterization of the imitation switch subfamily of ATP-dependent chromatin-remodeling factors in Saccharomyces cerevisiae. *Genes Dev*, 13, 686-697.

Valle, M., Gruss, C., Halmer, L., Carazo, J.M. and Donate, L.E. (2000) Large T-antigen double hexamers imaged at the simian virus 40 origin of replication. *Mol Cell Biol*, 20, 34-41.

van Attikum, H., Fritsch, O., Hohn, B. and Gasser, S.M. (2004) Recruitment of the INO80 complex by H2A phosphorylation links ATP-dependent chromatin remodeling with DNA double-strand break repair. *Cell*, 119, 777-788.

van Heel, M., Harauz, G., Orlova, E.V., Schmidt, R. and Schatz, M. (1996) A new generation of the IMAGIC image processing system. *J Struct Biol*, 116, 17-24.

Watkins, N.J., Dickmanns, A. and Luhrmann, R. (2002) Conserved stem II of the box C/D motif is essential for nucleolar localization and is required, along with the 15.5K protein, for the hierarchical assembly of the box C/D snoRNP. *Mol Cell Biol*, 22, 8342-8352.

Watkins, N.J., Lemm, I., Ingelfinger, D., Schneider, C., Hossbach, M., Urlaub, H. and Luhrmann, R. (2004) Assembly and Maturation of the U3 snoRNP in the Nucleoplasm in a Large Dynamic Multiprotein Complex. *Mol Cell*, 16, 789-798.

Watkins, N.J., Newman, D.R., Kuhn, J.F. and Maxwell, E.S. (1998) In vitro assembly of the mouse U14 snoRNP core complex and identification of a 65-kDa box C/D-binding protein. *Rna*, 4, 582-593.

Weber, V., Harata, M., Hauser, H. and Wintersberger, U. (1995) The actin-related protein Act3p of Saccharomyces cerevisiae is located in the nucleus. *Mol Biol Cell*, 6, 1263-1270.

Weinstein, L.B. and Steitz, J.A. (1999) Guided tours: from precursor snoRNA to functional snoRNP. *Curr Opin Cell Biol*, 11, 378-384.

West, S.C. (1994a) Processing of Holliday junctions by RuvABC--an overview. *Ann N Y Acad Sci*, 726, 156-163; discussion 163-154.

West, S.C. (1994b) The processing of recombination intermediates: mechanistic insights from studies of bacterial proteins. *Cell*, 76, 9-15.

West, S.C. (1996) The RuvABC proteins and Holliday junction processing in Escherichia coli. *J Bacteriol*, 178, 1237-1241.

Willert, K. and Nusse, R. (1998) Beta-catenin: a key mediator of Wnt signaling. *Curr Opin Genet Dev*, 8, 95-102.

Wood, M.A., McMahon, S.B. and Cole, M.D. (2000) An ATPase/helicase complex is an essential cofactor for oncogenic transformation by c-Myc. *Mol Cell*, 5, 321-330.

Yamada, K., Kunishima, N., Mayanagi, K., Ohnishi, T., Nishino, T., Iwasaki, H., Shinagawa, H. and Morikawa, K. (2001) Crystal structure of the Holliday junction migration motor protein RuvB from Thermus thermophilus HB8. *Proc Natl Acad Sci U S A*, 98, 1442-1447.

Yamada, K., Miyata, T., Tsuchiya, D., Oyama, T., Fujiwara, Y., Ohnishi, T., Iwasaki, H., Shinagawa, H., Ariyoshi, M., Mayanagi, K. and Morikawa, K. (2002) Crystal structure of the RuvA-RuvB complex: a structural basis for the Holliday junction migrating motor machinery. *Mol Cell*, 10, 671-681.

Yamamoto, T. and Horikoshi, M. (1997) Novel substrate specificity of the histone acetyltransferase activity of HIV-1-Tat interactive protein Tip60. *J Biol Chem*, 272, 30595-30598.

Yao, N., Coryell, L., Zhang, D., Georgescu, R.E., Finkelstein, J., Coman, M.M., Hingorani, M.M. and O'Donnell, M. (2003) Replication factor C clamp loader subunit arrangement within the circular pentamer and its attachment points to proliferating cell nuclear antigen. *J Biol Chem*, 278, 50744-50753.

You, Z., Ishimi, Y., Masai, H. and Hanaoka, F. (2002) Roles of Mcm7 and Mcm4 subunits in the DNA helicase activity of the mouse Mcm4/6/7 complex. *J Biol Chem*, 277, 42471-42479.

Yu, R.C., Hanson, P.I., Jahn, R. and Brunger, A.T. (1998) Structure of the ATP-dependent oligomerization domain of N-ethylmaleimide sensitive factor complexed with ATP. *Nat Struct Biol*, 5, 803-811.

Yu, X. and Egelman, E.H. (1997) The RecA hexamer is a structural homologue of ring helicases. *Nat Struct Biol*, 4, 101-104.

Yu, X., West, S.C. and Egelman, E.H. (1997) Structure and subunit composition of the RuvAB-Holliday junction complex. *J Mol Biol*, 266, 217-222.

Zawel, L. and Reinberg, D. (1993) Initiation of transcription by RNA polymerase II: a multi-step process. *Prog Nucleic Acid Res Mol Biol*, 44, 67-108.

Zhao, K., Wang, W., Rando, O.J., Xue, Y., Swiderek, K., Kuo, A. and Crabtree, G.R. (1998) Rapid and phosphoinositol-dependent binding of the SWI/SNF-like BAF complex to chromatin after T lymphocyte receptor signaling. *Cell*, 95, 625-636.